DOE/DP/40086-1 Vol. 1

UC-21

INERTIAL-CONFINEMENT FUSION CENTRAL-STATION ELECTRIC-POWER-GENERATING PLANT

FINAL REPORT FOR THE PERIOD MARCH 1, 1979 - SEPTEMBER 30, 1980

MASTER

VOLUME I

E. W. SUCOV

FEBRUARY 27, 1981

WORK PERFORMED UNDER CONTRACT
DE-AC08-79DP40086

PREPARED FOR THE
U.S. DEPARTMENT OF ENERGY
OFFICE OF INERTIAL FUSION

fusion power
systems department

Westinghouse Electric Corporation

WFPS-TME-81-001

DOE/DP/40086-1 VOL. I

UC-21

INERTIAL-CONFINEMENT FUSION CENTRAL-STATION ELECTRIC-POWER-GENERATING PLANT

FINAL REPORT FOR THE PERIOD
MARCH 1, 1979 - SEPTEMBER 30, 1980

VOLUME I

EDITOR

E. W. SUCOV

FEBRUARY 27, 1981

CONTRIBUTORS

R. V. BABCOCK
C. A. BOOKER
W. C. BRENNER
M. E. CULBERT
R. M. DEL VECCHIO
J. R. EASOZ
H. J. GARBER
R. E. GOLD
L. GREEN
R. A. HILL
J. R. HOLLAND
J. S. KARBOWSKI
A. Y. LEE
M. D. NAHEMOW
T. V. PREVENSLIK
R. J. RAVAS
D. A. SINK
G. S. SMELTZER
M. SNIDERMAN
L. H. TAYLOR
R. DE LUCA (STONE & WEBSTER)
B. K. JENSEN (PSE&G RESEARCH)

fusion power
systems department

Westinghouse Electric Corporation
P.O. Box 10864, Pgh. Pa. 15236

WFPS-TME-81-001

INERTIAL CONFINEMENT FUSION CENTRAL STATION ELECTRIC POWER GENERATING PLANT

FINAL REPORT FOR THE PERIOD MARCH 1, 1979 - SEPTEMBER 30, 1980

Approved by: _____
E. W. SUCOV
MANAGER
INERTIAL CONFINEMENT PROGRAMS

Approved by: _____
T. C. VARLJEN
MANAGER
ENGINEERING

fusion power systems department

Westinghouse Electric Corporation
P.O. Box 10864, Pgh. Pa. 15236

ACKNOWLEDGMENTS

This study has been conducted as an interdisciplinary and inter-organizational effort which involved contributions by a number of individuals. Two outside organizations were subcontractors to Westinghouse on this project, responsible for the following areas:

Stone and Webster	Balance of Plant
PSE&G Research	Utility Perspective

The principal individual contributors and their primary areas of responsibility are as follows:

Driver Design	M. D. Nahemow (Heavy Ion Beam) R. V. Babcock (CO_2 Laser)
Pellet and First Wall Physics	L. H. Taylor
Pellet Fabrication	R. M. Del Vecchio, J. R. Holland
Materials Technology	R. E. Gold
Stress Analysis and Cavity Design	T. V. Prevenslik
Thermal Design	A. Y. Lee
Nuclear Design	L. Green
Reactor Design, Interface with Stone & Webster	J. S. Karbowski
Maintenance	M. Sniderman
Balance of Plant	R. De Luca (Stone & Webster)
ICECAP Code Development	D. A. Sink

In addition to the above individuals, contributions were provided by:

C. A. Booker, Data Handling	R. A. Hill, Heavy Ion Power Supply
W. C. Brenner, Magnet Design	E. M. Iwinski, Computer Analysis
M. E. Culbert, Stress Analysis	R. J. Ravas, Pellet Injection
J. R. Easoz, Vacuum System	G. S. Smeltzer, Laser Power Supply
H. J. Garber, Tritium and Radwaste Handling	F. S. Malick, Cavity Design

ACKNOWLEDGMENTS (Cont.)

Special acknowledgment is given to our consultants who provided valuable orientation to our team members and participated in the study effort.

K. A. Brueckner (UCSD)	Pellet Implosion Physics; Driver Selection
G. A. Kulcinski (U. Wisconsin)	ICF Materials
R. W. Conn (UCLA)	ICF Systems
L. Teng (Fermilab)	Heavy Ion Technology
J. Benford (P.I.)	Light Ion Technology

Finally, we acknowledge the wholehearted cooperation of the national laboratories in guiding the effort and in supplying information and advice. In addition to many individuals at the weapons labs, we acknowledge the cooperation of the groups working under R. Martin, ANL, and D. Keefe, LBL. Special appreciation is expressed to the members of our Technical Review Panel

M. J. Monsler, LLL
I. O. Bohachevsky, LASL
D. L. Cook, Sandia

and to our contract administrator, Rex B. Purcell.

TABLE OF CONTENTS

VOLUME I

TABLE OF CONTENTS (Cont.)

TABLE OF CONTENTS (Cont.)

VOLUME II

TABLE OF CONTENTS (Cont.)

TABLE OF CONTENTS (Cont.)

LIST OF FIGURES

LIST OF FIGURES (Cont.)

LIST OF FIGURES (Cont.)

LIST OF FIGURES (Cont.)

LIST OF FIGURES (Cont.)

LIST OF FIGURES (Cont.)

LIST OF FIGURES (Cont.)

LIST OF FIGURES (Cont.)

LIST OF TABLES

LIST OF TABLES (Cont.)

LIST OF TABLES (Cont.)

LIST OF TABLES (Cont.)

LIST OF TABLES (Cont.)

1.0 ABSTRACT

The Westinghouse ICF Power Plant Design Study was undertaken 1) to investigate the comparative merits of commercial power plants based on ICF drivers, 2) to examine the technological problems that need to be confronted and solved in order to produce commercially competitive electricity acceptable to utilities and 3) to explore the technological and institutional implications of using classified pellets. Two conceptual designs, based on a CO_2 laser driver and on a heavy ion particle beam driver, were developed to provide the basis for the comparisons. Analytic descriptions of the performance and cost relationships for each of the subsystems that comprise the power plant were combined into an overall computer code which modeled the entire plant and permitted trade studies to be conducted. Utility requirements, based on legal and economic constraints, were identified.

This report contains a complete description of the subsystems of the power plant including driver, driver power supply, pellet fabrication, pellet injection and aiming, data handling and control, evacuation, tritium and radwaste handling, first wall protection, first wall and structure, heat removal, tritium breeding and neutron shielding, maintenance and repair and balance of plant. In addition, it contains analytic support for the conceptual designs developed for each subsystem. The emphasis of the effort was on designing a viable reactor cavity and on solving the problems of interfacing the driver systems with the reactor cavity. The reactors generate 3500 MWt by irradiating a pellet whose gain is 175 from two opposite sides with a total of 2 MJ driver energy at a 10 Hz repetition rate. Because the nominal laser driver efficiency is 10% and that for the heavy ion driver is 30%, the net electric power outputs are 1207 MWe and 1346 MWe; the net plant conversion efficiencies are 28.1% and 31.3%; and the recirculating fractions are 22.9% and 14.0% respectively. The increased power output is, however, only one of the factors considered by utilities in performing a cost minimization analysis of competing power sources for system expansion. These other factors include: capital costs, cost of construction time, operating costs, environmental and licensing costs and reliability cost.

The CO_2 laser delivers 2 MJ of 10.6 μm radiation through a cavity pressure of 10^{-1} Torr by combining 108 18.5 kJ beams arranged in 12 beam ducts (6 on a side), each carrying 9 beams. The driver efficiency of 10% is achieved by sequential extraction of energy from the power amplifier by different lines of the 10.6 μm complex. The final focusing mirror is 30 m from the target, allowing counter streaming gas to protect the mirror surface by absorbing the energy of the x-rays and debris ions. Neutron backstreaming to the entrance window is minimized by bending the laser beam through four right angle turns. The heavy ion driver accelerates singly charged Xe 131 ions to 10 GeV, accumulates and bunches them in 20 storage rings, each of which delivers 13 ns pulses containing 1 kA, and transports the ballistically aimed beams to the target through a pressure of 5×10^{-4} Torr. Neutron backstreaming through the accelerator tubes is prevented by magnetically bending the ion beam into the entry port and capturing the

undeflected neutrons in a beam dump. Pellet injection at 300 m/s is accomplished by a "rail gun" type accelerator; a precision bore tube provides accurate control over trajectory. The reactor cavity is spherical with a 10 m radius and contains two 6.5 m diameter openings on either side of the sphere for driver beam and vacuum system entry. Surface heating of 1.3 MW/m^2 due to x-rays and ions from the pellet explosion is carried away by flowing lithium in circular tubes of HT-9 steel, which constitute the first wall; protection of the first wall is provided by a thin Ta coating on the HT-9 steel. Debris which deposits on the Ta coating is periodically removed by introducing special pellets which vaporize it and collect it in the beam ducts. Neutron energy is captured in flowing lithium, 58 cm thick, directly behind the tubular first wall; the tritium breeding ratio is 1.22. Maintenance and repair procedures for the spherical first wall assembly are compatible with utility requirements of 30 days down annually and/or 4 months down every 5 years. The lithium cooling circuit provides lithium at 369°C to the intermediate heat exchanger; the sodium hot leg is at 363°C resulting in 1000 psia steam which generates electricity with a gross efficiency of 36%. The performance, size and cost of the two power plants were modeled and incorporated into a computer program called ICECAP.

2.0 EXECUTIVE SUMMARY AND CONCLUSIONS

In this study, two different electric power plants for the production of about 1000 MWe which were based on a CO_2 laser driver and on a heavy ion driver have been developed and analyzed. The purposes of this study were: (1) to examine in a self consistent way the technological and institutional problems that need to be confronted and solved in order to produce commercially competitive electricity from an inertial fusion reactor that uses classified pellets, and (2) to compare, on a common basis, the consequences of using two different drivers to initiate the DT fuel pellet explosions. Analytic descriptions of size/performance/cost relationships for each of the subsystems comprising the power plant (see Figure 2-1) have been combined into an overall computer code which models the entire plant. This overall model has been used to conduct trade studies which examine the consequences of varying critical design values around the reference point.

Our design irradiates the pellet from two opposite sides by using drivers which deliver 2 MJ to the pellet at a repetition rate of 10 Hz. The pellets have a gain of 175 and a yield of 350 MJ per shot. Because the laser efficiency at 10% is much lower than the 30% efficiency of heavy ion beams, the net electric power available from the laser plant is about 140 MW less than that from a heavy ion plant. The features of our reactor design are summarized in Table 2-1; the power flow through the two plants is shown in Figures 2-2 and 2-3.

The CO_2 laser delivers 2 MJ of 10.6 μm radiation to the pellet through a cavity pressure of 10^{-1} Torr by combining 108 18.5 kJ beams arranged in 12 beam ducts (6 per side) carrying 9 beams per duct. The nine beams in a given duct are sequentially extracted from a Power Amplifier Module (PAM) over a total period of 1.2 μs in order to achieve the design goal of 10% driver efficiency. These beams are recombined by introducing appropriate mirrors in a laser/mirror hall which equalize optical path length to the target. Entry windows

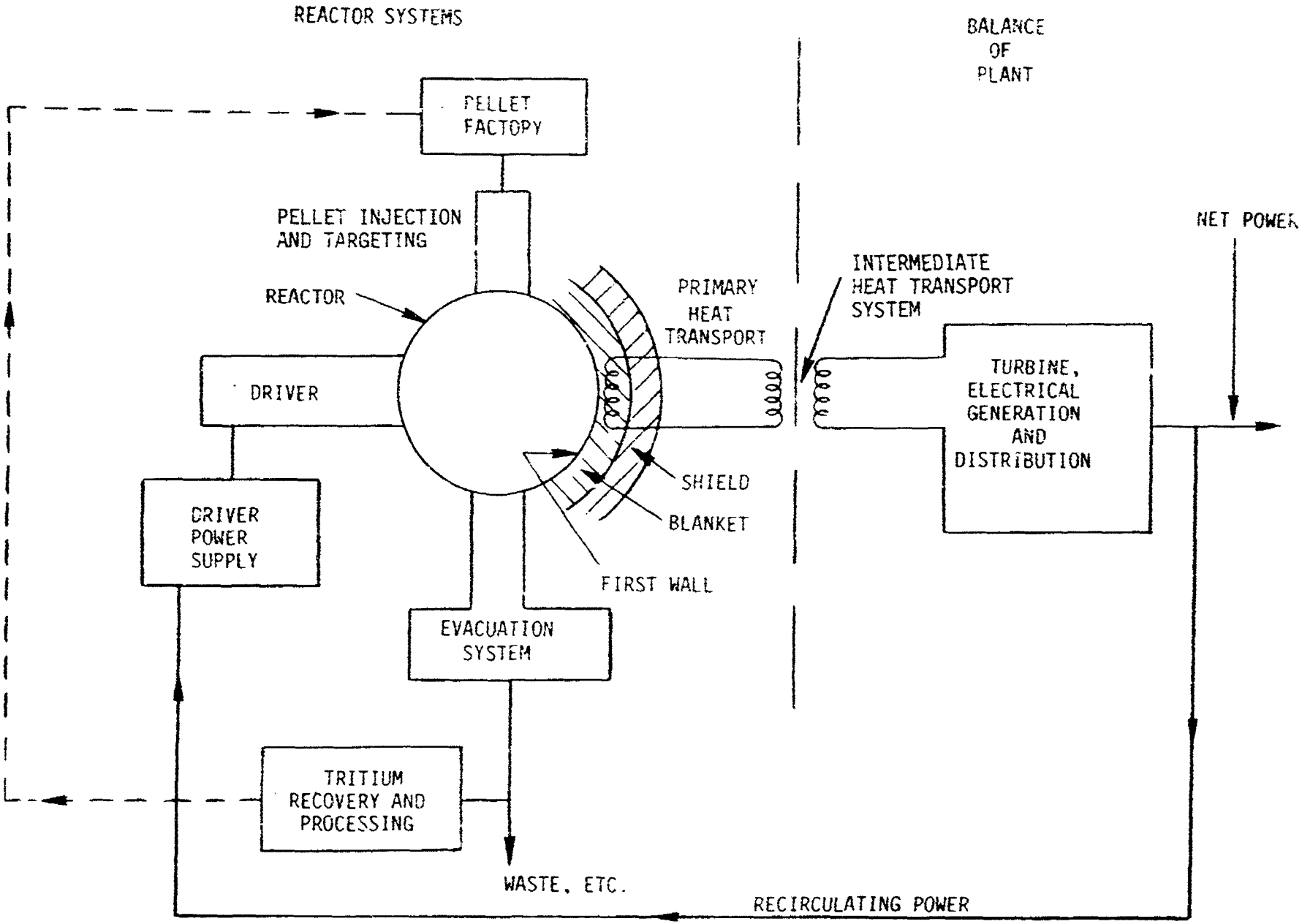

Figure 2-1. Functional Schematic of an Inertial Confinement Fusion Power Plant

TABLE 2-1

ICF ELECTRIC GENERATING PLANT SYSTEM PARAMETERS

	Laser	Heavy Ion
Pellet Thermal Power	3500 MWt	3500 MWt
Driver Energy	2 MJ	2 MJ
Pellet Gain, Q	175	175
Driver Efficiency, η	10%	30%
ηQ	17.5	52.5
Pellet Yield	350 MJ	350 MJ
Rep Rate	10 Hz	10 Hz
Driver Power	200 MWe	67 MWe
Total Blanket Thermal Power	4300 MWt	4300 MWt
Gross Electric Power	1565 MWe	1565 MWe
Net Electric Power	1207 MWe	1346 MWe
Thermal to Net Electric Conversion Efficiency	28.1%	31.3%
Recirculating Fraction	22.9%	14.0%
Cavity Gas Pressure	10^{-1} Torr	5×10^{-4} Torr
Cavity Radius	10 m	10 m
Cavity Shape	Spherical	Spherical
First Wall Configuration	Tubular	Tubular
First Wall Material	HT-9 Steel	HT-9 Steel
First Wall Protective Coating	Ta	Ta
Coolant/Blanket	Liquid Lithium	Liquid Lithium
Tritium Breeding Ratio	> 1.2	> 1.?

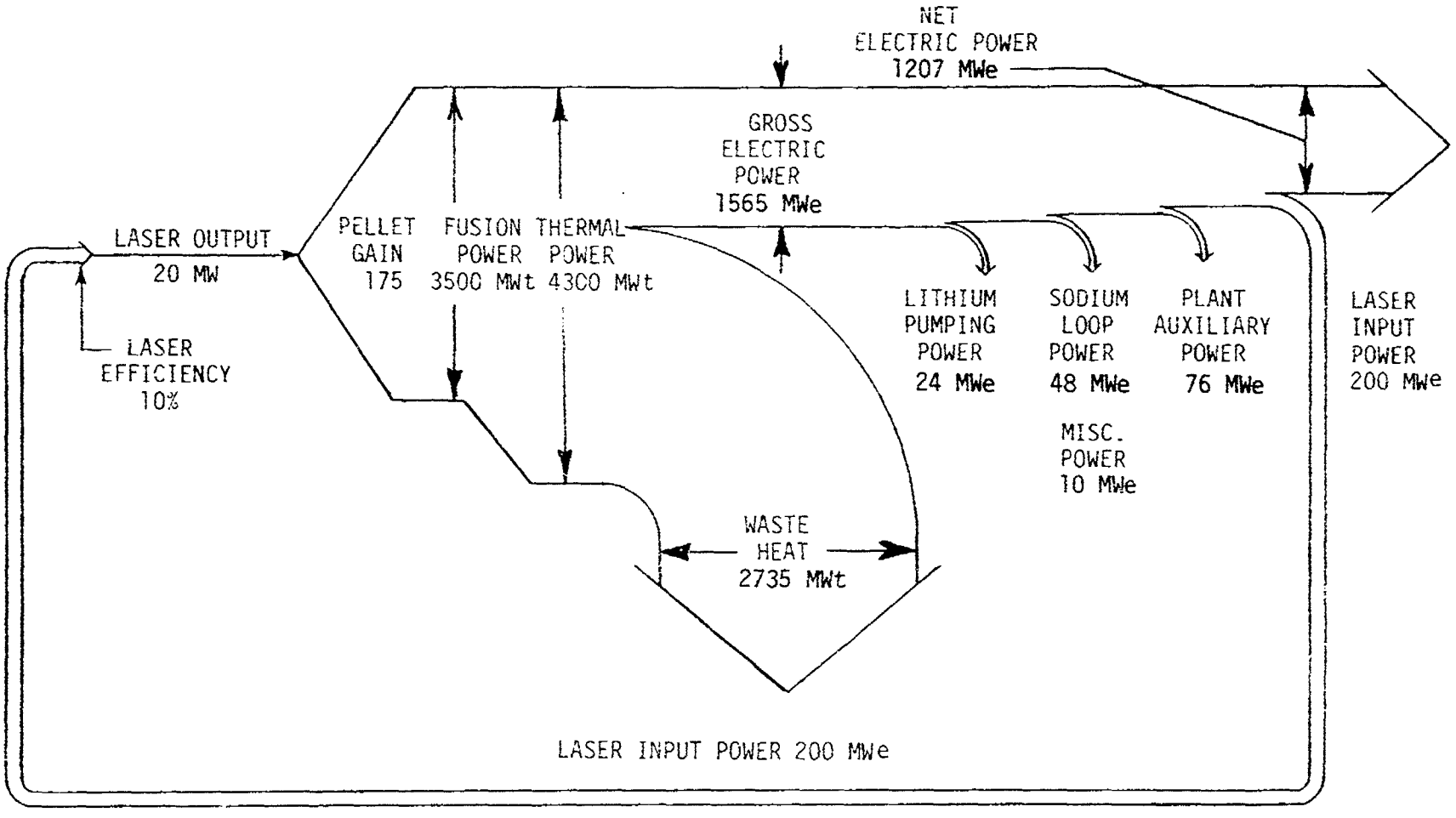

GROSS ELECTRICAL EFFICIENCY = 36.4%
NET ELECTRICAL EFFICIENCY = 28.1%
RECIRCULATING POWER FRACTION = 22.9%

Figure 2-2. Power Flow Diagram for the Reference Laser Fusion Reactor

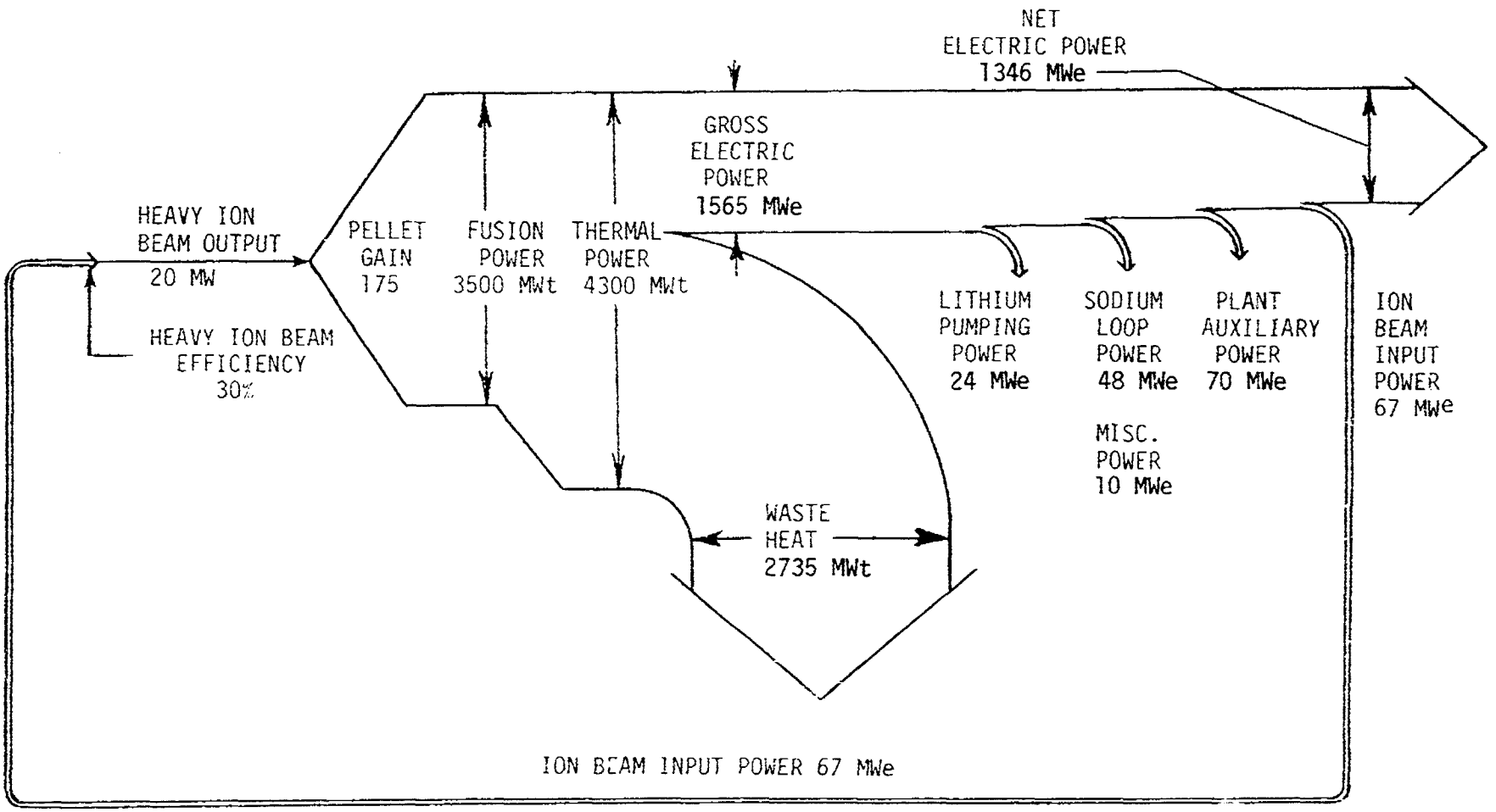

GROSS ELECTRICAL EFFICIENCY = 36.4%

NET ELECTRICAL EFFICIENCY = 31.3%

RECIRCULATING POWER FRACTION = 14.0%

Figure 2-3. Power Flow Diagram for the Reference Heavy Ion Beam Fusion Reactor

are made of salt (NaCl) which provides good transmission at 10.6 μm; however, salt windows are limited to peak fluxes of 3 J/cm^2 for ns pulses and the mechanical strength of flat salt windows limits their aperture to about 100 cm for a one atmosphere pressure differential. This defines the maximum energy per beam to be about 20 kJ. Diffraction laws applied to 10.6 μm radiation require the distance from the final mirror to a 1 mm pellet to be ∿ 30 m. Since the cavity radius is 10 m, the additional length allows the introduction of gas flowing from the final mirror to the cavity to act as a shield against pellet debris, particulate radiation and soft x-rays. To protect the environment against neutron radiation effects, the laser beams are brought from the entry window to the final mirror through four right angle turns in a labyrinth surrounded by shielding material. Additional protection against leaks or fractures of the NaCl windows is afforded by reducing the beam cross sections and passing all nine of them through a single 0.9 m diameter ball valve. The laser/cavity/containment building interface is shown in Figure 2-4.

The heavy ion beam driver accelerates bunches of singly charged Xe 131 ions through a sequence of low beta (v/c) Wideroe linacs up to 800 MeV followed by about 4 km of high beta Alvarez linacs to reach 10 GeV. Each beam goes into a storage ring of radius 113 m which accumulates and compresses the bunches to make 13 ns pulses containing 1 kA each. A total of 20 storage rings generate the 2 MJ pulse. To prevent neutrons from back streaming down the open accelerator tube, the ion beam is bent into the entry port by a 1.2 Tesla bending magnet that is 9 meters long; the neutron energy is absorbed in a neutron dump. A schematic representation of this design is shown in Figure 2-5. Cavity pressure is set at 5×10^{-4} Torr to allow ballistic aiming and transport of the ion beam to the target. Since pressure in the storage rings is set at 10^{-10} Torr to prevent excessive losses due to scattering during the 1 ms storage time, differential pumping is introduced over the distance between storage ring and cavity.

According to current understanding of pellet design, pellets capable of generating the required gain of 175 consist of an inner sphere containing the fuel and final tamper which is concentrically suspended inside an outer sphere containing the ablator and initial tamper. We have devised a novel method for

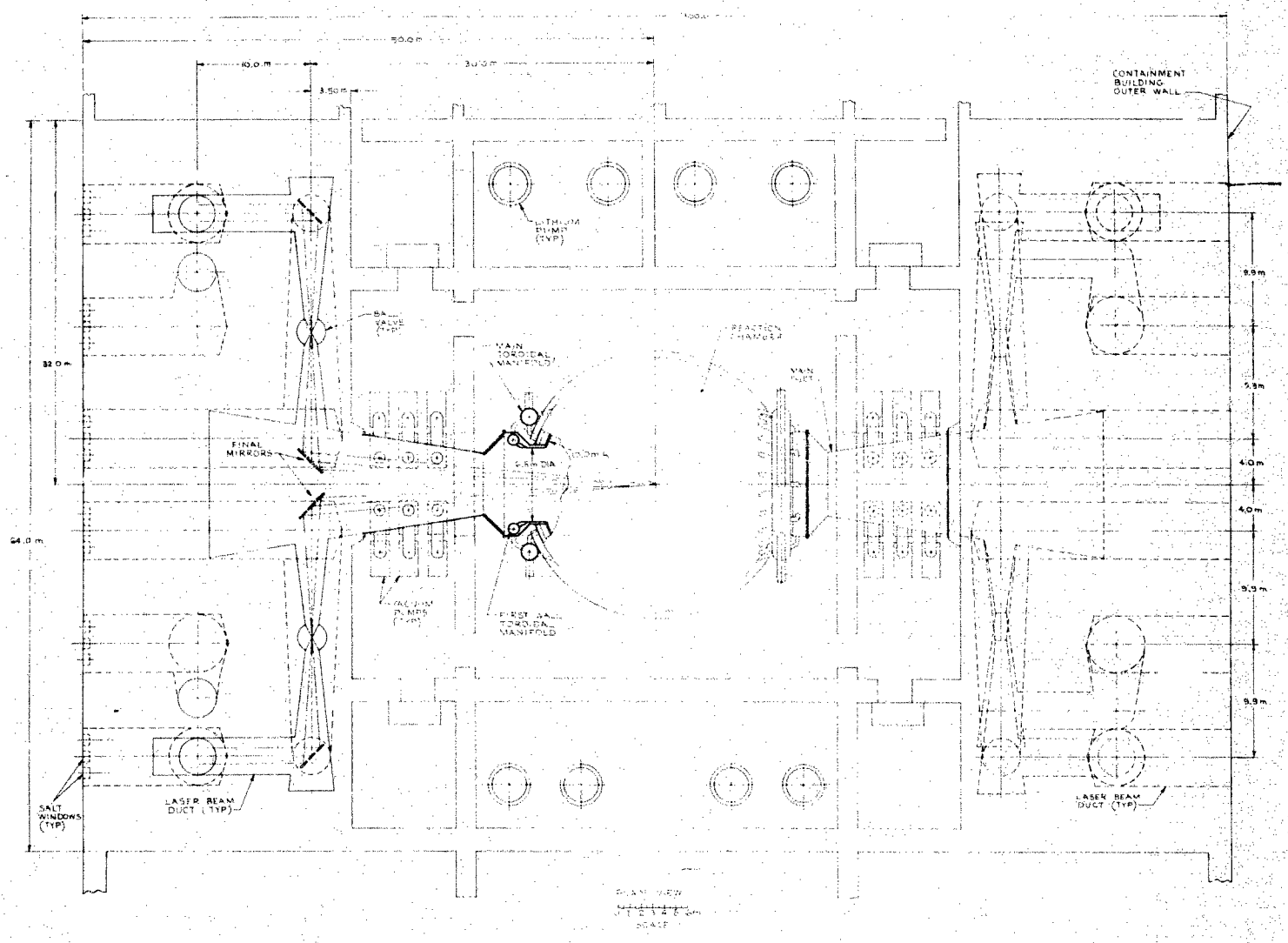

Figure 2-4. Plan View of the Reactor Building for the Laser Driver Concept

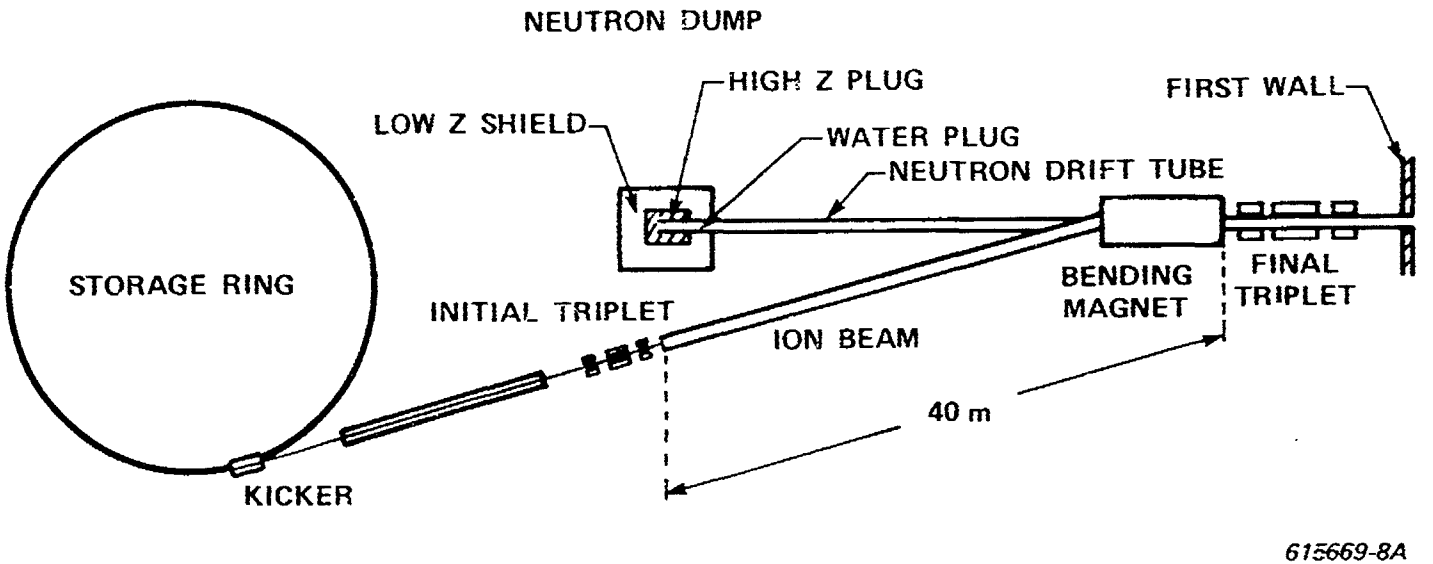

Figure 2-5. Schematic Illustration of the Interfaces Between the Storage Ring, Focusing Triplet, Bending Magnet and Reactor Chamber in a Heavy Ion Driven ICF Power Plant

suspending the inner sphere accurately and also maintaining the concentricity during injection into the reaction cavity. The essential concept is shown in Figure 2-6; it consists of an array of fibers in the two halves of the outer sphere which, when joined together, provide a confining nest for the inner sphere.

Pellets must be injected with velocity greater than 100 m/s in order to traverse the 10 m to the target region in a time small compared to the interval between pulses. A novel injection system has been conceived which provides extremely accurate control over the pellet velocity and direction by utilizing a linear synchronous motor to accelerate a sabot which carries the pellet in the vertically upwards direction. The pellet is separated from the sabot by introducing a coil near the end of the acceleration track which decelerates the sabot; the pellet continues through a precision bore tube at the final velocity while the sabot is captured and returned. This scheme maintains pellet cryogenic temperatures, does not introduce gas into the cavity and is compatible with high speed, repeated operation.

Debris from the pellet explosions consists of non-condensible gases (H, D, T, He, O, CO_2, etc.) and the condensible Ta. The vacuum system is designed to pump out the excess gas created by each explosion in less than 100 ms; total required pumping speed is 10^5 ℓ/s for the laser case, and 10^6 ℓ/s for the heavy ion beam case. Condensibles deposit about 95% of their mass on the inner surface of the first wall after each shot and about 5% in the major ducts on either side of the reaction chamber. The Ta deposit adds to the Ta which coats the first wall; it is removed by intermittently vaporizing it and allowing 5% of this vapor to redeposit outside the chamber on the duct walls. Vaporization is achieved by inserting a pellet into the firing system at preprogrammed intervals whose x-ray yield would cause the Ta to melt and vaporize. Final removal of the Ta deposit in the vacuum ducts is incorporated in the regular maintenance schedule.

The essential engineering problem to be solved in an ICF reaction chamber is to design a first wall which can carry away the steady state average surface

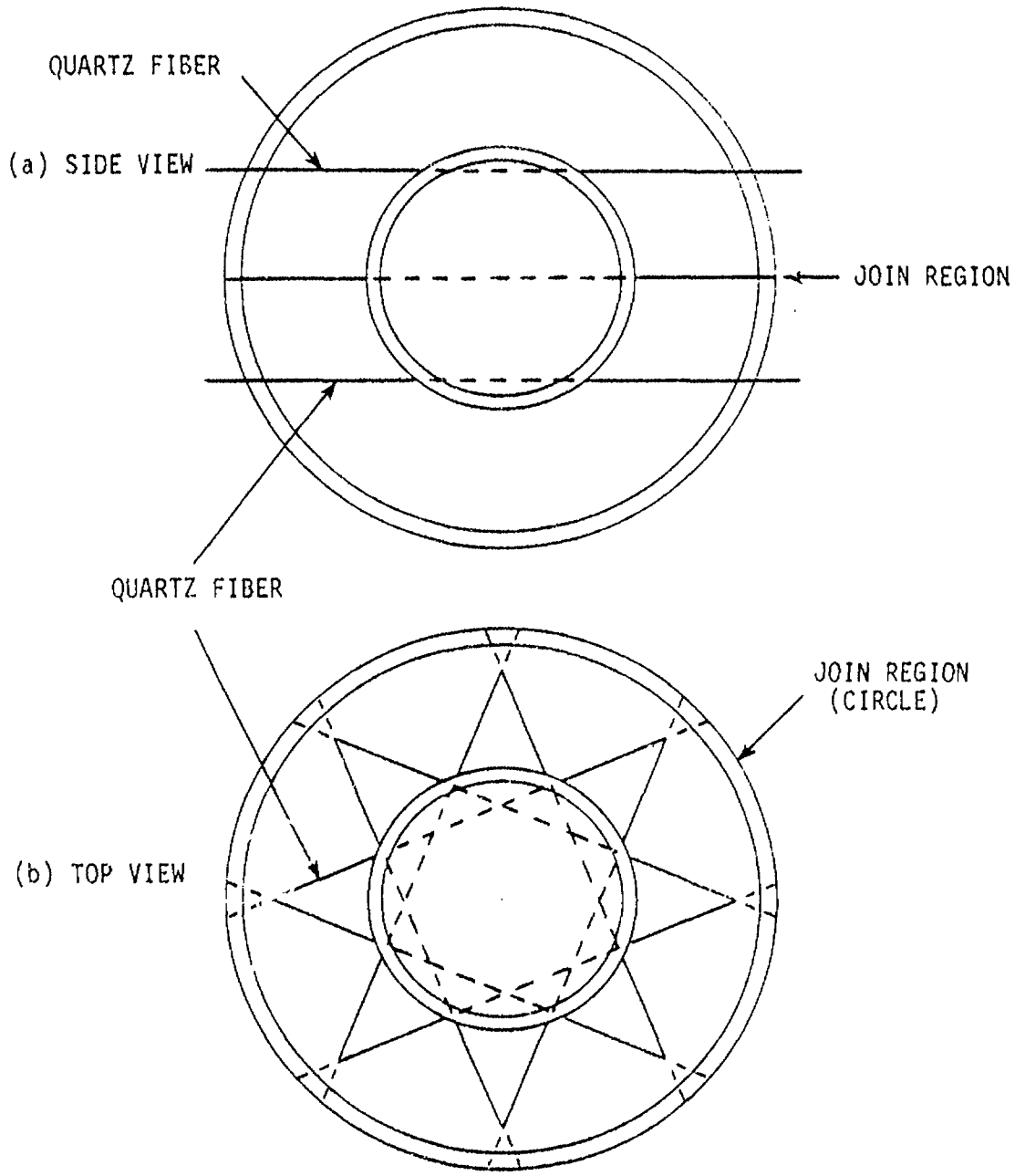

Figure 2-6. Suspension System for the Shell Within a Shell Pellet — (a) Side View, (b) Top View

heat and at the same time survive the transient temperature increase generated by x-rays and ions from the pellet explosion. Conditions for transmission of the laser beam and the ion beam to the target require cavity pressure to be $\leq 10^{-1}$ Torr and $\leq 5 \times 10^{-4}$ Torr respectively. These pressures were chosen as reference points in our design. While the presence of 10^{-1} Torr background gas in the laser cavity does offer some protection to the first wall against low energy x-rays and ions, it is not effective against the high energy x-rays and ions expected from high gain pellets. Thus, our design for the first wall is the same for both the laser and the ion beam drivers.

Our solution to the problem of handling both the steady state and the transient heat is to divide the functions of the first wall design. Thin steel tubes carrying flowing liquid lithium remove the steady surface heat while a metallic layer, whose melting temperature is above the peak temperature transient caused by the x-rays, protects the first wall surface of the tubes (facing the explosion). This coating buffers the steel tube from the large temperature transients which might otherwise destroy it due to thermal stress cyclic fatigue. Examination of the interaction between pellet heavy metal debris and first wall showed that, no matter what the original first wall material was, the rate of condensible metal deposition on the first wall was so great that the first wall coating material must be considered to be the same as the pellet metal. The choice of heavy metal for the pellet therefore becomes a joint decision of the pellet designer and the reactor designer. Candidate heavy metals were reviewed and Ta was selected because of its high melting temperature, ease of handling, cost, etc. The viability of the Ta layer was verified by computer calculations, including results from the CHART D code, which showed that: (1) the temperature of the Ta surface was always below its melting point, (2) internal stresses were not sufficient to cause spallation, and (3) the temperature increase at the Ta-steel interface was negligible.

This coated thin tube wall design handles fusion thermal power of 3500 MWt in a spherical chamber at a distance 10 m from the explosion. Because the x-rays and ions contain 45% of the fusion power and are absorbed on the surface of the wall, the surface heat flux is about 1.3 MW/m^2; this is removed by liquid lithium flowing through the tubes with a maximum velocity

of 18 m/s. The neutrons, on the other hand, carry 55% of the power and are absorbed in the first wall coolant and in the volume of the 58 cm thick flowing liquid lithium blanket situated behind the tubular first wall. This arrangement is shown in Figure 2-7. Tritium breeding ratio for this configuration is about 1.22.

Maintenance of the reaction chamber is based on removing the complete first wall assembly and replacing it with a new or refurbished first wall assembly during an annual planned down time of about one month. The time required to perform the sequence of operations is estimated to be about 27 days and contains the following procedures: removal of components and equipment which block access; draining of the coolant; uncoupling of any connections to upper half of external spherical shell; removal of upper outer shell from lower shell; uncoupling of inner spherical shell from its support; lifting, removing and placing inner spherical shell in a hot cell for cooldown. This process is summarized in Figure 2-8. Since the entire structure is radioactive, these operations are performed remotely.

The connection between the reactor and the balance of the plant is through the lithium cooling circuit which provides lithium at 369°C to the intermediate heat exchanger (liquid sodium). The sodium hot leg temperature is 363°C, resulting in superheated steam at 358°C and with pressure of 7.24 MPa (1050 psia) which is adequate to generate electricity with 36% efficiency. The major features of the balance of plant are the heat transport, steam generator and turbine generator systems. These must be housed in containment buildings to ensure the safety of the environment against possible accident. Major buildings in the balance of plant are the Reactor Building, Hot Cell Facility Building, Steam Generator Building, Turbine Building, Pellet Factory Building, Waste Disposal Building, Control Building, Emergency Generator and Standby Generator Building and Argon Storage Building.

The computer code which models the size/performance/cost of these two ICF power plants is called ICECAP, Inertial Confinement Energy, Cost and Performance Code. ICECAP was constructed such that the component models (beam

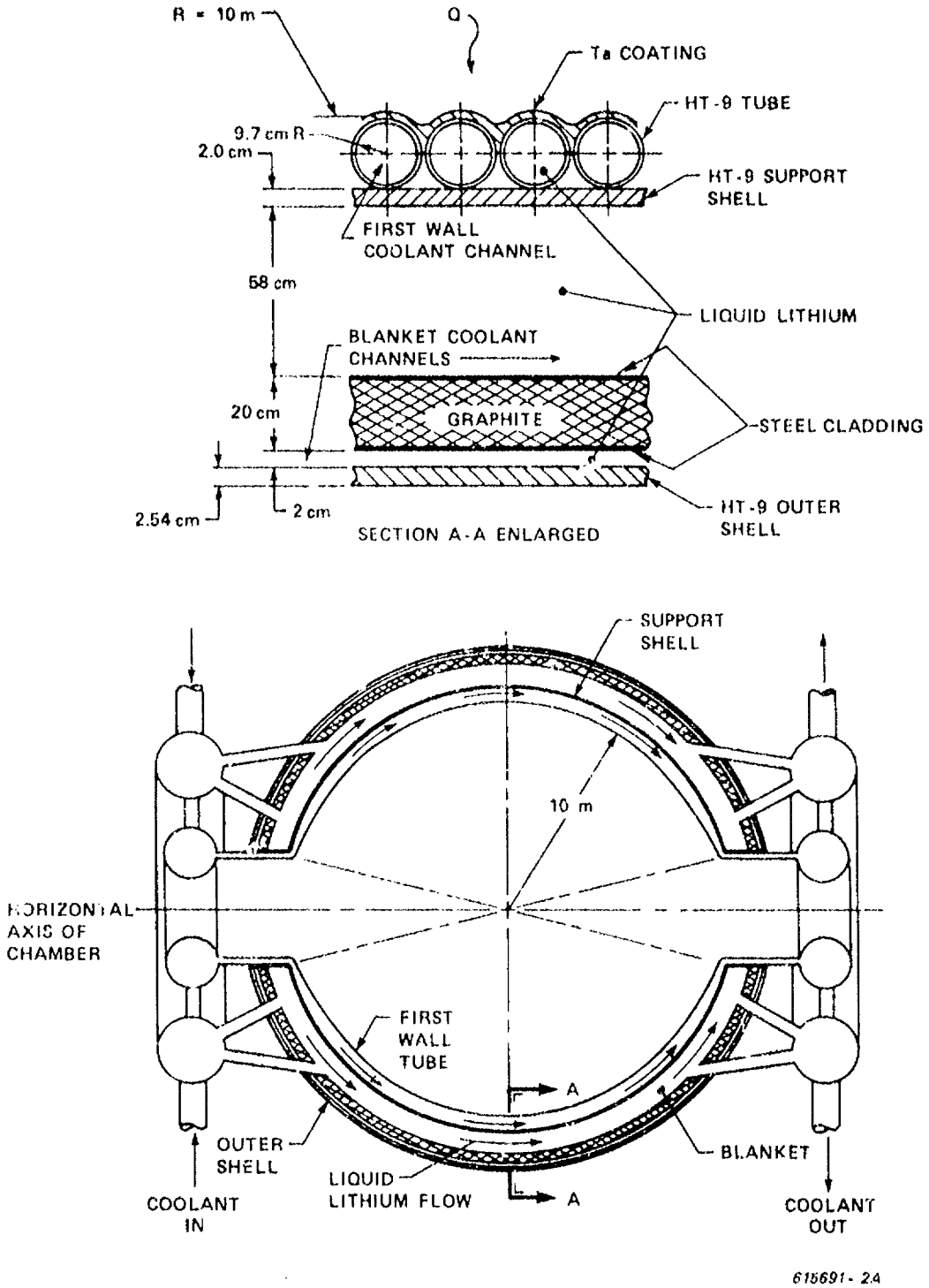

Figure 2-7. Schematic Representation of the Tubular First Wall and Blanket Concept

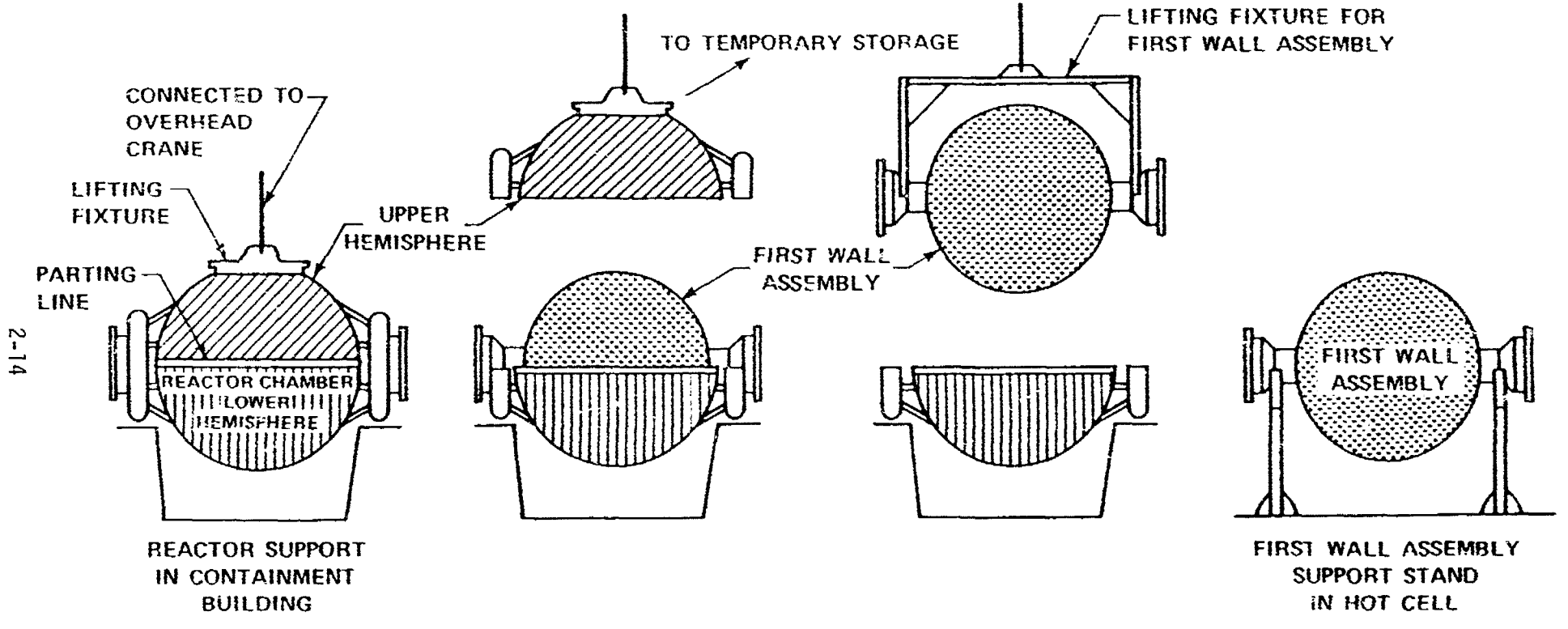

Figure 2-8. Sequence of Operations for the Maintenance of the First Wall

driver, blanket assembly, buildings/structures/equipment, etc.) are clustered into five groups. The pellet/plant data (pellet mass, repetition rate, cavity radius, plant availability factor, etc.) is read/calculated before the first component algorithm is called and the final calculations and output provide summary data for use in trade studies. The five clusters group the component systems as follows: (1) fusion support systems (drivers, pellet systems, and vacuum systems), (2) mechanical/thermal systems (first wall, blanket, shield, primary coolant loops), (3) power supply systems (for drivers, coolant pumping, distribution, etc.), (4) turbine plant systems (turbine, steam generator, heat rejection), and (5) facilities systems (buildings, controls, remote maintenance, etc.). The pellet/plant data is a set of internally self-consistent parameters which is used in each of the component models allowing for a single set of base assumptions in sizing and costing all subsystems. Various coding procedures are used to improve the user's ability to follow the FORTRAN as well as to identify the calculational results which are provided in the output print.

Trade studies were performed using ICECAP to investigate the impact on relative cost of electricity (COE) and on net electrical power delivered to the grid (P_{net}) of varying the following parameters one at a time: driver efficiency, rep rate, driver energy on target and cavity radius. Because our reference design operates at the maximum surface heat load that can be handled by our heat removal concept, parameter variations that led to heat loads greater than in the reference design were not allowed. Thus, rep rate and driver energy were varied below the reference values and cavity radius was varied above the reference value. Some interesting preliminary results for both laser and heavy ion driven reactors are listed below:

- COE drops by about 50% as rep rate increases from 5 to 10 Hz.
- COE increases by 5% as cavity radius increases from 10 to 20 m.
- COE decreases by factors of about 3 as driver energy increases from 1 to 2 MJ.

CONCLUSIONS

The major conclusions developed from this study are:

1. Protecting the first wall against temperature transients due to x-rays by using a Ta coating on steel appears to be viable and very attractive. This is a dry wall concept and is therefore compatible with cavity atmosphere requirements for all drivers. By choosing Ta, the coating material becomes the same as the heavy element in the pellet, and problems of incompatibility are removed.

2. Removal of the steady state heat load due to x-rays and ions is the limiting factor in thermal and mechanical design of the reaction chamber. The reference design generates 1.3 MW/m^2 which must be removed by rapidly flowing lithium; our design velocity of $\sim$ 20 m/s for this function is the maximum that is considered to be prudent in the absence of specific information on heat transfer coefficients and corrosion rates at these velocities.

3. Increasing cavity radius beyond 10 m will relax thermal constraints at little increase in cost of electricity but mechanical constraints may begin to emerge at larger sizes.

4. The penalty of the 10% laser efficiency, as compared to the 30% efficiency assumed for the heavy ion driver, is about 140 MWe. At today's rates, and assuming 50% availability, this represents a revenue of about \$30M/year. However, this is not the only factor considered by utilities in choosing a power source for system expansion.

5. Power source choice by utilities is the result of minimizing the future cost of electricity; factors considered are: capital and construction cost, operating and maintenance cost, reliability, environmental and licensing impact, safety and size of unit.

6. Capital cost for the heavy ion driven reactor is greater than for the laser driven reactor; both costs are about the same as for magnetic fusion reactors. The cost for the heavy ion accelerator is based on one-of-a-kind high energy physics machines in which there has been no effort to design components or systems for reduced cost. The costs for the CO_2 laser are based on current experience at LASL so the error associated with this estimate is lower than for the heavy ion driver.

7. Injection of the pellet can be done accurately, repeatedly and at 300 m/s by using the linear synchronous motor "rail gun" concept.

8. Mass production of double shell pellets is made possible by using two novel concepts: fabrication of the spheres using a porous ceramic called MODOX, and concentrically suspending one sphere inside the other on a nest of crossed fibers.

9. It is possible to design a tritium handling system which reduces environmental impact to 1 μCi/day and which minimizes proliferation problems. Concepts incorporated into the design include: double wall, counter flushing pipes; inert atmosphere at reduced pressure in containment buildings; storage as a solid.

10. The tantalum processing system is self-contained and has no environmental impact.

11. Radioactive tantalum will have to be stored for 4.5 years before it can be chemically processed; depending on the pellet design, this represents up to $25M worth of tantalum.

12. Planned maintenance operations can be made compatible with time available during utility down times. The structures must be designed in advance to accommodate the operational steps and special machines must be available.

13. Liquid lithium can be handled safely by using dry inert gas atmospheres and steel cover plates on floor and walls near lithium concentrations, removing crack causing stresses from pipes carrying lithium and surrounding lithium pumps with steel lined catch basins.

14. Radiation levels at the driver beam-reaction chamber interface can be made safe for personnel by proper combination of shielding and right angle bend labyrinths.

15. The ICECAP code provides a valuable tool for studying and comparing various ICF power plant designs and costs.

3.0 INTRODUCTION

The objectives of the effort performed under DOE Contract DE-AC08-79-DP40086 were as follows:

- Identification of key plant design requirements and design solutions necessary to allow the ICF plant to be used by utilities in anticipated electric grids
- Development of a conceptual design of the subsystems which make up ICF power plants based on two driver technologies and incorporating classified pellet information
- Development of a coupled ICF power plant performance/cost/economic assessment systems model sufficiently flexible to accommodate the major approaches and options for subsystems and component design
- A systematic assessment by means of trade-off, sensitivity, and parametric studies of the effects of key design features on power production and plant capital and operating costs
- Identification of Research, Development and Demonstration (RD&D) needs for the commercialization of ICF

In order to assure that the conceptual designs and the cost estimates developed in the study would be realistic, feasible and responsive to utility and government requirements, Westinghouse joined its knowledge and experience in fusion driver design and technology and fission reactor power plant engineering with the knowledge and experience of Stone and Webster, Inc. in architectural engineering and with the utility perspective provided by Public Service Electric and Gas Research Corporation. These organizations contributed significantly to the effort and to this Final Report.

The original contract terminated April 30, 1980; however, the contract was extended to February 28, 1981 at no cost to the government.

This volume is the first of two volumes which contain the unclas final report of work done under the contract. A separate volume contains a classified report of work done under this contract.

TECHNICAL ISSUES

A major long range goal of the United States Inertial Confinement Fusion (ICF) program is the successful development and demonstration of an ICF system for the generation of electrical power which is economical and competitive with other energy sources and can be successfully integrated into existing or projected commercial utility systems. A number of vigorous experimental programs are in progress or planned, and these are expected to provide definitive answers to many of the key physics feasibility questions associated with the various ICF options, particularly the demonstration of energetic breakeven at the beam-target level. If scientific breakeven is achieved in the 1980s, as expected, this could enable construction of an Experimental Test Facility (ETF) in the 1990s.

In order to produce an ICF reactor suitable for ultimate power production in a utility system, attention must be given to defining and solving technological and engineering problems in such a facility. The current state-of-knowledge in ICF is such that the physics of the processes, and therefore, the engineering design requirements, are not known with certainty and are changing rapidly; as a consequence, a wide range of subsystem technologies, design options, and performance parameters has been identified for ICF reactor systems. For example, three main driver technologies are under active consideration for use in the commercial fusion reactor; lasers, light ion beams, and heavy ion beams. And, in response to the range of expected performance levels attributed to various combinations of drivers, targets, and operating scenarios, a number of design approaches have been identified for the first wall cavity system or reaction chamber.

A clear requirement therefore exists for a systematic means for assessing the impact of the results of these ongoing experimental programs, and to provide guidance for the technical direction and priority of future programs which is consistent with the overall goal of the development of feasible central station

electric power plants based on ICF. If, as is likely, all three driver technologies demonstrate breakeven and can be extrapolated to commercial size, the commercial attractiveness will no longer be limited by driver-pellet technology; rather, issues such as engineering feasibility, construction and operation costs, safety, reliability, maintainability, and environmental impact will be of prime importance. The nation will need detailed appreciation of the consequences of the course leading to commercialization for each of the three driver systems. The first step in the development of this information must be design studies to identify and define potential concepts and problems so that appropriate solutions can be developed and evaluated. This contract effort is a contribution to that program.

Some of the major issues that need to be addressed in designing an ICF power plant are:

- Design first wall to withstand severe temperature transients
- Removal of surface heat deposited on first wall by ions and x-rays from the pellet explosion
- Accurate, repeatable injection of pellets
- Mass production of complicated pellets
- Design for reliable and continuous supply of electricity
- Isolation of radioactive sources from environment
- Design for minimum downtime due to planned maintenance/repair operations
- Failure and accident control and contingency
- Radwaste handling

Although the concepts that will be identified for the reactor systems in the present study may not be present in the ultimate design for a commercial reactor operating sometime after 2000, these concepts will have had to satisfy the joint requirements of technical feasibility and compatibility with the overall objective of acceptability by utilities. As such, they provide a realistic and acceptable basis for a plant design which will allow the identification of research and development efforts necessary to ensure the availability of key technologies in the 1990 time frame.

The technical approach used to develop the conceptual designs of ICF power plants is based on the recognition that the plant can be naturally divided into two major parts as shown in Figure 3-1. One part, the reactor system, consists of the following subsystems:

- Driver and beam transport
- Driver power supply
- Pellet factory
- Pellet injection and targeting
- Reactor, which includes cavity first wall and its protection system, blanket and shield, and heat removal system
- Evacuation system
- Tritium recovery and radwaste processing system

The second part, the balance of plant, consists of the steam and turbine generators and associated equipment, facilities, and structure necessary to produce and distribute the electrical power. The design of the balance of plant does not require access to classified data for successful execution, but it does need specific requirements information from the reactor system design. In general, the structures and systems can be designed from well established procedures based on fission reactor experience once these requirements have been specified.

Design effort for the reactor subsystems concentrated on defining two subsystems; the reaction chamber itself (especially the first wall and its protection and heat removal systems), and the interface between the two drivers and the reaction chamber. This approach was based on the recognition that driver and pellet design and development was a special responsibility of the national labs, while reaction chamber design was an area of special expertise in Westinghouse. However, enough effort was spent on designing the drivers and pellets to understand the implications of interface design solutions on the drivers and pellets themselves.

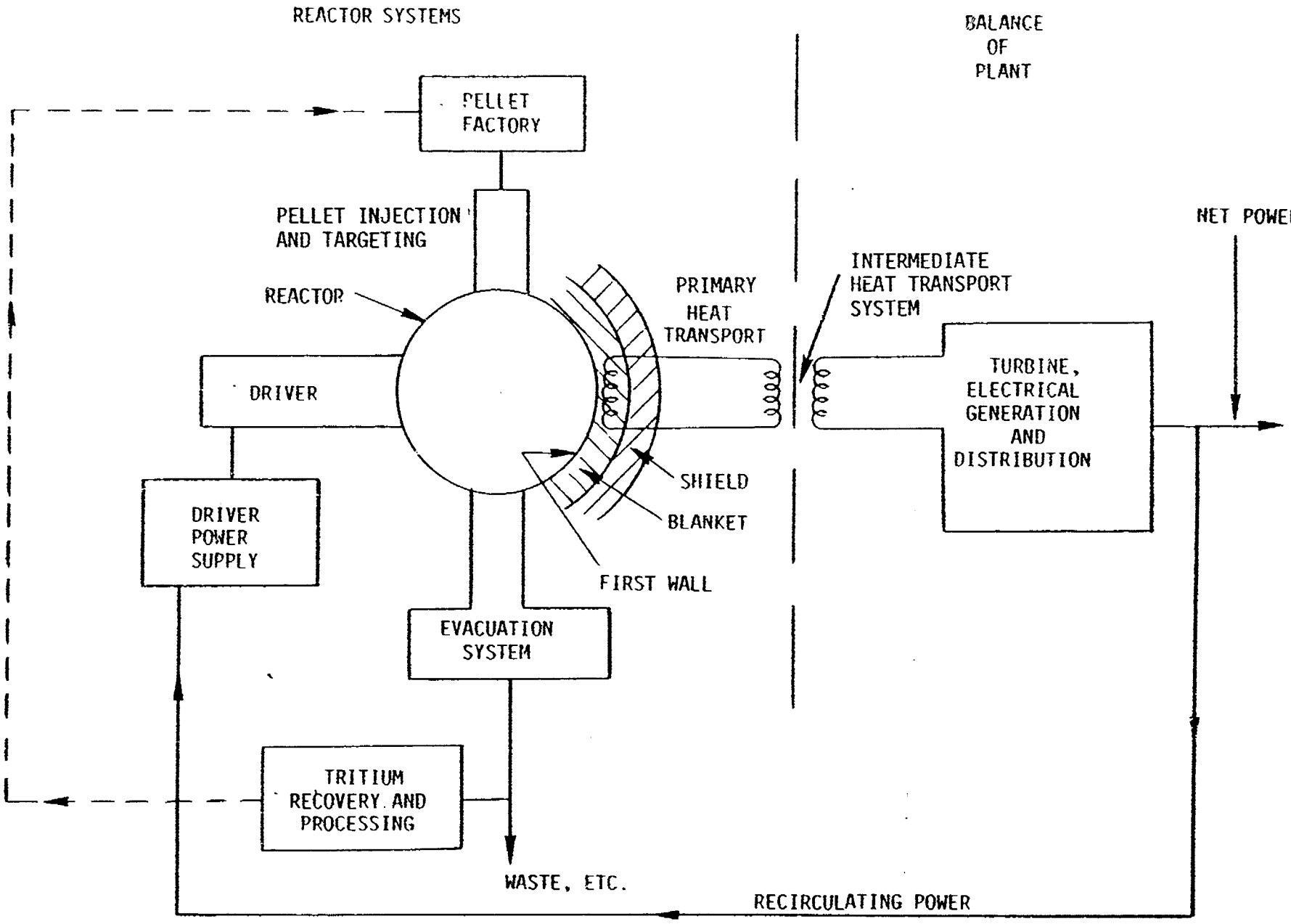

Figure 3-1. Functional Schematic of an Inertial Confinement Fusion Power Plant

DRIVER SELECTION

In order to examine and compare the consequences on the power plant of using various drivers, two different drivers were selected for study, based on the following criteria:

- Different cavity requirements
- One laser, one particle beam
- Ability to develop credible design in the shortest time
- Potential cost

Table 3-1 summarizes the analysis of the two laser candidates (CO_2 and KrF) of the two particle beam candidates (light ion and heavy ion); it identifies our choices for this study as the CO_2 laser and the heavy ion beam.

TABLE 3-1

COMPARISON OF FEATURES DESCRIBING
FOUR CANDIDATE DRIVERS FOR AN ICF POWER PLANT

	Laser Systems		Particle Beam Systems	
	CO_2	KrF	Light Ion	Heavy Ion
Available Data Base	Present	Absent	Present	Present
Cavity Conditions	<0.1 Torr	<0.1 Torr	10-100 Torr	10^{-4} Torr
Generic Driver Design	Yes	Yes	No	No
1 MJ Driver Cost	∿$500M	∿$500M	∿$50M	∿$1000M
1 GWe Plant Cost	∿$3000M	∿$3000M	∿$3000M	∿$3000M
Basic Uncertainties	Pellet Coupling	Scaleup of Laser; Pulse Compression	Beam Transport & Stability	Demonstrate System Performance
Final Choice	✓			✓

In analyzing the criteria for the laser candidates, we note that a large 10 kJ CO_2 system is presently operating and that a 100 kJ system is under construction at LASL, while the KrF laser is at the 10J level in development at LLL. However, both require <0.1 Torr gas pressure in the cavity and use electron beam excitation, flowing gas amplifiers and multiple pass mirror systems to shorten the pulse, increase the efficiency or equalize optical path lengths. The driver and plant costs are estimated to be very similar, given the uncertainties associated with making cost projections some 40 years into the future. Our final decision to choose the CO_2 laser was based on the absence of available data for a large KrF system and especially on the uncertainty as to which pulse compression scheme would be used.

The particle beam candidates are very different from each other. While both have a large data base to draw from, they are based on very different technologies. The light ion beam is accelerated electrostatically, while the heavy ion beam uses rf synchronized with the particle bundle velocity. Because the light ions carry low kinetic energy, the required power on the target necessary for implosion is achieved by using multi-kA magnitude currents. To prevent space charge from blowing up the beam, neutralization by electron capture as the beam passes through high pressure gas is necessary. On the other hand, the heavy ions can be focused to achieve the required power on target but must be transported through a good vacuum. Another major difference between the two concepts is the cost; light ions can be accelerated very inexpensively, while heavy ions are the most expensive of the four candidates. Our final decision to choose the heavy ion beam was based on the availability of straightforward concepts for ballistic focusing, while uncertainties remained as to the method by which the light ion beam would propagate repeatedly over several meters through the high pressure gas.

It must be stressed that our choices in no way represent a judgment as to the driver that will utimately be selected by DOE for use in a Single Pulse Test Facility (SPTF) or in an ETF. Future experimental results must be the basis for that choice.

CONCEPTUAL DESIGN APPROACH

In performing the conceptual design of a commercial power plant, operating some 40 years into the future, it was essential to assume that the drivers we had selected and their pellets had successfully demonstrated high gain operation at rates from 1 to 20 Hz. Furthermore, the overall design effort must optimistically extrapolate today's capabilities and costs. Within the limitations of available time and money, the goal of the effort was to develop a credible and viable conceptual design; however, in doing this, not all aspects of the design could be investigated, iteration within the design was limited to the most important issues, and optimization and design improvements were not undertaken. A further important element in the design approach was the early and continued incorporation of the utility point of view.

UTILITY REQUIREMENTS

Ideally, a utility needs an abundant fuel source, and a technology which is safe and clean and available at a reasonable cost with a plant potential capacity and reliability that are attractive. The siting and maintenance requirements of a generating plant using this technology should also be reasonable. There are other criteria which, if satisfied, would make the energy source ideal; but realistically, all that commercialization of a new energy source requires is that it be competitive with other available technologies.

Table 3-2 contains the principal parameters used to identify basic utility needs. It should be recognized that most of the parameters on this list can be traded off against each other. Ultimately, the final deployment decision for an ICF power plant, assuming the technological requirements can be met, will be based upon the cost of electricity comparison with cost of electricity of competing technologies.

The economic considerations are primary and will be treated in Chapter 8. The most significant remaining parameters are unit size, availability/reliability, and environmental impact. These will be discussed in the following paragraphs.

TABLE 3-2

PRINCIPAL PARAMETERS THAT IDENTIFY BASIC UTILITY CONCERNS

- Unit size
- Availability/reliability
- Site
- Safety
- Environmental impact
- Operation and maintenance
- Economics/finance
- Material availability
- Public acceptance
- Constructibility
- Lead time
- Plant electrical characteristics

Unit size refers to the MW electric power plant rating. The first step in a generating expansion study is to evaluate unit sizes and types, i.e., base load, intermediate load, or peak load types, that are needed to provide the necessary increase in system capacity. In general, the evaluations have shown that adding large, base load, units tends to increase reserve requirements because of the negative impact of the larger units on system reliability. However, economics of scale result in lower unit costs for larger units. For overall economy, the tradeoffs must be evaluated. Intermediate load and peak load units are used to intermittently supplement the base load units; they have smaller capacity than the base load units and also are required to be much cheaper, since they are not in full time use. The ICF reactor appears to be most appropriate for base load operation. Since the average size of base load units currently being installed on utility systems is approximately 1000 MWe, this size was selected as the reference size for the ICF power plant.

Availability is the fraction of time a unit is capable of producing power and considers time losses from scheduled maintenance, inspections, refueling and forced outages.

If possible, all generation capability should be available during peak load times. This means that maintenance during winter and summer peak times should be avoided and should be scheduled for off peak times like the fall or spring on an annual basis. Existing generating units are typically out of service for three to eight weeks each year for routine maintenance. Major maintenance on the turbine generator system is required approximately every five years and the unit may be out for as long as 16 weeks. Consequently, our design goal was to perform first wall changes or driver maintenance at the same time as routine annual or turbine generator maintenance.

The utility requirements in the area of environment and licensing are the most complex of all the parameters and involve judgements which in turn impact other parameters of the plant. Regulations defining the degree to which the environment may be changed by power plants result from the many laws passed by Congress over the last 10 years. The laws include the following:

- NEPA
- Coastal Zone Management Act
- Clean Water Act
- Clean Air Act
- Resource Conservation and Recovery Act
- Power Plant and Industrial Fuel Use Act
- OSHA
- Toxic Substances Control Act

These regulations provide the basis for utility acceptance of a given power plant design. It is anticipated that these limits will become more restrictive over the next 40 years as resources, space, and environmental flexibility get used up. Thus, designs performed in 1980 for power plants for the 2020 time frame must be sensitive to the anticipated stricter regulations.

A more complete set of utility requirements has been prepared as part of the Electric Power Research Institute's (EPRI's) Utility Requirements and Criteria for Fusion Options Project (RFP 1413). The project which is being carried out by Burns and Roe, Inc., Public Service Electric and Gas (PSE&G) and Northeast Utilities, has as its objective the development of a methodology to select the fusion options from those that, if successfully developed, will best satisfy the utility needs. Table 3-3, which is being included by special permission from EPRI, lists the dominant utility issues and rates them on a 0-5 scale of importance.

ORGANIZATION OF FINAL UNCLASSIFIED REPORT

The following chapters contain the complete technical report of our efforts in performing the design study of two commercial ICF power plants. Chapter 4, Plant Descriptions, is intended to provide the general interest reader with an understanding of the design and operation of each subsystem that makes up the plant. More detailed, technical analysis is found in Chapter 5.

TABLE 3-3

RELATIVE RANKINGS OF VARIOUS UTILITY REQUIREMENTS

Utility Requirement	Ranking of Importance
A. UTILITY PLANNING AND FINANCE	
1. Plant Capital Cost	5*
2. Plant O&M and Fuel Costs	3
3. Forced Outage Rate	4
4. Planned Outage Rate	4
5. Plant Life	3
6. Plant Construction Time	4
7. Financial Liability	5
8. Unit Rating	2
B. SAFETY, SITING AND LICENSING	
1. Plant Efficiency	0
2. Plant Safety	5
3. Dependence on Other Systems	0
4. Flexibility of Siting	4
5. Wast Handling and Disposal	4
6. Decommissioning	3
7. Licensability	5
8. Weapons Proliferation	3
C. UTILITY OPERATIONS	
1. Plant Operating Requirements	4
2. Plant Maintenance Requirements	4
3. Electrical Performance	4
4. Capability for Load Change	2
5. Part Load Efficiency	2
6. Minimum Load	2
7. Startup Power Requirements	3
D. MANUFACTURING AND RESOURCES	
1. Hardware Materials Availability	4
2. Industrial Base	4
3. Natural Resource Requirements	0
4. Fuel and Fertile Material Available	4

*Notes: Meaning	Code
Unimportant	0
Slightly Important	1
Moderately Important	2
Important	3
Very Important	4
Vital	5

In Chapter 4, the designer of each subsystem provides, as far as is possible, four kinds of information: 1) the functions or general purposes of the subsystem; 2) the design requirements on the system, that is, a quantitative statement of what the system has to do; 3) a description of the subsystem in words, tables and drawings; and finally, 4) a description of what the system does when the reactor is in operation. Because we have performed a design for two beam driven reactors, Chapter 4 contains two major sections; Section 4.1 - CO_2 Laser Driven Design, and Section 4.2 - Heavy Ion Beam Driven Design. Within each of these major sections, however, the subsystem descriptions are presented according to the above outline. In some cases, the design for a subsystem in the Heavy Ion Beam Driven System is the same as that for the Laser Driven System; rather than duplicate the discussion in Section 4.1, the authors refer the reader to it at the appropriate place in Section 4.2.

Chapter 5 provides the technical justification for the design choices embodied in the final design described in Chapter 4; it is intended for the specialist. As in Chapter 4, Chapter 5 contains two main sections; Section 5.1 - CO_2 Laser Driven Design, and Section 5.2 - Heavy Ion Beam Driven Design, each with the appropriate subdivision into subsystems. Each subsection describes the quantitative requirements as well as the constraints imposed on the subsystem either by other designers or by nature. In many cases, information was incomplete or nonexistent.

In conformity with the design philosophy of the project, optimistic assumptions had to be made; these are also specified in Chapter 5. Finally, analysis or narrative is presented to provide convincing evidence that the design will meet its goals. As in Chapter 4, if the discussion of the subsystem used for the Heavy Ion Driver is the same as that for the Laser Driver, the reader will be referred back to Section 5.1.

Chapter 6 describes the architecture of the computer code which models cost, size and performance of the entire plant. It is called ICECAP: Inertial Confinement Engineering, Cost And Performance code. This is not a documentation of the code; rather, it describes how the 20 subsystems are handled within the code to allow for their interaction and for rapid change of assumed operating

conditions. Chapter 7 reports on selected trade studies that were performed with this code. Our major interest was in identifying trends as particular parameters were varied, rather than striving for precision. This was especially important when we examined the cost of the plant and realized that many of the systems had never been built and that their cost could not be accurately estimated. In addition, cost estimates made in 1980 cannot take into account cost reductions which are certain to occur in the future due to inventions, new solutions to the problem, improved materials and manufacturing methods, nor to cost increases due to inflation, shortage of resources, difficulty in achieving design solutions, and increased environmental and safety requirements. Finally, emphasis on an actual dollar estimate serves to deflect attention away from the more important issue of demonstrating technical feasibility. For these reasons, the total costs are normalized to unity for each reference driver.

Chapter 8 presents a review of the designs for the commercial ICF power plant from the point of view of the utilities and also presents a description of the methodology used by utilities in evaluating the cost of electricity due to a given reactor.

Chapter 9 summarizes the technological areas which need further work, based on our efforts to arrive at conceptual solutions to design problems. In some cases, this listing is design specific; in other cases, the problems are generic and would apply to all reactors. No attempt has been made to generate an overall RD&D program for ICF; such an effort would require resources far beyond that which we were able to bring to this task. However, this chapter does identify material, component, technology and design areas that should be included in such a program.

4.0 PLANT DESCRIPTIONS

This chapter provides a description of the entire power plant associated with each of the two drivers investigated under this contract. Section 4.1 describes the CO_2 Laser Driven Power Plant and Section 4.2 describes the Heavy Ion Beam Driven Power Plant. The power plant has been divided into its eight major subsystems and each subsystem is described in a subsection of 4.1 or 4.2. The subsystem describing the reaction chamber and its supporting systems is itself divided into eight parts. These subsystems are listed in the Table of Contents and will not be repeated here. The discussion for each subsystem contains the following elements.

(1) Statement of the function or purpose of the subsystem. This will be in the form either of a short paragraph or an itemized list.

(2) Statement of the design requirements on the subsystem. This will be a quantitative description of what the subsystem is required to do. These requirements emerge from the overall design goals of the power plant and from the requirements of other systems which interface with it.

(3) A description of the design concept that was developed to satisfy the design requirements. This will include narrative, drawings and tables of parameter values. This element of each subsection contains the major conclusions of the design effort and reflects the early decision to invest the major portion of time and resources available from the contract to this task.

(4) The final element describes how the system operates, that is, what it does when the reactor is in operation.

The purpose of this chapter is to provide the interested, but non-specialist, reader with a detailed overview and description of the power plant concepts that emerged during this contract effort. Quantitative analysis of each subsystem will be found in Chapter 5.0.

4.1 CO_2 LASER DRIVEN DESIGN

4.1.1 DRIVER

REQUIREMENTS

The essential requirements on the driver point design are: (1) to deliver 1 MJ of 10 μm radiation to a 1 mm diameter spot on each of two opposed sides of a fuel pellet in a one ns pulse, repeated at 10 Hz, and (2) to accomplish this with an adequate overall (i.e., "wall plug") efficiency (design value = 10%) for an attractive power plant design. Other requirements include: to insure the survivability of the final focusing optics for an economic period, to limit the radiation field at the reactor building beam port windows to a safe level, to provide adequate isolation in the event of window failure, to provide for temporal pulse profiling if needed, and of course, to contribute to overall system economy.

SYSTEM DESCRIPTION

We accomplish this with a highly modular driver system which is amenable to system trade-off studies which vary beam energy, pulse length, repetition rate, etc., about the point design values.

The system is arranged as shown in plan view in Figure 4.1.1-1. Only one of two identical sides is shown — all following discussions refer to this one-half. The opposing beam arrays are exactly co-axial, so that if a pellet were missing (and the reaction chamber contained a good vacuum), each beam would appear as a particularly strong retro-pulse in the corresponding opposite beam line, and be dealt with at the power amplifier module (PAM). Actually, this does not happen for two reasons: first, most missing pellets are predicted by the pellet tracking system sufficiently in advance to disable the PAM gain, and second, if a pellet is unexpectedly missing, the gas background in the reaction chamber is enough to produce electrical breakdown at the beam focus, and the beam energy is absorbed in the resulting plasma. One result of this co-axial arrangement is that the reaction chamber first wall sees only reflected beam energy, which is negligible compared to design stress.

To describe the system, we briefly trace an optical pulse from the PAM to the pellet and then examine the component parts and the low power section, in more detail, following the same general order. There are six identical PAM's, each having a discharge volume of 0.95 x 0.95 x 4 m and a NaCl output window 1 x 1 m in size. Following one pumping discharge, we sequentially extract nine collimated beams, each 0.9 m square, from each PAM over a total period of 1.2 μs. The nine beams are slightly angled, so that they reflect from nine separate mirrors* situated 110 m from the PAM. Only one, the earliest one extracted, is shown in Figure 4.1.1-1.

Following either one or three more reflections, yielding appropriate time delays, the nine beams are simultaneous and parallel and arranged in a 3 by 3 array which passes directly from the laser building through nine 1 x 1 m NaCl windows into a tunnel in the reactor building. This tunnel is a four turn labyrinth designed to reduce the average fast neutron flux from the reactor chamber to a value permitting human occupancy at the window. At the first turn the beam pattern is converged to yield 0.6 x 0.6 m beams at the second mirror. The second turning mirrors recollimate the beams. The third set of mirrors directs these reduced, collimated beams to cross at the midpoint of the long tunnel run, so that all nine may pass through a single 0.9 m diameter ball valve, striking the final focusing mirrors (FFM) in the original (although transposed) pattern. The ball valve serves to mechanically isolate the reactor chamber if one of the nine windows fractures or leaks. Each FFM is 30 m from the pellet, and brings its beam to a focus at the pellet, through an open port in the chamber first wall, which is 10 m from the pellet. The FFMs are protected from pellet debris, particulate radiation and soft x-rays by an atmosphere of 0.5 Torr of Xe gas, which fills the beam tunnels. This gas is injected just inside the NaCl entrance windows, and extracted at pumping ports located just outside the first wall structure. The design

*Actually, three of the nine beams are separated on the second bounce, and three on the third bounce.

pumping rate provides a uniform gas velocity between the FFM and the pumping ports which exceeds the equilibrium diffusion velocity of the fastest diffusing particulate radiation.

The energy focused onto a 1 mm diameter spot on the pellet is 1 MJ, or 18.5 kJ per beam. The energy optically extracted from each PAM (total for nine beams) is 224 kJ. The input HV electrical energy to a PAM is 1.23 MJ delivered to the gas discharge from the sustainer HV energy store, plus 0.3 MJ to the electron beam supply, giving a total efficiency from HVDC to energy on target of 10.9%. Additional energy costs include about 0.08 MJ of compressor work for the PAM gas flow, electrical power conditioning losses, pre-amplifier and facility power. In all, the "wall plug" efficiency of the laser driver is likely to be slightly below the target of 10%.

The laser building is a one story structure 75 x 175 m, built on grade. The height is 5 m for beam clearance, plus headroom for a crane system having a capacity of 50 -100 Tonnes. The entire building space is moisture controlled to a dew point of -10°C, and is safe for occupancy whenever the driver optical pulse is absent. During operation, occupancy would be prohibited in output beam relay portion (from the PAM output to the reactor building) because these beams are exposed.

Because all input beams to the PAMs are derived from a single master oscillator pulse, an input beam delay field is required to produce similar total path lengths.

The building foundation is in three sections, vibrationally isolated from each other; a foundation for the high power optical system, a foundation for the low power end, and a partial basement in the vicinity of the PAMs which contains the low inductance portions of the PAM pulsed power supplies and the flow loops for circulating working gas through the PAMs.

LOW POWER END AND OPTICAL LAYOUT

Figure 4.1.1-1 traces the path of one beam (specifically, the first of nine beams to transit the indicating PAM) from source to fuel pellet. "Source" represents a master oscillator together with all the gating, amplification, temporal and geometric pulse shaping, etc., necessary to produce an appropriate 10J pulse of 1 ns duration. The pulse contains four different frequencies representing adjacent rotational transitions in the neighborhood of the highest gain line (P20 of of the 10 μm band). Because rotational relaxation times greatly exceed the chosen pulse duration, the multi-line operation utilizes more of the energy stored in the excited rotational manifold, thus giving ∿ 30% greater efficiency than single line operation.

We do not specify the source any further. The applicable technology has been well developed in the LASL laser fusion program, and the details do not significantly affect either our system cost or the design of other subsystems.

The source pulse is shuttled back and forth across a 400 m total delay path by the eight mirrors (a). Nine beam splitters (b) near the mid-plane extract 1J pulses from the source pulse sequentially at successive time intervals which match the gain recovery function of the excited gas in the PAM. Each one of these nine pulses travels past the six PAMs; opposite each PAM, a beam splitter (c) and a translatable mirror (d) extract and direct a pulse of ∿ 150 mJ into the PAM. The elements (c) and (d) shown are only one of nine separate systems. Following three passes through the PAM, the beam emerges with a size of 90 x 90 cm, and an angular separation $\geq$ 11 mrad* with respect to each of the eight other beams, sufficient to place each beam on a separate mirror (e). The high power beam suffers either 2 or 4 reflections, then enters a particular tunnel of the reactor building as one of nine parallel and simultaneous beams. The 54 now simultaneous beams undergo four more reflections before focusing on the pellet.

*Six of the beams are separated by lesser angles, and share one large mirror at (e).

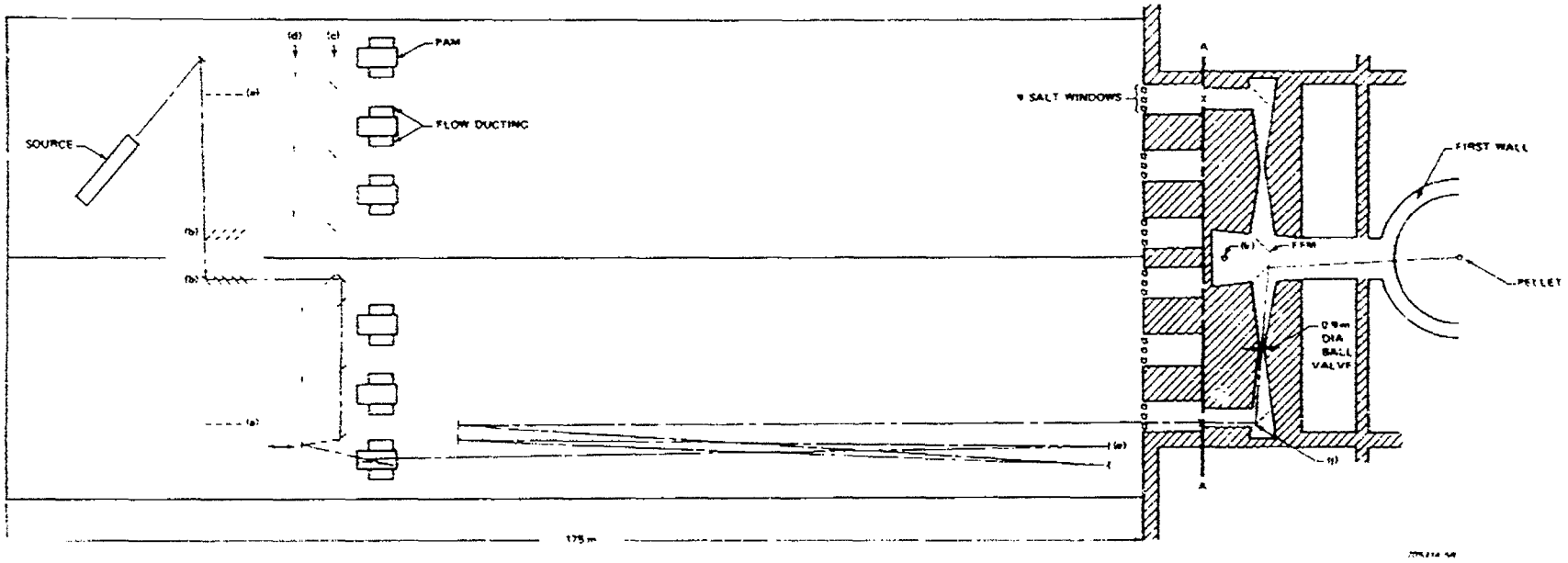

Note that level of plan is 23 m higher to the right of AA. Two turning mirrors per beam [(h) and (i) not shown] are at AA. The symbol (⌒) represents a beam splitter. The course of one beam (the earliest extracted from the lower PAM) is shown. Optical elements (a) through (e) are defined in text. Mirror (k) belongs to the visible frequency beam aiming system.

Figure 4.1.1-1. Plan View of 1/2 of CO_2 Laser Driver System

The total path length of each beam, from source to pellet, equals 715 m. Of this, (220 + 400k) meters is the path length at full power after leaving the PAM, where 400k ($0 \leq k \leq 1$) is the path length through the high power optical delay field, and 400 (1-k) is the path length in the low power delay field. Fine adjustments in total path length, to obtain simultaneous arrival at the pellet, are made by translating each of the 54 mirrors (d) along the axis indicated. These are the only mirrors whose mountings require translation adjustment of any kind. The translation is under active control, governed by arrival signals from detectors near each of the FFMs.

The mirror locations in Figure 4.1.1-1 correspond to equal time intervals of 150 ns between the successive passage of each of the nine beams through a particular PAM (i.e., k has nine values equally spaced from 0 to 1). This would result in each successive beam extracting less power from the PAM excitation, thus imposing an unnecessarily large peak power requirement on some NaCl windows. To equalize the power per beam, the intervals between successive k values are chosen to increase in accord with the gain recovery function in the excited PAM medium. This is done by relocating mirrors (a) closer to the center line for the earlier bounces, and correspondingly relocating mirrors in the high power delay field.

Table 4.1.1-1 gives the inventory of mirrors and beam splitters. Each of these has a very small range of motorized angular adjustment along two axes, and four simple diode detectors around the periphery. System alignment consists of an automatic sequence in which, beginning at the source, each element is centered on the succeeding element to balance the peripheral detector signals. Alignment is not under active control, but is updated when called for by peripheral detector error signals. Beam aiming requires active control of one mirror per beam line. This could be either the FFM or a preceding mirror if fast neutron damage considerations prohibit control at the FFM. Also, one deformable mirror per beam line might be needed to compensate for accumulated changes in optical figure. This is not provided in the present design.

TABLE 4.1.1-1

INVENTORY OF OPTICAL ELEMENTS FOR 1/2 OF LASER DRIVER SYSTEM.
ALL ELEMENTS HAVE TWO AXIS REMOTE ANGULAR MOTION EXCEPT AS NOTED.

Function	Key*	Size (cm)	Energy per Beam (J)	Figure	Number	Notes
Low power delay	a	4 x 4	10	Plane	8	
Sequence beam splitter	b	4 x 4	10	Plane	9	
PAM beam splitter	c	4 x 4	1	Plane	45	
PAM selector mirror	c	4 x 4	1	Plane	27	
Simultaneity adjustment	d	4 x 4	0.15	Plane	54	One axis translation
PAM second pass	f	20 x 20	< 80	Spherical diverging	6	9 beams, fixed
PAM final pass	g	95 x 95	20k	Spherical collimating	6	9 beams, fixed
High power delay:	e	175 x 250	20k	Plane	6	6 beams
		100 x 270	20k	Plane	6	3 beams
		100 x 100	20k	Plane	102	
Labyrinth:	h	100 x 140	20k	Spherical converging	54	
	i	60 x 84	20k	Spherical collimating	54	
	j	60 x 84	20k	Plane	54	
	FFM	60 x 84	20k	Off-axis paraboloid	54	
PAM output salt windows		100 x 100	20k		6	9 beams
Reactor building window		100 x 100	20k		54	
PAM input salt window		25 x 30	0.15		6	

*Figure 4.1.1-1

POWER AMPLIFIER MODULE

The geometry of one PAM is sketched in Figure 4.1.1-2. It provides a rectilinear electron beam controlled discharge with a volume of 95 x 95 x 300 cm. This is similar to one side of the dual PAM used in the HELIOS system at LASL, scaled up by a factor of four in discharge width and height, and has about the same energy input per unit volume of discharge (220 J/ℓ-atm). By sequentially amplifying nine beams over a total time of 1.2 μs, we expect to extract 18% of the energy in the discharge volume swept out by a 90 x 90 cm collimated beam. This amounts to $18\ (90/95)^2 = 16.2\%$ of the total discharge energy, or 224 kJ distributed among the nine sequential beams.

The triple pass optical path of one beam is shown. A collimated 4 x 4 cm beam, from one of the nine mirrors (d) in Figure 4.1.1-1, enters through a 25 x 30 cm salt window in the upstream wall of the gas flow duct, crosses the excited region, is diverged by the 20 x 20 cm mirror (f) which is common to all nine beams, is collimated by the 95 x 95 cm mirror (g), and exits through the 1 x 1 m salt window as a 90 x 90 cm beam containing 25 kJ.

Each of the nine beams crosses the identical 90 x 90 cm area at the mid-plane of the discharge during its final pass. Each of the eight outer beams is skewed from the central axis of the discharge by the angles in Table 4.1.1-2, which are sufficient to provide 150 cm center to center separation from all adjacent beams, when separated by an individual 1 x 1 m mirror at second or third bounce. Beams 7-8 are separated at the first bounce, after having diverged 130 cm. The result is that a rectangular area 96 x 95 cm of the 1 x 1 m PAM salt window is used. The corresponding area of mirror (g) which is used is 93.5 x 93 cm.

Assuming a filling factor $\eta_b = 0.8$, where η_b = peak beam intensity/average beam intensity, the peak energy density at the salt window is 3.85 J/cm^2. This must be compared to an assumed safe limit with respect to long term window damage of $3\sqrt{\tau_p}$ J/cm^2, where τ_p is the pulse duration in ns.

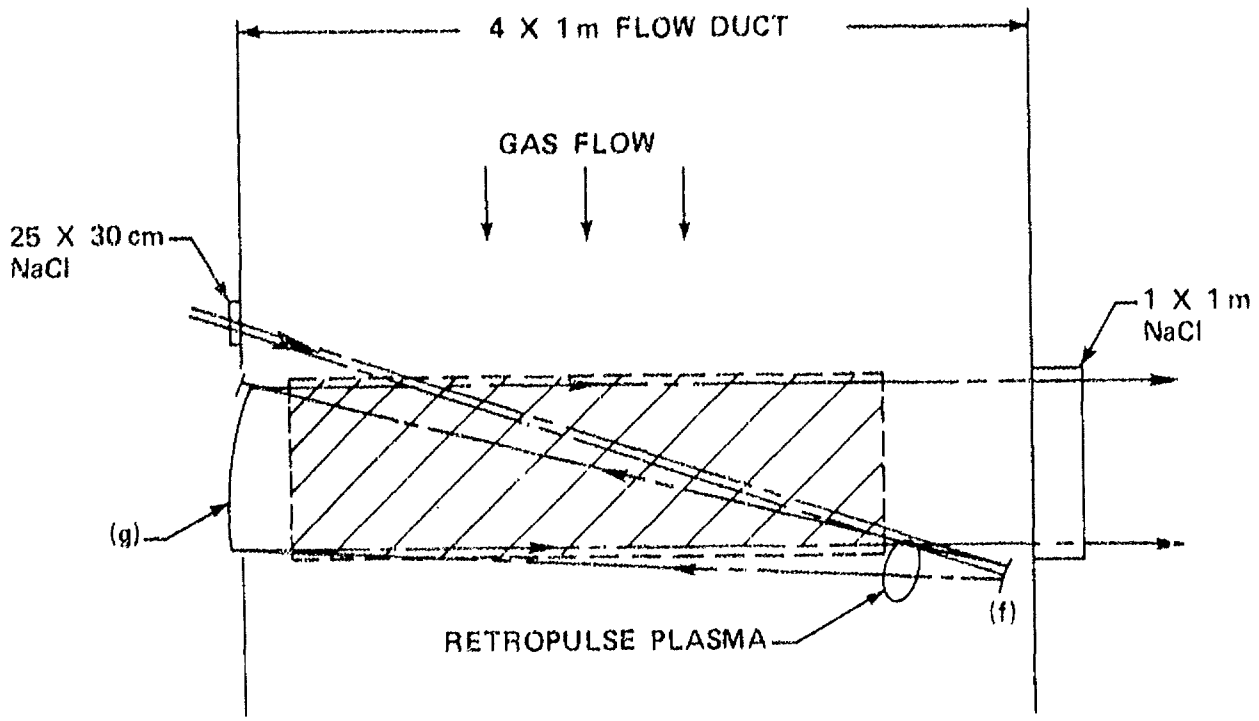

Figure 4.1.1-2. Plan View of Discharge Region of PAM, Showing Three Pass Path of One Beam. It enters as 4 x 4 cm collimated beam from mirror (d), Figure 4.1.1-1, is diverged by 20 x 20 cm common mirror (f), recollimated by 95 x 95 cm spherically figured mirror (g), and exits as 90 x 90 cm beam. The 95 x 300 cm discharge area is shaded.

TABLE 4.1.1-2

SKEW ANGLES OF SEQUENTIAL BEAMS

Beam No.	θ_{hor} (mrad)	θ_{vert} (mrad)	No. of Refl.	Path Length (meters at 1 atm)
1	-9.5	+ 4.9	4	515
2	-9.5	0	4	465
3	-9.5	- 4.9	4	415
4	-2.3	- 8.1	4	365
5	-2.3	+ 7.2	2	315
6	-2.3	0	2	265
7	+9.5	+11.8	2	215
8	+9.5	0	2	165
9	+9.5	-11.8	2	115
Envelope	19.0	23.6		

For τ_p = 1 ns, the PAM window would be severely stressed. We anticipate, however, that the eventual pellet design will call for a longer pulse duration, perhaps τ_p = 2 ns. Then the peak energy density at the window would be a more conservative 2.7 $\sqrt{\tau_p}$ J/cm^2. The average power transmitted by the PAM window, at the worst location, is 347 watt/cm^2.

The mechanical design of the window is not specified. Given the presently known strength coefficients for salt windows, a 1 x 1 m planar slab would have excessive thickness. This results from portions of the window being in tension, which salt does not support well. Alternative designs include:

(1) A curved shape which is convex inward (toward the 2.4 atmosphere discharge medium), and is designed to be everywhere in compression.

(2) A curved shape which is convex outward, supported by a mesh of tensioned wires on the outside surface.

(3) A composite sectional window.

The gain medium in the PAM consists of 360 Torr CO_2, 360 Torr N_2, and 1080 Torr He. The sustainer power supply delivers 1.23 MJ to the discharge in a pulse of 1 μs duration, having a rise time of ∿ 0.5 μs. The discharge voltage is 1 MV, giving a current density, over the 95 x 300 cm discharge area, of about 43 A/cm^2. The 1.23 MJ is delivered from a 2 MV sustainer energy store. In addition, 0.3 MJ is delivered to the electron gun at 1.3 MV. We have assumed that the electron beam energy is one-half as effective as the sustainer energy in exciting the appropriate levels, which implies a discharge energy loading of 220 J/ℓ-atm. The discharge turn-on time, relative to the arrival of the first input beam, is controlled to ∿ 20 ns, in order to control the fraction of energy extracted in the first beam.

This PAM is very similar to the well characterized final amplifiers of the HELIOS system at LASL with respect to gain length, optical extraction geometry, use of multi-spectral lines, and discharge energy loading. It differs primarily in being four times larger in both dimensions transverse

to the optic axis, and in having much greater total extraction efficiency, due principally to using nine sequential extractions.

The gas is circulated transversely at 15 m/s through the 1 x 4 m flow cross section, sufficient to move the perturbed gas 1.6 discharge widths between successive pulses. The estimated pumping power is about 5% of the total power requirement of the PAM.

Light reflected from the pellet back through the PAM produces gas breakdown at some point in the converging pass between mirror (g) and (f), and is absorbed harmlessly in the resulting plasma. Note that this plasma occurs on the downstream side of the gas flow, thus providing less disturbance to the succeeding discharge. This method has worked reliably in the HELIOS system. It is less of a problem in the proposed PAM for two reasons; much less gain remains in the medium because more was extracted, and the delay before the retropulse arrives is much longer.

HIGH POWER DELAY FIELD

Associated with each PAM are 19 plane mirrors, whose size and location are specified in Figure 4.1.1-3. Of the nine sequential skew beams listed in Table 4.1.1-2, beams 1-4 are reflected four times and beams 5-9 are reflected twice. This results in nine simultaneous and parallel beams arriving at the reactor building salt windows in a 3 x 3 array having adjacent beams separated by center to center distances of 150 cm. The individual beam paths can be traced in Figure 4.1.1-4 by the two-digit numbers attached to each mirror; the first digit identifies the sequential beam, and the second digit indicates the nth reflection (n = 1 to 4) of that beam.

The total beam path through the laser building atmosphere varies from 115 m for beam 9 to a maximum of 515 m for beam 1. The building atmosphere is maintained at a dew point of -10°C. Based on measured gross energy transmission of the P (20) line, the total absorption due to H_2O plus CO_2 then amounts to 3% over the longest path. After accounting

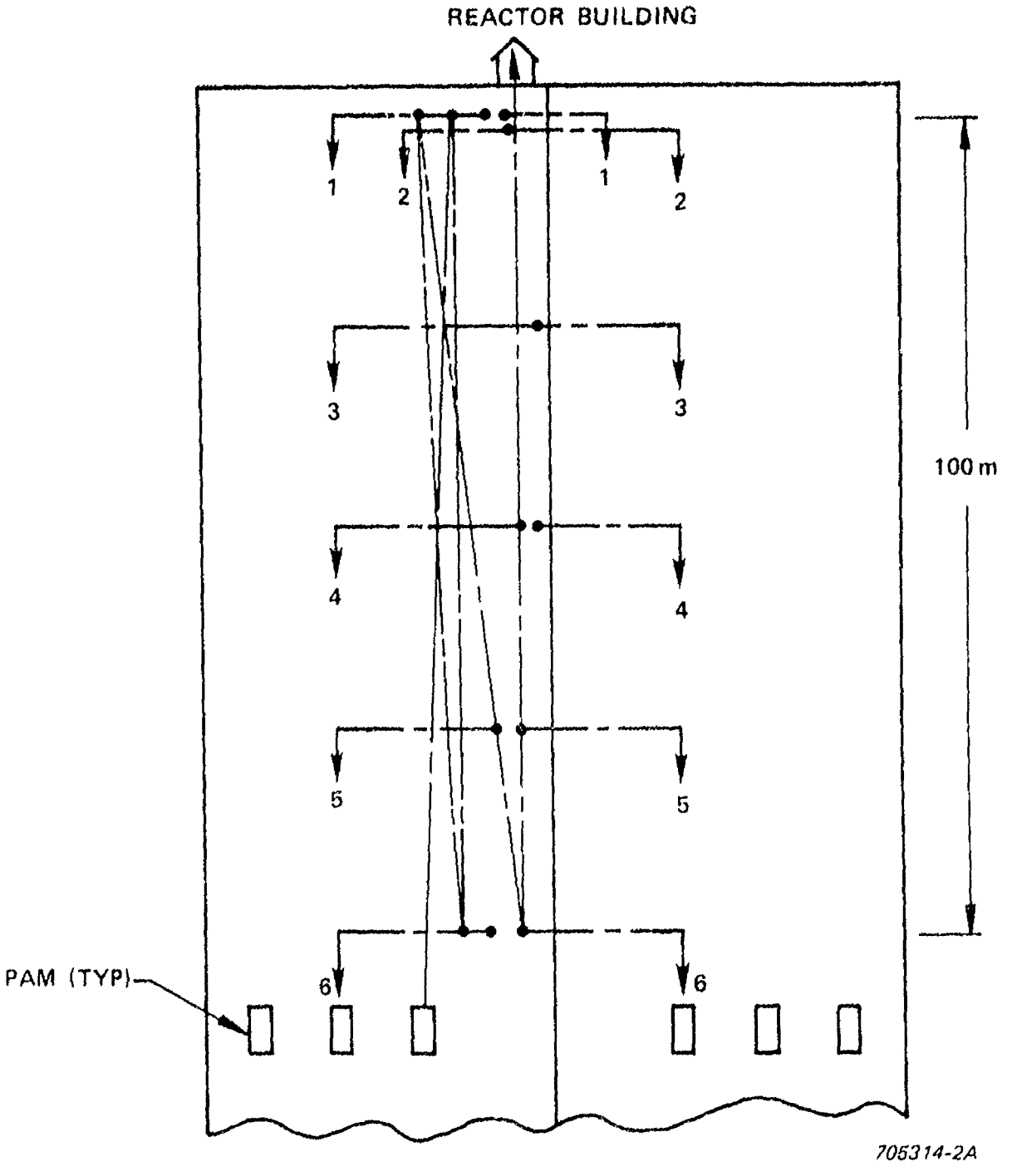

Figure 4.1.1-3. Schematic Arrangement of Mirrors to Introduce Optical Delay into Laser Beams. The thirteen dots show the location of the nineteen plane mirrors associated with one (of six shown) PAM. The path of the first beam extracted from this PAM is shown. The broad arrow at the top of the sketch indicates nine, now simultaneous and parallel, beams from this PAM passing through nine salt windows into one tunnel of the reactor building labyrinth.

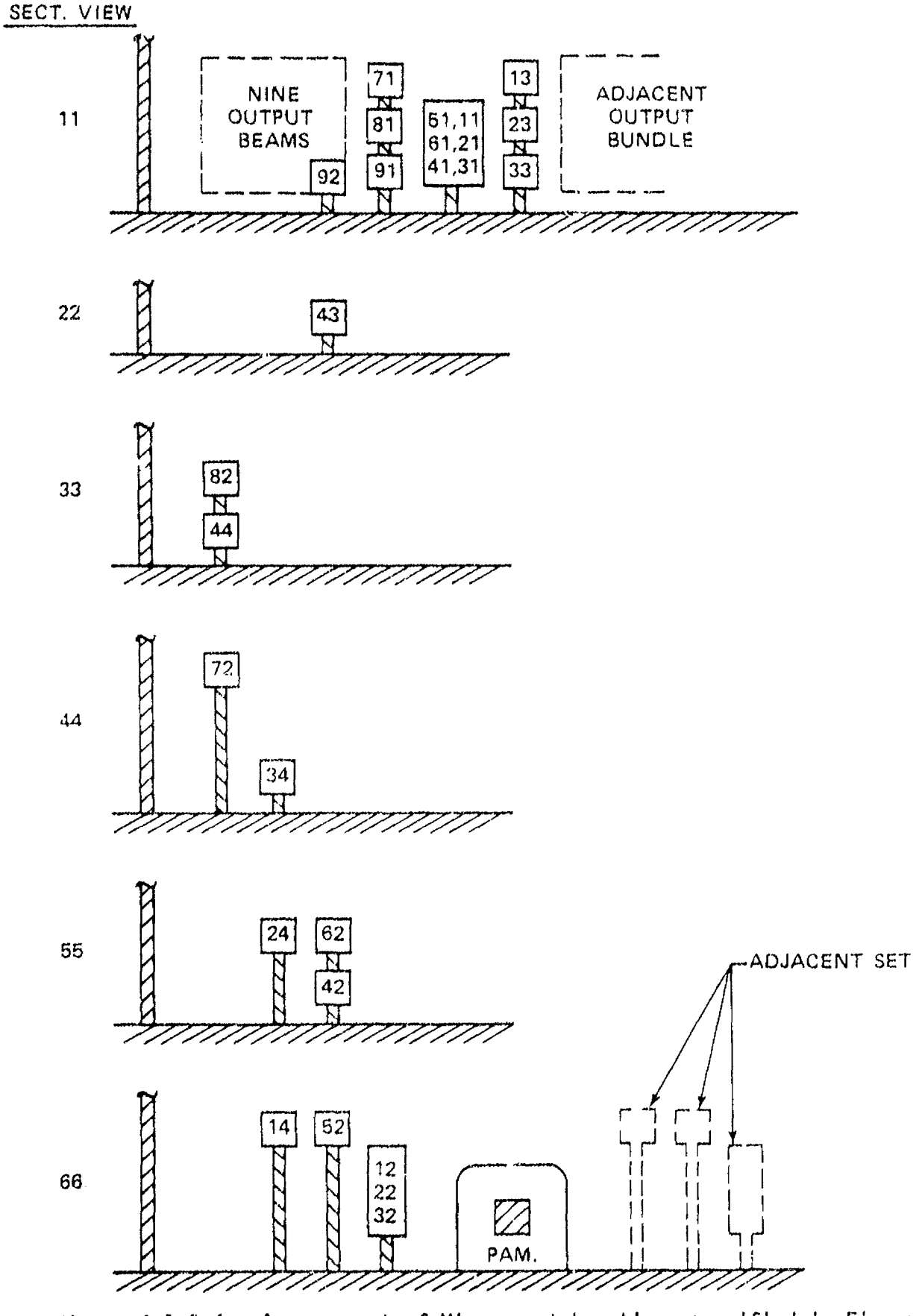

Figure 4.1.1-4. Arrangement of Mirrors at Locations specified in Figure 4.1.1-3. The number kn given for each mirror means that the k th sequential beam from the PAM suffers its nth reflection at that mirror. Square mirrors are 1 x 1 m.

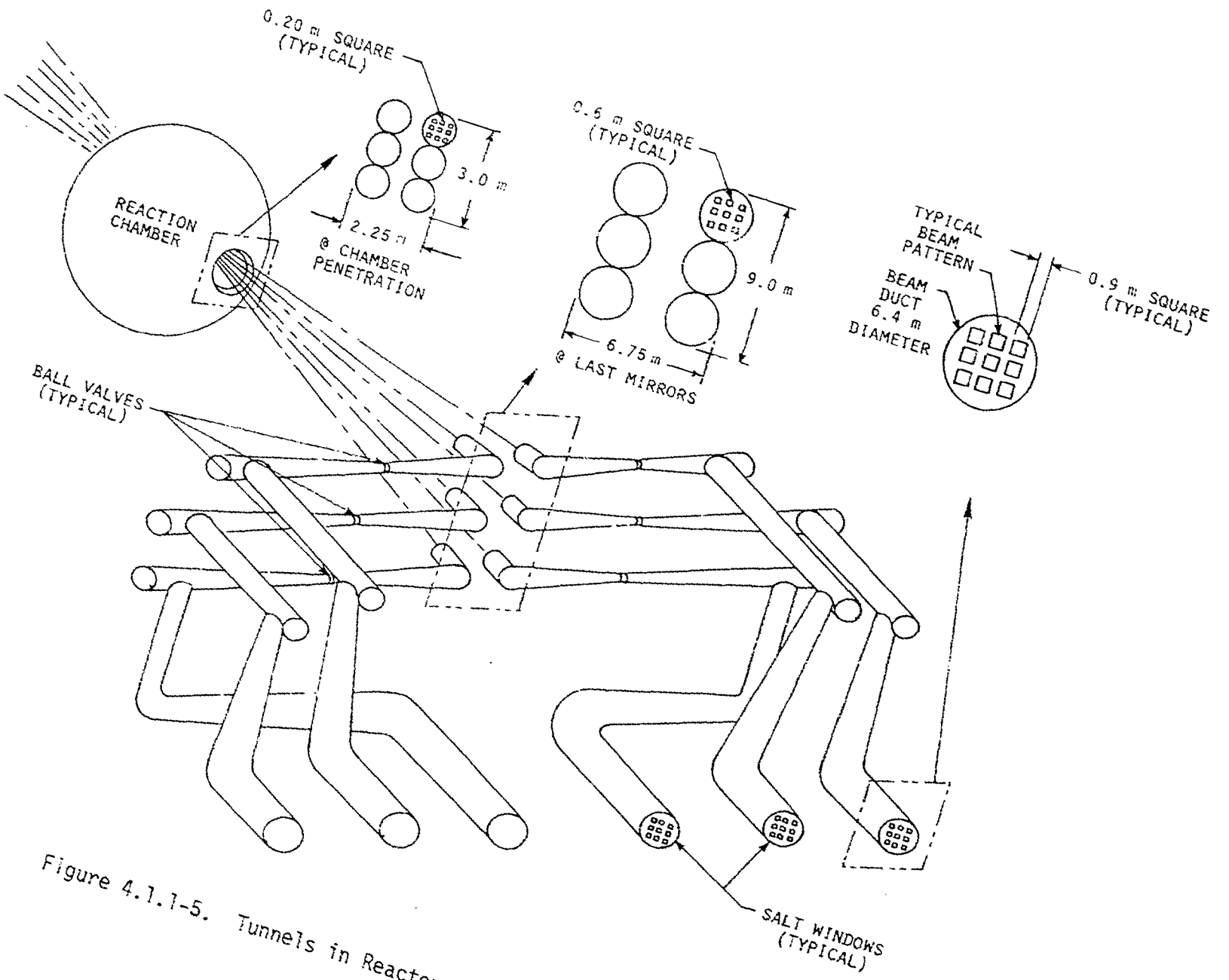

Figure 4.1.1-5. Tunnels in Reactor Building

for absorption and for mirror reflection losses, the effect of atmospheric speckle on beam focusability is included in the blanket assumption that 80% of the remaining beam energy can be focused onto the 1 mm diameter spot specified in the pellet design.

These mirrors are essentially static. Each is provided with a two-axis directional mounting having a modest pointing precision of about 100 μrad (i.e., $\lesssim$ 1 cm beam displacement at the following mirror). However, the specified stability of each mounting, when not energized is about 3 μrad (i.e., 0.1 mm at 30 m) at all frequencies > $1/\tau_i$, where τ_i is the integration time of the active beam pointing control of the FFM.

Pointing correction of these 19 mirrors (and the 27 associated static mirrors inside the reactor building) is called for only when an error signal indicates a beam footprint more than 1 cm off center on some mirror. The error signal is derived from imbalance in four peripheral diode detectors on the rim of each mirror. Because of the large number of mirrors involved, the pointing correction sequence is controlled by a mini-computer, and is integrated with pointing corrections of the low power input optical system.

In Figure 4.1.1-4, one sees that every mirror can have a direct, massive vertical mounting from the foundation, without obscuring any beam. The figure is drawn with up to three mirrors on a single vertical axis, but in every case the higher mirrors can be moved back slightly without penalty to provide individual vertical mounts.

OPTICS IN REACTOR BUILDING

Figure 4.1.1-5 illustrates the layout of the six optical tunnels on one side of the reactor building. The nine now parallel and simultaneous 90 x 90 cm beams from one PAM enter a single 6.4 m diameter tunnel, through nine 1 x 1 m salt windows. The internal pressure is about 1/2 Torr of Xe. The concave spherical mirrors (h) reduce each beam to 60 x 60 cm at the recollimating mirrors (i). The peak energy density normal

to the surface of mirrors (k), (j) and (FFM) is 5 J/cm^2. After traversing the 4.3 m diameter tunnel to plane mirrors (j), the beams cross at the midpoint between (j) and (FFM), passing through the 90 cm diameter circular orifice of a ball valve. The nine FFM are off-axis paraboloids which focus each beam on the pellet surface 30 m away.

At the radius of the first wall (10 m from the pellet) the total transverse area of the nine beam array is 80 x 80 cm. All six arrays together occupy only a small fraction of the 6.5 m diameter port in the first wall structure.

The salt windows are less heavily stressed than are those in the PAM. Peak energy density is about 10% lower, because of various transmission losses. Average power transmitted is nine times lower, because a separate window is required for each of the nine beams*. Also, the windows support only 1 atm pressure differential, rather than 1.4 atm, as in the PAM.

The ball valve in each tunnel serves to isolate the contaminated reaction space in the event of window failure. It is actuated by ultrasonic detectors behind each window of the appropriate tunnel. It can also be closed to permit maintenance of windows, plus all mirror assemblies, except for the FFM. The associated tunnel restriction also contributes to fast neutron attenuation. Behind each mirror assembly is a flux trap sufficiently deep to insure that only neutrons scattered by the mirror assembly can see the following mirror assembly. The entire optical tunnel system is intended to reduce the average dosage from neutrons at the salt windows to a level which permits human occupancy of the laser building.

---

*This provides the opportunity of using only 1/6 as many salt windows; if six path lengths inside the reactor building each differ by 2.5 m, a single window could transmit six beams at 7.5 ns intervals, without exceeding the damage limit of 3 $\sqrt{\tau_p}$ J/cm^2.

Active control of the aim of the fifty-four FFM is provided by a mini-computer processing diagnostic information over an integration time τ_i, which extends over many shots. Inputs to it include angle dependent yield data, pellet tracker output, and the most recent measurements of the location of the focal point of each of the 54 beams. These last data are obtained by a visible frequency optical measurement as follows.

At preselected times, one beam only is generated, with no pellet injected. This one beam produces breakdown of the background gas at a point one or two cm from the focal point. Mirror (k) in Figure 4.1.1-1, 4 cm in diameter, images the visible light from the breakdown onto a semiconductor diode array located 20 m directly below. The position of this image can be measured to an angular precision slightly better than the diffraction limited IR beam size at focus. The third dimension of the breakdown location is obtained similarly by observing the visible light directed toward the pellet injector (vertically downward) with an identical optical sensor. The mini-computer has sufficient information to calculate the IR focal point to the necessary precision. Absolute calibration of the visible sensing system is updated continuously by comparison with the yield and pellet position data.

During normal operation, both mirrors (k) are shielded by mechanical shutters.

PROTECTION OF FOCUSING MIRRORS

Protection of the figure surface of the FFM against ions, x-rays, and blast debris is afforded by an atmosphere of 1/2 Torr Xe in the 20 m flight path between the first wall penetration and the mirror surfaces. The gas is introduced into the tunnels near the salt windows and is exhausted through pumping ports just outside the first wall penetration. The effective path length in 1/2 Torr Xe is 10-15 m. The pumping rate is sufficient to provide a gas velocity near the FFM which is well in excess of the free diffusion velocities of all the components of the pellet debris, to prevent deposition of thermalized material on the optical surfaces.

Xe was specified as a compromise between high atomic number, which is effective in stopping x-rays, and high electrical breakdown threshold, to minimize the effects of IR induced breakdown near the pellet due to the unavoidable background of the protective gas within the reaction chamber. The specified 1/2 Torr estimated to be well in excess of the amount needed to reduce erosion of the mirror surface to a tolerable 3 μm over the life of the plant.

The fast neutron fluence at rated power is about 10^{20} n/cm^2-yr, a level which is not known to disturb bare Cu surfaces. However, the combined effect of this fluence level, and optical radiation intensities at near damage threshold, is not known. Our present assessment is that refurbishment of FFM optical surfaces at either annual or five-year scheduled plant shutdowns should be sufficient.

4.1.2 POWER SUPPLY

FUNCTIONS

- Take power from the 60 Hz system and provide controlled current pulses to the electron guns.
- Take power from the 60 Hz system and provide controlled current pulses to the gas discharge chambers in the power amplifier.

DESIGN REQUIREMENTS

Pulsing Power Supply System for the Gas Discharge Chambers

- The power supply system shall provide current pulse for each gas discharge chamber.
- The peak value of the current pulse for each chamber shall be regulated to a precision adequate for the laser needs.
- The current pulses in the chamber shall be brought up from zero to a specified peak and back to zero with a wave-shape determined by the parameters of the capacitor discharge circuits.
- The power supply system shall be capable of continuously supplying the full current pulses at the required rep rate.

Pulsing Power Supply System for the Electron Guns

- The power supply shall provide a current pulse for each cold cathode electron gun and a voltage for the grid of each electron gun.
- The grid of each electron gun shall be coupled to the supply so as to limit the total emission from the gun to the desired value.
- The gun current pulse shall provide the proper penetration of the anode foil by electrons into the gas chamber so as to satisfy the requirements for the current pulse of the gas chamber.

Each pulsing power supply system shall take power from the 60 Hz system in a manner that will not cause any unacceptable variations in the 60 Hz output of the main generator.

SUMMARY DESCRIPTION

The laser power supply consists of a gas pulser and an electron gun pulser. The circuits of each are basically the same. Each power supply takes power from the main 60 Hz system and feeds it through an isolation transformer and rectifier. The power is stored in capacitor networks which will be Marx generators. The capacitor energy of both systems is fed simultaneously into the laser power amplifiers as three microsecond pulses. The electron beam gun pulse may actually be slightly longer.

The basic system is shown in Figure 4.1.2-1. The circuit configuration of the two systems are the same except the electron-beam gun pulser has a grid network whose power and costs are minor. The engineering requirements and considerations of the design are described in the following paragraphs.

Transformer (T)

The transformer provides isolation from the ac system and thereby permits the electron gun pulser and the gas pulser to have a common circuit connection.

Rectifier (TR)

The rectifier supplies the dc power for charging the Marx generator. The bridge is shown with thyristors which provides fine control for charging at a constant voltage to offset any ac voltage fluctuations. There will actually be a number of bridges in series (as shown in Figure 5.1.2-1). Most of the bridges will actually have diodes which both reduces the cost and reduces the losses.

Back Diodes (BD)

A capacitor (C) charging through a reactor (L) has a peak voltage of double the source voltage. The back diodes are to block this additional voltage after the capacitor is charged.

Charging Reactor (L) and Capacitor (C)

The reactor and capacitor together set the basic operation of the circuit. The charging time is set by ($\pi\sqrt{LC}$) which is the time of one cycle or 0.1 seconds for ten Hertz. The capacitor is sized by the total stored energy and peak capacitor voltage (energy = 0.5 CV^2). The Marx generator voltages and capacitance are naturally adjusted for the series operation during discharge and the parallel operation during charging.

Marx Generator Resistors (R)

The resistors carry the charging current for the capacitors and function as voltage dividers during the discharge pulse of the Marx generators.

Discharge Switches (S)

The discharge switches initiate the dumping of the capacitor energy into the laser power amplifiers. They effectively change the Marx generator capacitors from a parallel network to a series network thereby providing the high voltage required by the laser.

SYSTEM PARAMETERS

The parameters of the laser power supply base design are shown in Table 4.1.2-1. The laser gas chamber voltage of 1 MV sets the capacitor voltage at double this value (2 MV) in order to efficiently transfer the capacitor energy to the gas chamber. In like manner the charging voltage of the rectifier will be one-half that of the capacitor voltage except the voltage used is that of the parallel capacitor network of the Marx generator. The electron-gun system voltages vary in the same manner.

TABLE 4.1.2-1

PARAMETERS OF THE LASER POWER SUPPLY BASE DESIGN

Rep Rate	10 Hz
Laser Beam Energy	2 MJ
Laser Efficiency	10%
Energy Input per Pulse	20 MJ
Input Power	200 MW
Driver Input Energy (Gas Chamber)	15 MJ
Peak Driver Capacitor Voltage	2 MV
Peak Gas Chamber Voltage	1 MV
Gas Chamber Pulse Width	3 μs
Jitter of Gas Chamber Pulse	± 0.25 μs
Electron Gun Energy	5 MJ
Peak Capacitor Voltage (EG)	1 MV
Peak Cathode-Anode Voltage (EG)	0.5 MV
Electron Gun Pulse Width	3-5 μs
No. of Power Amplifiers on Driver Output	12
No. of Marx Generators	
For Gas Chambers	12
For Electron Guns	12

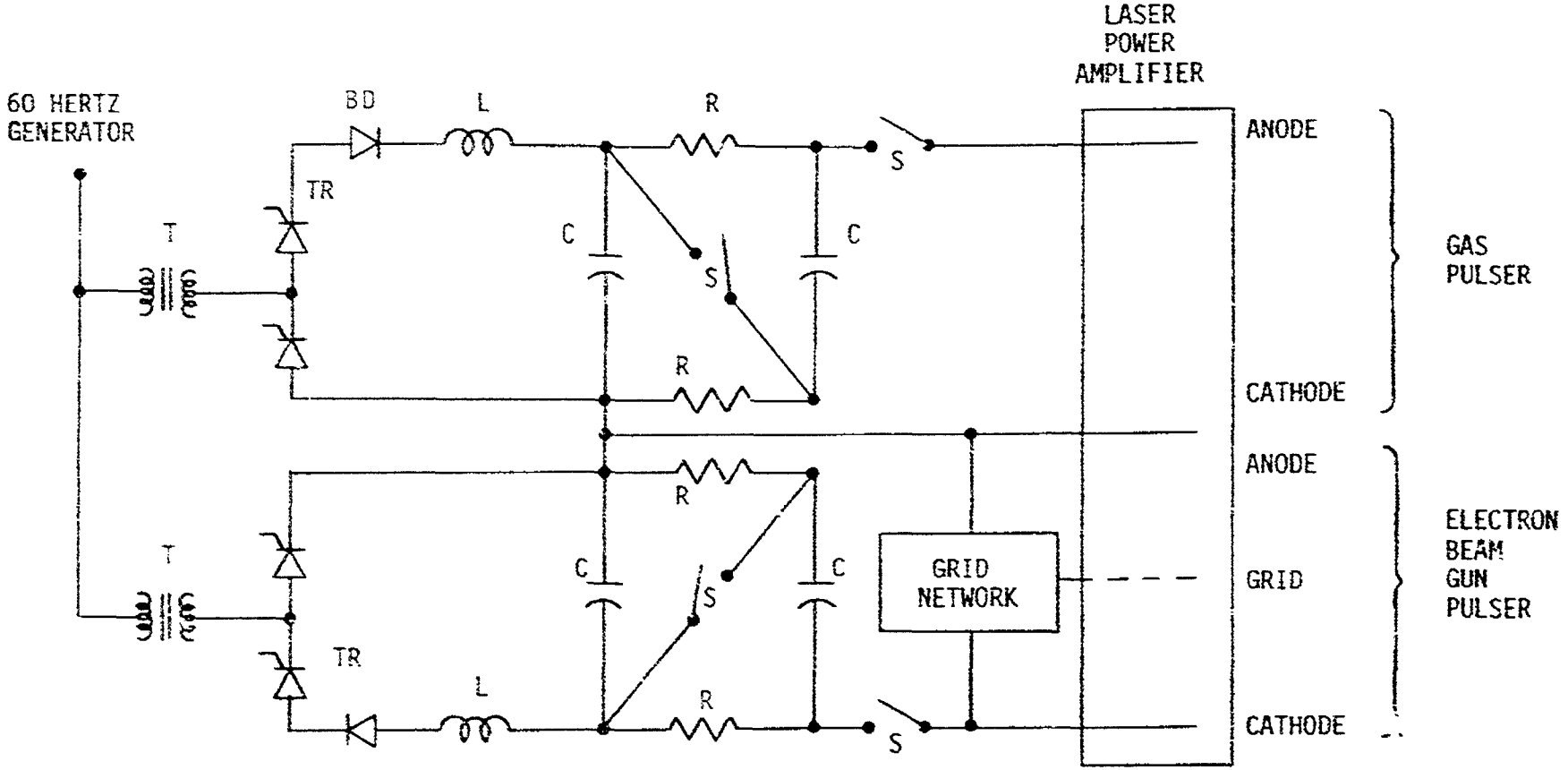

Figure 4.1.2-1. Schematic Diagram of the Power Supply for the CO_2 Laser

4.1.3 PELLET DESIGN AND FIRST WALL PROTECTION

FUNCTIONS

The pellet must convert the incident driver energy into an efficient implosive force which heats the DT fuel until a thermonuclear burn releases a substantially greater amount of energy than the incident driver energy. This output energy must be in a spectrum which can be easily converted to useful thermal energy without destroying the first wall.

The first wall is a spherical shell composed of banana-shaped HT-9 steel tubes which contain liquid lithium flowing at high speeds. This shell is large and heavy, and is the inner boundary for the liquid lithium neutron blanket. For these reasons it cannot be rapidly replaced or repaired. Thus, in order to have a long life, it must be protected from the adverse effects of the 8.64×10^5 daily explosions at the center of the chamber. This first wall protection must satisfy the following requirements:

- Convert the x-ray and ion energy from each explosion into thermal energy,
- Transmit this thermal energy to the first wall where it can be removed by the fast flowing liquid lithium within the steel tubes,
- Minimize the thermal cycling of the steel tubes which could eventually cause them to fail from thermal fatigue,
- Allow the vast majority of neutrons to reach the neutron blanket.

DESIGN REQUIREMENTS

The nominal design goals for the pellet are to produce a yield of 350 MJ for an incident driver energy of 2 MJ, to drive the thermal cycle, and put as much energy as possible into the kinetic energy of the thermonuclear neutrons. To reduce the high temperatures of reactor chamber materials which absorb a part of the pellet yield, the x-ray and ion spectra should have as little energy content as possible.

The first wall protection scheme must use materials which are either long lived or easily replenished, which are compatible with the pellet materials and HT-9 steel, and which do not:

- Suffer neutron damage,
- Allow high intensity shock waves to reach the HT-9,
- Introduce excessive radioactivity problems,
- Overload the gas pumping system,
- Impede the transport of the driver beams to the target.

SYSTEM DESCRIPTION

Pellet

The CO_2 laser pellet selected for this study is the low fuel mass POLARIS B design[1]. This cryogenic pellet, shown in Figure 4.1.3-1, features a double-shell exploding pusher design where the CHOW material in the original exploding pusher shell has been replaced by TaCOH and the high Z Au material in the original ablative pusher shell has been replaced by high Z Ta. The TaCOH material is a plastic, polymerized CH_2, that has been seeded with tantalum oxide, Ta_2O_5, until the tantalum constitutes about 1 atomic percent of the exploding-pusher shell. Since the choice of the high Z material in the shells is not critical, Ta is used in this design because it eliminates the need to process an additional material (Au), and because a significant component of the pellet is then completely compatible with the first wall coating of tantalum.

This pellet was scaled to a gain of 175 for an incident energy of 2 MJ. The scaled pellet is assumed to give a ρR of 6 g/cm^2 for the compressed fuel which means that 55% of the yield will be in the kinetic energy of thermonuclear neutrons and 45% will be in x-rays and ions[2]. This pellet has a total mass of 55.2 mg divided into 16.5 mg of oxygen, 14.7 mg of carbon, 10.5 mg of silicon, 9.0 mg of tantalum, and 4.5 mg of hydrogen and its isotopes. These masses include a nominal amount of SiO_2 from the glass shells which separate the different materials during pellet fabrication.

Although this pellet design is unclassified and is the result of crude scaling from a very small size, it is useful in elucidating many of the functional and design requirements of laser pellets and their effects on other systems of the reactor. However, the target design and systems studies groups at the Los Alamos Scientific Laboratory have furnished a detailed classified design which has been extensively used for the classified studies which are contained in the accompanying classified report, DOE/DP/40086-2.

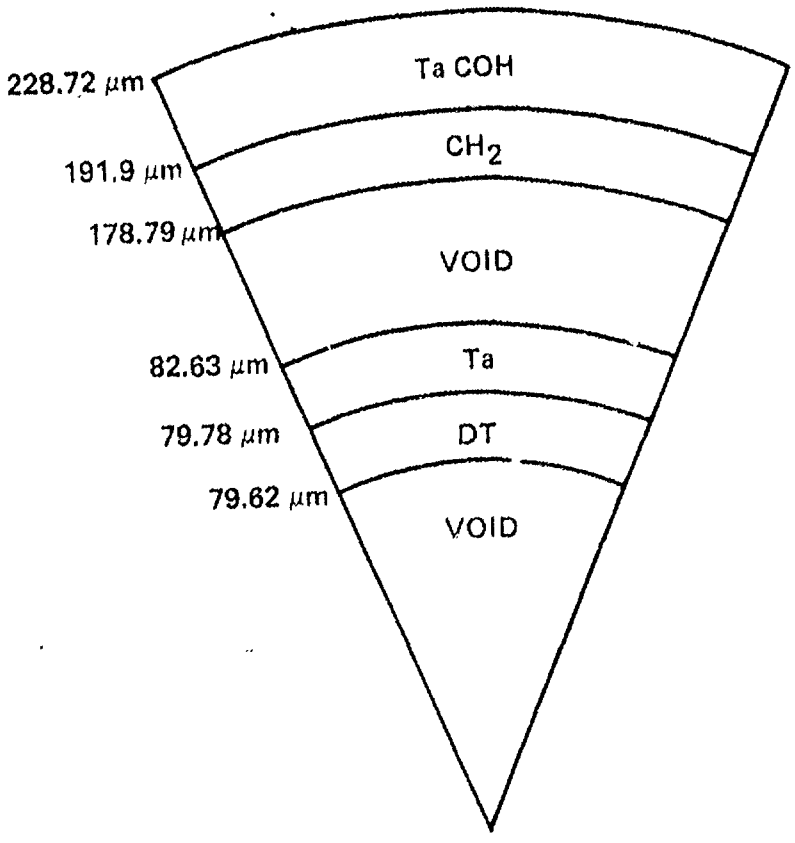

Figure 4.1.3-1. CO_2 Laser Pellet Design

First Wall Protection

A new concept for protecting the first wall has been developed in this study. This concept is similar to the bare wall concept, but is different in that it relies on a combination of two methods of protection: (1) a coating on the first wall, and (2) effective design of classified pellets.

The inner shell, or "first wall," of the 10 m radius spherical reactor chamber is formed by 324 HT-9 steel tubes which are closely nested and welded at their points of tangency. The surface of the tubes exposed to the interior of the chamber is covered with a 0.1 cm thick tantalum coating. Tantalum is used for the coating because it has very good material properties such as high values of density, thermal conductivity, heat capacity, and melting temperature. Furthermore, it is relatively easy to fabricate, remove, and process, is relatively cheap and abundant, and can be used as the high Z material in the pellets. This coating absorbs the x-rays and ions from the pellet explosion, and transmits the resulting thermal energy to the HT-9 steel tubes, whose outer surface temperature is nominally 773°K, with less than a $\pm$ 5% variation. This small variation minimizes the thermal stress at the tantalum-steel interface.

The gas pressure within the reactor chamber is limited to 0.1 Torr or less so as to not impede the transport and focusing of the CO_2 laser beams. This pressure is high enough to give some first wall protection. For this reason, Xe is chosen as the gas species since it is an inert gas and is a very good x-ray absorber.

The pellet is illuminated by 108 laser beams oriented within two opposing cones which have a 10° half angle. Each beam is focused to a 1 mm diameter spot size. The total energy incident on the pellet is 2 MJ and is delivered in 1 nanosecond. This irradiation produces a pellet yield of 350 MJ. The pellets are designed to not only have a gain of 175, but also to give x-ray and ion spectra under which the first wall and its coating can best survive. In particular, the selection of tantalum for the coating, of xenon for the gas, and of a properly designed pellet are all based on the premise that, in order to survive, the maximum temperature anywhere within the coating must be less than the melting temperature of the coating material.

SYSTEM OPERATION

The CO_2 laser pellet enters the reactor chamber from the very bottom at 300 m/sec and is continuously tracked. At the appropriate time the CO_2 laser is fired so that 2 MJ of energy, delivered in 108 beams, irradiates two sides of the pellet for one nanosecond at the exact moment that the pellet is centered within the reactor chamber.

The laser radiation on the pellet is absorbed by the TaCOH exploding-pusher shell, the inner half of which implodes with a high degree of symmetry. This imploding outer shell then collides with the Ta ablative pusher. The resulting velocity multiplication of the colliding shells effectively implodes the Ta shell which compresses the cryogenic DT fuel to a ρR value of 6 g/cm^2, and heats the fuel to a temperature near 20 keV.

Under these conditions thermonuclear reactions occur within the fuel with a tremendous release of energy in the form of kinetic energy of thermonuclear neutrons and alpha particles. Since the center of the compressed fuel has the hottest temperature, most of the thermonuclear neutrons and alpha particles originate there and must traverse the bulk of the compressed fuel before leaving the pellet. The high value of ρR in the fuel produces a high burn fraction of the fuel and signifies an efficient laser-driven implosion process. However, it also produces a high absorption of neutrons and alpha particles. Originally, 80% of the energy yield is in the kinetic energy of the neutrons. Absorption by the compressed fuel reduces the neutron energy escaping the pellet to 55%. On the other hand, the alpha particles have a much shorter range in the compressed fuel and are almost all absorbed. This absorption is very helpful because it significantly heats the fuel and generates a thermonuclear burn front which propagates radially outward through the fuel.

The total energy yield from the pellet is 350 MJ, 55% of which is in the kinetic energy of the neutrons which traverse the pellet shells surrounding the central fuel region with very little absorption. The remaining 45% of the energy yield is in the form of x-rays and the kinetic energy of charged particles formed from the pellet debris.

The neutrons traverse the Xe gas, the Ta coating, and the HT-9 steel tubes with very little absorption, depositing their energy in the liquid Li neutron blanket.

The x-rays and ions are absorbed somewhat by the Xe gas. This absorption has two effects: (1) it reduces the maximum temperature in the Ta coating, and (2) it produces a pressure wave which acts against the first wall. The former

effect is very desirable but not too significant since the classified calculations indicate that the temperature reduction is only 94°K. The latter effect is more significant since the maximum theoretical value of the pressure wave is about 1.7 atm, enough to cause the first wall to cycle between states of compression and tension — an undesirable situation which could reduce the lifetime of the first wall by fatigue. However, because of dissipative mechanisms it is unlikely that, in practice, it could be approached even within a factor of two. This reduction is sufficient to always keep the first wall safely in a state of compression.

The x-rays and ions are absorbed primarily in the Ta coating in a thin surface layer a few μm thick. If the temperature of this thin layer exceeds the melting temperature, 3269°K, of Ta, the layer will likely spall and the entire Ta coating would be gone in a few hundred shots. In the present design with the classified pellets, the maximum temperature reached in the Ta coating is about 2870°K, 400°K below the melting temperature and too low to initiate spallation. Furthermore, high temperatures in the Ta coating exist for such a short time that evaporation of the Ta is an insignificant loss mechanism.

The temperature rise per shot at the Ta coating-HT-9 steel interface is about 50°K for a 0.1 cm thick coating and proportionately lower for thicker coatings. This temperature increase introduces at most a $\pm$ 5% amplitude oscillation at 10 Hz on the steady-state temperature of 773°K. The amplitude of this oscillation is small enough that thermal fatigue at the interface should not be a problem.

These results indicate that, to first order, the Ta coating should survive the reactor chamber environment. However, further analysis identified two potential problems. First, the numerous stress waves produced in the coating by each pellet explosion may eventually fatigue the bonding between Ta and HT-9. Application of Ta by means of a detonation gun may produce a sufficiently strong bond. This problem deserves further study. Second, although the absorbing surface layer does not become hot enough to melt or spall, it does become hot enough to engage in plastic flow. This action will subsequently lead to thermal fatigue of this surface layer. It is not clear what effect

the fatigue will have on the coating since the fatigued material is in such a small volume at the surface. One possible scenario is that after a few thousand shots, the fatigued material would crack orthogonal to the surface to a few μm depth. The resulting checkboard pattern of cracks would then stabilize with no further crack growth and the coating would then have a very long lifetime.

This conclusion is supported by the following considerations. First, once the cracks are formed the lateral stresses which led to their formation are relieved and should no longer be effective. Second, the Ta from the pellet debris will be deposited on the wall and will tend to fill the cracks with fresh material, albeit at the slow rate of 11 μm/month. However, if plastic flow should be an insurmountable problem, the stresses can be restricted to the elastic regime by reducing the energy yield to 175 MJ. However, this would require an increase in repetition rate to 20 Hz to maintain the original thermal power of 3500 MWt.

The deposition on the Ta coating of the Ta in the pellet debris also tends to compensate for variations in coating thickness. The thinner portions will be nearer the cooler liquid lithium in the steel tubes and will therefore be at a lower temperature than the thicker portions. The Ta in the pellet debris will more likely stick to a cooler surface than to a hotter surface. The result will be a preferential buildup of the pellet debris Ta onto the thinner portions of the coating.

The deposition on the coating of the Ta in the pellet debris clearly has some advantages, but one disadvantage is that at an accumulation rate of 136 μm per year, the desirable thermal and physical properties of the coating may be altered, particularly since the deposited Ta may not have the same crystalline structure or be as pure as the original coating. The excess Ta deposited on the coating can be simply removed by occasionally injecting a pellet with a modified yield to evaporate the excess Ta which could then be removed by the gas pumping system.

4.1.3 REFERENCES

1. J. M. Kindel and M. A. Stroscio, "Double-Shell Target Designs for LASL EBS," p. 109, Laser Fusion Program Progress Report LA-7328-PR (1977).

2. J. A. Blink, P. E. Walker, and H. W. Meldner, "Target-Dependent Effects," p. 8-25, Laser Program Annual Report UCRL-50021-77 (1977).

4.1.4 PELLET FABRICATION

FUNCTION

The pellet fabrication system produces spheres of DT fusile fuel, encapsulated in various light and heavy shells, which are delivered to the center of the reaction chamber where they are imploded by absorbing energy from laser beams.

DESIGN REQUIREMENTS

The pellet fabrication plant must be capable of producing approximately 10^6 pellets per day to fuel the power plant. In addition, it should have the facilities to store about a 30 day supply of pellets to ensure continuous plant operation in the event of pellet factory shutdown. The pellet plant could be located in a separate building near the power plant since a day's supply of pellets would occupy about a cubic meter of space and be easy to transport to the power plant on a daily basis. Safety precautions against T leakage will be required in the transport process as well as in the plant itself. Because the pellets under consideration for commercial fusion have extremely stringent requirements on tolerance and uniformity, the plant should include inspection systems at various stages of pellet manufacture to insure a high quality product.

A useful, high gain pellet for laser fusion will probably be of the shell within a shell design as shown in Figure 4.1.4-1. There is a near vacuum region between the shells which allows the outer shell to absorb much of the beam energy and accelerate inwards before striking the inner, fuel-rich sphere. This results in a nearly isentropic compression of the fuel which is highly desirable for maximizing gain. The inner sphere contains the DT fuel in gaseous form during manufacture but it is subsequently frozen to provide a solid inner shell before ignition. The two shells will consist of a low density material, probably plastic, impregnated with a high atomic number metal such as tantalum to shield the fuel from preheating due to x-rays and fast electrons. The shells are required to be spherical

to ∿ 1%, to have surface imperfections not exceeding ∿ 200Å and to be concentric to ∿ 1 μm.

The pellet shown in Figure 4.1.4-1 is somewhat idealized. It is apparent, for instance, that some supporting structure is necessary to keep the inner sphere suspended within the outer sphere. The perturbation caused by a support system should be minimized, however, in order to maximize the compressive force on the inner sphere. Another compromise will probably be necessary with regards to the plastic inner shell. If this inner shell is filled with DT by gaseous diffusion, then it will not be able to withstand the elevated temperatures and pressures normally associated with this diffusion process. Thus, it will probably be necessary to include an additional glass or ceramic shell, through which the DT filling occurs, and to subsequently coat this with the required plastic shell. Again, this extra glass shell should be kept as thin as possible so as not to greatly perturb the original design.

The final step in the manufacturing process will be to solidify the DT into a uniform inner shell and to preserve this as a solid shell up to the instant of ignition. This solidification step should probably occur near the pellet injector in the reactor building.

SUMMARY DESCRIPTION

The pellet described above poses formidable manufacturing difficulties, particularly when we realize that the requirement on shell surface perfection rules out the use of seams or join regions. While the creation of near perfect single glass shells can be accomplished by a drop tower technique, the creation of a shell within a shell with both shells meeting the stringent surface and concentricity requirements discussed above has, to our knowledge, not been achieved. We propose a solution to this manufacturing problem involving the development of new technology. We will present it in the context of the overall manufacturing process beginning with the inner shell.

We propose making the inner shell out of glass by means of a drop tower technique. This technology has been considerably advanced by the work at LLL[1]. While the shells made so far are much smaller than would be useful for commercial fusion, the method appears capable of working far larger shells. Essentially a droplet generator creates droplets of liquid glass at the top of a drop tower by vibrating a jet of liquid. As the drops fall in the partially evacuated and heated top zone of the tower, they expand and form bubbles because of the entrapped gasses. These bubbles solidify in cooler regions of the tower and are eventually collected in an oil bath at the bottom. The success of this procedure depends on careful control of conditions in the tower and on careful selection of parameters such as the lengths of the heated and cooled regions of the tower. With proper care, the yield of acceptable shells is as high as 90%[1].

This initial glass shell will have to be filled with DT before additional shells are added. Diffusion calculations, which will be presented in Section 5.1.4, show that filling a glass shell with gaseous DT at 500°C requires several days' time. This time would increase considerably were diffusion required to occur through additional shells. In addition, this high temperature would be damaging to any plastic layers. The glass shells should be made thick enough to withstand the internal DT pressure when they are removed from the diffusion chamber (autoclave) and brought to room temperature and pressure for subsequent processing steps. This thickness depends on the tensile strength of the glass which should be chosen as high as possible to minimize the thickness.

The glass shell is then coated with the required thickness of plastic impregnated with tantalum (TaCHO). This plastic coating will be applied by physical vapor deposition with an RF discharge to polymerize the plastic. In addition, it will be necessary to individually levitate the pellets in a gas jet during the coating process to prevent collisions[2].

Conceptually, the method we propose for fabricating the outer shell with the inner shell suspended inside it, involves making a temporary, sacri-

ficial outer shell. This sacrificial shell is formed by joining two hemispheres together. The join region is acceptable here because this shell will not be present in the final pellet. The two halves of this shell will contain a network of quartz fibers to suspend the inner shell as shown in Figure 4.1.4-2. This network is designed so that when the two half shells are joined, the quartz fibers are placed in tension for positive positioning of the inner sphere. The quartz fibers project beyond the sacrificial shell but are attached by glue or cement to the sacrificial shell in the region where they pass through it. The join region must be smoothed over by filling in the crack and smoothing off any rough edges by polishing so that the outer surface of the temporary shell has the required finish.

The sacrificial shell with projecting quartz fibers is then coated with a porous material, having a pore size smaller than the surface finish tolerance of $\sim$ 200 Å. The projecting quartz fibers embed in this porous shell which is expected to be free of imperfections because of the smoothing of the surface of the sacrificial shell. The sacrificial shell is then removed by a gasification reaction through the pores of the just deposited outer shell, leaving the glass fiber suspension system intact since the fibers are now attached to the porous shell. The porous shell is then coated with the desired thickness of TaCHO, just as the inner shell was coated previously. This method introduces an additional shell which for reasons cited previously should be kept as thin as possible consistent with having sufficient strength to anchor the suspension system.

As a concrete realization of the preceding fabrication scheme, the sacrificial shell will be made of nickel and the gasification reaction will be the carbonyl reaction: $Ni + 4\ CO \rightarrow Ni(CO)_4$ where the nickel carbonyl is gaseous at the reaction temperature of about 100°C. This temperature is low enough that the plastic coating will be unaffected. The nickel may be recovered by essentially reversing the above reaction and may then be reused to make new sacrificial shells.

For the porous shell, we use a relatively new type of ceramic called a metal-organic-derived-oxide (MODOX). This ceramic or glass is made by means of easily controlled chemical reactions that take place at low temperatures (below 500°C). It is formed by the molecular mixing and subsequent reaction of soluble metal alkoxides in the presence of water. The metal alkoxides are readily obtainable, often as liquids of high purity. Thus the composition of the MODOX can be varied by mixing together several metal alkoxides before allowing them to react.

For example, a MODOX reaction involving silicon alkoxide, $Si(OR)_4$, and aluminum alkoxide, $Al(OR')_3$, where R and R' are hydrocarbon groups, would proceed as follows:

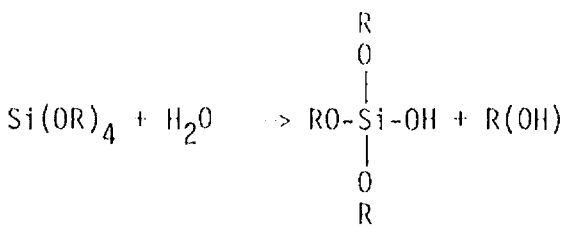

$$Si(OR)_4 + H_2O \rightarrow RO\text{-}Si(O\text{-}R)_2\text{-}OH + R(OH)$$

The active OH group on the soluble silanol reacts further:

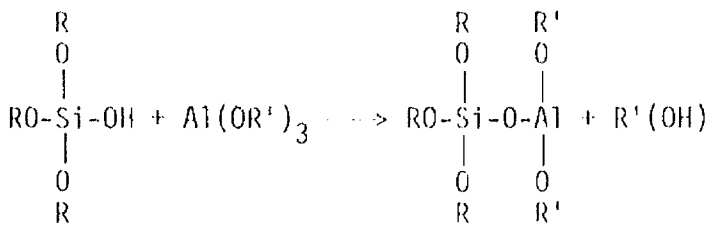

$$RO\text{-}Si(O\text{-}R)_2\text{-}OH + Al(OR')_3 \rightarrow RO\text{-}Si(O\text{-}R)_2\text{-}O\text{-}Al(O\text{-}R')_2 + R'(OH)$$

As more water is added, polymerization continues until the entire solution gels into a clear, stiff single phase containing a matrix of silicon and aluminum cross-linked by means of oxygen bonds.

The glass formed by the above process is quite porous. The pores occupy about 60% of the volume. Significantly, the pore size distribution is sharply peaked about some mean value. The average pore size may be adjusted by varying suitable parameters during the polymerization process. Average pore sizes in the range of 40-100 Å are easily attainable with standard deviations of only a few Angstroms[3].

2 OF 4

DOE/DP

40086-1

(VOL I)

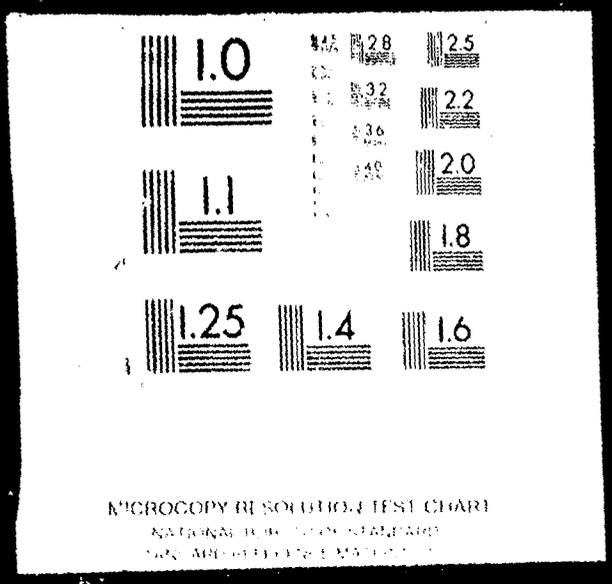

We note the possibility that the composition of the MODOX shell may be chosen to enhance pellet performance; for example, a high atomic number metal may be incorporated. After the nickel shell is removed, any residual gas in the pellet may be evacuated through the pores of the MODOX shell before the outer plastic shell is deposited. The composition and pressure of the gas in the inter-shell region may be selected by depositing the final plastic shell in the desired gas mixture. Since the pressure is expected to be small, this should not seriously interfere with the vapor deposition of the plastic shell. The quartz fiber support system should be designed to withstand the inertial forces which will develop when the pellet is accelerated in the injection device. These forces appear to be modest for the inner shell masses of interest and for the injection systems under consideration.

A diagram of a pellet factory which provides for the major tasks outlined in this section is shown in Figure 4.1.4-3. The factory will require a total floor space area of about $1000m^2$. The drop towers will be about 20m high. The storage area keeps the pellets at liquid nitrogen temperatures. Sufficient cooling power should be provided to remove the heat generated by the tritium beta decay. The inspection area will contain the necessary x-ray or optical inspection equipment and computer system for automatically inspecting the pellets. Possibly only a statistical sample of the pellets will need to be inspected. The factory is designed so that tritium cannot escape to the outside in the event of an accident. A list of the major subsystems of the pellet factory and some important parameters are given in Table 4.1.4-1. These parameters apply to a 350 MJ pellet that is being fired at the rate of 10 per second. The estimated total power consumption of this pellet factory is 500 kW.

TABLE 4.1.4-1

MAJOR SUBSYSTEMS OF THE CO_2 LASER PELLET FACTORY

1. Drop tower (need at least 2 for redundancy)

Height	20 m
Diameter (of structure)	7 m
Power Consumption	50 kW

2. Autoclaves

Number required (500 liter capacity)	20
DT Fill Temperature	500°C
DT Fill Pressure	60 MPa (600 atm)
DT Fill Time	~ 1 week
Power Consumption	200 kW

3. Vapor deposition (for TaCHO shells) including jet sources for levitation

4. Nickel shell processing with equipment to attach quartz fibers

5. MODOX shell deposition

6. Nickel gasification facility

   Closed system required because of gas toxicity

7. Inspection area

   Computers, x-ray, optical equipment

8. Storage area (30 day supply)

Storage volume	30 m^3
Storage temperature	77°K
Cooling power (including refrigerator efficiency)	50 kW

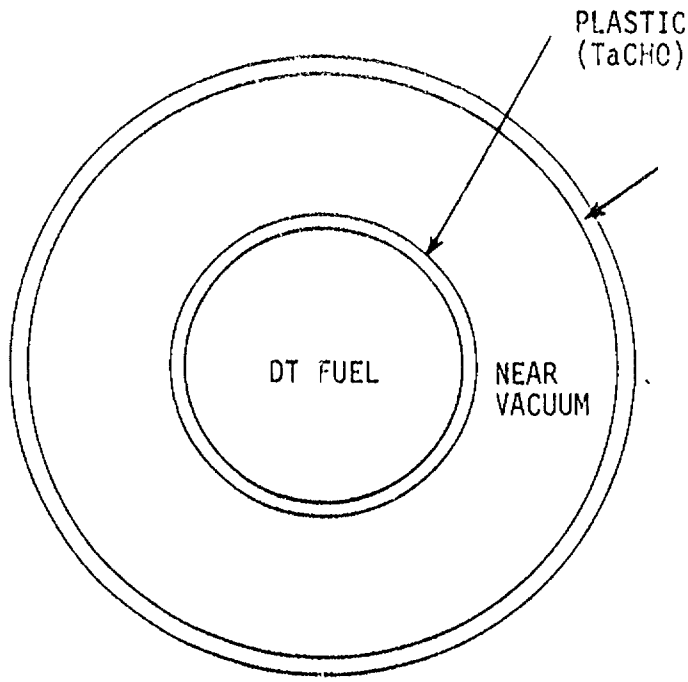

Figure 4.1.4-1. Shell Within a Shell Pellet

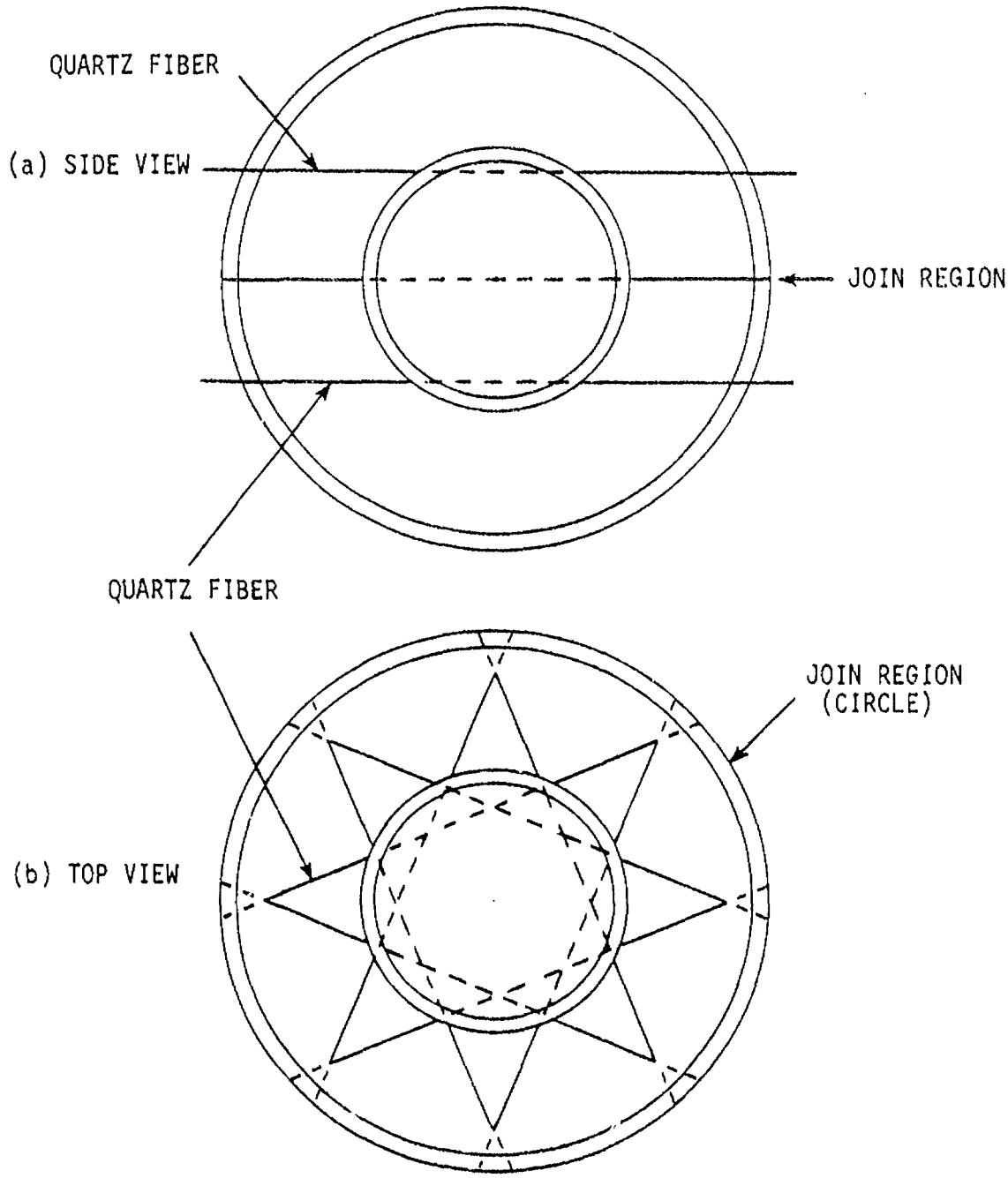

Figure 4.1.4-2. Suspension System for the Shell Within a Shell Pellet — (a) Side View, (b) Top View

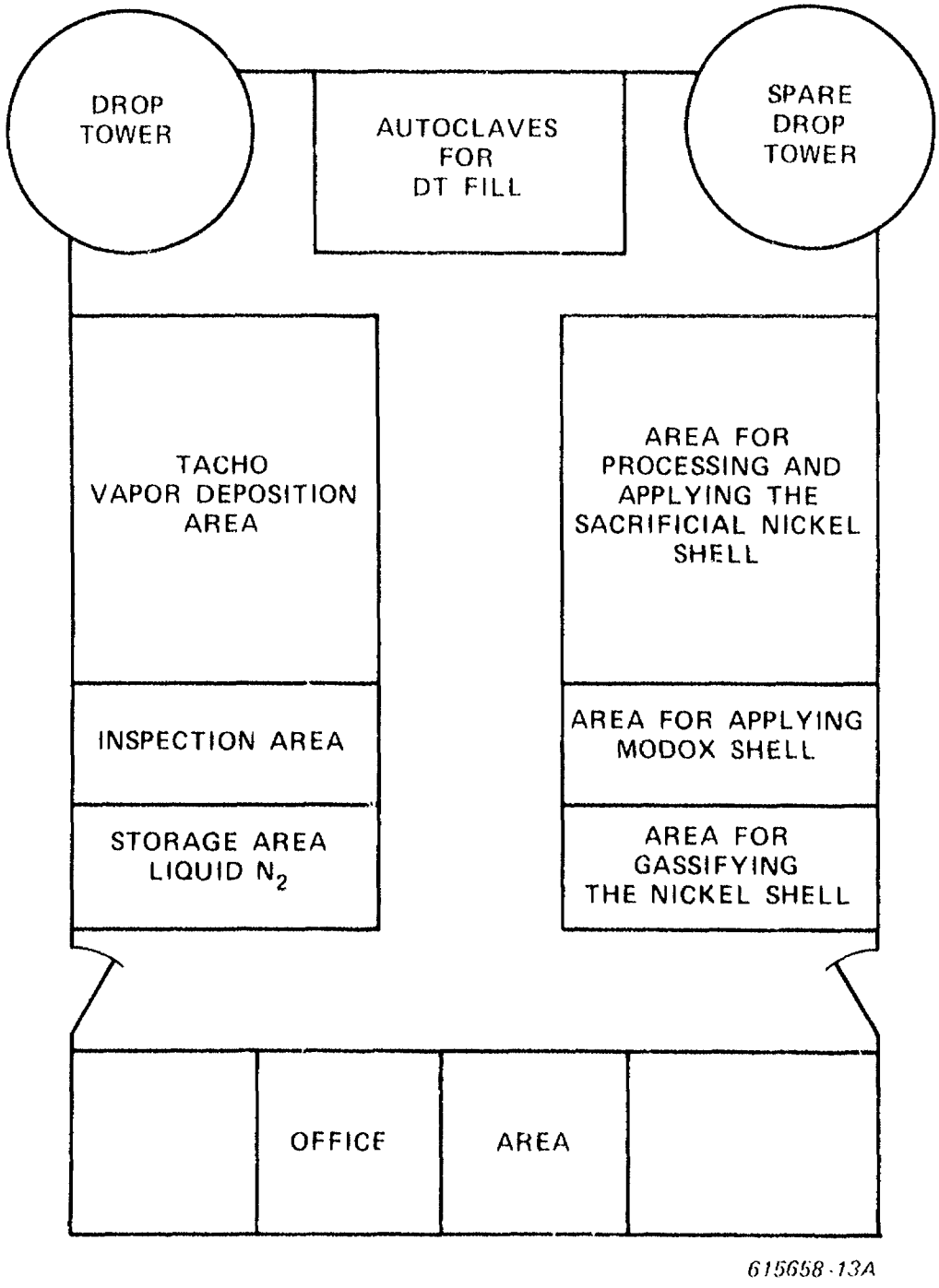

Figure 4.1.4-3. General Plan View Arrangement of a CO_2 Laser Pellet Factory

4.1.4. REFERENCES

1. A. Rosencwaig, J. L. Dressler, J. C. Koo, and C. D. Hendricks, "Laser Fusion Hollow Glass Microspheres by the Liquid-Droplet Method," Lawrence Livermore Laboratory Report: W-7405-ENG-48, June 5, 1978.

2. C. D. Hendricks and W. L. Johnson, "Electrostatic Levitation, Control and Transport in High Rate, Low Cost Production of Inertial Confinement Fusion Targets," Lawrence Livermore Laboratory Report: PREPRINT UCRL-82752, May 25, 1979.

3. B. E. Yoldas, "A Transparent Porous Alumina," The Am. Cer. Soc. Bull., Vol. 54, No. 3, March, 1975, pp. 286-288.

4.1.5. PELLET INJECTION AND TRACKING

FUNCTION

The function of the pellet injector is to transfer the cryogenic pellet from the pellet factory to the center of the reaction chamber without significant absorption of heat by the pellet. The pellet velocity must be sufficient for it to travel from the injector to the center of the reaction chamber during the time interval between shots. Very precise trajectory is necessary.

The function of the tracking system is to enable the driver beams to accurately strike the pellet during its free flight through the reaction chamber. Alignment is corrected by adjusting the aim of the injector between shots.

DESIGN REQUIREMENTS

The nominal design goals for the pellet injection and tracking system are presented in Table 4.1.5-1.

TABLE 4.1.5-1.

INJECTION PARAMETERS

Nominal pellet free flight path length	15m
Trajectory precision at end of free flight path	0.25mm
Nominal pellet injection velocity	300m/s
Nominal pellet position accuracy (gating driver beams)	0.25mm
Nominal pellet injection rate	10/s

DESIGN DESCRIPTION

Figure 4.1.5-1 presents an overall conceptual design of the fusion pellet injection and tracking system. Vertical injection is mandatory since any slight deviation in pellet injection velocity would result in variations of trajectory if gravity were allowed to act on a pellet with a horizontal trajectory component. Upward injection is chosen to

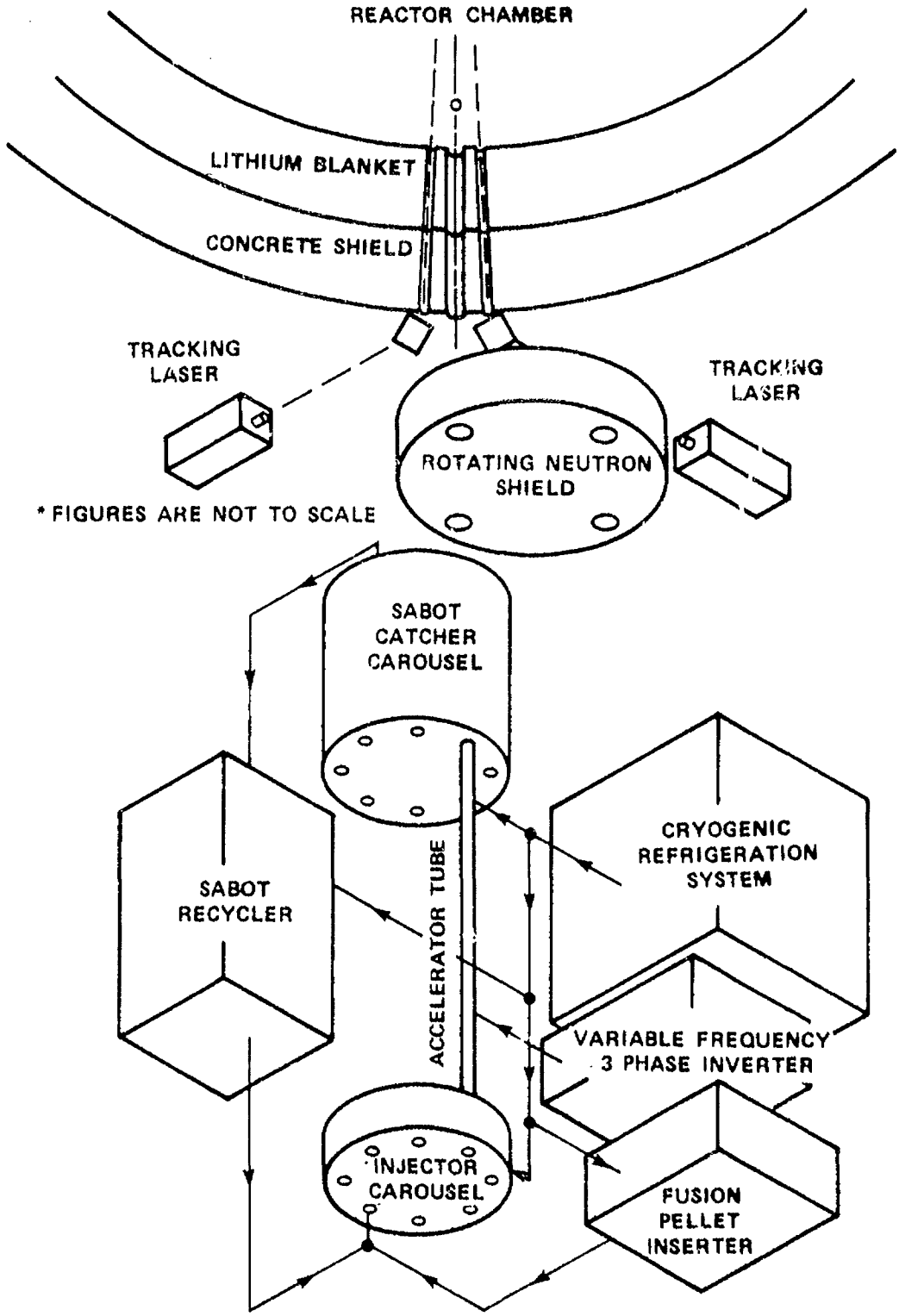

Figure 4.1.5-1. Conceptual Arrangement of Pellet Injector System Interface with Reactor

allow for structural and maintenance considerations relative to the reaction chamber.

The pellets are encased in sabots which serve to isolate them from the accelerator tube while applying the accelerating force to the pellets. The mechanical isolation prevents the pellet from acquiring any components of velocity perpendicular to the launch axis or from acquiring any spin components. Thermal isolation afforded by the sabot prevents the pellet from heating up during handling or launch. The sabot is cooled to cryogenic levels prior to insertion of the sabot. Pellet and sabot are placed in individual chambers in an injector carousel which rotates each into position just prior to launch.

The launch tube is a smooth bore guide tube with cryogenically cooled propulsion coils embedded axially within the tube walls. These coils act upon a permanently magnetized sabot with a frequency swept three phase current drive in such a way as to form a linear synchronous motor. Most of the initial length of the guide tube acts to accelerate the sabot while the final portion decelerates the sabot by electromagnetic dynamic braking. This separates the sabot from the pellet in a nonturbulent manner when the pellet reaches full injection velocity. The pellet then proceeds in free flight along the established trajectory to the exact center of the reaction chamber.

The sabot catcher carousel rotates into position such that the pellet passes through an unobstructed hole enroute to the reaction chamber. The sabot on the other hand has been greatly but not completely decelerated within the accelerator tube and it is brought to rest in the sabot catcher carousel. The carousel retains the sabot and rotates to remove the sabot from the launch axis. The sabot is subsequently ejected and routed back to the sabot recycler where it is inspected for possible replacement, remagnetized, cooled to cryogenic temperature and sent back to the injector carousel.

The pellet, after passing through the sabot catcher carousel, passes through one of the tunnels in the rotating neutron shield. This shield is rotated at constant velocity and synchronized with other pellet accelerator components so that it offers a free flight path to the reaction chamber during injection. During the pellet flight time, the neutron shield rotates to obstruct the flight path and thus shield the injection mechanism during fusion.

The azimuthal tracking lasers (three 1 watt argon lasers) are used to determine the extent to which the pellet deviates from the intended injection axis. They are shielded from direct reactor radiation by using mirrors to deflect their beams. Optical receiver ports corresponding to these laser input ports are placed at the top of the reactor chamber and are also protected by deflection mirrors.

In addition to azimuthal tracking, there is need for an accurate position sensor to determine when the pellet is about to reach the exact center of reactor chamber, the designated target area. This is done with a fourth laser beam positioned at right angles to the pellet trajectory and intersecting the pellet's path about 1 cm. prior to the designated target point. The velocity of the pellet is relatively uniform from pellet to pellet, and thus if one knows the exact instant that the pellet is within 1 cm. of the target point, one can use this time plus a slight fixed delay to ensure that the fusion drivers pulse when the pellet is in position.

Details of the pellet accelerator tube are presented in Figure 4.1.5-2. Rather than apply the accelerating force directly to the pellet, it is advisable to accelerate a recoverable sabot which carries the pellet to its injection velocity and then separates and is caught prior to entering the reaction chamber. The intent is to isolate the pellet from both the propulsive medium and undesirable friction and bumping on the walls of the guide tube. By doing so, it is felt that the pellet will acquire a minimum of heat, spin and velocity normal to the intended injection path. The sabot will be precooled to the pellet temperature

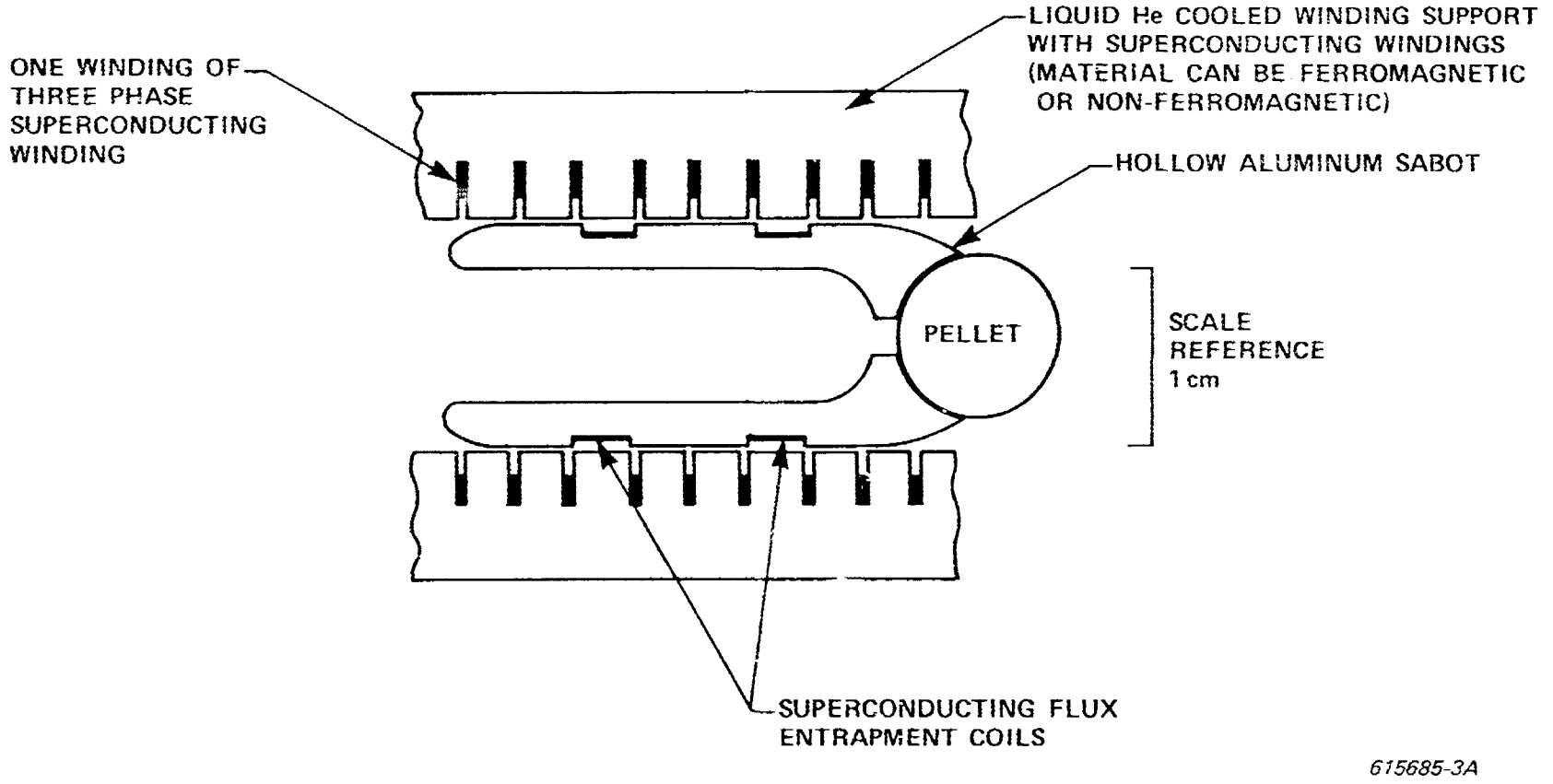

Figure 4.1.5-2. Cylindrical Sabot in Tubular Launcher

or lower and by virtue of its mass and bulk thermal resistance, it will have little tendency to transfer heat into the pellet during the brief interval of acceleration. Although pneumatic propulsion has been considered, the problems introduced by the propulsive gas and the inaccuracies of pellet speed indicate electromagnetic acceleration is preferable.

To achieve practical operation, the coupling of energy to the sabot must be accomplished by purely electromagnetic means. The necessary permanent magnetic field of the sabot could be achieved by building it of a permanent magnetic or ferromagnetic material, but these techniques are limited by the material saturation flux density and require relativley dense materials. Instead, one can take advantage of the cryogenic temperatures associated with the sabot and pellet to fabricate a permanent magnet by superconducting flux entrapment. This is accomplished by building the sabot of some non-superconducting material such as aluminum and fabricating superconducting bands around it.

If such a sabot is placed in a reasonably intense magnetic field of 1 Tesla or more and then cooled to cryogenic temperatures, the flux becomes entrapped by the currents induced in the superconducting band and it is retained so long as the sabot tmeperature remains below the critical temperature of the superconductor. This allows the fabrication of a high intensity permanent magnet having the low mass of a hollow aluminum sabot.

The proposed accelerator configuration is a cylindrical sabot within a cylindrical guide tube. Tne sabot is symmetrical so that it can be inserted either end forward and still function properly. It has its magnetic flux entrapped axially by means of two superconducting bands and thus the flux lines complete their required path by emerging radially from the sabot to interact with the drive windings of the launch tube. To minimize sabot mass, it is hollow.

Superconducting windings in the launch tube are in the configuration of a stack of foil washers in each slot. This is done to force all of the sabot flux to cut each of the drive windings and thus achieve maximum force. Every third coil of the drive windings is driven by the same phase of a variable frequency three phase current supply and thus the accelerator is actually a three phase linear synchronous motor. To achieve proper operation, such a synchronous machine requires that the frequency of the power supply be linearly proportional to the speed of the sabot. The sabot will thus move at exactly the same velocity as the propagating magnetic field and thus the pellet injection velocity can be controlled as precisely as the frequency of the power source. Characteristic of synchronous machines, the speed is not a function of applied drive power or pellet mass once a minimum threshold of drive is exceeded.

The vertical pellet injection system, made possible by the high force electromagnetic accelerator, avoids the influence of gravity on the pellet trajectory. This overcomes the need for precise pellet tolerances and for dynamic pellet or beam steering. Theoretically, the pellet will always pass through the exact center of the reactor chamber although its time of arrival is subject to some variation.

The pellet is intended to be a fixed point of reference in this system. In other words, the injection and tracking system will attempt to always cause the pellet to pass through the exact center of the reaction chamber and to precisely indicate the time when the pellet arrives at the chamber center.

The pellet tracking concept is illustrated in Figure 4.1.5-3 Since it is difficult to construct an isometric drawing of adequate clarity in this case, perhaps it will be helpful to describe the geometry as similar to the Chinese finger trap. Consider three parallel beams passing parallel to the axis of injection and through two imaginary discs which are perpendicular to the axis of injection. Now imagine that the

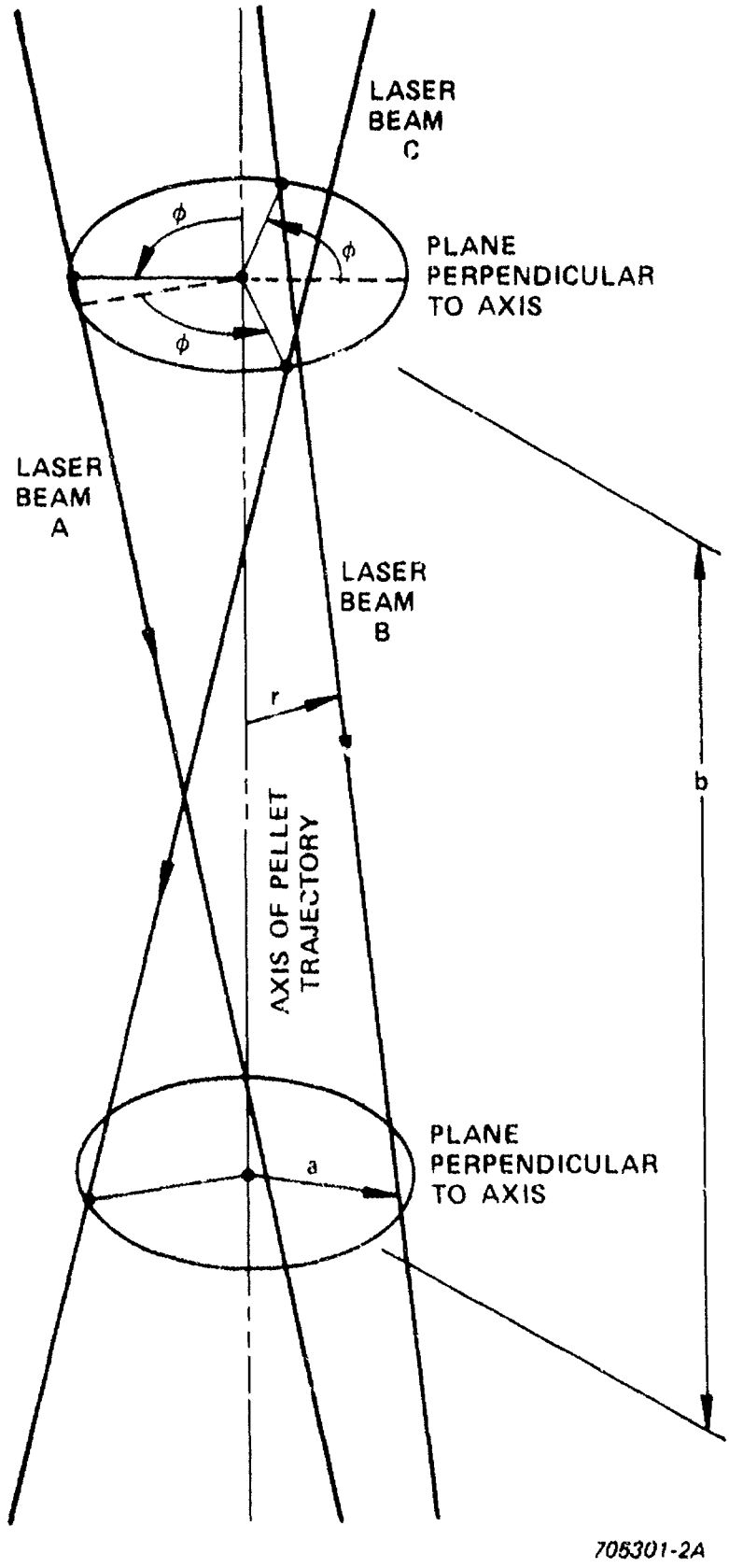

Figure 4.1.5-3. Pellet Tracking Beam Concept

two discs are rotated with respect to each other while the beams intersect each disc at the same point as they did originally. The distance between any beam and the axis of injection is a function of the position along the axis and is a minimum half way between the imaginary discs.

To illustrate how this technique is employed, consider the beams as being positioned around the injection axis. Although the beams themselves are straight, the beam to axis separation bows in toward the axis and back out again at both ends of the beam. The narrowest region of the beam array is positioned half way between the chamber center and the first wall. It is in fact made somewhat less than the diameter of the pellet so that any pellet moving exactly along the axis will break all three beams simultaneously and will maintain the interruption for a large fraction of the flight path. If the pellet is not exactly on axis, it will break one of the beams sooner and maintain the interruption for longer than the other two beams. This is easily detected and since the detection occurs well in advance of the pellet reaching the chamber center, it could be used to beam steer the drivers for each shot. It is anticipated that such dynamic corrections will not be necessary and thus the tracker will serve only to correct pellet or beam position on a consecutive shot basis.

Determination of the pellet's position in the axial direction is not important until it is at the target area. This will be done by a fourth laser beam intersecting the injection axis at a right angle and positioned to intercept the pellet 1 cm prior to its arrival at the designated target point.

Concern over the long term effects of neutron or driver radiation on the beam sources and detectors will have to addressed, but at present it looks as though the best approach is to use mirror deflection and shielding such that the laser beam is reflected more easily than the driver beam or the reactor neutron output. This requires tracking

lasers of much higher power than one would normally employ. If CO_2 drivers are used, it is possible to insert SF_6 absorption cells in the optical sensor path to absorb the reflected CO_2 light. Pellet heating should be no problem since the power levels are still very small and they intercept the pellet only briefly during its flight.

Focusing and alignment of the driver beams is a matter not directly measured by the proposed instrumentation. Apparently, means exist to perform an initial alignment of the drivers to some "optimal" standard. The problem is that there is expected to be some alignment drift during extended operation. The proposed pellet injection system can be considered capable of repeatedly placing the fuel pellet in the center of the target area and precisely detecting its position during repeated operations. Thus, the pellet position can be considered as a fixed point of reference. Assuming that during the course of repeated shots the system will drift to a new equilibrium position, one would expect that an iterative optimization over many shots to be an effective means of system alignment. Computer search and optimization algorithms exist which allow optimization of a multivariable system by methodically peaking one parameter at a time to maximize output. Although these techniques sometimes converge to local optima rather than true maxima, they generally perform well in systems where a good initial starting point is available and where the increments of adjustment are relatively small for each iteration.

4.1.6 REACTION CHAMBER AND SUPPORTING SYSTEMS

4.1.6.1 MECHANICAL AND STRUCTURAL CONSIDERATIONS

FUNCTION

The functions of the reaction chamber are to accommodate the pellet micro-explosion energy release in a controlled fashion in order to breed tritium and transfer the thermal energy to a heat transport system from which it can be converted to electrical power. In addition, the chamber should provide some degree of shielding to attenuate irradiation and reduce the amount of external shielding to protect the concrete building structure and minimize activation of reactor and auxiliary system components. In order to perform these functions, a first wall and blanket are necessary components of the reaction chamber. The first wall must absorb energy primarily attributed to x-ray irradiation and ion bombardment (about one half of the total) while the blanket must absorb the bulk of the neutron energy in order to produce tritium and convert the neutron energy to heat. An active coolant system is required to transfer the heat from the blanket for conversion to electrical power and for transferring bred tritium for processing for use as fuel. The chamber shall also provide suitable penetrations for interfacing with the laser driver beams, vacuum pumps, pellet injector and pellet tracking system. The reaction chamber requirements and parameters are tabulated in the following section.

DESIGN REQUIREMENTS

The reaction chamber shall be designed to satisfy the requirements and parameters specified in Table 4.1.6.1-1. Requirements for the chamber with both the Heavy Ion Beam (HIB) and laser driver system are included for comparison and are seen to be identical except for the driver interface and chamber pressure.

TABLE 4.1.6.1-1. REACTOR CHAMBER REQUIREMENTS AND PARAMETERS

	LASER	HIB
PELLET THERMAL OUTPUT	3500 MWt	3500 MWt
ENERGY DISTRIBUTION		
X-RAYS AND IONS	45%	45%
NEUTRON	55%	55%
CHAMBER PRESSURE	$< 10^{-1}$ Torr	$\sim 5 \times 10^{-4}$ Torr
REACTION CHAMBER		
SHAPE	Sphere	Sphere
RADIUS TO FIRST WALL	10 m	10 m
FIRST WALL AND STRUCTURE		
MATERIAL	Steel	Steel
TEMPERATURE	500° C Max	500° C Max
PENETRATIONS/WALL COVERAGE	Consistent with achieving Tritium Breeding Ratio of $\geq$ 1.1	Consistent with achieving Tritium Breeding Ratio of $\geq$ 1.1
COOLANT	Liquid Lithium	Liquid Lithium
LIFETIME		
CHAMBER	30 Years	30 Years
FIRST WALL	5 Years	5 Years
BLANKET		
BREEDING MATERIAL	Liquid Lithium	Liquid Lithium
REFLECTOR	Graphite	Graphite
INTERFACING COMPONENTS	Laser Beams, Vacuum Pumps, Pellet Injector, Pellet Tracking Systems	Ion Beams, Vacuum Pumps, Pellet Injector, Pellet Tracking Systems
TOTAL NUMBER OF DRIVER BEAMS (2-SIDE ILLUMINATION)	108	20

SUMMARY DESCRIPTION

The spherical shaped reactor chamber is lined with 324 tapered HT-9 steel tubes which are closely nested to form the first wall surface located at a radius of 10 m. The tubes enter at the equator at a penetration in the sphere, expand to a maximum diameter at the pole region beyond which the tubes converge in diameter until they exit at the chamber penetration at the opposite side (see lower schematic of reactor chamber, Figure 4.1.6.1-1). The tubes which are welded together at their points of tangency are contained in a surrounding HT-9 sphere to provide additional structural support. HT-9 was selected as the first wall material because of its greater strength and higher thermal conductivity (as compared to stainless steel). The relatively high operating temperature capability (500° C) is also compatible with removing the high heat flux on the first wall while maintaining a reasonable temperature drop through the wall to achieve high coolant exit temperatures necessary for acceptable thermal performance. The temperature drop across the wall is low enough to avoid excessive thermal stress.

The first wall surface of the tubes (see upper schematic of 4.1.6.1-1) is covered with $\sim$ 0.1 cm tantalum coating to isolate the tube from the high thermal spikes that accompany each pellet microexplosion which occurs at a rate of 10 Hz. This coating prevents thermal cycling of the tube which could lead to high cycle stress fatigue. The first wall is expected to have a 5 year life. Flowing lithium serves as the first wall coolant. A lithium blanket region, which contains a graphite reflector clad with steel, is located behind the first wall. In-situ tritium removal can be accomplished by removing a portion of the total flow from the reactor chamber and passing it through a tritium extraction system. Finally the entire assembly of first wall, blanket and reflector, Figure 4.1.6.1-2, is enclosed in a steel outer sphere which acts as the overall support structure for the above components. The sphere is split at the horizontal centerline and is fitted with flanges on the upper and lower hemisphere to permit the upper hemisphere to be lifted off for removal of the first wall assembly. The flange will be clamped and seal welded to prevent leakage of lithium to the surrounding environment. The outer sphere is expected to last for 30 years.

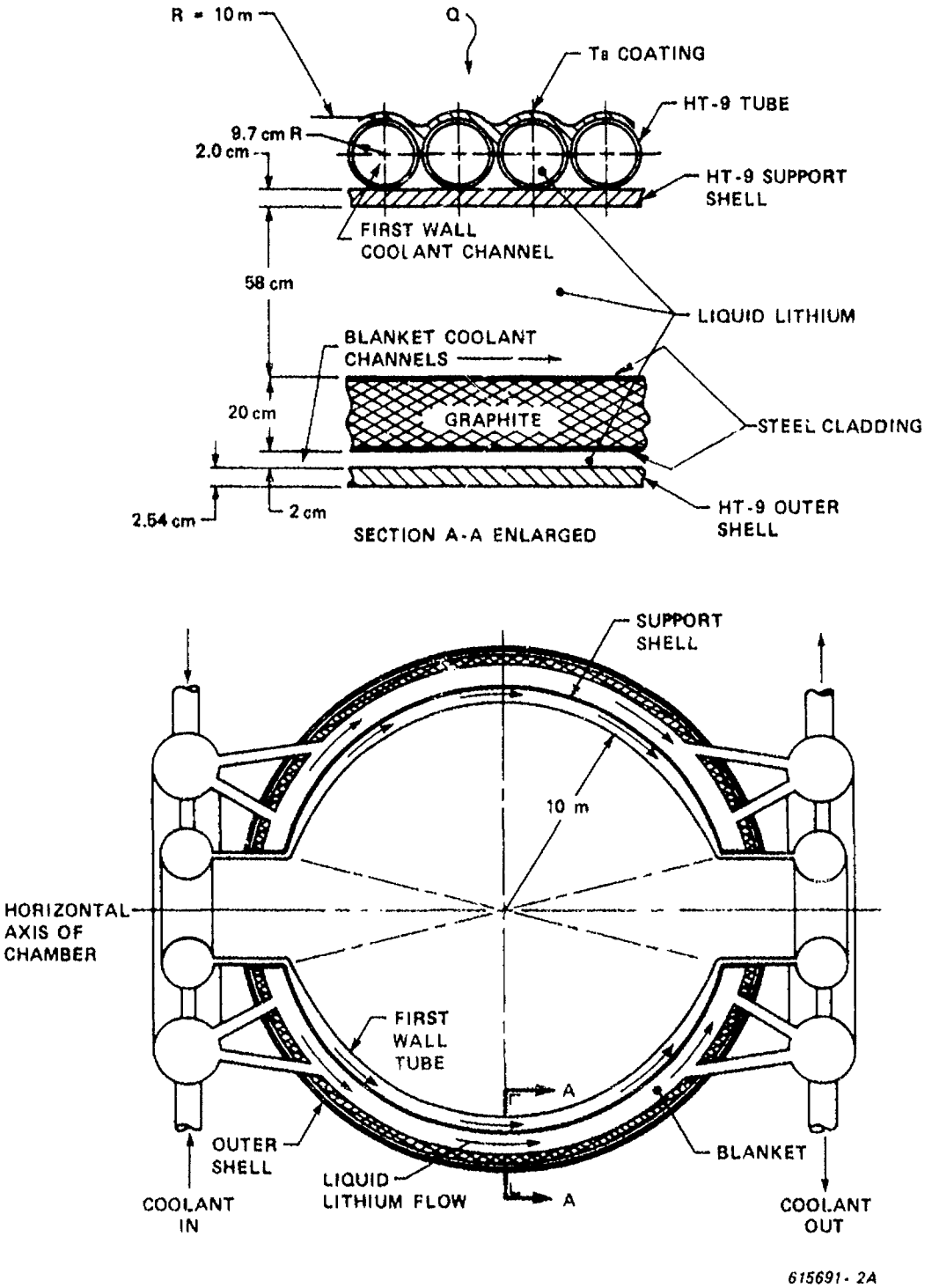

Figure 4.1.6.1-1. Schematic Representation of the Tubular First Wall and Blanket Concept

The reaction chamber provides for the penetrations necessary to interface with the laser driver beams, pellet injector, pellet injector tracking system, vacuum pumps and primary heat transfer system piping and components. The major penetrations (for the laser beams) are two 6.5 m openings on opposite sides of the horizontal centerline. The outside of the reaction chamber is covered with alumina silica insulation to minimize heat losses from the chamber.

Performance and design parameters for the reactor system, which include the primary heat transport system interfacing components and reaction chamber, are tabulated in Table 4.1.6.1-2. Because of the similarity between the reaction chamber designs, both the laser and HIB reactor systems are included for comparison. The essential differences in chamber configuration lie only in the entry beam angle, beam penetration requirements and vacuum pumping loads and will be discussed later.

The chamber concept depicted in Figure 4.1.6.1-2 shows the size relationship of the chamber, first wall, blanket, piping, and major penetrations. The concept description and operation will be addressed in more depth in the following section.

INTERFACING SYSTEMS

The reaction chamber concept investigated to meet the requirements presented in the previous section and the pertinent features necessary for interfacing systems and components will be discussed in greater detail in this section. The chamber (Figures 4.1.6.1-1 and 4.1.6.1-2) contains two concentric shells, consisting of an inner support shell surrounding the tubular first wall and an outer shell of larger diameter to provide for an annular primary blanket region between these shells. Two 6.5 m diameter openings are provided for laser beam entry and vacuum pumping. Space is provided in the blanket annulus for a graphite reflector to enhance breeding. Because the first wall is cooled by liquid lithium flowing through the tubes, additional breeding is achieved to supplement the tritium breeding obtained in the primary blanket region. Toroidal coolant manifolds are provided at each side of the chamber at the 6.5 meter penetrations to supply lithium to the chamber and from the chamber to the primary heat transport system (PHTS) coolant loops.

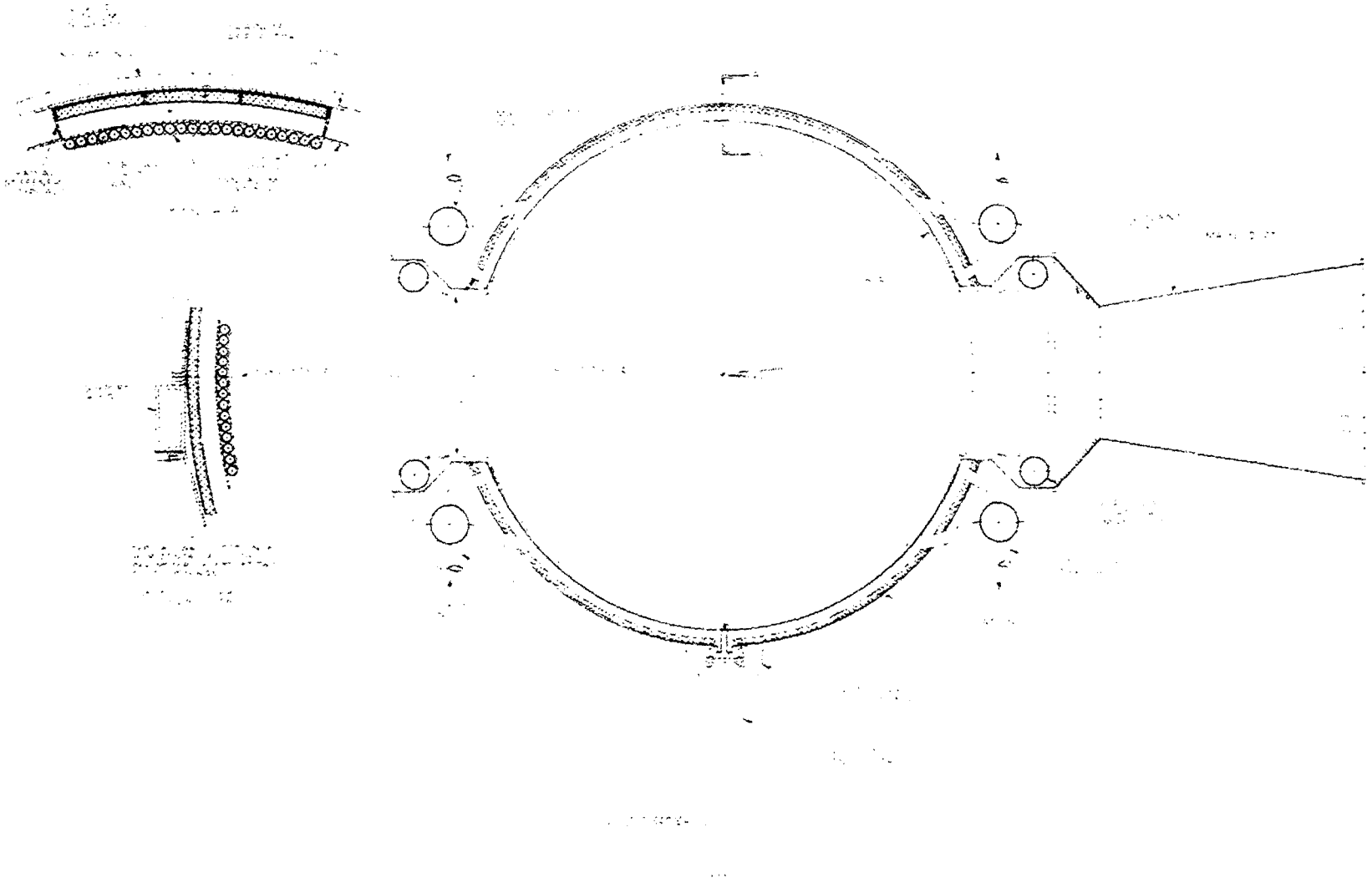

Figure 4.1.6.1-2. Reaction Chamber Concept for the Laser Driven Reactor

TABLE 4.1.6.1-2 REACTOR SYSTEM PERFORMANCE AND DESIGN PARAMETERS

Driver	CO_2 Laser	Heavy Ion Beam
Thermal Output	3500 MWt	3500 MWt
Chamber Pressure	$\sim 10^{-1}$ Torr	$\sim 5 \times 10^{-4}$ Torr
Protective Atmosphere	Xenon	---
Reaction Chamber		
Shape	Sphere	Sphere
Radius to First Wall	10 m	10 m
First Wall Configuration	Tubular	Tubular
Material/Coating	HT-9/Ta	HT-9/Ta
Tube Diameter - Variable, OD	19.4-6.23 cm	19.4-6.23 cm
Tube Wall Thickness	0.18 cm	0.18 cm
Ta Coating Thickness	0.1 cm	0.1 cm
Tube Temperature, Max	500° C	500° C
Structural Support Sphere		
Material	HT-9	HT-9
Thickness	2.0 cm	2.0 cm
Blanket Annulus Thickness	80 cm	80 cm
Lithium Thickness	60 cm	60 cm
Graphite Reflector	19.8 cm	19.8 cm
Graphite Clad Thickness	0.1 cm	0.1 cm
Outer Sphere		
Material	HT-9	HT-9
Outer Radius	$\sim$ 11 m	$\sim$ 11 m
Thickness (Exclusive of Flanges, Fittings, etc.)	2.5 cm	2.5 cm

TABLE 4.1.6.1-2 (Continued)

Driver	CO_2 Laser	Heavy Ion Beam
Outer Sphere Insulation		
Material	Alumina Silica	Alumina Silica
Thickness	30.5 cm	30.5 cm
Lithium Flow Requirement		
First Wall, gallons per minute (m^3/s)	261,400 (16.5)	261,400 (16.5)
Outer Blanket, gallons per minute (m^3/s)	213,900 (13.5)	213,900 (13.5)
Total Lithium Flow, gallons per minute, (m^3/s)	475,300 (30)	475,300 (30)
Maximum Velocity (m/s)		
First Wall	17.8	17.8
Blanket	1.2	1.2
Piping	9.1	9.1
Lithium Pump Requirement, gallons per minute (m^3/s)		
First Wall + Outer Blanket, 8 required	∿ 60,000 (3.8)	∿ 60,000 (3.8)
Lithium Inlet Pipe Size (Equiv. Dia.)		
First Wall	∿ 1.5 m	∿ 1.5 m
Blanket	∿ 1.4 m	∿ 1.4 m
Lithium Coolant Temp., (T_{in}, T_{out})	300, 369° C	300,369° C
Total No. of Beams (2-Sided Penetrations)	108	20
Chamber Beam Penetrations		
Beam Opening Requirements @ First Wall (each side)	∿ 2.3 x 3.0 m	10 Openings, ∿ 0.3 m Dia. on ∿ 7.3 m Pitch Circle
Available Opening	∿ 6.5 m Dia.	∿ 6.5 m Dia.(1)
Beam Half- Angle	< 10°	23° (Cone)

(1) Min of 4 m diameter required for vacuum pumping

TABLE 4.1.6.1-2 (Cont.)

Driver	CO_2 Laser	Heavy Ion Beam
Vacuum Pumps		
Type	Roots Blower	Hg Diffusion
Quantity	24	16
Pumping Speed (each)	10,000 l/sec per pump	100,000 l/sec per pump
Wt. (each)	~ 10,200 kg	~ 1600 kg
Effective Blanket Coverage, %	94.5	94.3
Electrical Power Requirements, MW		
Driver	200	67
Li Pumps (3.0 MW each)	24	24
Na Intermediate Loop (6.0 MW each)	48	48
Vacuum Pumps	4	4
Auxiliaries (steam system, HVAC, etc.)	76(2)	70(2)
Net Electric Power Output	1207 MW	1346 MW
Li Wt (Reactor Chamber Only)		
First Wall	63 Tonnes	63 Tonnes
Blanket	415 Tonnes	415 Tonnes
Toroidal Manifolds	32 Tonnes	32 Tonnes
Chamber Wt		
Tubular Wall and Ta Coating	384 Tonnes	384 Tonnes
Toroidal Manifold Assembly (2 required 31 Tonnes each)	62 Tonnes Total	62 Tonnes Total
Support Sphere	324 Tonnes	324 Tonnes
Graphite Reflector (Upper & Lower)	427 Tonnes	427 Tonnes
Outer Sphere (Upper) w/o Reflector	183 Tonnes	183 Tonnes
Outer Sphere (Lower) w/o Reflector	218 Tonnes	218 Tonnes

(2) Final Focus Magnet Not Included

First Wall

Because of the high heat flux which must be removed from the first wall (approximately one half of the pellet energy released) it was necessary to provide a wall which was as thin as practical to minimize the thermal stress through the wall while still providing structural integrity and permitting the coolant temperature to be high enough to achieve a reasonable thermal performance. In order to carry the circulating coolant pressure with thin walls, an efficient circular tube structural shape was necessary. The first wall steel tubular structure is protected by a tantalum coating which is thick enough to prevent any significant thermal cycling of the HT-9 tubes during successive pellet microexplosions. The tubes taper from a 6.23 cm outer diameter at the 6.5 m penetration at each side of the chamber to a maximum of 19.4 cm at the polar region of the sphere. First wall cooling is achieved by tapping off lithium flow from the main toroidal manifold which also supplies lithium to the main blanket annulus between the support shell and the outer shell. The flow area through the tubular wall is relatively small, compared to the 60 cm blanket lithium annulus. However, because of the higher flow velocity required to achieve first wall cooling, the flow rate in the first wall tubes is 22% higher than in the main blanket.

The first wall coolant flow energes from the tubular wall and exits into a toroidal manifold from which it is combined with blanket flow in the main toroidal outlet pipes to the lithium coolant pumps for distribution to the four PHTS coolant loops. A total of 8 lithium pumps (2 per loop) of 60,000 gpm (3.8 m^3/s) capacity are required to supply the total flow of 475,300 gpm (30 m^3/s).

Main Blanket

The main blanket region is supplied with lithium coolant from the main toroidal mainfold. The lithium flows through the 58 cm annulus between the support shell and graphite reflector to cool the shell and back of the reflector. Another parallel 2 cm annulus between the reflector and outer shell provides a lithium path for cooling the shell and back of the reflector. After flowing through the blanket, the coolant mixes with that from the first wall outlet toroidal mainfold.

Radial stiffeners (Section A-A of Figure 4.1.6.1-2) are welded to the support shell and extend to the outer shell in order to provide additional stiffness to the support shell and to channel the coolant flow through the blanket so that swirl will be reduced.

Laser Beam Interface

The reaction chamber interfaces with the laser driver beams through main ducts at the two 6.5 m penetrations on each side of the reaction chamber. Figures 4.1.6.1-3 and 4.1.6.1-4, which are plan and elevation views of the containment building, show the laser beam interfacing between both the reaction chamber and containment building. The beam penetrations in the containment building consist of six separate circular ducts which enter the containment from each of the two laser buildings near ground level. After passing through salt windows at the outer wall of containment, the beams undergo four 90° bends to minimize neutron streaming. Figure 4.1.6.1-3 shows a cross section through two of the beam ducts (containing nine beams each) at the third and fourth mirror or final bend. The duct arrangement is shown schematically in Figure 4.1.6.1-5. At the first bend, the beams (which are initially 0.9 x 0.9 m square when they pass through the salt windows) are bent 90° and focussed to a smaller diameter to minimize space.

After the first focus, three additional 90° bends are incorporated before final focus by the last mirror to ~ 1 mm at the center of the reaction chamber. The salt windows and mirrors are sized to subject them to a maximum of 3 J/cm^2 and 5 J/cm^2 loads respectively in order to permit use with beam energy up to 5 MJ. Figure 4.1.6.1-5 shows the duct space requirement and beam sizes at the salt windows, mirrors and at the reaction chamber where the beam envelope converges to ~ 2.3 x 3.0 m. The four bend arrangement is intended to limit the radiation level at the outside of the salt windows so that personnel could occupy this area for a 40 hour week without exceeding the allowable dose.

By crossing the beams within the ducts, it is possible to converge the beam pattern and duct to less than 1 m diameter which permits incorporation of ball valves as shown in Figure 4.1.6.1-5. In the event of a fracture of a salt window, the reaction chamber can still be isolated from the outside of the

containment building by use of these valves. The valves need not be fast acting, since the pressure is normally inward toward the reactor to preclude release of any of the pellet debris ouside of containment through the ducts.

The last mirror is located 30 meters from the center of the cavity and is protected from microexplosion debris by a counter streaming gas flow.

Vacuum Pumps and Duct Arrangement

In order to minimize the number of penetrations in the reaction chamber, the vacuum pump ducts are connected to the main ducts which interface with the laser beams at the wall of containment and the reaction chamber. These main ducts (Figures 4.1.6.1-3 and 4.1.6.1-4), because of their low impedance, are large enough to permit pumping without extra penetrations in the reaction chamber. The pump and duct arrangement shown in the figures include 24 Roots blower pumps each of ~ 10,000 l/sec capacity to provide adequate pumping capability to permit the 10 Hz repetition rate. The intermediate ducts between the pumps and the main duct are long enough to permit a reasonable packaging arrangement of the pumps within the containment building and short enough to provide low impedance for vacuum pumping.

Pellet Injector

The pellet injector is mounted at the bottom of the reaction chamber and injection is upward along the vertical centerline of the reaction chamber. The pellet injector interfacing concept is shown in Figure 4.1.6.1-6 and shows the penetration through the blanket, center shell, support shell and first wall. The pellet entry tube can be installed in the tubular first wall without significant perturbation to lithium coolant flow. In addition, the joint between the injector and first wall assembly is accessible from below the reaction chamber. Location of the pellet injector below the reaction chamber has the inherent advantage of facilitating removal of the first wall with minimum delay since both the pellet injector and the lower half of the outer shell remain in place during this major maintenance and servicing operation. The maintenance operation is discussed in Section 4.2.6.8.

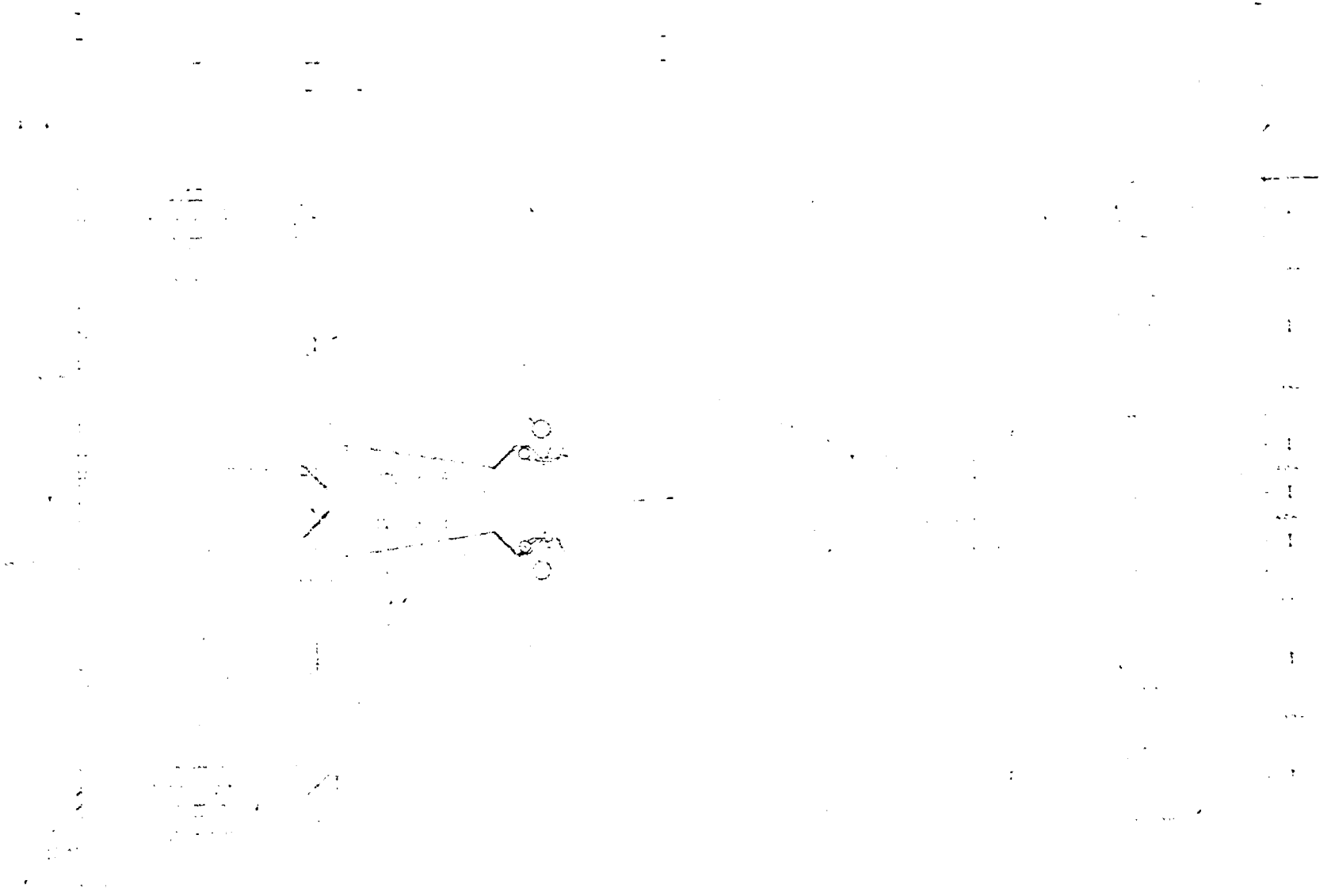

Figure 4.1.6.1-3. Plan View of Reactor Containment Building and Reaction Chamber Interfaces for Laser Driven Reactor Concept

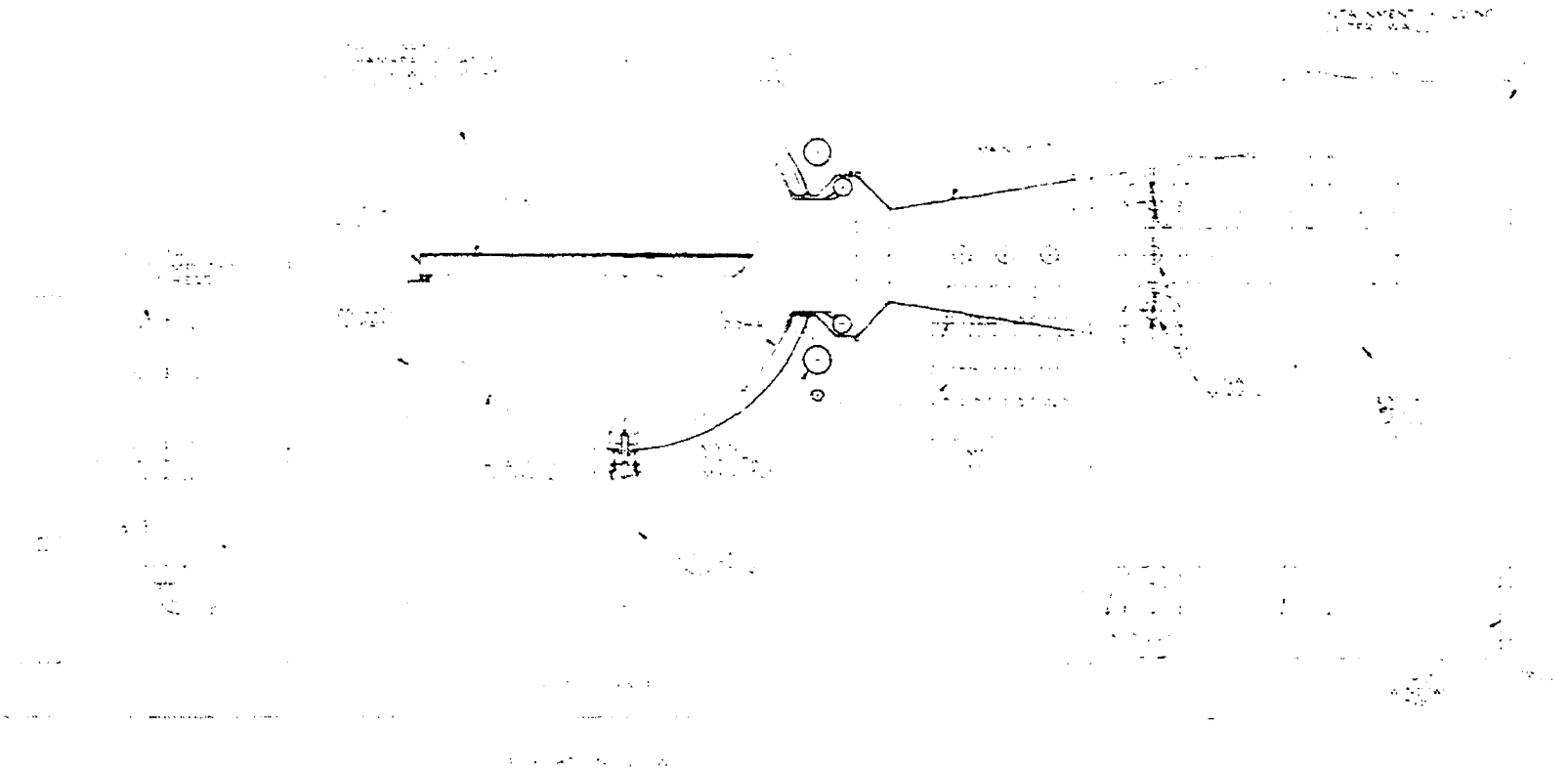

Figure 4.1.6.1-4. Elevation View of Reactor Containment Building and Reaction Chamber Interfaces for Laser Driven Reactor Concept

Reaction Chamber Support

The entire reaction chamber assembly, which includes the first wall assembly, graphite reflector, the outer shell and its insulation is supported by a circumferential support ring surrounding the chamber and located just below the equator of the chamber. The support ring is fitted with high capacity roller assemblies similar to the Hillman* Roller Assemblies. The rollers, Figure 4.1.6.1-7, rest on the cylindrical concrete support skirt below the reactor. The roller arrangement between the support skirt and support ring permits free radial motion of the reaction chamber due to temperature changes encountered between hot and cold operation of the reactor. Roller assemblies in the 100 tonne range are commercially available and there is enough space around the chamber to provide for more than adequate vertical support. The concrete skirt which supports the reaction chamber extends to the base mat of the containment building and provides shielding to protect components below the center of the reaction chamber.

*Hillman Equipment Co. Inc., Wall, New Jersey

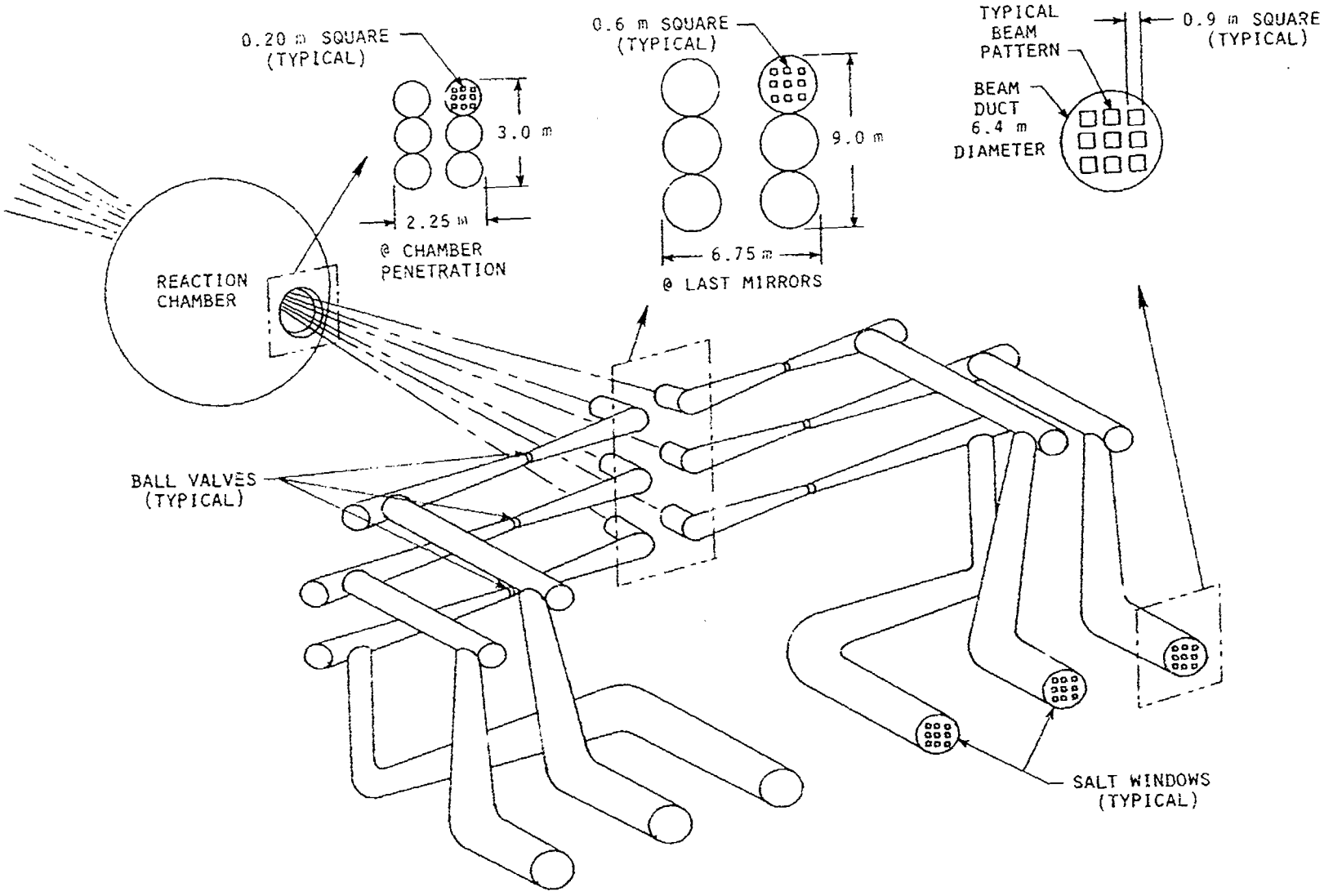

Figure 4.1.6.1-5. Laser Duct and Beam Concept Showing Duct Arrangement and Beam Pattern for 4-Bend Configuration

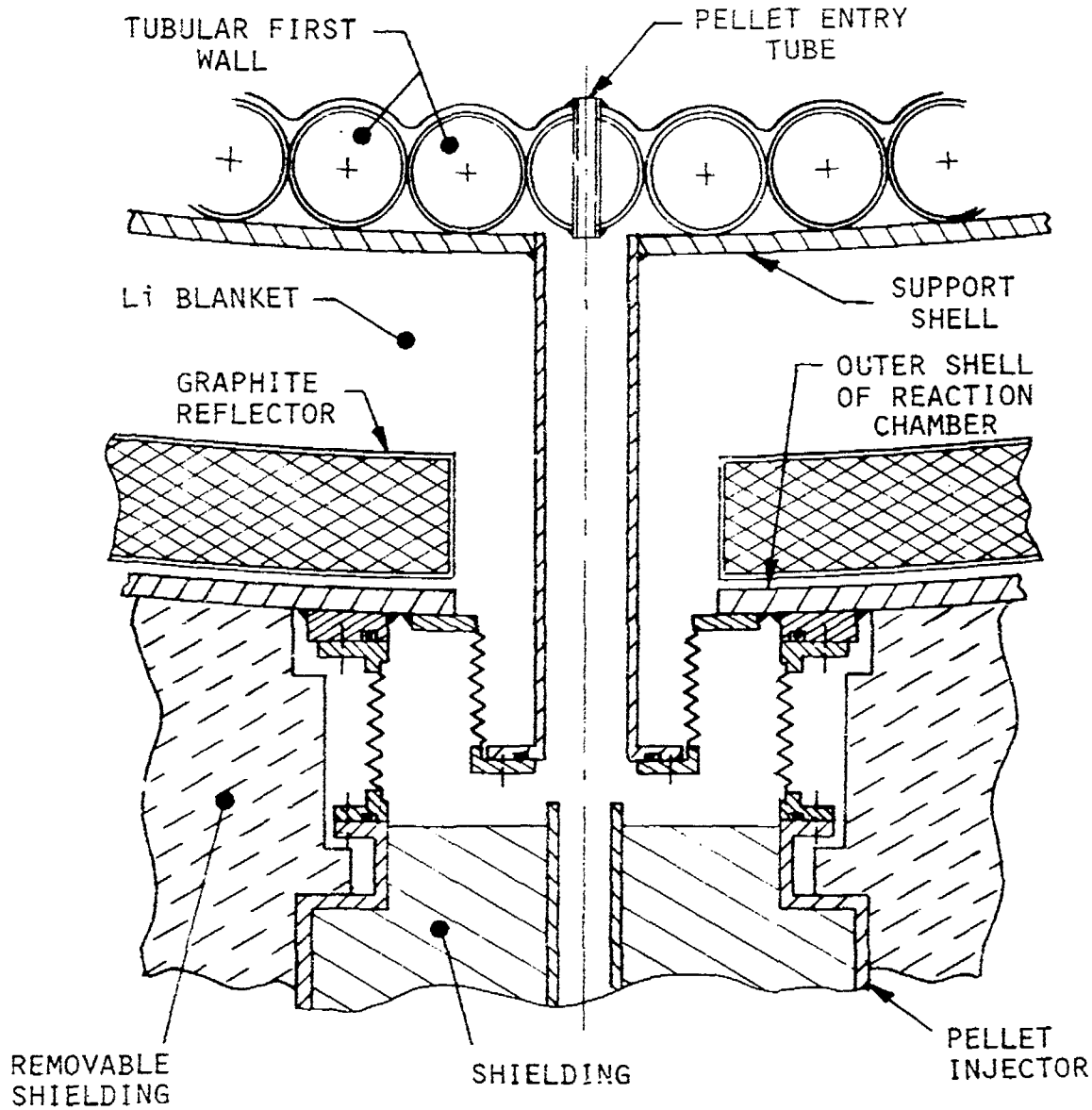

Figure 4.1.6.1-6. Pellet Injector/Reaction Chamber Interface Concept

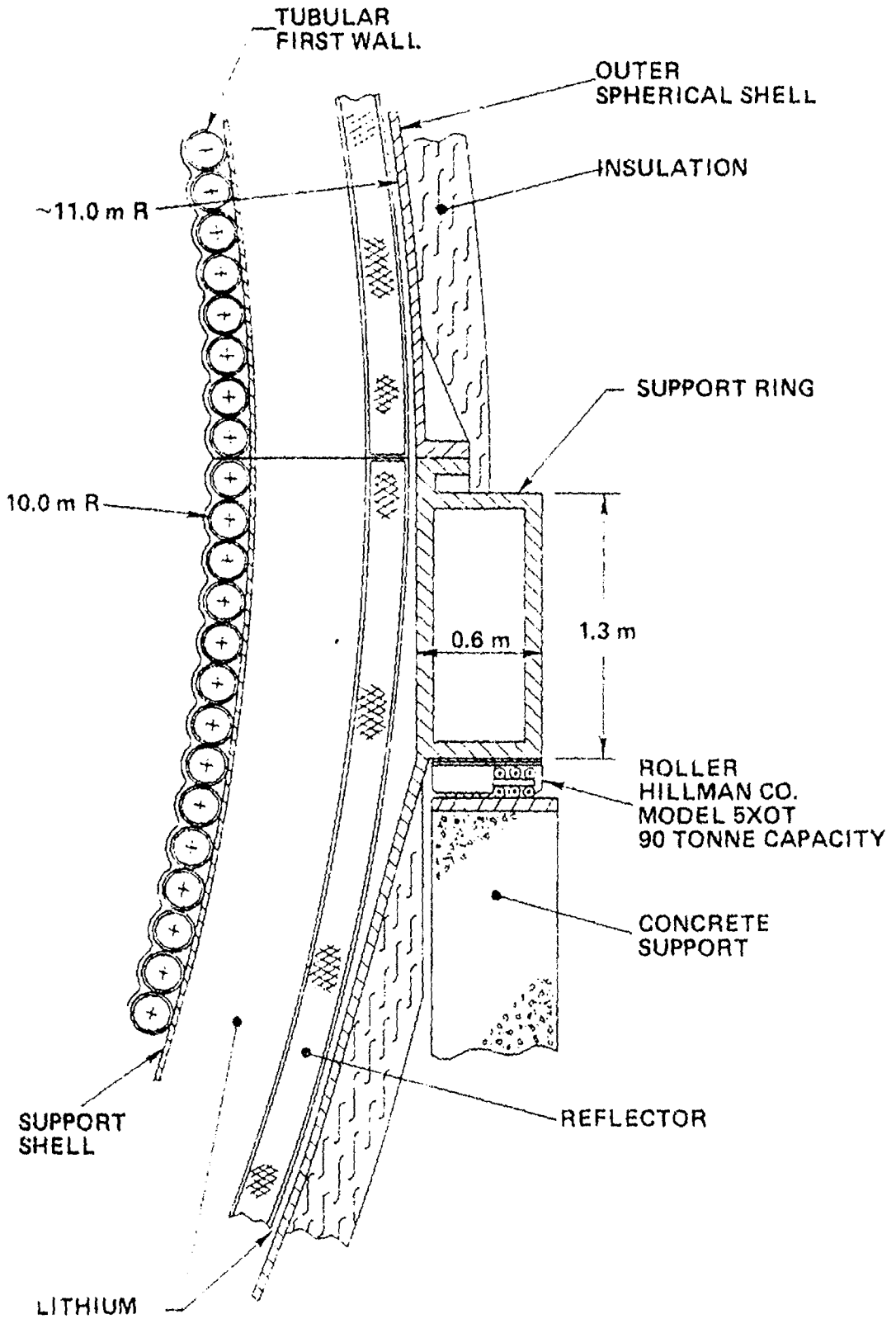

Figure 4.1.6.1-7 Reaction Chamber Support Concept Showing Roller Arrangement to Accommodate Radial Expansion

4.1.6.2. MATERIALS SELECTION AND DESIGN CONSIDERATIONS

The reaction products of the D-T pellet micro-explosions create an extremely hostile environment at the reaction chamber inner — i.e., plasma-facing — surface. In contrast to the situation for quasi-steady state devices such as tokamaks or mirrors, where the energy deposition occurs relatively uniformly with time and where the energy is transported by neutrons and charged particles (D, T and α particles), the pellet microexplosions in inertially confined concepts result in significant energy transport to the reaction chamber wall in the form of x-rays and heavy ions as well as neutrons and light ions. Moreover, the cyclic nature of inertial confinement operation implies that cyclic thermal and mechanical stresses must be accommodated.

The major effect of the high energy x-rays and debris ions will be extreme and rapid heating of the first surface. This can lead to melting and evaporation and will also produce a stress pulse which will propagate inward through the structure. This stress pulse can lead to spallation of either the rear surface, or upon reflection, at the front surface of the chamber wall. In addition, the phenomena of physical sputtering and bulk neutron radiation damage must be considered.

In the interests of design simplicity a decision was made to use a bare, rather than liquid or wetted, wall design. Preliminary calculations of the thermal stresses which would occur due to x-ray and debris ion heating indicated the yield strength of essentially any solid structural material used for the pressure boundary would be exceeded. Closer examination of the materials parameters which control the magnitude of the temperature rise, and hence induced stress, suggests a distinct advantage for materials of low atomic number[1]. For first wall and blanket structures cooled with lithium this is not practical due to liquid metal corrosion of candidates such as carbon (graphite), aluminum, beryllium, etc. Therefore a decision was made to use a coating over the "first wall" structural material.

The reaction chamber wall therefore consists of two elements — the structural load-bearing substrate and the overlayer or coating used to protect it by

attenuation of the effects of the x-ray and debris ion depositions. Selection of materials for these applications is discussed in the following paragraphs.

STRUCTURAL WALL MATERIAL

As was mentioned in the preceding section, the reference structural wall concept employs an array of contiguous tubes, joined at their points of tangency and cooled internally by liquid lithium. The maximum temperature of this tube wall was set at 500°C. Primary candidate materials for this application are the ferritic alloys such as Croloy (2-1/4 Cr-1 Mo) or HT-9 (Fe-11.5 Cr-1 Mo + W, V, C), or one of the austenitic stainless steels such as type 316. For temperatures above about 400°C the distinct strength advantage of HT-9 over 2-1/4 Cr-1 Mo suggests HT-9 be considered as the favored ferritic alloy.

Factors which affect the choice between HT-9 and 316SS include:

- Strength at Maximum Temperature (500°C)
- Coolant Choice (Liquid Lithium)
- Thermal Stress Response
- Bulk Radiation Damage Characteristics
- Cost
- Availability
- Fabricability.

At 500°C the allowable design stress intensity, S, is roughly the same for both candidate alloys. Corrosion behavior in liquid lithium at that temperature, particularly at the high flow rates encountered in the present design, favors HT-9 as do considerations of cost and availability (chiefly due to the lack of nickel in the Cr-Mo-V-W ferritic alloy). Comparison of the thermal stress "figure of merit," proportional to $\alpha E/k\ (1-\nu)$ where, α = coefficient of thermal expansion, k = thermal conductivity, ν = Poisson's ratio and E = Young's Modulus reveals a factor of two advantage for HT-9.

On the basis of very limited data, the irradiation response characteristics of HT-9 appear to be somewhat better than those of austenitic stainless steels. These data, developed on the LMFBR Advanced Cladding and Duct Program, indicate very little void swelling for a fast reactor neutron fluence (EBR-II) of 10^{23} n/cm^2 (E > 0.1 MeV). There may be, however, some reason for concern over an increase in the ductile-brittle transition temperature (DBTT) since a significant decrease in upper shelf impact energy and increase in the high strain rate DBTT have been seen for HT-9 irradiated to only 10^{22} n/cm^2 (E > 0.1 MeV).

Consideration of the final design factor, fabricability and weldability, favors austenitic stainless steel where pre- and postweld heat treatments are not required. HT-9, on the other hand, is normally used in the tempered martensite metallurgical condition. To achieve this, a heat treating schedule of 1050°C for one hour (plus air cool) and one hour at 760°C (again air cool) is required. The need for the secondary heat treatment could imply difficulty in design and fabrication of complex hardware, particularly since fusion-welded structures require this heat treatment to avoid heat-affected zone cracking.

Potential limits on the radiation data base and concerns over fabricability notwithstanding, HT-9 has been selected for detailed evaluation by the Alloy Development program of the Office of Fusion Energy as a candidate first wall alloy for magnetic fusion reactors. As the result of this selection the fabrication characteristics, including mechanical performance of welded structures, and the irradiation response of HT-9 are under considerable investigation at the present time[2].

In view of the advantages offered by HT-9 in the important areas of thermal stress response, lithium corrosion resistance, and cost, this alloy was selected for use as the structural wall tubing.

FIRST WALL COATING

Since the energy deposition due to x-rays and debris ions occurs on a time scale which precludes accommodation by thermal diffusion or relaxation processes, there is an advantage to choosing a material with low x-ray energy attenuation properties so that the effects are spread over a relatively greater volume (depth) of material. Other properties which are attractive for various reasons include the thermal conductivity, coefficient of thermal expansion, and Young's modulus; these will affect the magnitude of the thermal stress which develops due to the background "steady-state" temperature gradient which will exist through the coating. It is also advantageous to use a material which is relatively soft or ductile, and which has a relatively high melting temperature.

As was mentioned previously, many of these factors suggest use of a low Z (low atomic number) material. With the exception of melting temperature, unalloyed aluminum appears very attractive and represented the initial choice during this design study. Early analysis of the effects of the x-ray and debris ion energy deposition indicated the aluminum coating would efficiently suppress the thermal and mechanical cycling of the underlying structural tubes. However, a significant volume of Al would be lost at each microexplosion due to the melting and evaporation of a (3 μm) surface layer. Even allowing for the 95-98% recondensation which should occur, this would lead to an unacceptable loss in a relatively short time.

This conclusion, coupled with selection of tantalum for the heavy element component of the unclassified target pellet, forced reconsideration of the first wall coating selection. Since selection of a higher melting point metal might preclude melting and evaporation, it would also guarantee that essentially all of the pellet debris and reaction product ions would strike the wall. [This seems certain to be the case for the heavy ion design case where the chamber pressure is $\sim 10^{-4}$ Torr. It may not be equally true for the CO_2 laser driven design where the 0.1 Torr inert gas background pressure will significantly attenuate both the x-rays and debris ions during their passage to the wall.] Hence, since accumulation of tantalum should occur on the

chamber's inner surface, a substantial argument could be offered for the use of unalloyed tantalum for the first wall coating.

Unalloyed tantalum is quite ductile at modest temperatures despite its 2996°C melting temperature and good mechanical strength. It possesses a combination of thermal and mechanical properties which appear to make it at least an acceptable coating selection. Moreover, it is compatible with operation at cavity background pressures of interest without suffering melting and evaporation of its surface.

Thus, unalloyed tantalum was chosen for the first wall coating. It should be noted that a change of the high atomic number material in the pellet should be carefully weighed since other possible heavy element choices may not possess the combination of properties required. For example, tungsten and molybdenum, despite high melting temperatures (3410°C and 2610°C, respectively) and attractive thermal properties are almost certainly too brittle to be used as a shock and heat absorbing coating.

4.1.6.2 REFERENCES

1. J. Hovingh, "Design Issues and Materials Problems in Inertially-Confined Fusion Reactors," UCRL-82943, preprint of a paper prepared for submission to the Proceedings of the Impact Fusion Workshop, July 10-13, 1979, Los Alamos, NM.

2. Alloy Development for Irradiation Performance, Quarterly Progress Report for Period Ending March 31, 1980, U. S. Department of Energy, DOE/ER-0045/2, June, 1980.

4.1.6.3 BLANKET AND SHIELD DESIGN

FUNCTION

The blanket and shield of the ICF reactor plant perform the following functions:

(1) Absorb the neutron energy emerging from the pellet and convert it to useable heat.

(2) Produce tritium for makeup of fuel burned in pellets.

(3) Provide bulk biological radiation shield for reactor building.

(4) Provide support wall radiation damage lifetime consistent with chamber servicing requirements.

(5) Reduce neutron activation of components requiring regular service and maintenance (e.g., lithium pumps, heat exchangers).

(6) Provide adequate shielding of activated chamber during shutdown and servicing.

(7) Provide shielding against radiation streaming through ducts and chamber penetrations.

DESIGN REQUIREMENTS

The design requirements will be discussed in the context of each of the functions above.

(1) Approximately 55% of the thermonuclear energy of the exploding pellet, in the reference design, is in the form of kinetic energy of the emerging neutrons. This energy is multiplied by exothermic (energy producing) reactions as the neutrons are absorbed in the blanket. The blanket must be thick enough to absorb most of the energy. As an objective, the energy lost should be much less than recirculating power fraction of the ICF plant.

(2) The tritium breeding ratio (TBR) should be high enough to compensate for losses due to chamber penetrations, reprocessing, radioactive decay of the tritium, and calculational uncertainties. An objective

of approximately 1.2 for the TBR was established, considering typical loss values.

(3) The bulk radiation biological shield must be adequate to provide access by radiation workers during normal operation. Current limits are 5000 mr/year or 2500 mr/quarter. However, it is likely that these values will be significantly reduced in the near future.

(4) Radiation damage of the HT-9 support wall, in the form of gas production and atomic displacements, will cause swelling, loss in ductility, and eventual failure. A lifetime goal of five years was established to be consistent with the major plant shutdown and overhaul schedule.

(5), (6) A number of plant components will require scheduled and unscheduled maintenance while the plant is in a shutdown condition. It is important that these operations be performed in a limited hands-on mode. This requires adequate care in the design of the shield, which serves a dual purpose in this case. It must shield against neutrons leaking through the blanket, which may cause activation of the components, and it must provide gamma ray shielding of the activated chamber internals.

(7) Radiation will pass out of the reaction chamber through the openings required for admitting the laser or ion beams. The radiation constitutes both a heating and a radiation shielding problem. Active cooling systems, so that primary duct walls and beam dump do not exceed allowable temperature limits, are required. Duct configuration and radiation traps must be designed to minimize neutron streaming effects so that excessive shielding and beam bends are not needed.

DESIGN DESCRIPTION

The 1-dimensional spherical geometry representation of the reference first wall, blanket and shield used for the neutronic analysis is shown in Figure 4.1.6.3-1, and is identical for both drivers. It consists of 12 concentric spherical shells or zones, centered at the pellet. The

constituents of each zone were homogenized over the shell volume, according to their respective volume fractions.

This one-dimensional representation does not allow description of penetrations and ducts, or the phenomena associated with them. These must be treated separately, and are discussed in Section 5.1.6.3.

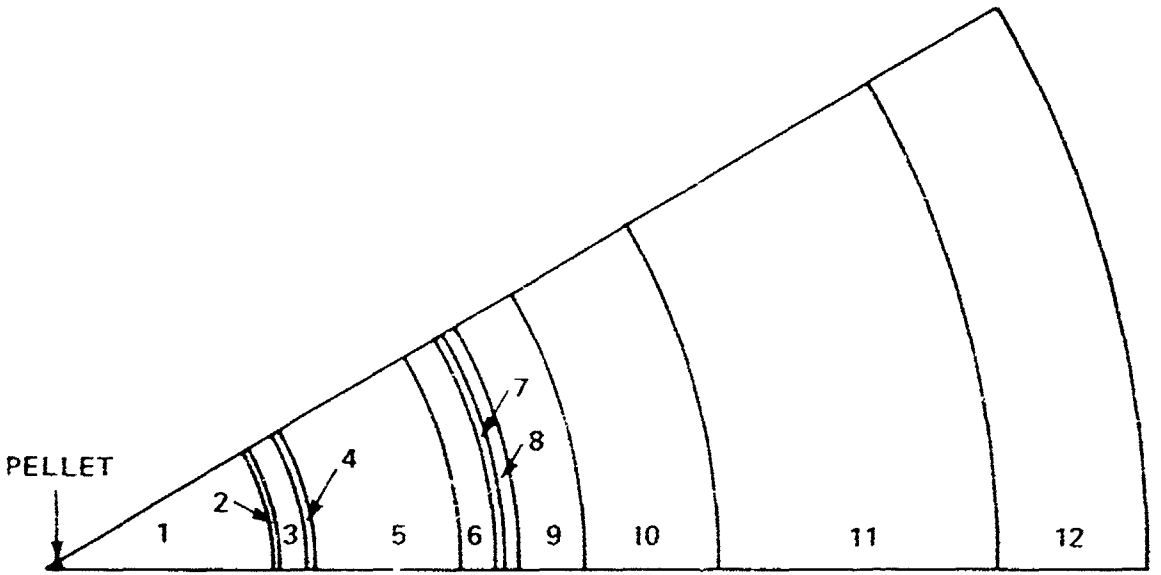

ZONE	COMPOSITION	THICKNESS (METERS)
1	CHAMBER (VOID)	10.0
2	Ta COATING	0.01
3	Li IN HT-9 TUBES	0.12
4	HT-9 STEEL SUPPORT	0.02
5	Li + 4 v/o STRUCTURE	0.58
6	GRAPHITE REFLECTOR + 10 v/o STRUCTURE	0.20
7	Li + 4 v/o STRUCTURE	0.02
8	STEEL SHELL	0.025
9	THERMAL INSULATION	0.305
10	CONCRETE + 5 v/o IRON	1.0
11	MACHINERY SPACE	7.7
12	CONCRETE + 5 v/o IRON	2.0

G15658-7A

Figure 4.1.6.3-1. Neutronics Model for the Reference Arrangement of the Reaction Chamber

4.1.6.4 HEAT REMOVAL SYSTEM

FUNCTION OF SYSTEM

The function of the reactor chamber heat removal system is to remove the thermal energy deposited in the first wall and the blanket from the pellet microexplosion and to transport the energy to a steam turbine/generator system for power conversion. The first wall surface heat flux amounts to about 45% of the pellet yield and the neutron heatings results from the remaining 55% of the pellet yield. The first wall is protected from the x-ray and the ion debris heat load and particle interactions by a thin coating of tantalum metal. Liquid lithium is used as the coolant of the first wall and the blanket structures as well as the tritium breeding material. A sodium intermediate heat transfer loop is utilized to separate the primary lithium loop and the water/steam loop to minimize tritium transfer from lithium to water and to avoid possible lithium-water interaction.

DESIGN REQUIREMENTS

The design requirements of the heat removal system are:

- The coolant flow rate must maintain the temperature of the first wall and the structures to a maximum of 500°C for the selected structural material of HT-9 ferritic steel. The flow rates should not be excessive, so that liquid metal pumps of reasonable sizes can be utilized.
- The maximum coolant flow velocity in a cooling channel is below 20 m/sec.
- The coolant pressure in the blanket region should be minimized, so that the pressure acting on the first wall structure is acceptable in view of the selected chamber radius of 10 m.
- The coolant operating temperature is to be as high as practical to result in a high power conversion cycle thermal efficiency to assure at least 1000 MWe of power production.

Note that the requirements given above are not entirely compatible. For example, the maximum allowable structural operating temperature limits how high the coolant outlet temperature can be. In order to raise the coolant inlet temperature, to increase the power conversion efficiency, the coolant flow rate must be increased for a given thermal power input. High coolant flow rate results in high flow channel velocity and attendant corrosion problems. Trade-offs must then be carried out to obtain compromises, so that the design requirements can be satisfied.

SYSTEM DESCRIPTION

The reactor chamber heat removal system consists of three parallel cooling channels: (1) first wall tubes; (2) main blanket region and, (3) outer shell. The first wall construction of this reactor design is of the "dry wall" concept consisting of circular steel tubes. The diameter of each tube varies so the tubes can form a spherical shell covering the reactor cavity. The inner surface of the tubular shell is coated with a thin layer of tantalum metal which absorbs the cyclic surface heat flux spike after each microexplosion, so that the temperature response of the tubes outer wall would be in a nearly steady state pattern. In this conceptual design analysis a steady state condition for the tubes and the blanket was assumed. The liquid lithium coolant flow rates in the three channels were sized to limit the maximum temperature in the structures to about 500°C. A schematic of the three lithium flow channels used in the analysis model is given in Figure 4.1.6.4-1. The entrance ports of the laser beams are located on the two ends of the horizontal axis of the chamber. The coolant inlet and outlet manifolds are located outside the beam ports. The manifolds are circular rings connected to the channels by feeder tubes. The half cone angle of the beam port opening on each side of the chamber is 19°. With these two openings the first wall and blanket area coverage is reduced to about 94.5% of the total interior area of the chamber (the other penetrations and pellet injection port are assumed to be small compared to the chamber area). The incident heat flux directed toward the beam duct openings will thus be deposited on the duct walls and the other hardware outside

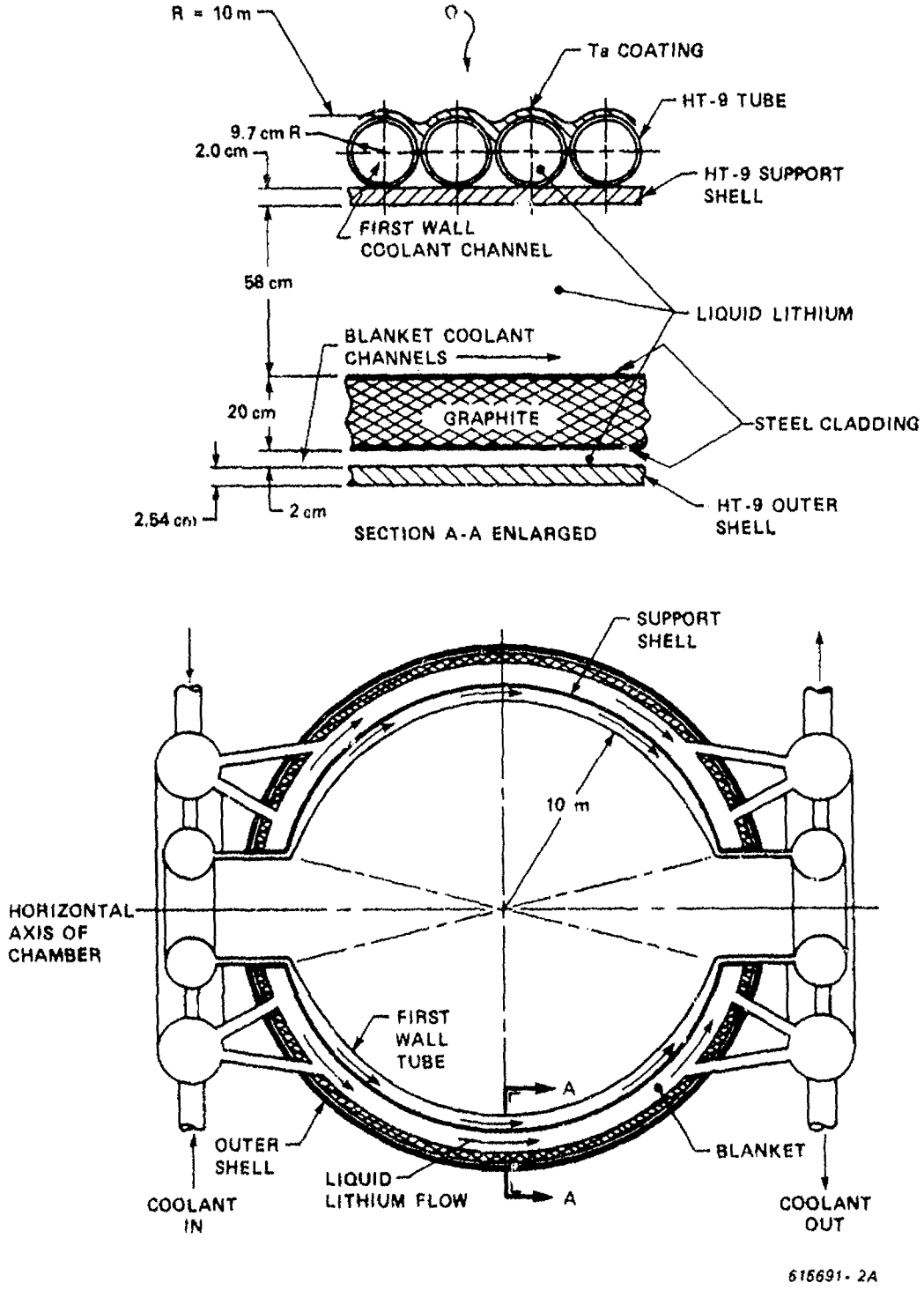

Figure 4.1.6.4-1. Heat Removal System of the Reactor Chamber

the chamber. This portion of thermal energy was not included in the heat removal systems for power conversion, but might be recovered and utilized for other purposes in the power plant.

The thermal power distribution on the various components of the first wall and the blanket as obtained from neutronic calculations (see Section 4.1.6.3) is shown in Table 4.1.6.4-1. With a total of 3500 MWt thermal power from the reference design pellet, the net first wall surface heat load due to x-ray and ion debris is 0.45 x 3500 x .945 = 1489 MWt while the net neutron thermal power deposited in the structures and lithium is 2811 MWt because the blanket power multiplication is 1.54. The total heat to be removed by the cooling system is therefore, 4300 MWt.

The thermal and hydraulic design parameters of the heat removal system are shown in Table 4.1.6.4-2. The lithium coolant inlet temperature was selected to be 300°C. The total lithium flow rate required to maintain the maximum structural temperature to the allowable limit of 500°C is about 30 m^3/sec. (475,000 gpm). For this conceptual design study a four loop heat transport plant was selected with each loop having two pumps. The flow rate in each pump is hence 3.75 m^3/sec. (59,400 gpm). A pump of this capacity is well within present liquid metal pump technology. The time averaged surface heat load from the pellet x-ray and debris amounts to about 1/3 of the total thermal power which is equivalent to a surface heat flux of 1.25 MW/m^2 for the 10 m radius chamber. With this heat flux the first wall tube thickness must be thin to reduce the temperature drop across the tube wall. The tube wall thickness of the present first wall design is 0.18 cm. The resulting average temperature drop across the wall is 87°C. Since the tubes are heated from the front half only, the temperature difference across the tube diameter is 129°C. With these temperature gradients the thermal stresses were found to be satisfactory.

In order to keep the coolant pressure in the reactor chamber low, the liquid pumps are to be located at the hot leg of the primary loop.

TABLE 4.1.6.4-1

FIRST WALL AND BLANKET THERMAL POWER DISTRIBUTIONS

First wall and blanket coverage = 0.9455 of total spherical area

Total pellet fusion power = 3500 MWt

Blanket Power multiplication = 1.54

	Full Coverage	94.55% Coverage
First Wall Surface Power	1575	1489
Tantalum Coating	297	281
First Wall Zone: Lithium	703	665
Tubes	45	43
First Wall Support Shell	210	199
Blanket Zone: Lithium Main Channel	1405	1328
Lithium Outer Channel	40	38
Structures	113	107
Graphite Reflector and Structures	130	122
Chamber Outer Shell	30	28
Total, MWt	4548	4300

TABLE 4.1.6.4-2

THERMAL AND HYDRAULIC PARAMETERS OF THE FIRST WALL AND BLANKET HEAT REMOVAL SYSTEM WITH LASER DRIVER

Chamber radius, m	10	
Pellet Fusion Power, MWt	3500	
Percent X-Ray and Ions/Neutron, %/%	45/55	
First Wall Surface Power, MWt	1489	
Neutron Thermal Power, MWt (blanket multiplication = 1.54)	2811	
Total Thermal Power, MWt	4300	
Structural Material	HT-9 Steel	
Maximum Structural Design Temperature, °C	500	
Lithium Coolant Inlet Temperature, °C	300	
Lithium Flow Rates:		
First Wall Tubes, m^3/sec. (gpm)	16.5	(261,000)
Blanket, m^3/sec. (gpm)	13.5	(214,000)
Total Lithium Flow Rate, m^3/sec. (gpm)	30.0	(475,000)
Lithium Temperature Rise:		
First Wall Tubes, °C	72.5	
Blanket, °C	64.5	
Lithium Mixed Mean Outlet Temperature, °C	369	
Maximum Lithium Flow Velocity, @ First Wall Tube Ends, m/sec.	17.8	
Temperature Drop Across Tube Wall, °C	87	
Temperature Difference Across Tube Diameter, °C	129	

TABLE 4.1.6.4-2 (CONT'D)

Lithium Coolant Inlet Pressure MPa, abs. (psia)	0.45 (65)
Lithium Coolant Pressure Loss Across First Wall/ Blanket Channels, MPa (psi)	0.27 (39)
Lithium Primary Loop Hot Leg Temperature, °C	369
Lithium Primary Loop Cold Leg Temperature, °C	300
Sodium Secondary Loop Hot Leg Temperature, °C	363
Sodium Secondary Loop Cold Leg Temperature, °C	272
Total Sodium Flow Rate, m^3/sec. (gpm)	41.40 (656,000)
Steam Power Conversion System	
Steam Pressure, MPa abs. (psia)	7.24 (1,050)
Steam Temperature, °C	358
Estimated Gross Cycle Thermal Eff., %	36.4
Gross Electric Power Output, MWe	1565
Power Consumptions:	
Laser Driver, MWe	200.0
Lithium Loop, MWe	24
Sodium Loop, MWe	48
Vacuum Pumps, MWe	4.0
Tritium, Pellet & Radwaste Systems	6
Plant Auxiliary Power, MWe	76
Total Power Consumption, MWe	358
Net Electric Power Output, MWe	1207
Overall Plant Conversion Efficiency, %	28.1
Recirculation Power Fraction, %	22.9

The lithium pressure distributions in the first wall and the blanket channels are shown in Figure 4.1.6.4-2. In the figure the pressure difference above the pressure at the outlet manifold was plotted. The pressure gradients included the frictional losses, elevation and flow area changes and the entrance and exit losses. The overall pressure loss across the first wall channel is about 0.27 Mpa (39 psi) and that across the blanket channel is about 0.014 MPa (2 psi) which is small compared to that across the tubes. The coolant flow to the blanket channels would have to be orificed to drop the channel inlet pressure to the level shown in the figure. Since the lithium flow is axially symmetric with respect to the horizontal axis of the chamber, the effect of elevation change on the coolant pressure is not the same at all planes through the axis. The pressure profiles along the three major flow directions on the vertical and the horizontal planes of the chamber are shown in Figure 4.1.6.4-2. The difference in shape is small, therefore we can use the top curve for design purposes.

The selection of the operating pressure level for the lithium flow loop depends on the net positive suction head (NPSH) required to operate the lithium pumps and the coolant pressure required inside the blanket main coolant annulus to alleviate the thermal stresses in the first wall support shell. For this reference point design the coolant pressure at the channel exit was selected to be 0.172 MPa abs. (25 psia). This results in a maximum coolant pressure inside the tubes of 0.448 MPa abs. (65 psia) and inside the main blanket channel of 0.221 MPa abs. (30 psia). These are the design pressures for structural design of the first wall and blanket systems. The pressure distributions in the primary lithium loop and the secondary sodium loop are discussed in the design of the balance-of-plant.

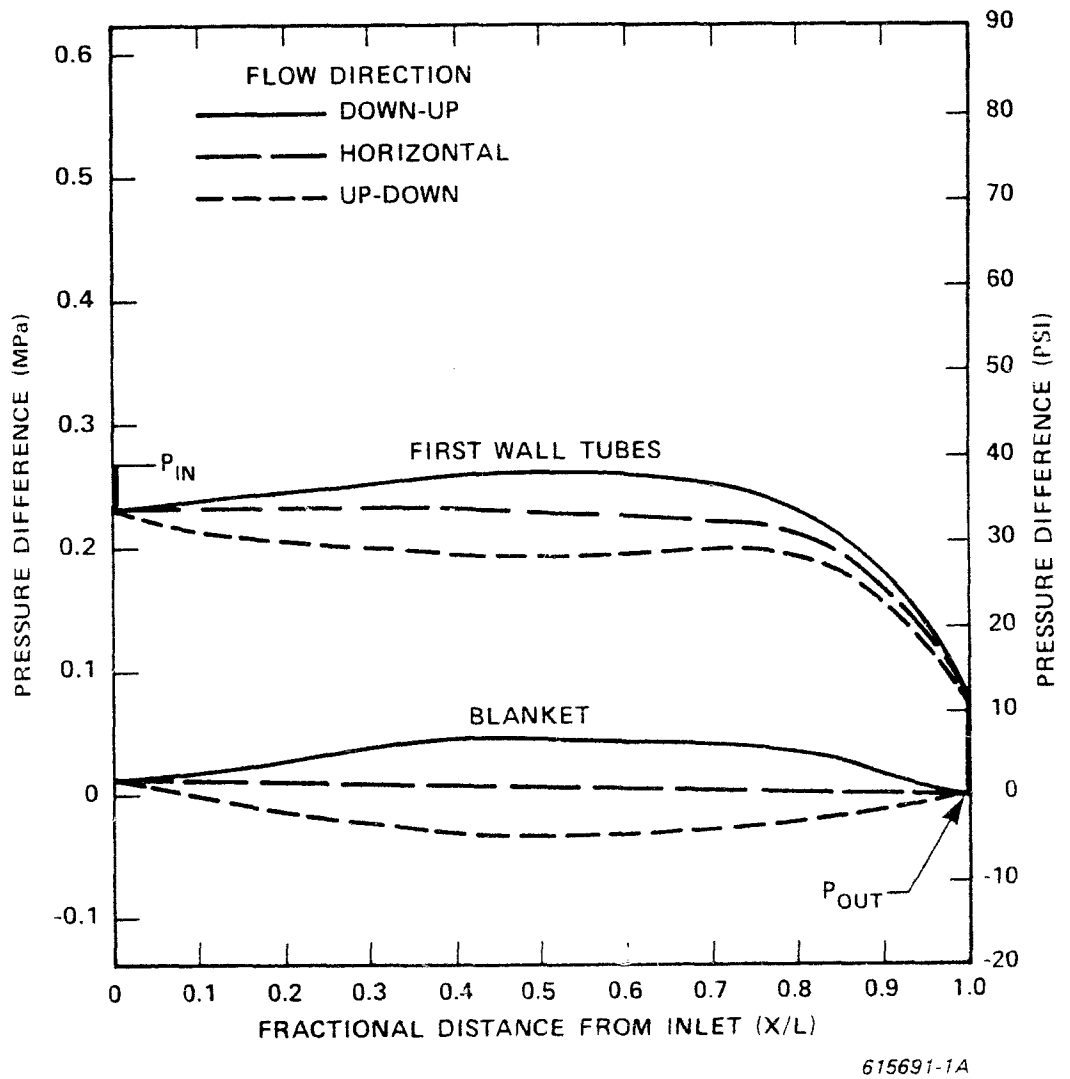

Figure 4.1.6.4-2. Lithium Pressure Profiles in First Wall and Blanket Cooling Channels

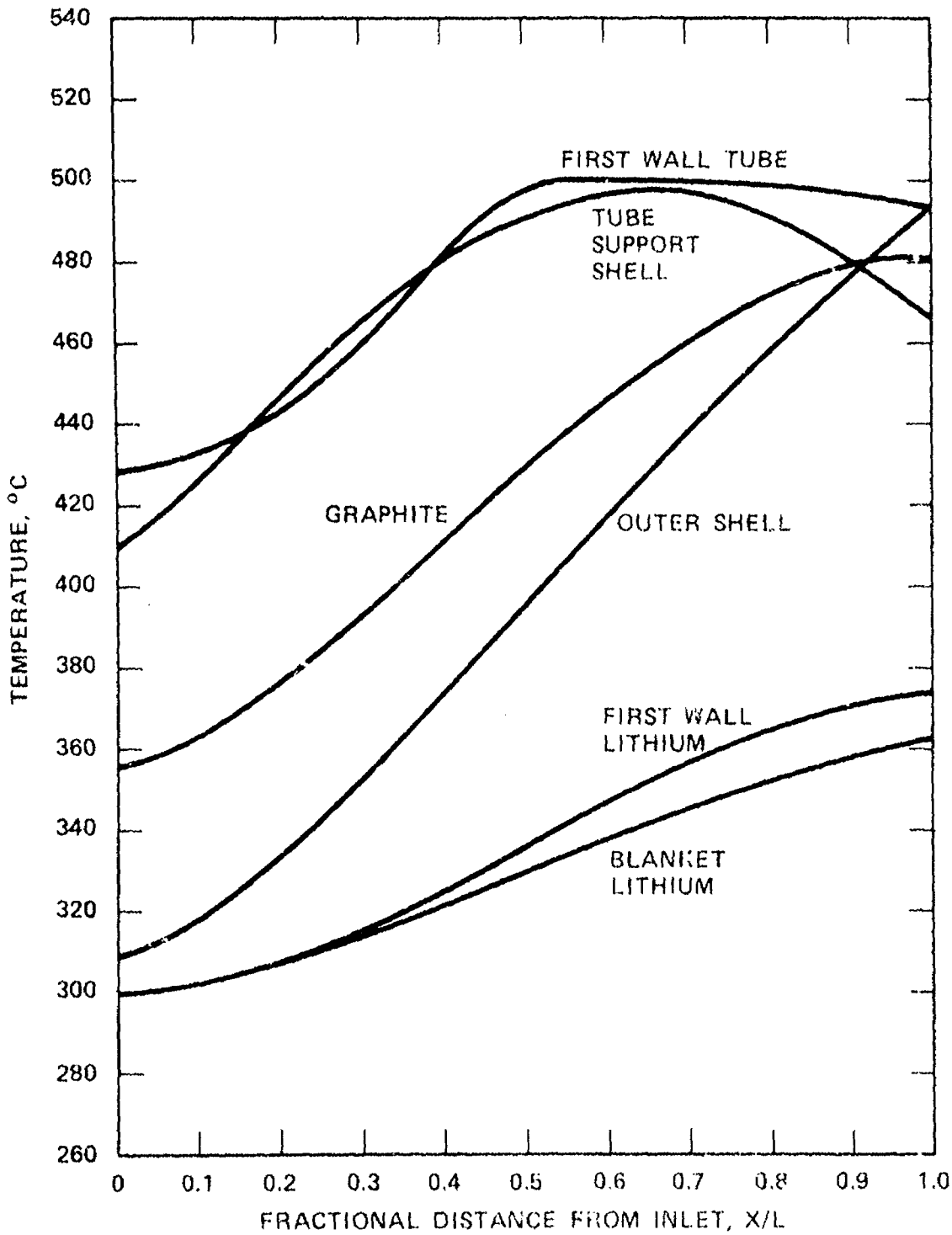

Figure 4.1.6.4-3. Temperature Distributions in the First Wall and Blanket Heat Removal System Components and Structures

The temperature profiles along the coolant channels are shown in Figure 4.1.6.4-3. The maximum material temperature of the first wall tubes, the tubes support shell and the chamber outer shell are at or near the allowable limit of 500°C. The graphite reflector peak temperature is below 500°C. The liquid lithium coolant temperatures are also shown in the figure. The mixed mean lithium outlet temperature is 369°C.

The thermal parameters of the sodium secondary loop and the steam turbine power conversion cycle are also shown in Table 4.1.6.4-2. The gross electric output of this plant design is 1565 MWe. The total power consumption with the laser driver is 358 MWe, so that the net electric power output is 1207 MWe. The overall plant conversion efficiency is 28.1% and the recirculation fraction is 22.9%.

The thermal power deposited in the insulation and concrete vessel outside the reactor cavity amounts to about 60 MWt. Since the maximum steady state operating temperature of a reinforced concrete containment vessel is on the order of 200°C, the coolant temperature will be lower than 200°C which is too low to be included in the reactor heat removal power conversion system. A separate cooling loop using air or helium gas can be used to cool the vessel. The heat could be disposed of in the cooling tower or utilized for other purposes in the plant.

4.1.6.5 VACUUM SYSTEM

FUNCTION

The function of the vacuum system is to remove from the reaction chamber any additional gaseous material introduced during a single pellet burn.

DESIGN REQUIREMENTS

The ambient pressure inside the vacuum chamber and driver entrance ducts must be maintained at the prescribed values prior to each repetitive shot. Any gaseous waste must be properly discharged to the waste handling system. In addition, protection of the final focusing laser mirror surfaces from chamber debris must be compatible with the vacuum system design.

The vacuum system must maintain a xenon buffer gas pressure of approximately 0.1 Torr (evaluated at 300K) in the reaction chamber a minimum of once every 100 ms. All other gases in the chamber must have a partial pressure small compared to the buffer gas pressure. It is assumed this "debris" partial pressure is maintained at 0.01 Torr. The gas removal system is "closed," terminating at the beginning of the waste processing system. Mirror protection requires that none, or an amount small enough not to affect mirror performance, of the debris from the reaction chamber is allowed to accumulate on the mirror surfaces.

DESIGN DESCRIPTION

Table 4.1.6.5-1 describes the parameters of the vacuum system and Figure 4.1.6.5-1 is a schematic of the same. Basically, the system involves a group of 12 Roots blowers (mechanical booster pumps), backed by an appropriate array of backing pumps which exhausts the pellet debris from the vacuum chamber between shots. The gas is exhausted through the main beam ducts. Secondary ducts connect the main ducts with the pumps. Xe gas flow from the mirrors to the pumps provides protection of the mirrors from chamber debris by countering diffusion of the debris toward the mirrors. The first wall is utilized as a condensation pump for the gaseous tantalum in the system.

TABLE 4.1.6.5-1

VACUUM SYSTEM PARAMETER LIST FOR THE LASER DRIVEN REACTOR

• Rep Rate	10 Hz
• Chamber Pressure	10^{-1} Torr @ 300K
• Chamber Radius	1000 cm
• Chamber Volume	4.2×10^{9} cm^3
• Wall Surface Temperature	800°K
• Time Averaged Gas Temperature	832°K
• Buffer Gas/Density	Xenon/3.2×10^{15} cm^{-3}
• Operating Debris Density	3.2×10^{14} cm^{-3}
• Per Shot Particle Load	1.9×10^{21} particles
• Effective Particle Mass	14.6 amu
• Single Shot Debris Density Rise	0.1%
• Pump Speed at Chamber	5.9×10^{4} ℓ/sec
• Effective First Wall Pumping Speed for Ta	1.2×10^{6} ℓ/sec
• Ta Filter Saturation Time	∿ 2 weeks
• Primary Vacuum Pump	10^{4} ℓ/sec - Roots Blowers
• Number of Primary Pumps	12
• Primary Pump Size	1.5 m x 2.0 m x 3.2 m
• Pumping Power	1.0 MW
• Pump Speed for Mirror Protection	2.3×10^{3} ℓ/sec
• Backing System	One - 10^{3} ℓ/sec Roots Blower One - 250 ℓ/sec Rotary for each primary pump

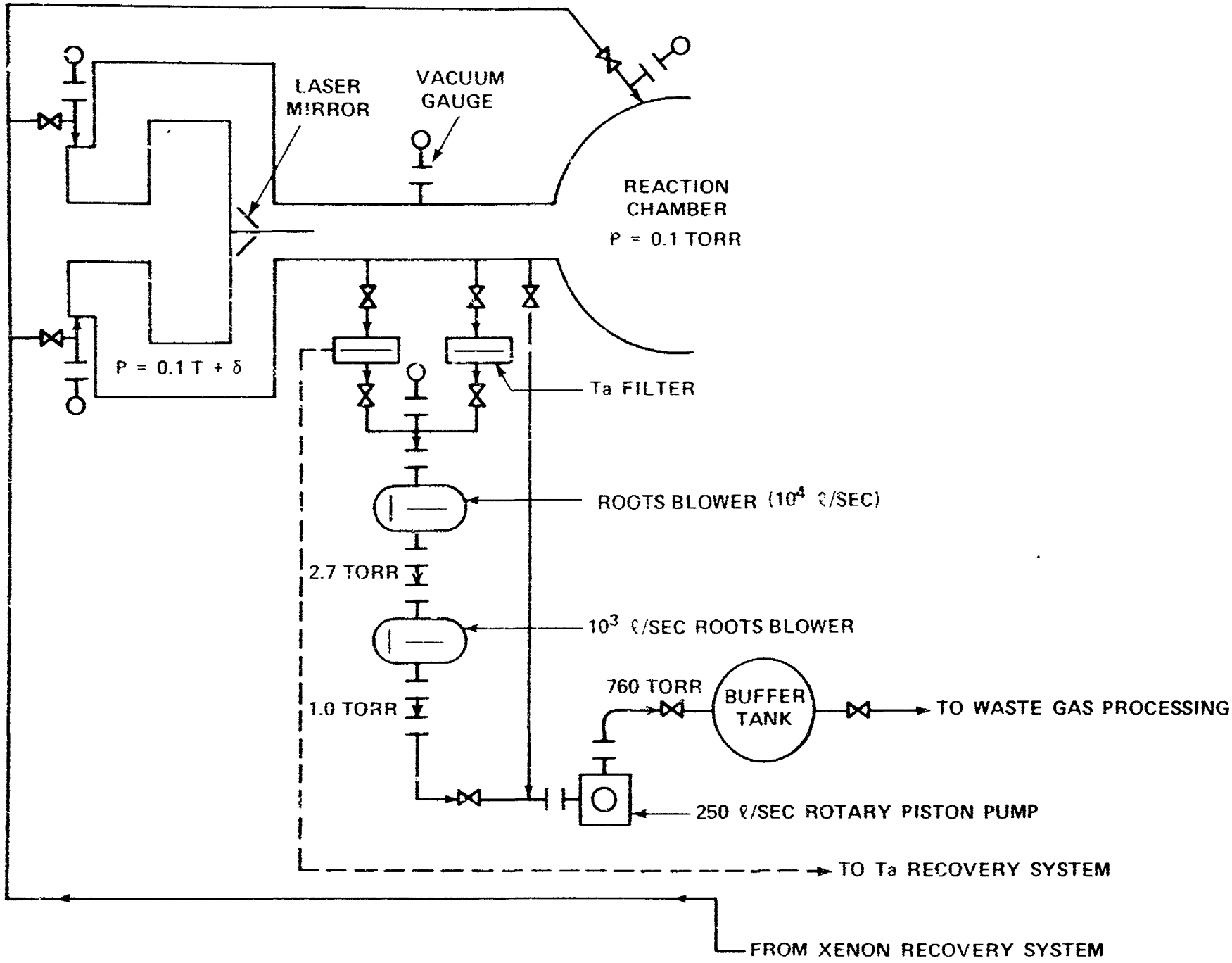

Figure 4.1.6.5-1. Vacuum System Schematic for the Laser Driven Reactor

615699-1A

SYSTEM OPERATION

The system operation involves continuous operation of the vacuum pumps. The pumps work at a constant speed while the gas bursts due to the pellet burns impose a cyclic characteristic on the chamber pressure. The pumps are sized to always return the pressure to about 0.1 Torr before the beginning of a shot. The Ta in the pellet condenses on the first wall while approximately 5% is sucked through the vacuum ducts and towards the pumps where that Ta which does not plate out on the duct walls is trapped by a Ta filter before reaching the pumps. The noncondensibles flow through the traps and are passed on to the gaseous recovery system via a buffer tank at atmospheric pressure. Xenon gas which is drawn out through the pumps is recovered and continuously bled back into the chamber to maintain the one-tenth Torr of Xe in the chamber as a buffer gas.

Recovery of the Ta which has plated out on the first wall is accomplished with the aid of a special pellet which evaporates many times the amount of Ta deposited by a regular pellet. About 95% of this evaporated Ta recondenses on the first wall; approximately 5% of this amount passes into the vacuum ducts and either plates out on the duct walls or is caught up in the Ta filters. The accumulation of Ta on the filters makes it necessary to replace the filters about once every few weeks. This is accomplished by remotely valving in a parallel filter and removing the saturated filter for Ta recovery. This procedure need not involve reactor shut down.

To protect the final focusing mirrors of the lasers, Xe gas is bled into the beam tunnels at about 0.3 Torr. This gas flows towards the chamber where it is removed by the vacuum pumps. The flow of gas displaces the flow of diffusing pellet debris, effectively stopping the debris far in advance of the mirror position (approximately 7 meters before the mirrors).

4.1.6.6 TRITIUM HANDLING SYSTEM

FUNCTIONS

The functions of the tritium handling system, which is primarily a chemical processing complex, include:

- Storing the fusile fuel inventories, including any excess bred tritium.
- Supplying deuterium and tritium to the pellet factory.
- Processing the microexplosion debris to recover and recycle the residual fusile fuels and reactor chamber inert gas, and eliminate the impurities and fusion generated helium (He-4).
- Eliminating the protium from the mixed hydrogen isotope stream recovered from the microexplosion debris.
- Adjusting the isotope mixes of the fusile fuels recovered by processing the microexplosion debris and supplying these to the pellet factory.
- Abstracting the tritium bred in the lithium flowing through the breeding blanket and heat transport modules.
- Holding the escape of tritium into the facility and into the environment to acceptably low levels.
- Providing tritium trapping capability to insure containment integrity in the event of emergencies such as power or cryogenic system failures or loss of vacuum.
- Providing adequate parallel flow path and vital equipment redundancies to ensure operational continuity of the facility in the event of process equipment malfunctions.
- Collecting the bulk of the He-3 generated by radioactive decay of tritium, handling it as a "special nuclear material."
- Reconstituting and recycling tritium that has been converted into tritiated water by the microexplosion debris processing operations.

The functions do not include the handling/processing/recovery of the heavy metal content of the pellets which operations are the responsibility of Radwaste Handling or disposal of other "hot materials" which operations are the responsibility of Radioactive Waste Handling (a Balance of Plant subsystem).

DESIGN REQUIREMENTS

Fulfilling the aforementioned functions dictates that the tritium handling complex comprise seven subsystems, operated in interconnected fashion, having the design requirements enumerated below.

Tritium Storage

- Provide compact, ultra-safe, flexible bulk storage for all on-site tritium inventory, with built-in means for maintaining tritium high purity.
- Storage capability must accomodate: (1) all fuel required for plant startup and "pipe-line fill," (2) steady state operation tritium content in the pregnant lithium stream, (3) pellet factory nominal supplies, and (4) accumulation of excess bred tritium, approximately 25% in excess of doubling of the plant startup required inventory, amounting in total to 150 full operating days' worth of tritium injected in the pellets.
- Storage subsystem must consist of multiple units for reasons of safety and operating flexibility; capability must exist for simultaneously dispensing and receiving tritium.
- Design must incorporate means for separating and collecting He-3 generated via tritium radioactive decay; decay amounts to 5.45% per year.

Deuterium Storage

- Provide bulk storage of all on-site deuterium supply inventory in highly compressed gaseous form, in amounts adequate for pellet factory needs.
- Deuterium, which is to be procured from a commercial supplier, is stored on-site in plant dedicated tube trailers which are manifolded to the dispensing lines.
- A multiplicity of tube trailers is required to allow for plant operating continuity when one of the depleted trailers is in transit for refilling.

Debris Primary Processing

The microexplosion debris will consist of a host of materials, the principal ones being H_2, D_2, T_2, He-4, HD, HT, DT, H_2O, CO_2, Xe, SiC, SiH_4, C_2H_2, SiO_2, Ta among others. The underlying design requirements for this subsystem include a sequence of steps and provisions:

- Separating out the particulates that may by-pass the vacuum system or that are generated during processing the debris, mainly SiC and SiO_2.
- Removing the readily condensible components (CO_2, C_2H_2, SiH_4, H_2O) and recovering their contained D and T.
- Removing the residual minor impurities (CO, H_2S, NH_3, PH_3, AsH_3, H_{2n+2}, etc.) carried in the non-condensibles, generating a stream consisting of the elements H, D, T, He-4, He-3, and Xe.
- Separating the hydrogen isotopes (H, D, T) from the rare gases (He-3, He-4, Xe).
- Recycling the bulk of the Xe back to the reaction chamber.
- Dispatching the off-gases generated to the Secondary Processing Subsystem for elimination/recovery of the contained tritium.
- Dispatching the purified hydrogen isotope stream to the H isotope mix adjustment facility (Cryogenic Distillation Subsystem).
- Providing secondary containments about the processing equipment to minimize T escape to the plant or environment, including dynamic inert buffer gas flow through the containment annuli, which gases are dispatched to the atmosphere cleanup units of the Processing Atmospheres Detritiation Subsystem.

Processing Atmospheres Detritiation

The dynamic inert cover gases (He or Ar) that sweep through the secondary and tertiary containments around the processing equipment (including T storage units and T emergency dump for the Cryogenic Distillation Complex) are continuously detritiated in closed loop fashion by the cleanup units of this subsystem, down to levels at or below MPC

(5×10^{-6} $\mu Ci/cm^3$) at the cleanup unit discharge. Any tritiated water generated by these operations is collected and dispatched to the electrolyzer of the Secondary Processing Subsystem for recovery/recycle of the contained T.

Secondary Processing

The Secondary Processing Subsystem is a multipurpose complex that fulfills the following design requirements:

- Detritiates all of the other gas streams including: He-3 generated by radioactive decay of in-storage T; He-4/He-3 generated in the Li of the T breeding system; off-gas stream of the H-isotope mix adjustment operations; O_2 stream generated by the tritiated water electrolyzer; inert gas sweep through the secondary containments for the heat transport system; all other off-gases prior to collection of these for monitoring, holdup, and discharge to the environment.
- Collects and stores the bulk of the He-3 generated by facility operations.
- Collects all tritiated water generated by facility operations, dispatching reclaimable level liquids to the electrolyzer and low level liquids to the facility radioactive waste system (balance of plant operation) for holdup or disposal.
- Electrolyzes the reclaimable level tritiated water, dispatching the H-D-T cathode product stream to the H-isotope mix adjustment facility.

Hydrogen Isotope Mix Adjustment

The main design requirements for this subsystem are: (1) adjusting the isotopic mix of the D and T recovered from the microexplosion debris, in conformity with the composition needed at the pellet factory, and (2) eliminating protium from the various feeds to the H isotope mix adjustment facility. Because of differences in the diffusion rates of D and T through the fuel enclosing capsule of a pellet, the principal product of this subsystem is a 55 a/o T:45 a/o D mixture. To provide for

operational flexibility at the pellet factory toward producing pellets having a 1:1 D:T makeup, this facility also provides small product streams of essentially pure D and T. The waste product stream contains the protium fed to the facility along with small amounts of D.

Bred Tritium Abstraction

As detailed in the section on Blanket and Shield Neutronics, tritium is bred in the liquid lithium flowing through the breeding blanket and heat transport systems. The breeding reactions also generate equal atomic amounts of He-4 and T. Additionally, the circulating Li will contain He-3 resulting from radioactive decay of T and small amounts of various corrosion-erosion products, including activation and decay daughter nuclides of these.

At plant startup the circulating Li will be virgin material. Reactor operation will create T which will be accumulating initially up to a point where the T level attains the design-point steady state value, at which time the Bred Tritium Abstraction Subsystem will start treating the pregnant Li on a continuing basis.

Design requirements for this subsystem include the following:

- Supplying capability to abstract the bred T at a rate equal to the plant breeding rate plus adequate stretch capacity, while producing high purity T, free of Li, He-4, and He-3.
- Providing capability to detritiate all of the Li inventory of the blanket and heat transport systems, if the need for this should arise.
- Recovering and collecting the He-4/He-3, for subsequent dispatching to a government facility for isolation of the special nuclear material He-3.

DESIGN DESCRIPTION

In basic makeup, the designs of the Tritium Handling System for both the CO_2 Laser and Heavy Ion Beam drivers are identical. Quantitatively there are some differences in the nominal materials throughput rates and hence design capability and hardware cost for five of the seven subsystems, stemming from the variances in the pellet compositions for the two drivers shown in Table 4.1.6.6-1.

TABLE 4.1.6.6-1

PELLET COMPOSITION FOR THE DRIVER OPTIONS

Pellet Mass Makeup, mg/pellet	CO_2 Laser	Heavy Ion
Carbon	14.7	20.0
Oxygen	16.5	18.6
Silicon	10.5	10.5
Tantalum	9.0	160.0
Hydrogen-Deuterium-Tritium	4.5	5.5
Total	55.2	214.6

Because the basic designs are identical, magnitudes for subsystem parameters and other relevant quantities for both fusion driver options are reported in this subsection only. In addition to making for terseness, this also provides ready comparison of system details for the two driver options treated.

The designs of the subsystems comprising the Tritium Handling System are dictated directly by some of the parameters prescribed for the plant operation. Magnitudes of these are listed in Table 4.1.6.6-2.

TABLE 4.1.6.6-2

PLANT PARAMETERS THAT IMPACT ON TRITIUM HANDLING SYSTEM DESIGN

Item	Magnitude
Pellet DT fusion energy yield, MJ/microexplosion	350
Pulse repetition rate, microexplosions/s	10
Tritium breeding ratio, atoms T created/atom consumed by fusion	1.220
Tritium inventory in pellet factory, full operating days worth	30
Tritium nominal inventory in standby storage, full operating days worth	5
Tritium storage subsystem full inventory capability, full operating days worth	150
Lithium circulating content in tritium breeding and heat transport systems, g atom Li	4.7×10^{8}
Mean tritium concentration in the circulating lithium	
g atom T/g atom Li	1.6×10^{-5}
wppm T	7

To the extent practicable, the design uses processing schemes that minimize moving parts in the interest of attaining high plant reliability and minimizing need for maintenance. To that end the processing hardware design in the main is based on fixed bed type of contactors. This applies particularly to the equipment specified for tritium storage, microexplosion debris purification, bred tritium abstraction, cold trapping of condensible compounds, and removal of tritiated water from gas atmospheres. In this kind of design approach the overall operation is continuous, although the individual components operate on a batch basis. This entails the need for a pair of contactors, one of which is in operation while the other is in standby status, going on stream when its twin is removed from the processing flow loop by remotely controlled valving for regeneration. Additionally, operational continuity and stretch capability are ensured by augmenting the

pairs of contactors by a third unit. Design conservatism is incorporated by including excess reacting medium within a contactor.

In general, three contactors are located within an Ar inerted hermetically sealed steel-lined, thick-concrete wall vault. A contactor consists of an inner and outer body, with the intervening annulus inerted with a controlled He flow. Counting the structure that houses the processing equipment, four levels of containment are provided for those pieces of equipment that contain substantial amounts of tritium. Each of the contactors are provided with sets of resistance heaters, remotely operated valving, and instruments. Each triplet of contactors is provided with gas coolers, emergency protection unit (thermal quench), and instrumentation to control temperatures and flow rates. The annuli He inerted zones and vault Ar inerted volumes are manifolded to a dedicated pair of continuously operated atmospheric detritiation units, valved so as to alter flow rates as may be required.

Table 4.1.6.6-3 summarizes the processing modes applied in the design of the Fuel Handling System. Tables 4.1.6.6-4 and 4.1.6.6-5 provide additional details regarding the principal contactor unit configurations, reactive metal requirements, internal dimensions of the contactor inner bodies, external dimensions of the containment vaults and unit operating temperature ranges.

Figure 4.1.6.6-1 is a simplified flow schematic that delineates the equipment hookup and flow sequence for processing the microexplosion debris, and companion Figure 4.1.6.6-2 is a simplified flow schematic for the bred tritium abstraction operations. Not shown on these are schematics for the cryogenic distillation complex, which involves a four column array, and a typical atmosphere cleanup system based on catalytic oxidation of the tritium and trapping the resulting tritiated water on molecular sieves.

TABLE 4.1.6,6-3

SUMMARY OF PROCESSING MODES APPLIED FOR FUEL HANDLING

	Mode
RESERVE FUSILE FUEL STORAGE	
1. Tritium	Solidified on depleted uranium
2. Deuterium	Compressed gas in trailer tubes
MICROEXPLOSION DEBRIS PROCESSING	
1. Removal of particulates (SiC, Ta wall spallations)	Mechanical separation
2. Removal of condensible vapors (C_2H_2, SiH_4, H_2O, CO_2)	Regenerative cryogenic trapping
Recovery of contained T	Catalytic oxidation, mechanical separation of SiO_2, trapping of tritiated water on molecular sieves followed by desorption, electrolysis of tritiated water, recovery of T by cryogenic distillation from H-D-T
3. Elimination of trace impurities (C, N, Si, S, P, As)	Hot uranium trapping
4. Separation of He-3, He-4 and noble gases from H isotopes	Cold uranium trapping
5. Further elimination of trace impurities to prevent column plugging	Cryogenic trapping
6. Elimination of H, recovery of D and T and adjustment of D:T mix	Cryogenic distillation

TABLE 4.1.6.6-3 (Cont.)

SUMMARY OF PROCESSING MODES APPLIED FOR FUEL HANDLING

	Mode
BRED TRITIUM ABSTRACTION	
1. T-removal from Li breeding stream	Gettering on yttrium beds
2. Recovery of T from Y getter beds	
Removal of adhering Li	Draining and moderate temperature vacuum distillation
Recovery of bred T	High temperature desorption - vacuum distillation
Elimination of associated He-3 and He-4	Gettering on Zr Al alloy and selective permeation through Pd-Ag diffusers
RECOVERY OF He-3 FROM IN-STORAGE TRITIUM	
1. Separation of He-3 from associated T	Gettering on Zr Al alloy and selective permeation through Pd-Ag diffusers
RECOVERY OF TRITIUM FROM SWEEP STREAMS AND OFF-GASES	
1. Separation of H isotopes from carrier gas	Catalytic oxidation, trapping of tritiated water on molecular sieves followed by desorption and electrolysis of tritiated water
2. Recovery of T and D and elimination of H	Cryogenic distillation

TABLE 4.1.6.6-4

DESIGN CONFIGURATION AND MATERIALS FOR PROCESSING EQUIPMENT

T Storage-Generators, U Cold and Hot Traps, Bred T Abstractors, Cryogenic Distillation Emergency Dump

	Uranium Getter	Yttrium Getter
Number of Units/Containment Vaults		
T storage-generators	3/1	
U cold-traps	3/1	
U hot-traps	3/1	
Bred T abstractors	-	3/1
Cryogenic distillation emergency dump	1/1	-
Inner Body		
Material	316-SS	Inconel
Wall thickness, cm	2.5	3.0
Head thickness, cm	4.0	6.0
Inside height to diameter ratio	1	2
Bulk getter density, g/cm^3	2	1
Inner volume to bulk getter volume ratio	3	3
Outer Body		
Material	316-SS	316-SS
Wall thickness, cm	2.5	2.5
Head thickness, cm	4.0	4.0
Vault Liner		
Material	304-SS	304-SS
Thickness, cm	1.0	1.0
Vault Enclosure		
Material	Concrete	Concrete
Shape	Cylindrical	Cylindrical
Thickness, cm	30	30

TABLE 4.1.6.6-4 (Cont.)

DESIGN CONFIGURATION AND MATERIALS FOR PROCESSING EQUIPMENT (Cont.)

	Uranium Getter	Yttrium Getter
Clearances, cm		
Annulus between inner and outer bodies	3	6
Radial spacing between unit outer bodies and vault center-line	60	60
Radial spacing between outer bodies and vault interior wall	30	30
Combined vertical spacing (top plus bottom) between outer bodies and vault interior	120	120

TABLE 4.1.6.6-5

CONTACTOR GETTER MASSES, DIMENSIONS AND OPERATING TEMPERATURES

Item	Uranium Getter		Yttrium Getter
	Laser Driver	Heavy Ion Driver	
Total Getter Mass, kg			
Tritium storage-generators	6360	6360	
Hot uranium traps	1145	2190	
Cold uranium traps	1250	2090	
Cryogenic distillation emergency dump	570	1820	
Bred tritium abstractors			12000
Inner Body Dimensions, radius/height,cm			
Tritium storage generators	80/160	80/160	
Hot uranium traps	45/90	56/112	
Cold uranium traps	46/92	55/110	
Cryogenic distillation emergency dump	36/72	53/105	
Bred tritium abstractors			96/385
Vault External Dimensions, diameter/height, m			
Tritium storage generators	2.9/3.6	2.9/3.6	
Hot uranium traps	2.2/2.9	2.4/3.2	
Cold uranium traps	2.2/3.0	2.4/3.1	
Cryogenic distillation emergency dump	2.0/2.8	2.3/3.1	
Bred tritium abstractors			2.3/6.0
Operating Temperature Range, K			
Tritium storage generators	290-660	290-660	
Hot uranium traps	800-830	800-830	
Cold uranium traps	330-830	330-830	
Cryogenic distillation emergency dump	290-660	290-660	
Bred tritium abstractors			
Tritium sorption phase			570
Lithium drain phase			570
Lithium distillation phase			770
Tritium desorption phase			950

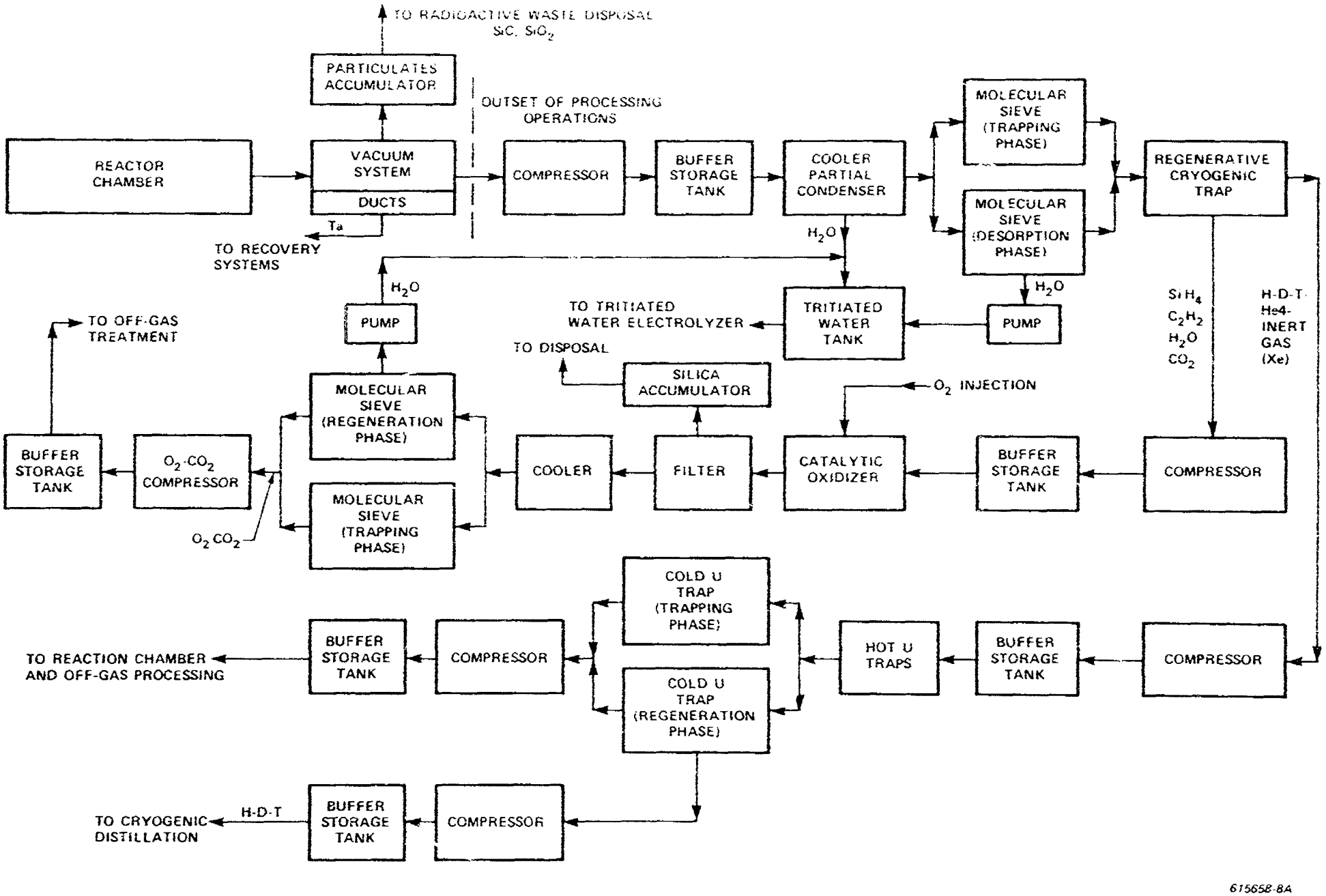

Figure 4.1.6.6-1. Simplified Flow Schematic for Microexplosion Debris Processing

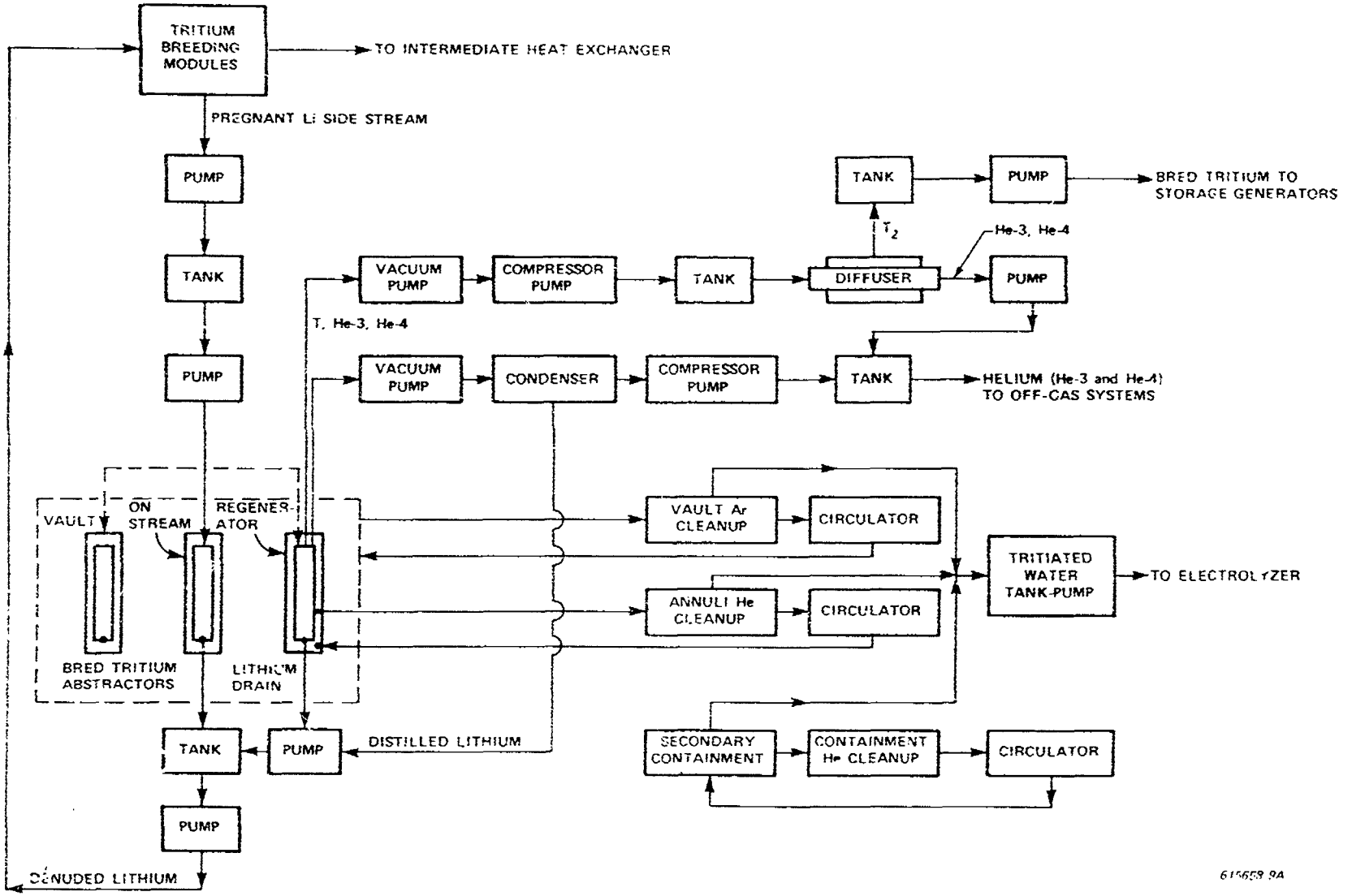

Figure 4.1.6.6-2. Simplified Flow Schematic for Bred Tritium Abstraction

SYSTEM OPERATION

Initially the reaction chamber contains inert gas (Xe) and the Li in the coolant/breeder loop is T free. With the onset of plant startup two main transients occur in the fuel handling portions, en route to establishment of steady state operating conditions:

- The microexplosion debris level in the reaction chamber increases to a steady state value as determined by the rates of fuel addition, gas removal by the vacuum system, and recycle of the Xe. At the steady state condition the rate of debris removal by the vacuum system which is passed along to processing is equal to the rate of debris generation.
- Abstraction of the bred T from the Li is deferred for the first 35 full operating days, during which time the T level builds up to 7 wppm. At this point the abstraction operations are initiated. Associated with the T rise are similar transient buildups of the He-4 and He-3 levels in the Li to 9.3 and 0.034 wppm respectively.

Treatment of the microexplosion debris involves the sequence of processing steps shown schematically in Figure 4.1.6.6-1. The not readily condensed components, which consist mainly of H-D-T-He are purified by hot U trapping, with separation of the H-D-T effected by cold U trapping. The hot U traps operate continuously, whereas the cold U traps operate in a batch mode, nominally on-stream for one full operating day, followed by valving out of the processing circuit and regenerating the trapped H-D-T by a heat-up. Subsequent to a cooldown the denuded cold trap is valved back into the processing circuit, while its twin is removed for denuding. Operating in this tandem fashion, the net result is an essentially continuous processing operation.

The feed to the cryogenic distillation complex consists of the H-D-T stream recovered from the cold U traps augmented by the substantial H-D-T cathode product of the tritiated water electrolyzer. The complex operates continuously around-the-clock in the range 20-25 K, producing three main

product streams (∿ 0.45:0.55 D:T, T, D) and a waste stream (H containing D in the ratio D:H = 0.0002:1). When the reactor is shut down for maintenance or otherwise not operating the complex is nevertheless kept in operation under total reflux conditions, in order to preserve the concentration gradients required for successful performance.

Abstraction of the bred T from the pregnant Li is accomplished by the processing steps diagrammed schematically in Figure 4.1.6.6-2. A triplet of Y abstractors sorb the T out of the pregnant Li, one of which is on-stream in a batch operating mode at any time. The nominal on-stream time per cycle is one full operating day. Flow to the abstractor amounts to 72 kg Li/min corresponding to a daily turnover of 3.2% of the contained Li in the breeding blanket-loop-heat exchanger complex. A loaded abstractor is valved out of the circuit for recovery of the sorbed T, and one of the other abstractors is valved into the Li loop. Abstraction/regeneration of a loaded unit is accomplished by a three step process: (1) draining of the Li adhering on the Y chips; (2) preferential controlled temperature distillation of the Li not removed by the drain; (3) recovering the sorbed T by combined thermal dissociation-vacuum distillation. During these operations the associated He-4 and He-3 are also removed. Separation of the T from the He-4 and He-3 is accomplished by selective permeation through Pd-Ag diffusers.

4.1.6.7 RADWASTE HANDLING SYSTEM

Radwaste Handling is confined solely to consideration of the heavy metal content of the pellets. Treatment/ultimate disposal of all other radioactive wastes generated by ICFR operations are not included, and would normally be a responsibility of the Balance of Plant Systems.

FUNCTIONS

The functions of the radwaste handling system, which like the tritium handling system is also primarily a chemical processing complex, include:

- Receiving the neutron activated tantalum collected in the reaction chamber and duct walls after it is removed by the remote maintenance operations.
- Packaging and holding up the radioactive tantalum in safe suitable containers for the necessary decay times to allow essentially hands-on processing of the decayed material.
- Processing the cooled material to remove impurities and activation generated elements so as to result in gross recovery of purified tantalum and in a chemical form best suited for fuel preparation at the pellet factory.
- Using the by-products of the tantalum incorporation schemes of the pellet factory, to the extent possible, in the tantalum recovery/recycle processing facility.
- Collecting and storing the more valuable by-products of the tantalum recovery/recycle processing facility for potential sale to rare and precious metal processors/vendors.

DESIGN REQUIREMENTS

Compliance with foregoing functional duties imposes the design requirements enumerated below:

1. The tantalum will be radioactive, the principal nuclide being Ta-182

with a 115.1 day half-life and with most of the gammas having an energy of ∿ 1.2 MeV. A batch of machinings removed from the ducts may have a gross activity of several millions of curies. Consequently the machinings initially will have to be generated-handled-packaged for cooling under "hot cell conditions."

2. In view of the 115.1 day half-life of Ta-182, a storage-cooling period for the machinings on the order of four years will be required to lower the activity by a factor of ∿ 6000 if something approaching "hands on" processing is to be attempted.

3. Economics and conservation of strategic materials considerations dictate the need for Ta reclamation/recycle at the plant site rather than disposal otherwise.

4. Due to the chemical inertness and refractory nature of the oxides and nitrides of Ta and the processing complications that could arise from the presence of these, precautions must be exercised to minimize their formation. To that end, storage of the Ta machinings must be in tightly sealed weather-proof durable containers that are evacuated and back-filled with an inert gas (Ar).

5. To the extent practicable the processing scheme adopted for recovering/recycling the Ta should yield a final product that can be applied directly in the pellet factory for incorporating the heavy metal into the fuel pellets.

6. Ideally, the processing scheme should achieve very close to 100% closed-cycle operation when tied into the operations of the pellet factory. Reagents consumed in one place should be regenerated elsewhere in the operations, with minimal creation of waste products and need for makeup of chemicals.

7. In addition to unreacted natural Ta and residual Ta-182, there is a high probability for the presence of more than threshold levels of

transmutation nuclides of tungsten, rhenium, osmium, iridium among others, which if carried over into the recovered Ta, may interfere with operations at the pellet factory. Consequently, the recovery/recycle process evolved must include means for separating/eliminating such potentially objectionable nuclides.

8. To the extent possible the processing schemes adopted should be based on state-of-the-art technology, involving minimal or no development effort.

DESIGN DESCRIPTION

The design basis and the operating modes of the Radwaste Handling Systems for both the laser and heavy ion driven plants are identical. The only differences are in the required component sizes and materials throughput capabilities. The facility for the heavy ion driven plant is significantly larger and costlier than that for the laser driven plant, due to the larger Ta content in the fuel pellets, 160 vs. 9 mg/pellet. In view of the identical nature of the designs, magnitudes of the parameters for the facilities are reported only in this subsection.

The design capability of the Radwaste Handling System is set at double the nominal Ta injection Rate (assuming 100% plant availability) to provide stretch capacity, resulting in design throughput rates of 5,700 and 102,000 kg Ta/yr for the laser and heavy ion driven plants respectively.

The proposed means for packaging-storing the radioactive machinings is an array of 55 gallon stainless steel (type 304) shipping-storage drums with removable seal-tight heads provided with valving for evacuation and inert gas back-filling. Based on a machinings anticipated bulk density of 4.2 g/cm^3, the Ta content of a typical packed drum will amount to 870 kg.

The main product is high purity tantalum pentachloride ($TaCl_5$). The $TaCl_5$ is dispatched to the pellet factory where it is used in the

preparation of the TaCHO that is incorporated in the fuel and in the application of the Ta metal coating on the pellets via the chemical vapor deposition (CVD) technique. The by-product of the Radwaste Handling System is a mixture of chlorides of various transmutation daughters, particularly W, Re, Os, Ir. Separation of the $TaCl_5$ and by-product chlorides which result from the chlorination of the aged machinings is accomplished by fractional distillation.

The dry chlorine required for the metal chorination operations is generated by the electrolysis of aqueous potassium chloride (KCl); the electrolysis cathode product is hydrogen, which is dispatched to the pellet factory and used there in the chemical vapor deposition operations. A third product of the electrolysis is aqueous potassium hydroxide, which is also dispatched to the pellet factory where it serves to trap the hydrogen chloride (HCl) by-product of the Ta chemical vapor deposition operations, thereby forming KCl.

The simplified flow schematic shown in Figure 4.1.6.7-1 indicates the processing sequence and interfaces between the involved ICF major systems.

Completely 100% closed-cycle operation will not be achieved. Ta, KCl (or KOH), and H_2O replacements will have to be introduced from time to time to make up processing and transmutation losses.

Table 4.1.6.7-1 provides details regarding the chlorinator and electrolyzer configurations, operating modes and temperatures, number of units installed, and operating characteristics.

SYSTEM OPERATION

Packaging-storing operations for the Radwaste Handling System will commence at the time of generation of the first batch of radioactive Ta machinings. On the basis that this will occur after one-half year of uninterrupted operation of the plant, the amounts of materials to be packaged and placed into storage will amount to 1,420 and 25,230 kg

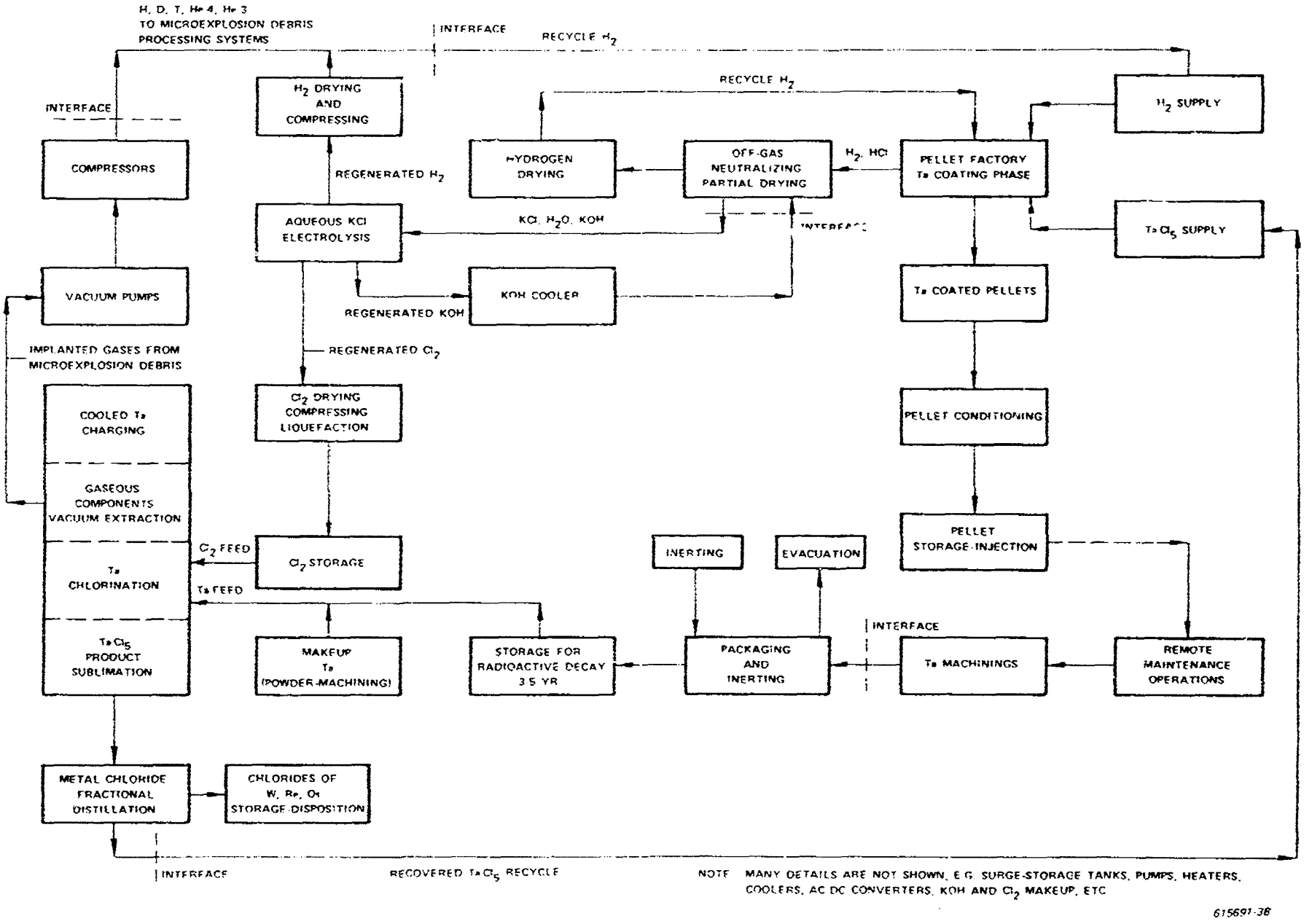

Figure 4.1.6.7-1. Simplified Schematic for Radwaste Processing

TABLE 4.1.6.7-1

DESIGN CONFIGURATION -
OPERATING MODES OF KEY RADWASTE PROCESSING COMPONENTS

ITEM	LASER DRIVER	HEAVY ION DRIVER
Chlorinators		
Number of units	12	12
Inner Body		
Material	Hastelloy C	Hastelloy C
Wall Thickness, cm	3	3
Head Thickness, cm	6	6
Inside Height/Diameter Ratio	2	2
Bulk Machinings Density, g/cm^3	4.2	4.2
Inner Volume/Bulk Machinings, Volume Ratio	3	3
Inner Diameter, cm	19.3	50.3
Inner Height, cm	38.5	100.5
Outer Body		
Material	Hastelloy C	Hastelloy C
Wall Thickness, cm	2.5	2.5
Head Thickness, cm	4.0	4.0
Annular Clearances, cm	6.0	6.0
Operations Mode	Batch	Batch
Loading Time, hr	1	1
Evacuation-Degassing Time, hr	44	44
Chlorination Time, hr	8	8
Product Sublimation Time, hr	3	3
Temperature Range, K		
Evacuation-Degassing	600	600
Chlorination	570-620	570-620
Product Sublimation	750	750
Electrolytic Diaphragm Cells		
Type	Hooker S	Hooker S
Current, Amp	7000	7000

TABLE 4.1.6.7-1 (CONT'D)

ITEM	LASER DRIVER	HEAVY ION DRIVER
Potential Drop, volts/cell	3.5	3.5
Current Efficiency, %	95	95
Operating Temperature, K	360	350
Total Design Capability, kg KCl electrolyzed/day	32	570
Number of Cells Installed	2	3

respectively for the laser and heavy ion driven plants. This material would then be held in storage for four years of radioactive decay before being withdrawn for processing/recovery/recycle of the Ta. On the basis that the half-year frequency applies throughout for removal of the accumulated pellet heavy metal, the amount of Ta held up in storage and the reactor nominally would amount to 12,770 and 227,100 kg respectively for the laser and heavy ion driven plants, and the corresponding number of drums would total 15 and 261.

The packaging campaigns nominally occur at half-year intervals. The machinings generated by the Remote Maintenance operations are weighed, placed in the drums, the lids are applied and clamp-sealed. The drums are then evacuated to 0.1 Torr, back filled to 760 Torr with dry Ar, appropriately marked, logged into the materials inventory records, and then conveyed to the drum storage area.

Subsequent to undergoing storage for radioactive decay, the drums are externally monitored (gamma ray spectrometry) for determination of residual activity, and passing this, are transported to the Radwaste Handling facility. Here the following processing steps are conducted on the heavy metal:

- The machinings are charged into the chlorinators by automatic loading devices.
- The units are heated to 600K and subjected to an evacuation-degassing operation (10^{-5}-10^{-6} Torr) for a period of 44 hr to drive off the imbedded/sorbed gaseous elements (H, D, T, He-3, He-4), which gases are dispatched to the Debris Primary Processing Subsystem of the Tritium Handling System.
- The heavy metal chlorination phase is conducted under batch closed conditions at 570-620 K and nominally at 760 Torr over an 8 hr period, with the controlled addition of dry chlorine gas to the chlorinators. Progress and completion of the chlorination is indicated by monitoring the system pressure.
- Removal of the heavy metal chlorides from the chlorinators is accomplished by subliming these compounds via a 750 K, 3 hr treatment phase.
- Separation of the transmutation daughter nuclide chlorides from the $TaCl_5$ principal product is accomplished by a subatmospheric multicomponent fractional distillation operation.
- The $TaCl_5$ is dispatched to the pellet factory, and the by-product heavy metal chlorides are stored, pending disposal by sale to precious metal processors/vendors.

The associated main activity conducted at the Radwaste Handling facility is the electrolysis of the spent aqueous KOH-KCl generated at the pellet factory to produce: (1) chlorine, which is consumed in the heavy metal chlorination operations; (2) hydrogen, which is dispatched to the pellet and consumed there in the fuel pellet Ta coating operations; (3) regenerated aqueous KOH, which is dispatched to the pellet factory and used there to trap the HCl generated by the fuel pellet Ta coating operations.

Although full scale operation of the Radwaste Handling facility on Ta machinings would be deferred on the order of 4.5 full operating years of the reactor, the electrolysis activities could begin with reactor startup. This would minimize accumulation of large amounts of spent aqueous KOH and consumption of hydrogen, albeit with the associated accumulation of substantial amounts of chlorine. In this connection the following numbers would apply:

ITEM	LASER DRIVER	HEAVY ION DRIVER
Nominal Treatment Rate, kg/day		
KCl Electrolyzed	16	285
KOH Generated	12	214
H_2 Generated	0.22	3.9
Cl_2 Generated	6	107
Chlorine Accumulation in 4.5y, kg	12,510	222,450

The Ta contents of the pellets are relatively low, at 9 and 160 mg for the laser and heavy ion driven cases respectively. Consequently, the time required to build up a substantial thickness of deposited Ta on the reactor chamber are large, corresponding to 22,870 and 1,290 full operating days for a 1 cm thick shell.

The value of the 4.5 year held-up Ta is substantial, amounting to $1.5M and $26.6M respectively for the laser and heavy ion driven plants.

4.1.6.8 MAINTENANCE AND SERVICING SYSTEM

FUNCTION

The function of the maintenance and servicing system is to:

a) determine which major components or portions of the reactor require inspection and or repair,

b) provide the means of disassembling the reactor to remove the identified components,

c) reinstall new or refurbished components into the reactor,

d) thoroughly inspect and repair the removed components for subsequent evaluation and reuse.

DESIGN REQUIREMENTS OR CRITERIA

- The "Planned" maintenances and/or repair functions should be capable of being completed during the normal utility annual and/or five year shutdown periods.
- The maintenance and servicing functions should be capable of being performed remotely.
- "State-of-the-art" concepts should be utilized to the maximum extent practical with advancements in technology utilized if found necessary.
- The operation must be capable of being performed in a manner so that the safety of the personnel and reactor are fully guaranteed.
- The maintenance equipment must be campatible with the environment to which they will be exposed when used in and near the reactor chamber and the reactor vessel intervals.

SYSTEM OPERATIONS

The major maintenance operations which are to be performed on a yearly basis involve the removal and reinstallation of a complete first wall assembly, a detailed inspection of this first wall and a means of refurbishing the first

wall by crack repair and the removal or addition of tantalum to the first wall inner surface. Once every five years the vacuum ducts, which are the connection between the reactor vessel and the laser beams, would also be removed, inspected and refurbished.

The particular operations which must be performed start with the draining of the lithium coolant followed by the removal of components, equipment, shielding, etc., which block access to the outer spherical shell of the reactor and the vacuum ducts. Then any joints or connections which are attached to the upper spherical half, such as coolant lines, support structure bolts, clamps, etc., would be disconnected or uncoupled so that the upper spherical half (approximately 23 m diameter, 400 tonnes) can itself be parted from the lower spherical half and then lifted and moved to temporary storage by the 1000 tonne overhead crane. Once this is accomplished, the first wall assembly (approximately 750 tonnes) will be disconnected from its support structure, all coolant connections between the first wall assembly and the outer sphere disassembled and the first wall unit lifted and moved to the hot cell (Figure 4.1.6.8-1). Table 4.1.6.8-1 lists the weights and sizes of some servicing equipment.

Since the first wall assembly which is being removed is highly radioactive, the majority of the operations would have to be performed remotely and a personnel exclusion area established so that the movement of the unit will not present radioactive exposure problems to any personnel. It will also be necessary for numerous remote control actions to be used during the maintenance operations which will require specially designed components to be incorporated into the reactor design. This will include: a) means of guiding and aligning components such as the upper spherical half, the first wall assembly and the vacuum ducts for installation and removal, b) the placement and operation of automatic seal welding and cutting equipment and c) the incorporation of flanged joint duct installation and removal equipment.

After the reactor has been reassembled, the first wall assembly which was removed from the reactor will be thoroughly inspected and reworked for subsequent

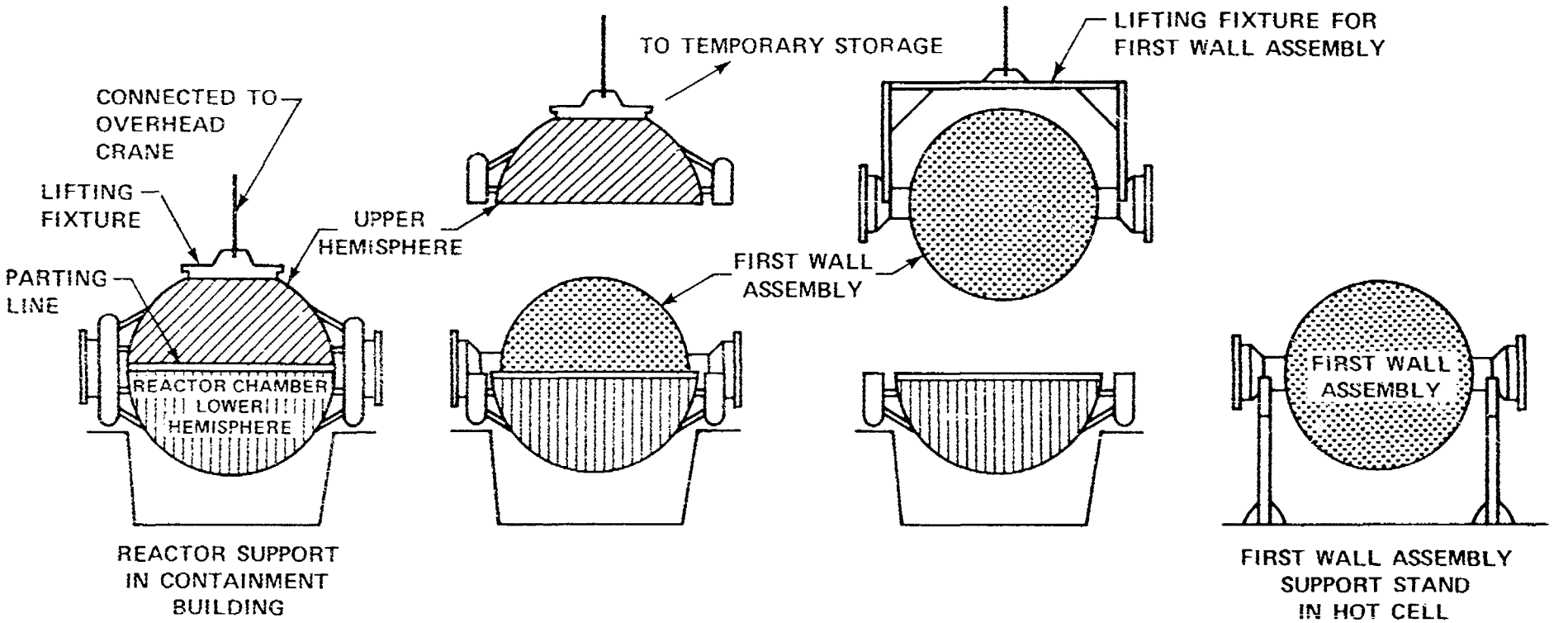

Figure 4.1.6.8-1. Sequence of Operations for the Maintenance of the First Wall

reinsertion into the reactor at a later shutdown. This scenario provides maximum usage of maintenance personnel by providing useful work which can be performed on a normal yearly work schedule and not have an adverse effect on the plant availability.

During the major five year shutdown, in addition to the first wall assembly, the two vacuum ducts (approximate weight of 125-150 tonnes each) will be removed and replaced. These ducts will be disconnected at the side ports of the sphere, coupled to the lifting rods of linear actuators which would be mounted on a commercially available Gantry type self propelled handling device. The duct would be raised and simultaneously rotated to a vertical position where it would be lifted through an access hatch and positioned in an area where it could be attached to move it to the transfer bay and then into the hot cell (See Figure 4.1.6.8-2).

These ducts will also be fully examined and a determination made as to any refurbishment required for future use. These repairs would involve crack location and the removal or addition of tantalum coating on the inner surfaces.

Detailed step by step procedures were developed for the various maintenance operations discussed above. These procedures are discussed in Chapter 5 and appear in the Appendix to this report. The analysis of these tasks indicated that the complete first wall assembly (without the vacuum ducts) could be removed and replaced in approximately 26 days which is consistent with the criteria of being performed within the normal yearly utility shutdown period.

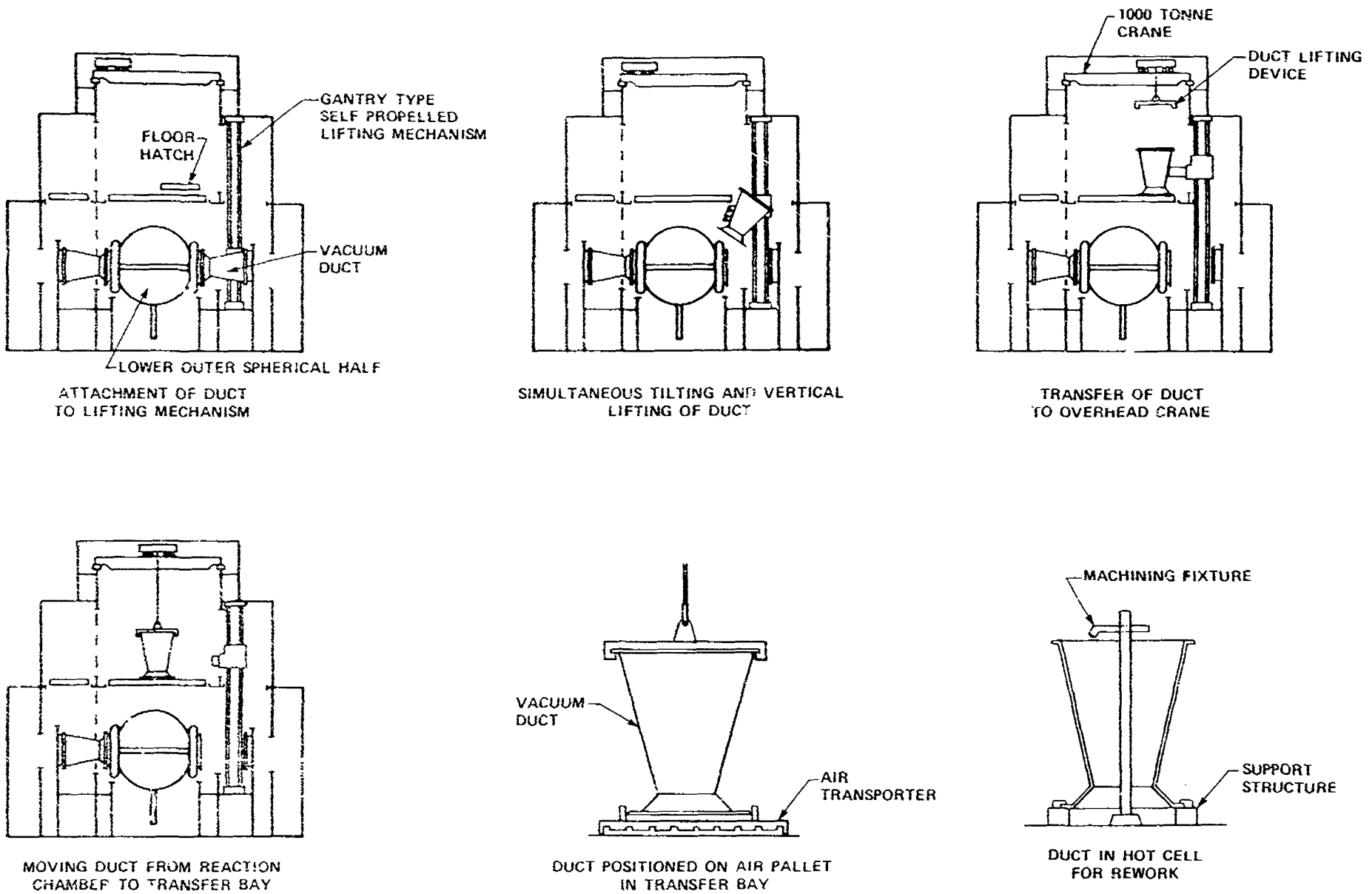

Figure 4.1.6.8-2. Schematic Showing the Removal Operations for the Vacuum Duct for the Laser Driver

705317-28

TABLE 4.1.6.8-1

LIST OF WEIGHTS AND SIZES OF SERVICING EQUIPMENT
FOR BOTH LASER AND HEAVY ION DESIGNS

		Driver	
		CO_2 Laser	Heavy Ion Beam
Components to be Lifted			
Upper Spherical Half (with Graphite Reflector Attached)		400 Tonnes ∿23 m dia.	400 Tonnes ∿23 m dia.
Spherical First Wall Assembly (Prior to Tantalum Deposit caused by Pellets)		750 Tonnes ∿26 m dia.	700 Tonnes ∿26 m dia.
Vacuum Duct		∿125 Tonnes ∿ 12.3 m Long	∿150 Tonnes ∿ 10 m Long
Tantalum Build-up/Year (50% plant availability, 95% surface area)		∿ 2.4 Tonnes	∿ 43 Tonnes
Lifting Device for Large Components		∿ 34 Tonnes 24 m long x 0.6 m wide x 1.0 m deep	∿ 34 Tonnes 24 m long x 0.6 m wide x 1.0 m deep
Shielding Blocks		20 Tonnes each	20 Tonnes each
Crane for Reaction Chamber			
Main Hook		1000 Tonnes	1000 Tonnes
Hoist Speed (Meters/Minute)	Slow	0.3	0.3
	Medium	0.45	0.45
	High	0.6	0.6
Auxiliary Hook		75 Tonnes	75 Tonnes
Trolley Speed (Meters/Min.)	Slow	3.0	3.0
	Medium	6.0	6.0
	High	9.0	9.0
Bridge Speed (Meters/Min.)	Slow	4.0	4.0
	Medium	6.0	6.0
	High	9.0	9.0
Bridge Span		33.5 m	33.5 m

TABLE 4.1.6.8-1 (Cont.)

LIST OF WEIGHTS AND SIZES OF SERVICING EQUIPMENT
FOR BOTH LASER AND HEAVY ION DESIGNS

	Driver	
	CO_2 Laser	Heavy Ion Beam
Remote Operated Shielded Mobile Floor Unit	~4 m x 3 m x 4 m High	~4 m x 3 m x 4 m High
Remote Operated Shielded Crane Cab	~4 m x 3 m x 3 m High	~4 m x 3 m x 3 m High
Main Seal Welding/Cutting Machine - Track Mounted on Outer Sphere	~1 m x 1 m x 0.5 m	~1 m x 1 m x 0.5 m
General Utility Tool	~14 m (long) x 5 m dia.	~14 m (long) x 5 m dia.
Remotely Operated Transport Units Operating Between Transfer Bay, Hot Cell and Storage Areas	Air Pallet - Sized to Handle 22 m Spherical Unit	Air Pallet - Sized to Handle 22 m Spherical Unit

4.1.7 DATA HANDLING AND CONTROL

FUNCTION

The functions of the data handling and control system are: a) to read transducers connected to plant, b) to read operator inputs, c) to provide control signals to actuators governing plant operation, d) to maintain operation within prescribed parameter space, e) to log operation for diagnostic purposes, f) to log parameters for archival purposes, g) maintain safe operating conditions, and h) provide timely warning of drift from established parameters.

DESIGN REQUIREMENT

The basic requirements of the system are: 1) that it be able to accept data at the rate generated by the plant, 2) that it be able to analyze the data in accordance with the desired plant operating parameters, 3) that it be able to produce the appropriate control signals, 4) that it be able to provide suitable indications to the operators.

SYSTEM DESCRIPTION

The system is a distributed system which communicates between units by a CAMAC protocol using optical fibers. The center of the system is a main frame computer with a real time operating system. The subsystems are, in general, minicomputers which may in turn have microcomputers under them. The subsystems in most cases behave as set point controllers with provisions for data reduction, alarm setting, and local display. The injector, pellet tracking and aiming system differs from the other systems in that, at this time, it is felt that dedicated hardware is required for this function. A block diagram of the system is shown in Figure 4.1.7-1. The data logging function has three classes of storage. A short term storage which may be disc, or in the near future magnetic bubble, is used for storing data for the last N hours and may be used for diagnostic purposes and trending. The long term storage may be magnetic tape and is used for archival storage of operating data. The hard copy is a printer which may be used to produce

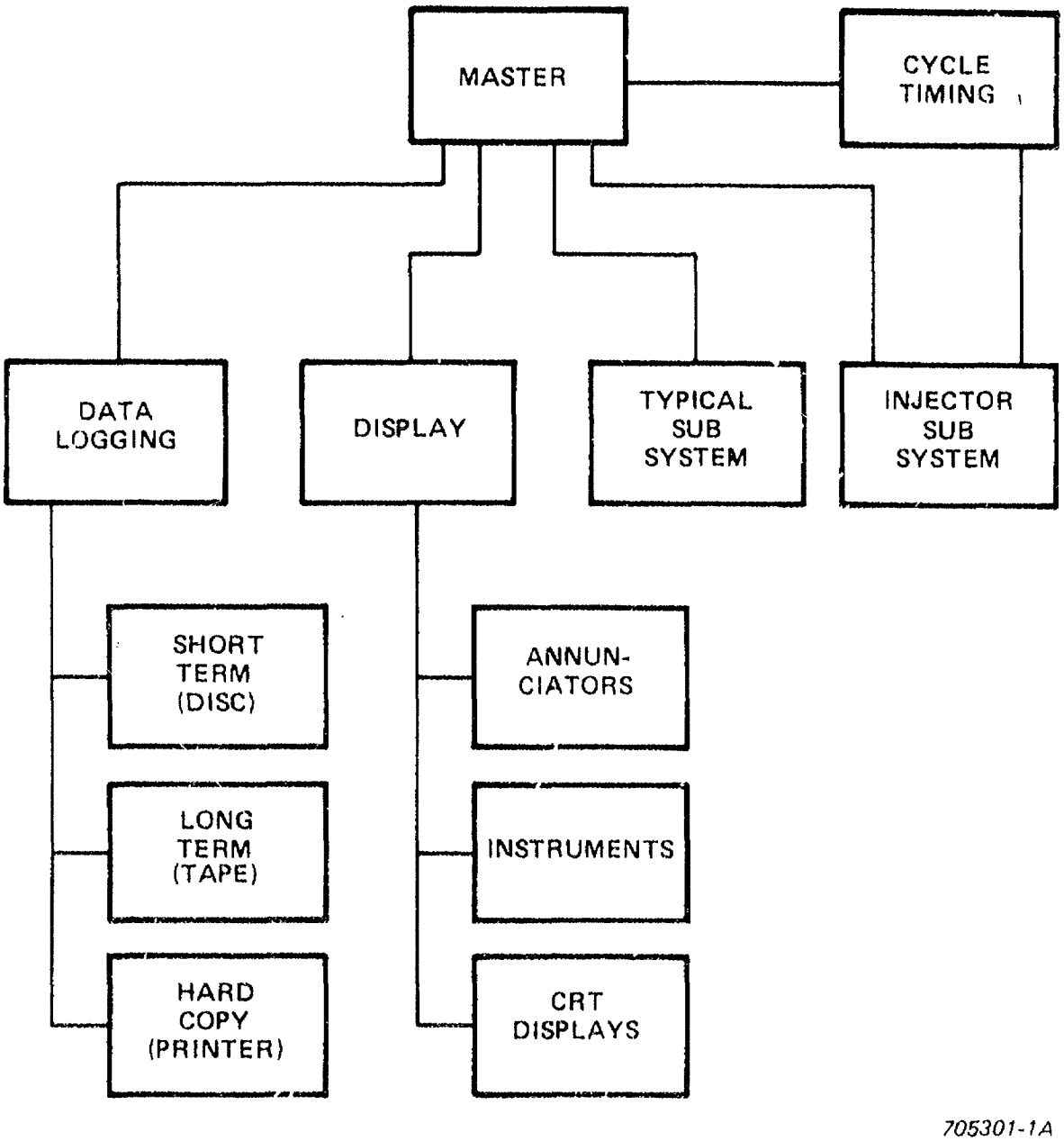

Figure 4.1.7-1. Block Diagram of System to Control Pellet Injection, Pellet Tracking and Beam Aiming

daily operations reports and other data for which human analysis is required. The display functions are provided on an operator's panel in the form of signal and alarm lights, digital and analog instruments and a CRT display for various data and information.

The typical subsystem will be a remote minicomputer which will receive its operating parameters from the master, or from the operator through the master, by means of a fiber optic communications channel. The function of the subsystem is to maintain operation at the prescribed parameters and to send to the master its status and any out of tolerance conditions.

The cycle timing is used to initiate the pellet injection cycle. The master provides to the cycle timer the desired repetition rate of pellet injections and the cycle timer will provide the required injection sequence starting pulse.

The injection subsystem provides the sequencing necessary to perform the pellet injection. This includes the delivery of the pellet and sabot at an appropriate time, the initiation of injection, timing of the flight of the pellet, determination of position of the pellet, generation of an abort signal if pellet is not properly positioned and aiming correction signals.

SYSTEM OPERATION

In response to the energy demand, which is an operator input subject to parameter limits, the master will generate a number for the injection cycle period. This will be passed to the cycle timer which will produce the sequence of signals required to load a pellet and sabot and initiate an injection. The injector subsystem will time the flight of the pellet from initiation to entry into the chamber for an indication of proper operation of the injector. The time of flight from entry into the

chamber until intercept of the tracking beams permits the calculation of the ETA at the center of the chamber. The variation in the time of breaking of the tracking beams permits a measure of the pellet position relative to the axis, and the generation of an abort signal if the position error is too great. If the pellet position is satisfactory, a beam firing signal is generated at such a time as to permit the beams and pellet to arrive at the center of the chamber simultaneously.

At the same time, other subsystems are monitoring the vacuum, coolant flows, and temperatures, etc., and if an abnormal condition is detected the abort signal may be produced. In the event of an abort, a printout could be made either automatically or upon demand giving the cause of the abort and the status of all systems.

For each shot the results will be monitored and stored on the short term storage. This record may be examined to aid in the diagnosis of faulty operation to see if a trend had been established previously which eventually led to the false operation.

4.1.8 BALANCE OF PLANT

4.1.8.1 INTERFACE WITH REACTOR

FUNCTION

The ICF plant has two principal liquid metal circuits; the lithium cooling circuit for the Reaction Chamber in series with the primary lithium heat transfer loop, and the secondary sodium heat transfer loop.

The lithium cooling circuit extracts the pulsed fusion energy from within the Reactor Chamber and converts it to heat energy and transfers the heat to the secondary sodium heat transfer loop within the Intermediate Heat Exchangers. The sodium heat transfer loop transfers the heat to the steam circuit within the Steam Generators, producing superheated steam.

DESIGN REQUIREMENTS

Table 4.1.8-1 enumerates the parameters imposed on the Heat Transport System by the Reactor Design, namely maximum heat load, lithium flow and lithium inlet and exit temperatures. In addition, the parameters that are imposed on the system as a consequence of these and the Turbine Generator requirements are included.

TABLE 4.1.8-1 HEAT TRANSPORT PARAMETERS

	Intermediate Heat Exchangers	Steam Generators
Maximum Heat Load	4,300 MW	4300 MW
Lithium Flow	1800 m^3/min	
Lithium Inlet Temperature	369°C	
Lithium Exit Temperature	300°C	
Sodium Flow	2500 m^3/min	2500 m^3/min
Sodium Inlet Temperature	272°C	363°C
Sodium Exit Temperature	363°C	272°C
Steam Flow		134,000 kg/min
Feed Water Inlet Temperature		254°C
Feed Water Inlet Pressure		7.34 MPa absolute

3 OF 4

DOE/DP

40086-1

(VOL I)

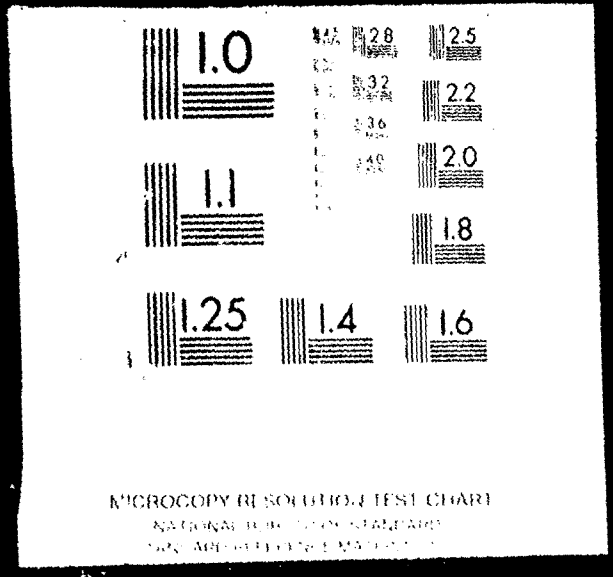

TABLE 4.1.8-1 HEAT TRANSPORT PARAMETERS (CONT.)

	Intermediate Heat Exchangers	Steam Generators
Superheated Steam Exit Temperature		358 C
Superheated Steam Exit Pressure		7.24 MPa absolute

DESIGN DESCRIPTION

Because of limitations in scope, many of the details discussed in the following paragraphs have not been shown on the listing of drawings that illustrate the Heat Transport System.

Figure Title	Figure Number
Containment Structure - Plan El. 0.15 Meters	4.1.8-1
Containment Structure - Plan El. 42.75 Meters	4.1.8-2
Containment Structure - Section 1-1	4.1.8-3
Containment Structure - Section 2-2	4.1.8-4
Steam Generator Building - Plan	4.1.8-5
Steam Generator Building - Section	4.1.8-6
Steam Generator	4.1.8-7
Liquid Metal Heat Transport System Flow Diagram	4.1.8-8
Intermediate Heat Exchanger	4.1.8-9

Four Intermediate Heat Exchangers, each with two sets of parallel lithium and two sodium pipes per loop located within the Containment Structure along with the Reactor Chamber, as shown on Figures 4.1.8-1 to 4.1.8-4. Lithium is circulated through the Reactor Chamber and each of the Intermediate Heat Exchangers by one Lithium Circulating Pump in each of the eight lithium pipes. The eight Lithium Circulating Pumps are also located within the Containment Structure. Four Steam Generators each with two sodium pipe systems and one steam loop are located within the Steam Generator Building, as shown on Figures 4.1.8-5 and 4.1.8-6. Sodium is circulated through each Steam Generator in series with an Intermediate Heat Exchanger by one Sodium Circulating Pump in each of the eight sodium pipes. The eight Sodium Circulating Pumps are located with the Steam Generator Building. The Lithium Drain and Storage Tank is located in the Contain-

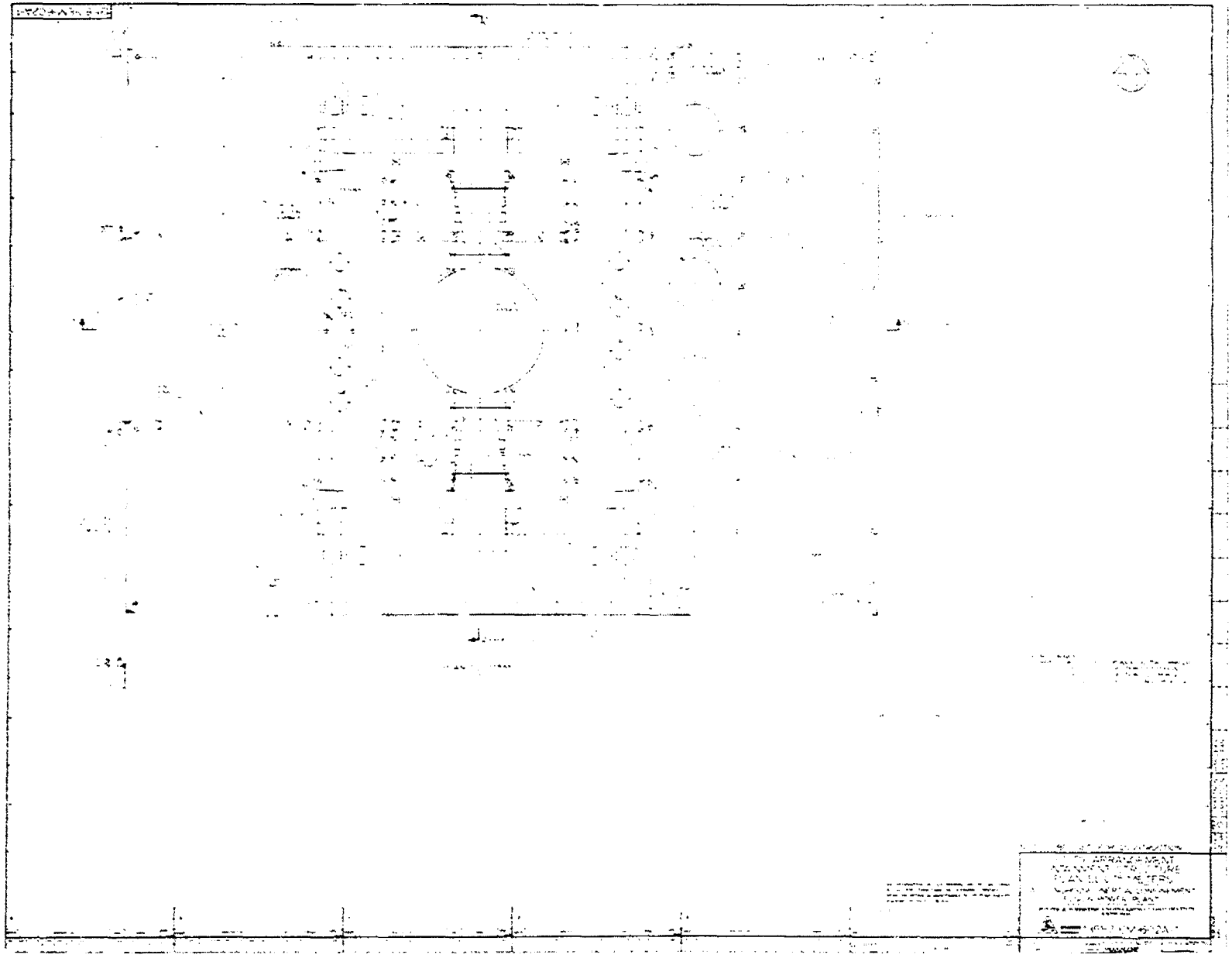

Figure 4.1.8-1. Containment Structure, Plan El. 0.15 meters

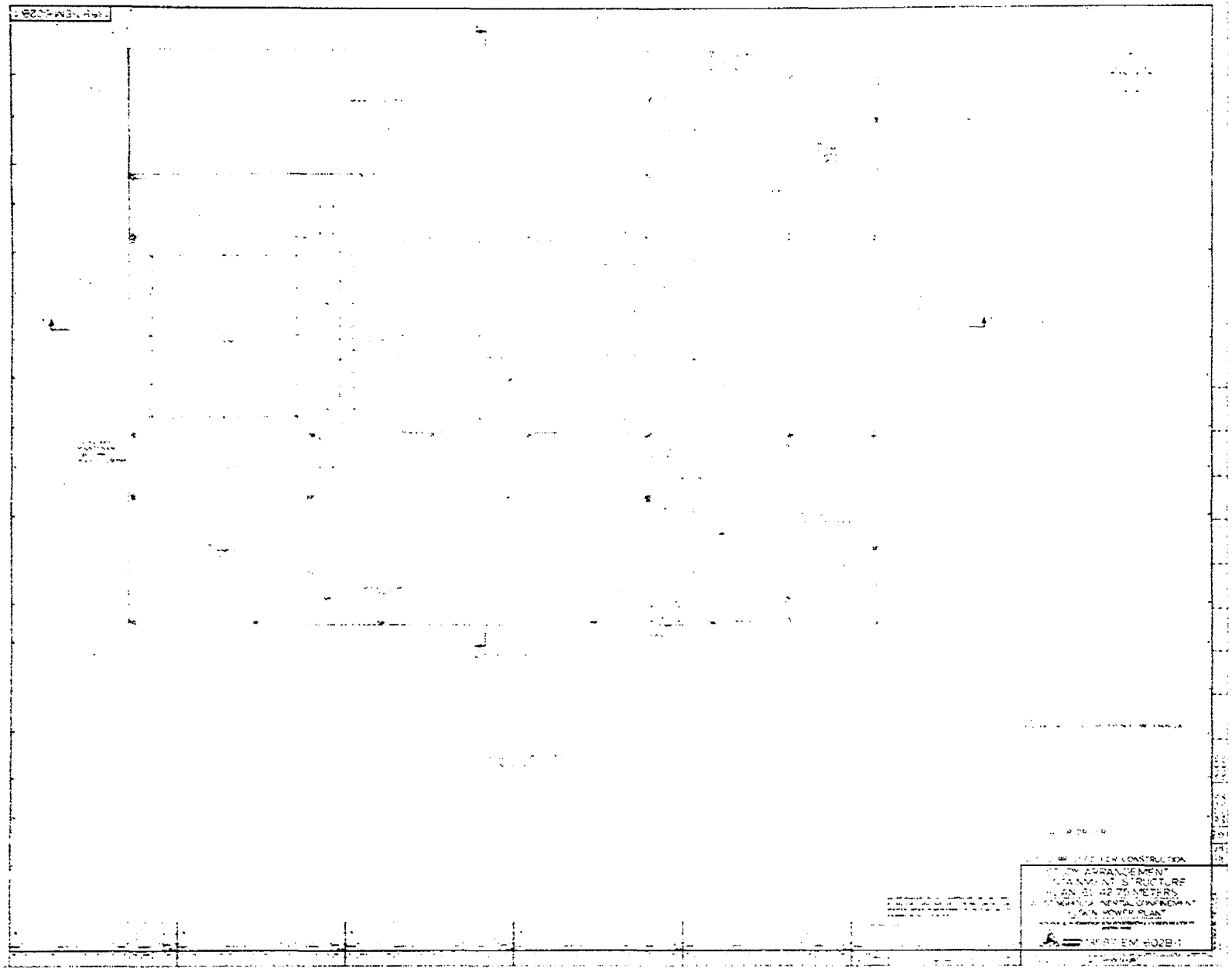

Figure 4.1.8-2. Containment Structure, Plan El. 42.75 Meters

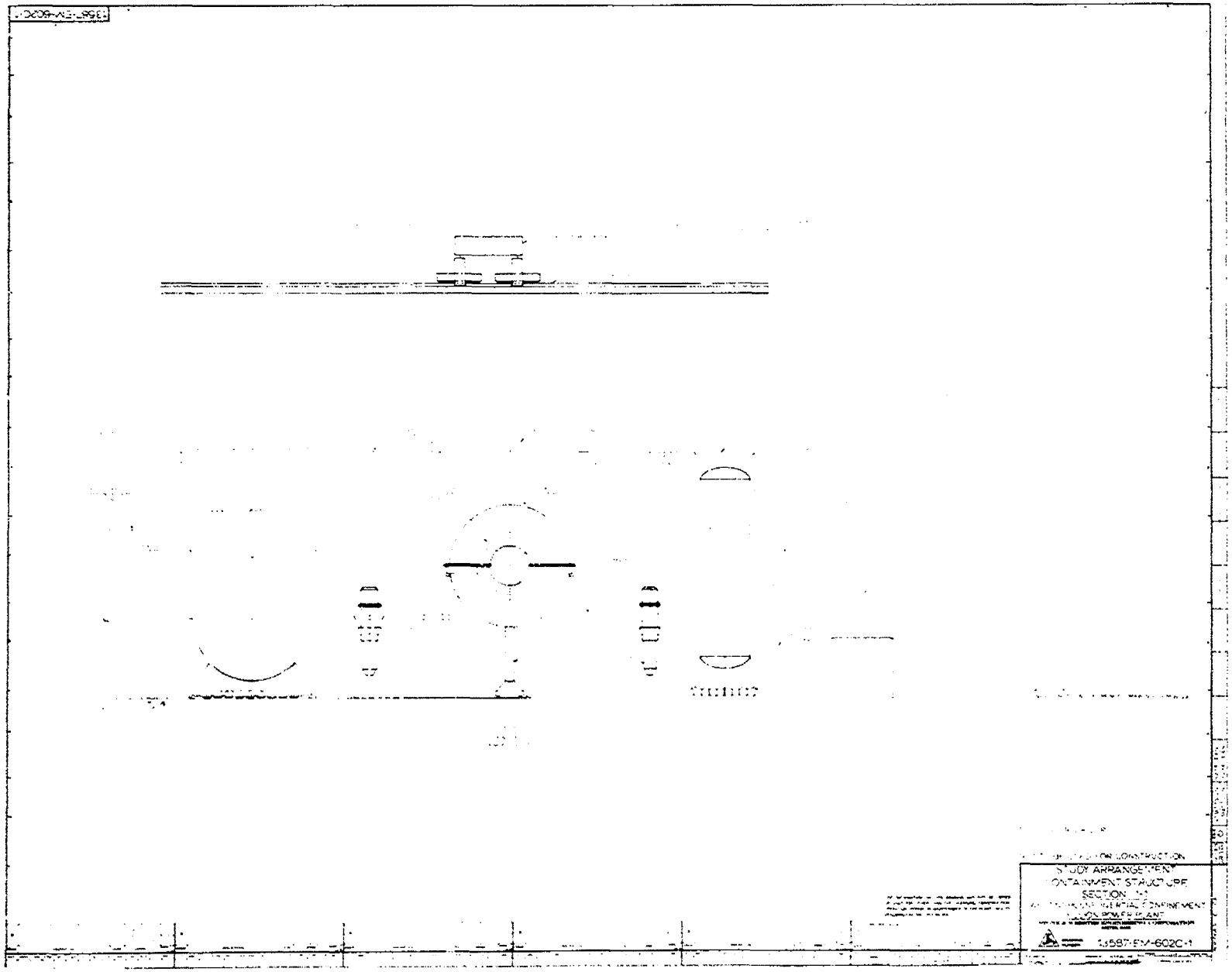

Figure 4.1.8-3. Containment Structure, Section 1-1

Figure 4.1.8-4. Containment Structure Section 2-2

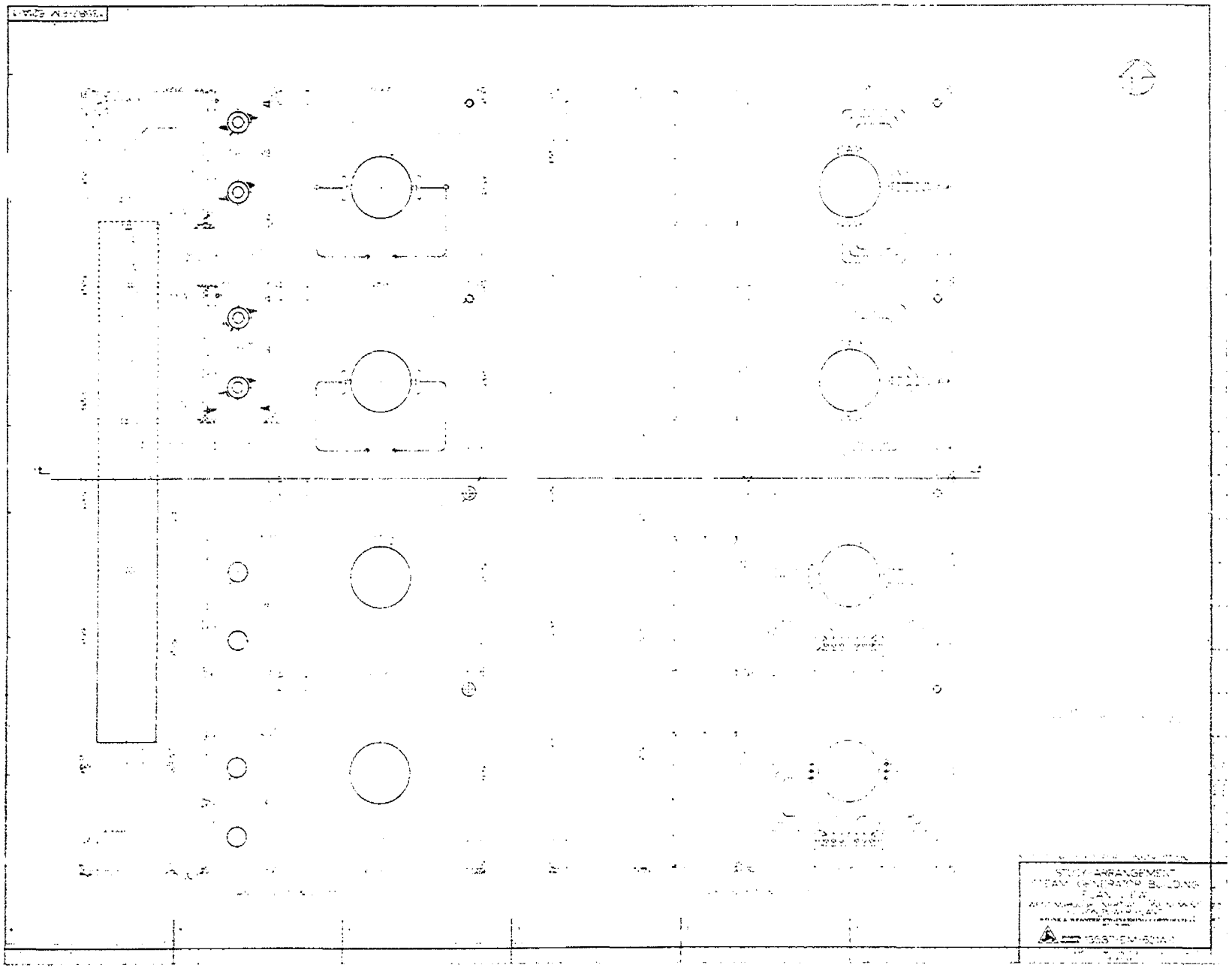

Figure 4.1.8-5. Steam Generator Building, Plan View

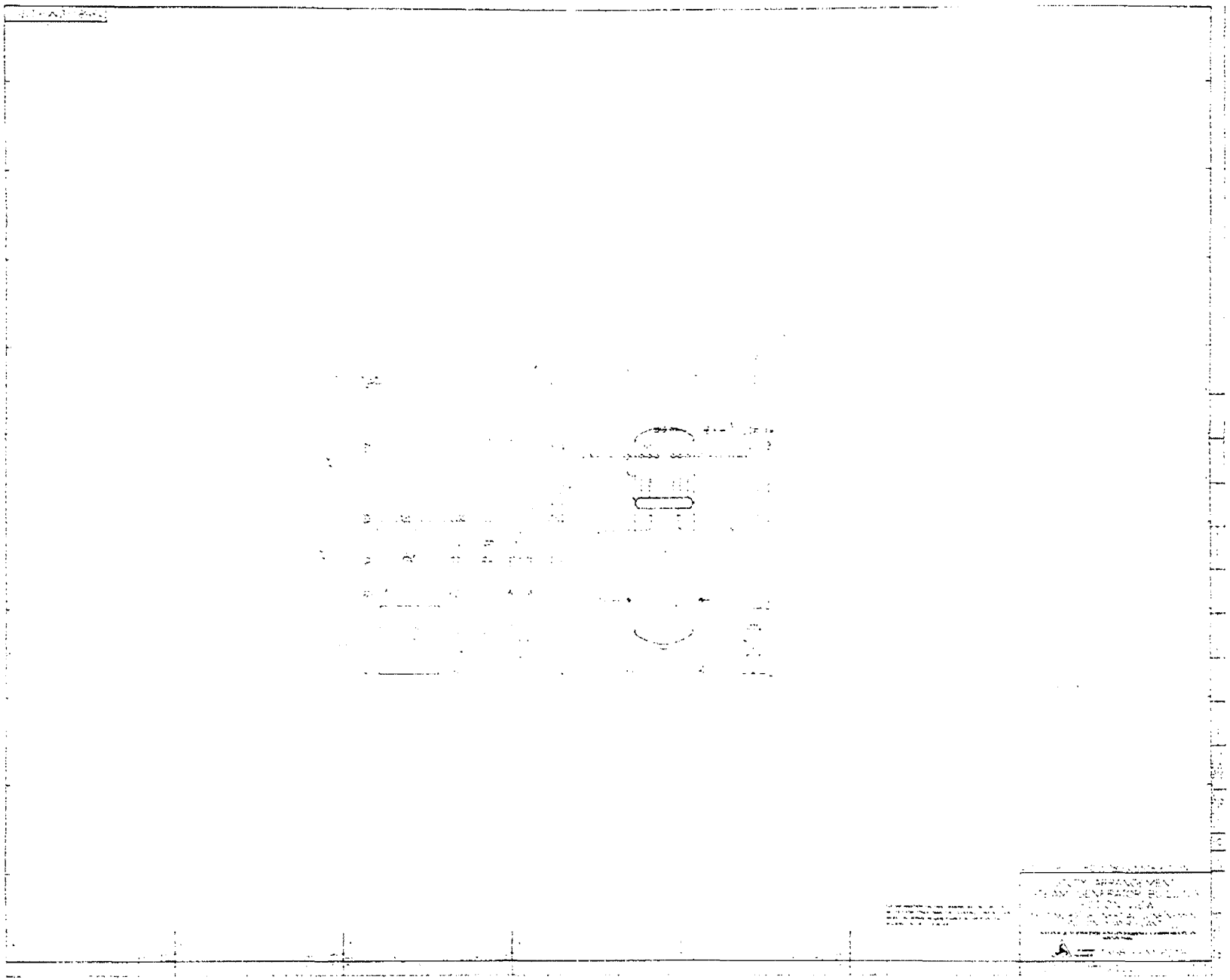

Figure 4.1.8-6. Steam Generator Building, Section View

ment Structure adjacent to the Intermediate Heat Exchangers and the Sodium Drain and Storage Tank is located in the Steam Generator Building.

The Reaction Chamber, each Intermediate Heat Exchanger, each Steam Generator, each Lithium Circulating Pump, each Sodium Circulating Pump, the Lithium Drain and Storage Tank, the Sodium Drain and Storage Tank and all of the piping comprising the liquid metal loops are located within individual compartments to contain accidental liquid metal spills.

All of the equipment and piping, and valves containing liquid metal are electrically heated to maintain surface temperature at a minimum of 205°C to ensure that the liquid metal does not solidify during an accidental outage.

As illustrated on Figures 4.1.8-7 (Steam Generator) and 4-1.8-8 (Heat Transport System) a Steam Generator is comprised of an evaporation section, a steam drum with separator and scrubber elements and a superheating section.

Sodium from the Intermediate Heat Exchanger sodium hot loop enters at the upper chamber and flows by gravity through the superheating section, into the central holding chamber and thence by gravity through the evaporation section into the lower chamber. From the lower chamber, the sodium enters the sodium cold loop where it is pumped through the Intermediate Heat Exchanger. The flow of sodium through both the superheating section and the evaporation section is regulated by a fixed orifice fitted at the discharge end of each tube.

One of the functions of the upper, central and lower chambers is to provide adequate expansion volume to accommodate operational variations in sodium temperature and rate of flow. A second function of these chambers is to provide pressure equilibrium at the entrance and exit of the sodium tubes in both the superheating section and the evaporation section. All three chanbers are interconnected and continuously inerted with argon gas.

Feed water enters the steam drum and washes the saturated steam entering from the evaporation section. The feedwater and the fraction of steam condensed in the washing process, flow downward from the steam drum and enter the evaporation

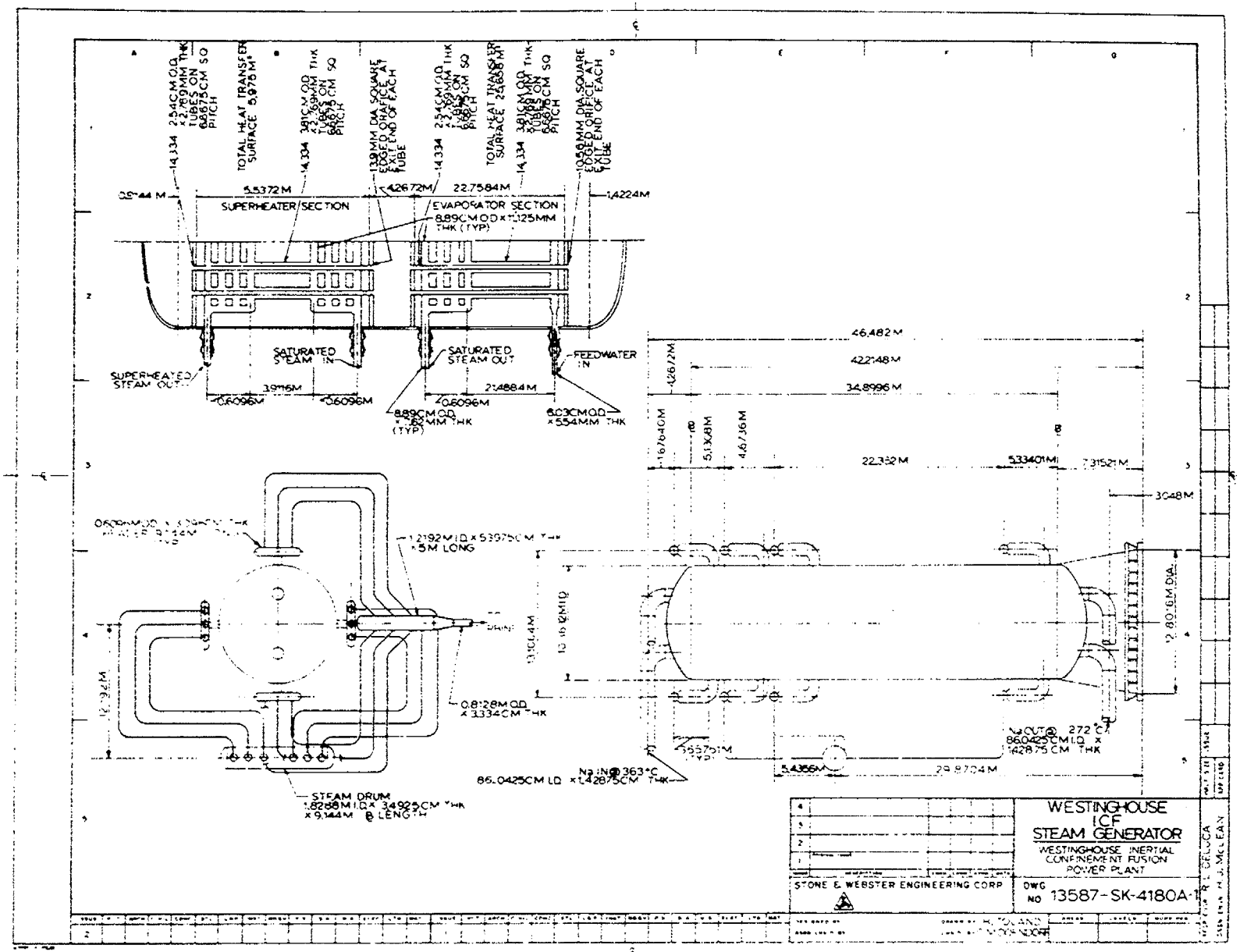

Figure 4.1.8-7. Conceptual Design of Steam Generator for ICF Power Plant

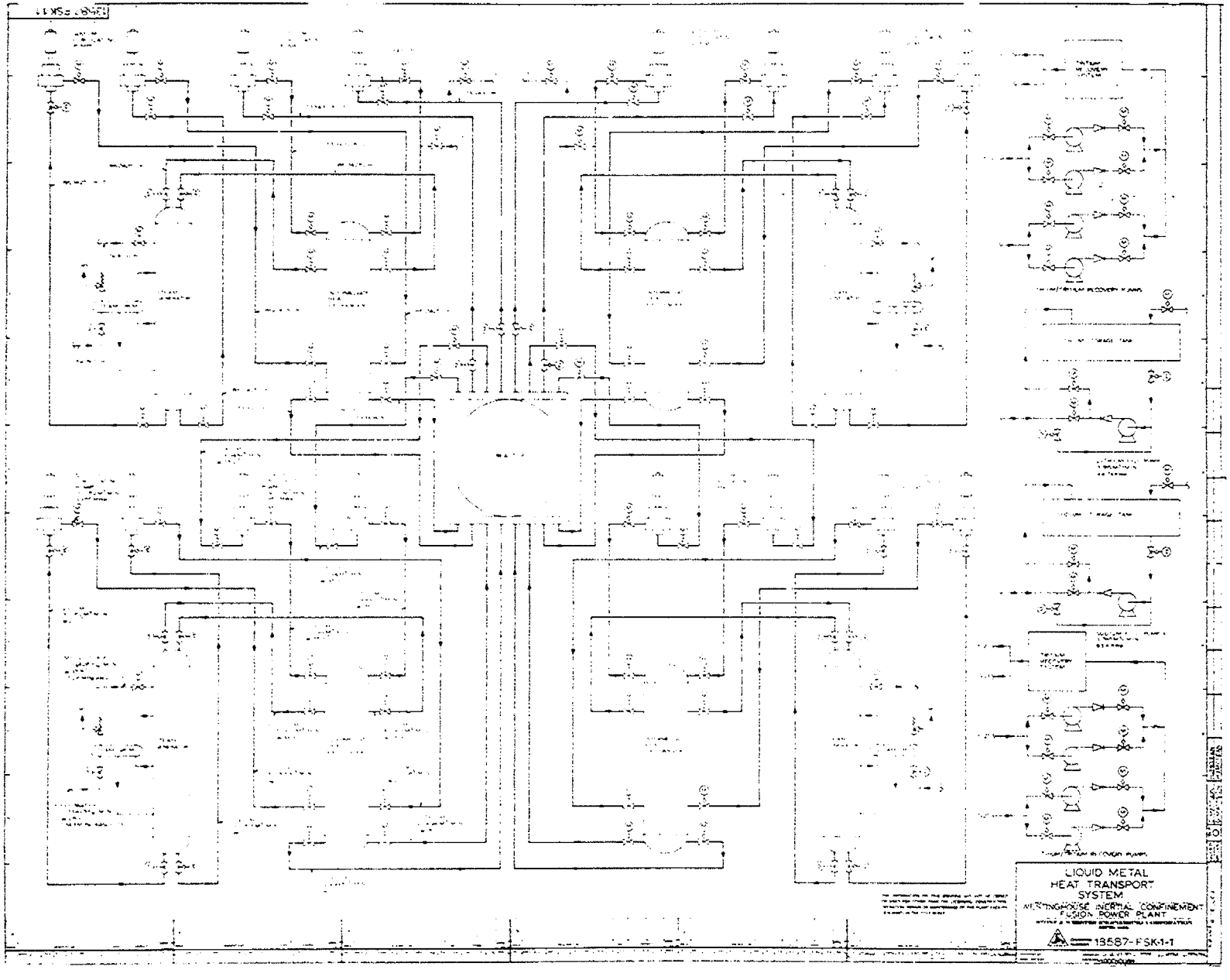

Figure 4.1.8-8. Liquid Metal Heat Transport System Flow Diagram

section. Saturated steam leaves the evaporation section and enters the steam drum where it is washed, dried in its passage through the separator and scrubber elements, and then is superheated in its passage through the superheating section.

Both the evaporation and the superheating sections are constructed as a multitude of co-axial tubes, with the sodium flowing downward through the central tube and the steam flowing upward through the annulus formed by the control and outer tubes.

The volume bounded by the outer shell and the evaporation and superheating section tubes is filled with argon gas maintained at 0.2 MPa absolute. The argon is at approximately the same temperature as the steam within the tubes thereby minimizing heat losses and thermal stresses.

As illustrated on Figures 4.1.8-9 (Intermediate Heat Exchanger) and 4.1.8-8, the Heat Exchanger is composed of a multitude of coaxial tubes with lithium flow downward through the central tube and sodium flowing upward through the annulus formed by the central and outer tubes.

Lithium from the Reactor Chamber is pumped through the lithium hot leg where it enters the upper lithium chamber, flows downward by gravity through the central tubes into the lower lithium chamber, then into the lithium cold leg where it is returned to the Reaction Chamber.

Sodium is pumped through the sodium cold leg to the lower sodium chamber, flows upward through the annulus formed by the central and outer tube to the upper sodium chamber, into the sodium hot leg and then conducted to a Steam Generator.

The function of the upper lithium chamber is to provide adequate expansion volume to accommodate operational variations in lithium temperature and rate of flow. The lithium chamber is inerted with argon gas maintained at 0.53 MPa absolute for the purpose of controlling the minimum pressure within the Reaction Chamber.

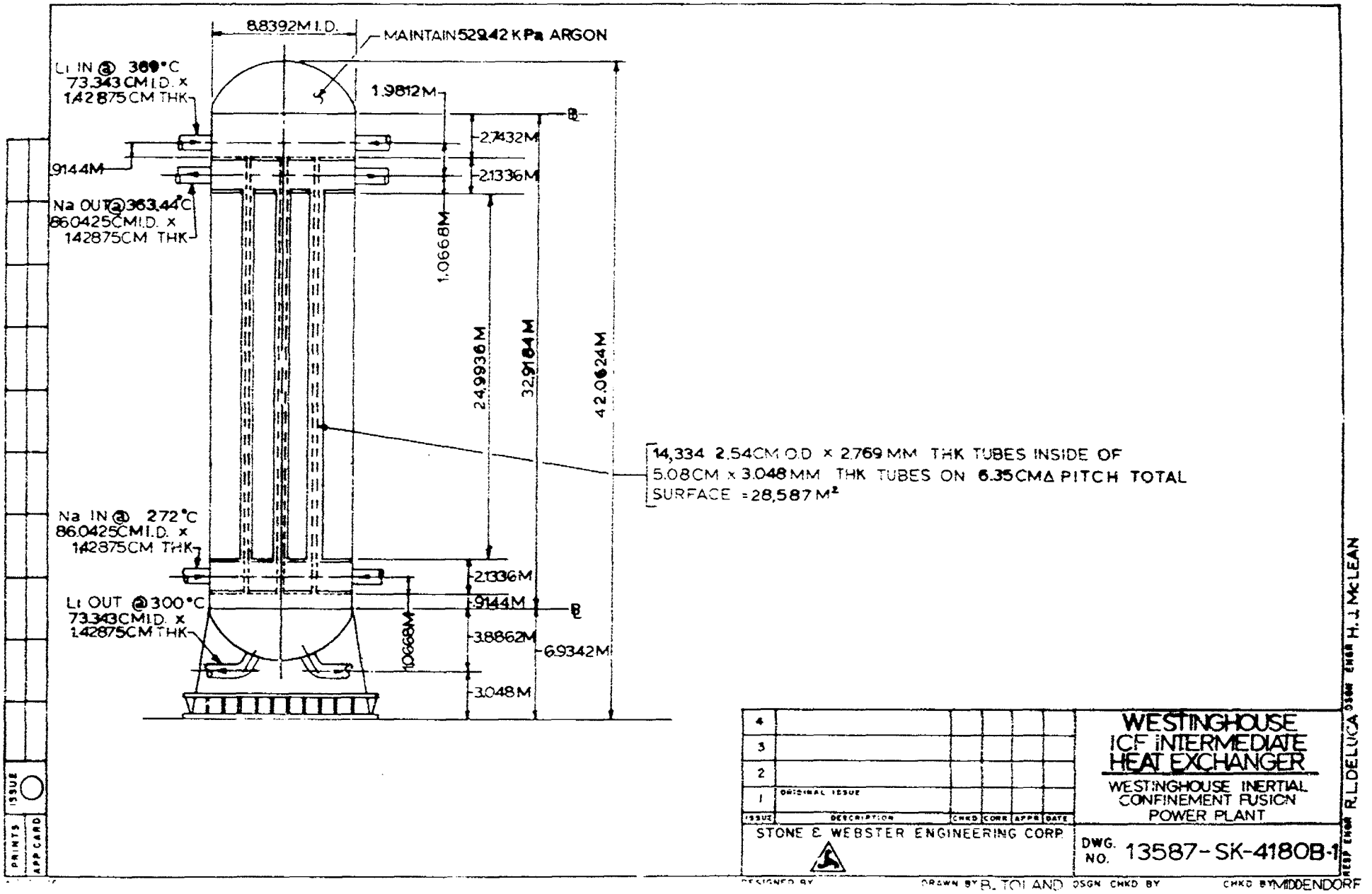

Figure 4.1.8-9. Schematic of Intermediate Heat Exchanger Concept

The volume bounded by the outer shell and the sodium tubes is filled with argon gas maintained at 0.2 MPa absolute. The argon is at approximately the same temperature as the sodium within the tubes thereby minimizing heat losses and thermal stress.

The Lithium Drain and Storage Tank and the Sodium Drain and Storage Tank are each horizontal rectangular cross-section tanks supported at two points, and electrically heated and insulated on all surfaces to maintain the stored product at 205° C minimum. Both tanks are inerted with argon gas.

The pumps for the lithium circuits are vertically mounted, free surface double stage centrifugal pumps, with single bottom suction and side discharge.

Table 4.1.8-2 enumerates the salient features of the Heat Transport Equipment that comprise the Heat Transport System.

TABLE 4.1.8-2 HEAT TRANSPORT EQUIPMENT

Intermediate Heat Exchanger

Number Required	4
Diameter of Shell	8.8 m
Length of Shell	33 m
Overall Height	42 m
O.D. of Sodium Tubes	5 cm
Thickness of Sodium Tubes	3 mm
O.D. of Lithium Tubes	2.5 cm
Thickness of Lithium Tubes	2.8 mm
Number of Lithium Tubes	14,334
Number of Sodium Tubes	14,334
Tube Pitch	6.35 cm Triangular Pitch
Total Heat Transfer Surface	28,600 m^2
Total Sodium Flow	10.3 m^3/s
Velocity of Sodium Through Tubes	0.6 m/s
Total Lithium Flow	7.5 m^3/s
Velocity of Lithium Through Tubes	1.7 m/s

TABLE 4.1.8-2 HEAT TRANSPORT EQUIPMENT (CONT.)

Steam Generator

Number Required	4
Diameter of Shell	10.4 m
Length of Shell	35 m
Overall Height	46.5 m
O.D. of Sodium Tubes	2.5 cm
Thickness of Sodium Tubes	2.8 mm
O.D. of Steam Tubes in each of the Evaporator Section and Superheater Section	3.3 cm
Thickness of Tubes	2.8 mm
Number of Sodium Tubes in each of the Evaporator and Superheater Section	14,334
Number of Steam Tubes in each fo the Evaporator Section and Superheater Section	14,334
Total Heat Transfer Surface in the Evaporator Section	25,700 m^2
Total Heat Transfer Surface in the Superheater Section	6,000 m^2
Tube Pitch	6.67 cm Square Pitch
Total Sodium Flow	10.4 m^3/s
Velocity of Sodium Through Tubes	2.3 m/s
Total Steam Flow	557 kg/s
Velocity of Steam in Evaporator Section	6.2 m/s
Velocity of Steam in Superheater Section	6.2 m/s

Lithium Circulating Pump

Number Required	8
Flow Rate	3.75 m^3/s
Number of Stages	2
Speed	430 rpm
Developed Head	108 m
Net Positive Suction Head, (NPSH) Required	15.1 m
Specific Speed, Ns	2160
Suction Specific Speed, Ss	2,056
Power Consumption (each)	3 MWe

TABLE 4.1.8-2 HEAT TRANSPORT EQUIPMENT (CONT.)

Sodium Circulating Pump

Number Required	8
Flow Rate	5.2 m^3/s
Number of Stages	1
Speed	480 rpm
Developed Head	84.7 m
Net Positive Suction Head, (NPSH) Required	15.1 m
Specific Speed, Ns	2020
Suction Specific Speed, Ss	6150
Power Consumption (each pipe)	6 MWe

Lithium Hot Leg

Number of Pipes	8
Pipe Inside Diameter	73.3 cm
Pipe Thickness	14.3 mm
Lithium Flow (each pipe)	3.75 m^3/s
Lithium Temperature	309° C
Flow Velocity	8.9 m/s

Lithium Cold Leg

Number of Pipes	8
Pipe Inside Diameter	73.3 cm
Pipe Thickness	14.3 mm
Lithium Flow (each)	3.75 m^3/s
Lithium Temperature	300° C
Flow Velocity	8.9 m/s

Sodium Hot Leg

Number of Pipes	8
Pipe Inside Diameter	86 cm
Pipe Thickness	14.3 mm
Sodium Flow (each pipe)	5.2 m^3/s

TABLE 4.1.8-2 HEAT TRANSPORT EQUIPMENT (CONT.)

Sodium Hot Leg (Cont'd)

Sodium Temperature	363° C
Flow Velocity	8.9 m/s

Sodium Cold Leg

Number of Pipes	8
Pipe Inside Diameter	86 cm
Pipe Thickness	14.3 mm
Sodium Flow (each pipe)	5.2 m^3/s
Sodium Temperature	272° C
Flow Velocity	8.9 m/s

SYSTEM OPERATION

The sodium and the lithium are received at the plant in solid form in 114 m^3 (30,000 gallon) capacity tank cars equipped with heating coils.

Because both lithium and sodium ignite spontaneously in air, both the Lithium Storage Tank and the Sodium Storage Tank and all of the pumps and piping from the receiving docks to the storage tanks are purged and inserted with dry argon gas heated to 370° C. The argon is circulated until surface temperatures of 205° C are attained. These surface temperatures are maintained with electric heaters.

The lithium and the sodium are melted in the tank car by circulating "Downtherm A" at a temperature of 260° C through the heating coils and the melted metal is pumped to its drain and storage tank. Each metal has its own melting and storage facility to obviate the possibility of mixing the metals. Before the heat transport systems are loaded with the liquid metals, the Reaction Chamber, the Intermediate Heat Exchangers, the Steam Generators and the circulating pumps, piping and valves are purged and inerted with dry argon gas, heated to 370° C, until all of the metal parts that contact the liquid metal are heated to a minimum of 205° C. The surface temperature of all of the above items is

prevented from dropping below this limit for all in-plant conditions, except for maintenance or replacement, by electric strip heaters.

The Auxiliary Boiler produces 205° C, 1.72 MPa absolute steam. This steam is circulated through the Steam Generator, the turbines and the heaters to warm up the steam system and to augment the argon heating of the sodium conducting tubes within the Steam Generators. While the heat transport system is being heated, all of the compartments within the Containment Building and the Steam Generator Building, in which all items of equipment or runs of piping that will contain either lithium or sodium is located, are purged and inerted with dry argon gas to a pressure slightly below atmospheric.

The argon gas from each compartment is maintained at 32° C with individual unit coolers and is provided with an atmospheric clean-up system.

Each atmospheric clean-up system consists of a fan, a detritiating adsorber and a HEPA filter. All tritium removed is returned to the Waste Handling Building.

The individual unit coolers are each provided with an intermediate heat exchanger circulating refrigerant R-11 as the coolant.

Once the heat transport system has had its temperature raised to its minimum of 205° C, lithium is pumped from the Lithium Drain and Storage Tank to fill the lithium system, sodium is pumped from the Sodium Drain and Storage Tank to fill the sodium system, the lithium and Sodium Circulating Pumps are started, and normal Steam Generator water levels are established.

In the Turbine/Generator Building, the Main Condenser Circulating Water System is placed into operation, the condenser dump valves are placed in the pressure control mode and set for "no-load" pressure and the condensate system is prepared for operation.

The auxiliary feedwater system is aligned to feed all Steam Generators, and all valves are positioned. The Turbine Driven Feed Water Pump is started, using the steam generated in the Auxiliary Boiler, and the Main Turbine is rolled up to 600 rpm.

After all Turbine Generator Auxiliary Systems are placed in operation, the Reactor is placed in operation and the Turbine Generator is brought slowly up to 1,800 rpm. The Turbine Driven Feed Water Pump is placed in main steam operation, and when required steam flow has been established, the Generator output is synchronized and tied into the grid.

4.1.8.2 INTERFACE WITH GRID

FUNCTION

The Turbine Generator portion of the plant receives superheated steam from the Steam Generator and transforms the thermal energy in the steam to electrical energy.

DESIGN REQUIREMENTS

Table 4.1.8-3 enumerates the salient parameters of the electric generating portion of the Balance of Plant.

TABLE 4.1.8-3 TURBINE GENERATOR PARAMETERS

Turbine Type	Tandem compound, 6-flow condensing, double reheat machine consisting of one double-flow high pressure cylinder, and three double-flow low pressure cylinders
Turbine Speed	1,800 rpm
Throttle Flow	7.78×10^6 kg/hr
Throttle Pressure	72 kg/cm^2
Generator Type	Liquid-cooled stator and hydrogen inter-cooled rotor, with exciter to control the voltage of the generator
Generator Power Factor	0.9
Total Generator Power	1,565 MWe
Unit Output	1,207 MWe

Unit Heat Rate	3,063 kcal/kWhr
Unit Efficiency	28%
Condenser Duty	2.34×10^9 kcal/hr
Auxiliary Power	358 MWe

DESIGN DESCRIPTION AND SYSTEM OPERATION

Because of limitations in scope, many of the details discussed in the following paragraphs have not been shown on the listing of drawings that illustrate the Turbine Generator System.

The Turbine Generator System is illustrated on the following drawings:

Figure Title	Figure Number
Heat Balance Diagram	4.1.8-10
General Arrangement, Turbine Building - Ground Floor	4.1.8-11
General Arrangement, Turbine Building - Operating Floor	4.1.8-12
General Arrangement, Turbine Building - Section	4.1.8-13
Electrical Main One Line Diagram	4.1.8-14

A moisture separator-reheater unit is provided to dry and superheat the steam between the high and low pressure cylinders.

An electrohydraulic control system provides speed and acceleration control for startup, load control, load limiting, emergency trip, manual trip, and valve testing function.

Steam from the Steam Generators is carried in four carbon steel lines, which join into a common manifold. A main steam isolation valve and a main steam isolation bypass valve are located in each line in the Turbine Building. Four carbon steel lines carry steam from the manifold, located in the turbine building, to four main steam turbine stop valves and four main steam turbine control valves.

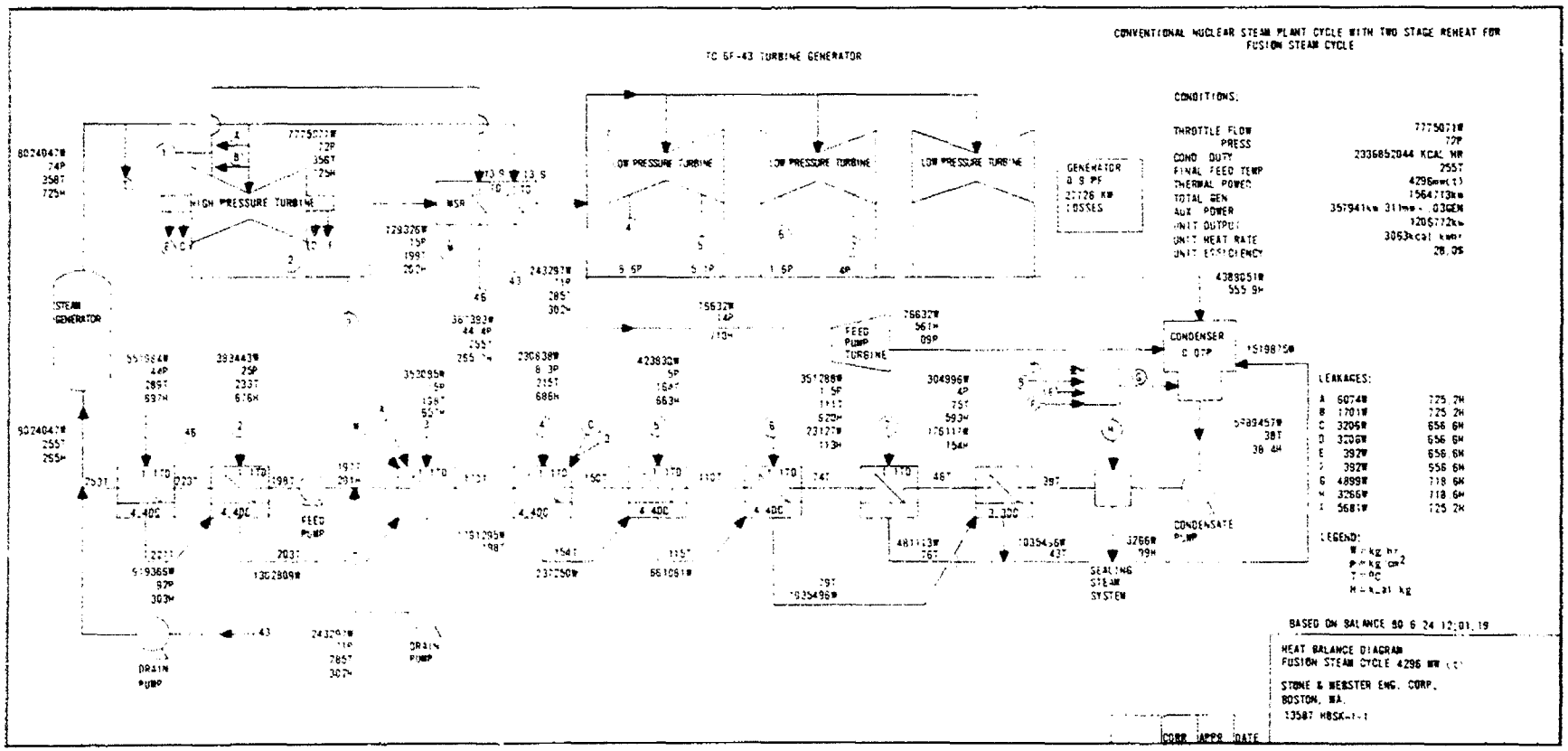

Figure 4.1.8-10. Heat Balance Diagram for Fusion Steam Cycle

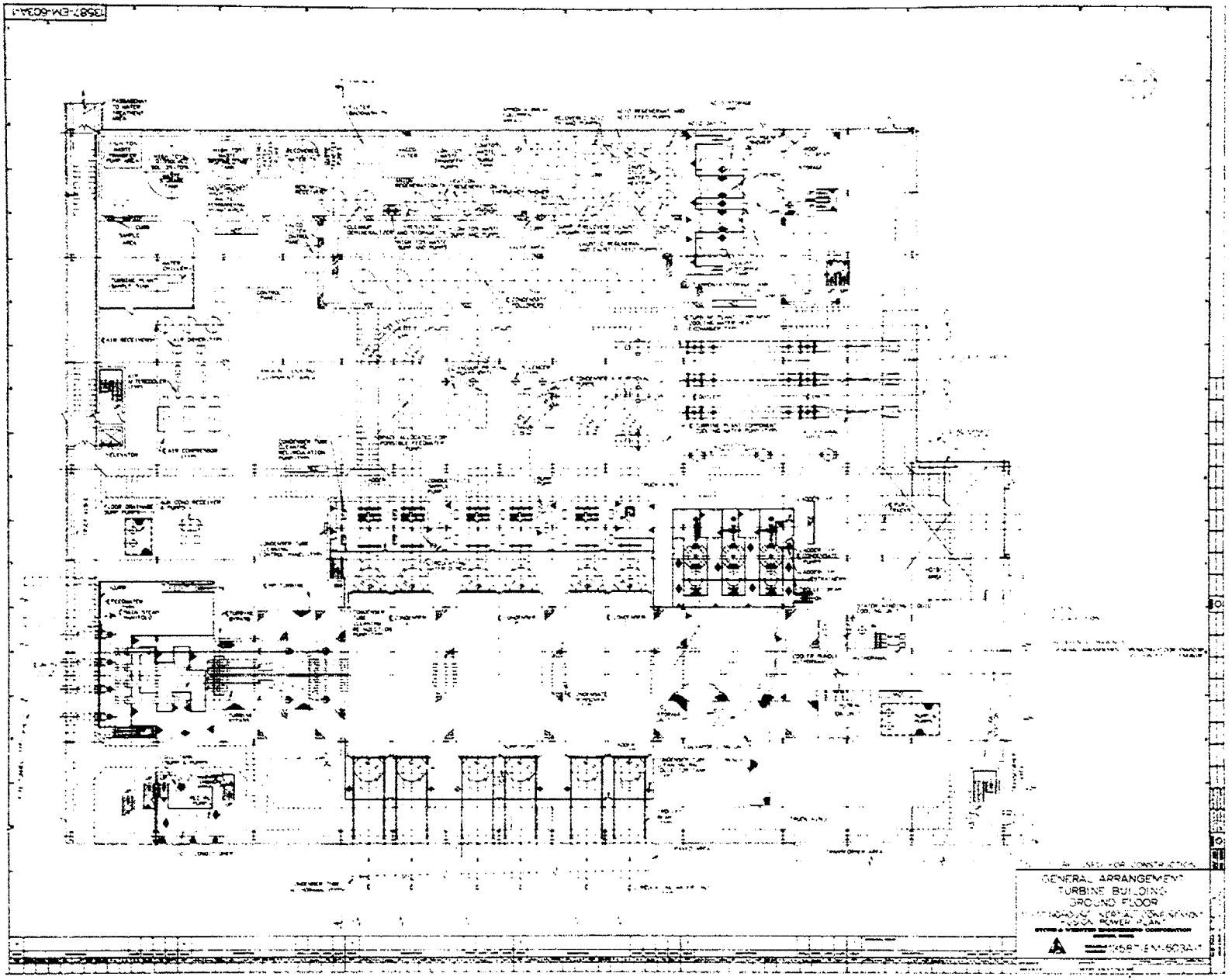

Figure 4.1.8-11. General Arrangement, Turbine Building Ground Floor

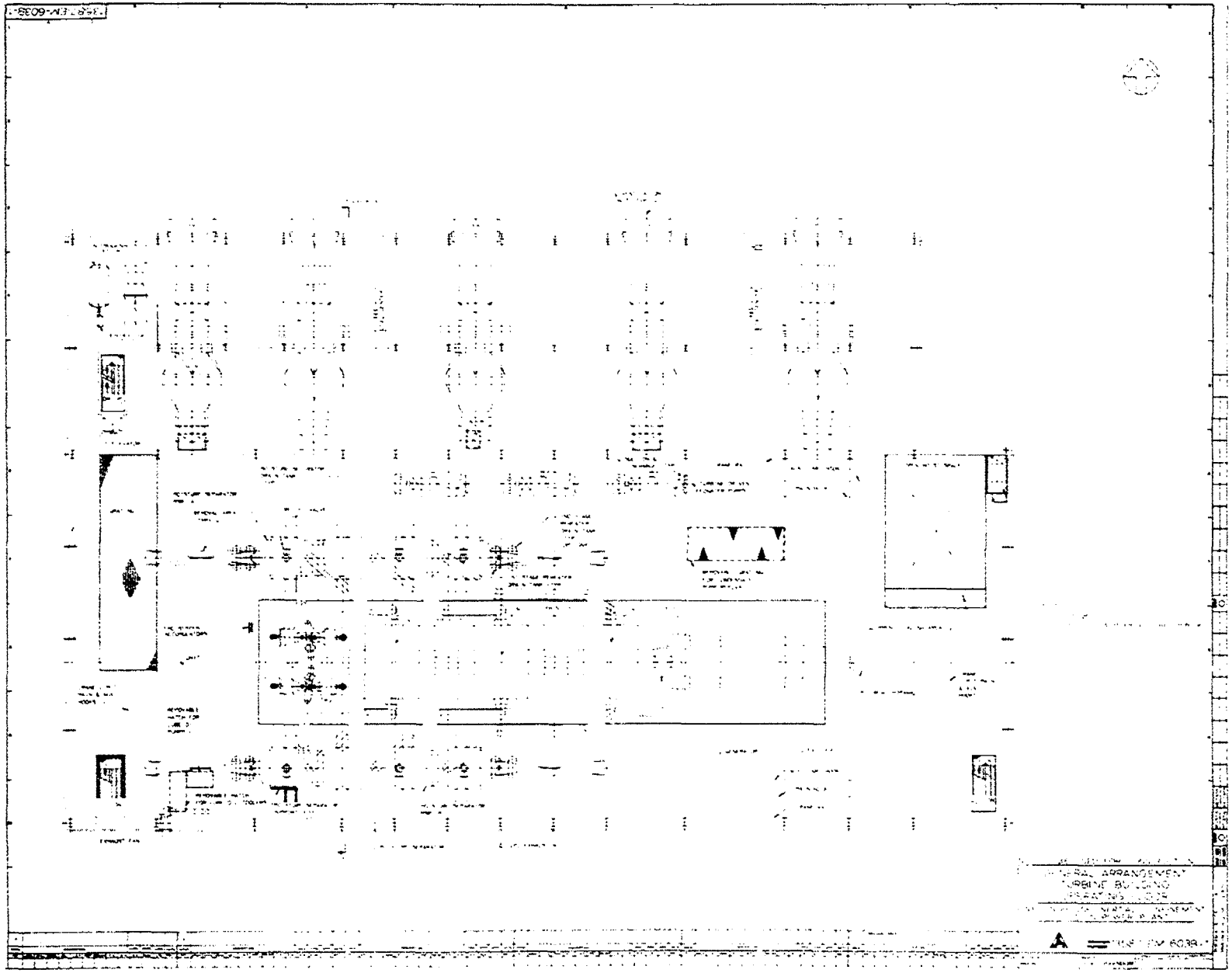

Figure 4.1.8-12. General Arrangement, Turbine Building Operating Floor

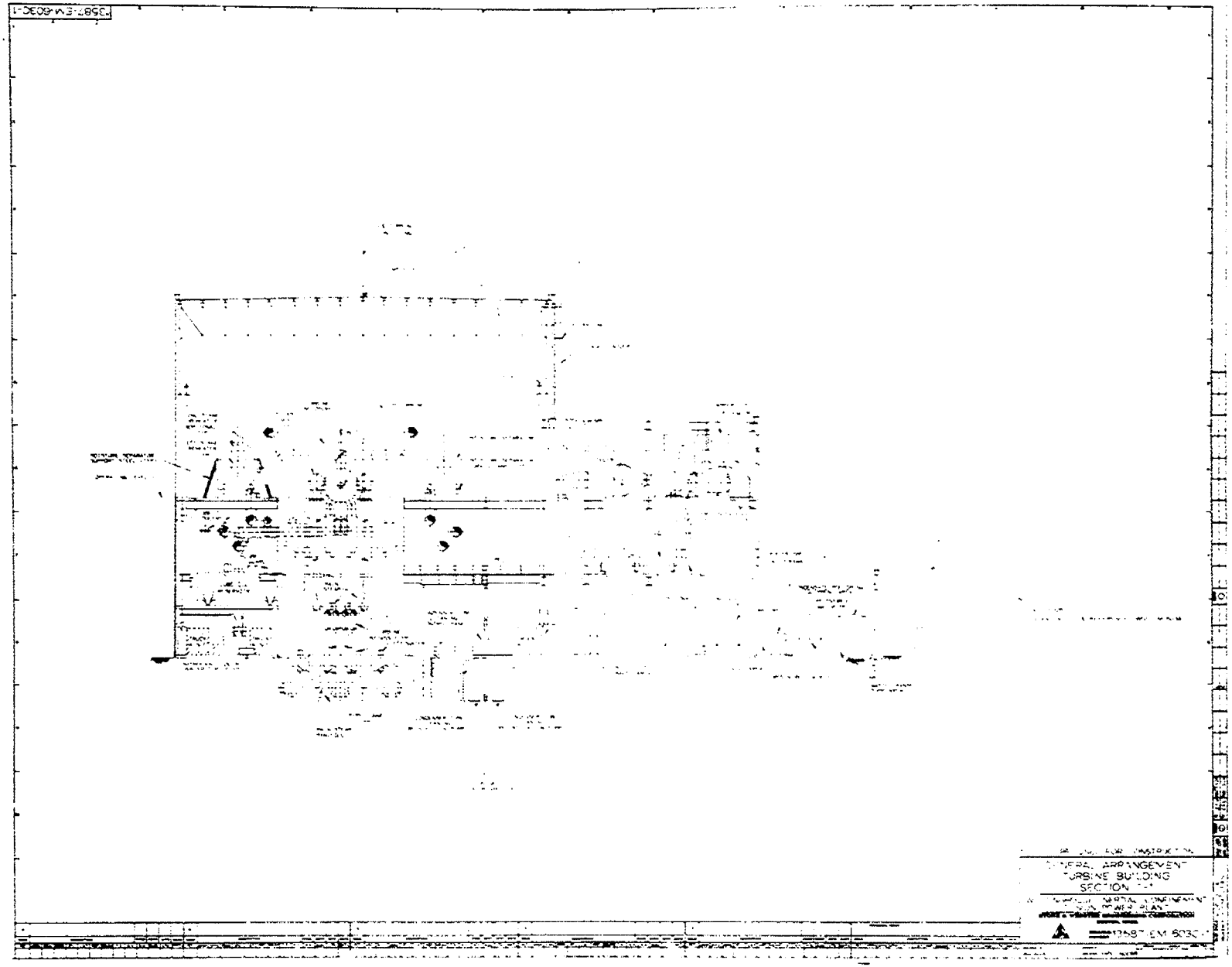

Figure 4.1.8-13. General Arrangement, Turbine Building Section 1-1

Steam leaving the high pressure turbine passes through the moisture separator-reheaters to the inlets of the three low pressure turbines. Each of the steam lines between the reheater outlet and low pressure turbine inlet is provided with a combined intercept-stop valve. Main steam stop-check valves in the steam supply connections automatically prevent reverse flow of steam in the event of accidental pressure reduction in any Steam Generator or its piping and also provide a manual shutoff of steam from its associated steam generator.

The main steam system is capable of disposing of heat from the heat transport system following sudden load rejection or unit trip, by automatically bypassing main steam to the condenser through the turbine bypass system and/or by relieving to the atmosphere. Relief valves installed in the moisture separator-reheater protect this vessel and the crossover system from overpressure. These valves are designed to pass the steam flow resulting from a complete turbine load rejection, or other shutoff of main steam flow, to the condenser.

The extraction steam system conducts steam from the high pressure turbine, cold reheat lines, and the low pressure turbines to the feedwater heaters. The extraction steam is required for feedwater heating to increase cycle efficiency.

The Auxiliary Boiler provides steam for process systems when plant steam is not available, in addition to steam for heating the Turbine Plant and the Steam Generator when starting from a cold condition. This includes an oil fired water-tube boiler, a condensate receiver, a condensate pump, a condensate makeup pump, a deaerator, a boiler feed pump, and controls. Fuel oil is supplied to the Auxiliary Boiler from one above ground fuel oil supply tank. A fuel oil supply pump transfers oil from the supply tank to the Auxiliary Boiler.

The condenser is a triple shell, multipass, multipressure, divided water box design. During normal operation, two steam jet air ejectors remove noncondensible gases from the condenser shells. The feedwater system receives partially heated feedwater from the condensate system. It completes heating the feedwater and raises its pressure to the values required to feed the Steam Generators. Two one-half capacity, variable speed turbine-driven feedwater pumps with one one-half capacity motor-driven backup pump take suction from the condensate

system and discharge to a common header. Three stages of regenerative feedwater heating are provided to two feedwater heater strings connected in parallel between the pump discharge header and a headering system designed to provide sufficient mixing to ensure that uniform temperature feedwater is supplied to each Steam Generator.

The feedwater is directed to the Steam Generator feed lines. Each feed line has a feedwater flow control valve and two feedwater isolation valves. The flow control valves are positioned by a signal from the Steam Generator Water level control system. The flow control valves in conjunction with the variable speed feedwater pumps maintain the desired Steam Generator water level during normal operation. The redundant feedwater isolation valves ensure isolation of feedwater flow to the Steam Generator on a feedwater isolation signal.

The auxiliary feedwater system is used to supply an emergency source of feedwater to the Steam Generators in the event of loss of the normal feedwater system. The auxiliary feedwater system can also be used to provide feedwater to the Steam Generators in conjunction with the condensate pumps during plant startup and shutdown when sufficient steam cannot be generated to operate the turbine-driven main feedwater pumps. The auxiliary feedwater system can also be used to provide feedwater to the Steam Generator during an operation as hot standby.

The circulating water system is a closed loop cooling system using one natural draft cooling tower. The turbine plant service water system cooling water discharge is used as makeup water for the cooling tower. The circulating water system consists of four circulating water pumps, pumphouse, circulating water piping, steam condenser, cooling tower and associated hydraulic, mechanical, and electrical equipment. The total design circulating water flow rate is constant at 2,050 m^3/min.

To control and maintain the required system water chemistry, chemical solutions are fed to the main condensate system, to the Auxiliary Boiler condensate system, and to the makeup and circulating waters of the natural draft cooling tower. To perform these functions, the following systems are provided: Steam Generator wet layup, chamical feed hydrochlorite, chemical feed-condensate, chemical

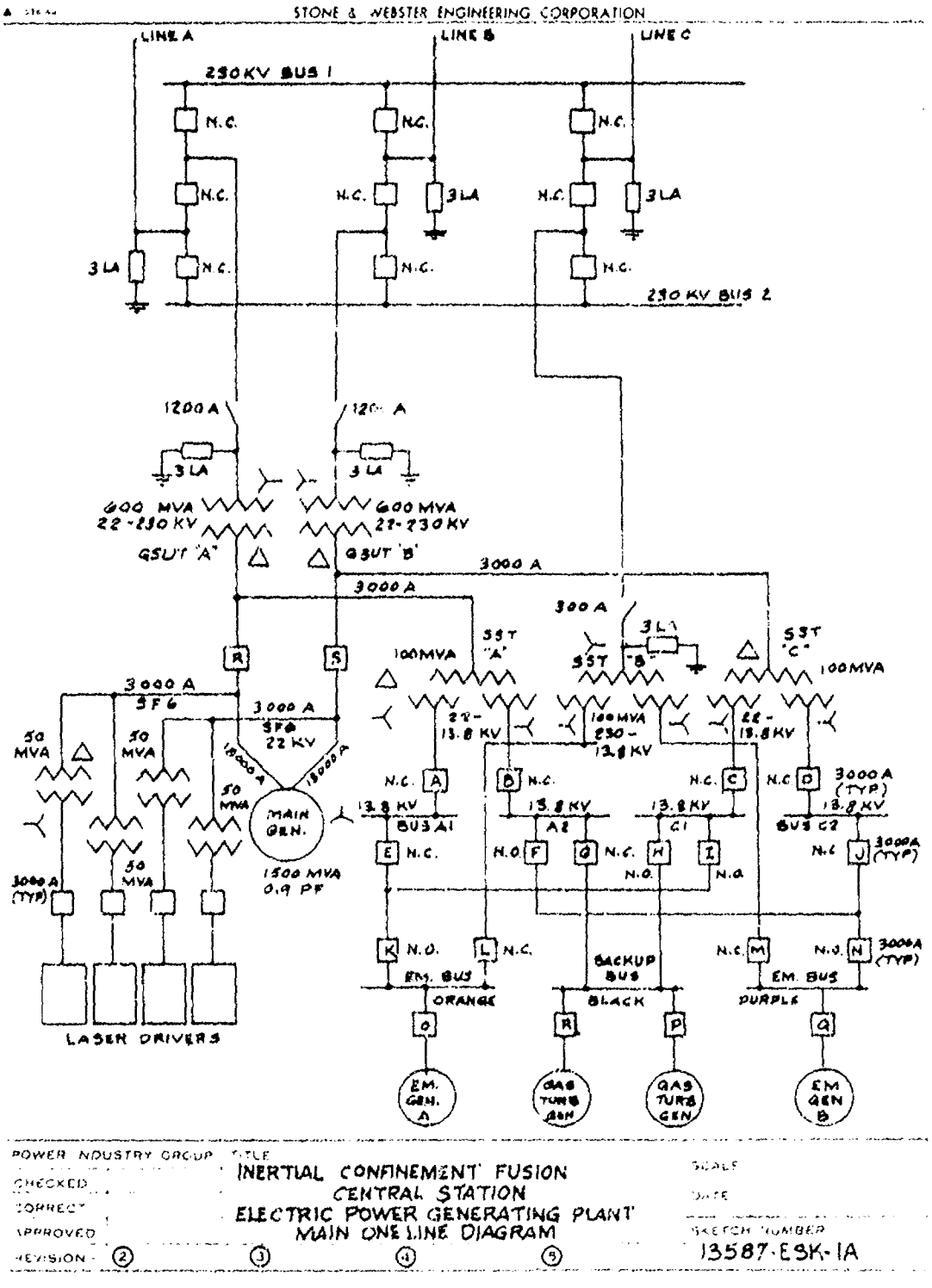

Figure 4.1.8-14. Electrical Main One Line Diagram

feed - Auxiliary Boiler and Chemical feed-acid. The Steam Generator wet layup system allows chemistry control when the Steam Generator is isolated in a full wet layup condition during cold shutdown. Hydrazine and ammonia solutions are added to the water for conditioning while the Steam Generator is being filled to provide corrosion protection during cold shutdown periods.

The chemical feed-hypochlorite system allows sodium hypochlorite solution to be injected into the makeup water line, circulating water, and the service water systems for biofouling control. The chemical feed-condensate system introduces hydrazine and ammonia solutions into the condensate system to scavenge the oxygen and control the pH, respectively. The chemical feed - Auxiliary Boiler system introduces hydrazine and morpholine solutions to the Auxiliary Boiler feedwater to scavenge oxygen and control the pH of the feedwater, respectively. The chemical feed-acid system feeds the makeup water lines to the natural draft cooling tower with sulfuric acid for scale control during the summer months.

The station electrical system, Figure 4.1.8-14, receives ac power from the turbine generator during normal operation. The power flow is via 2 three winding normal station service transformers. The power output of the main generator is split between two generator lead isolated phase bus runs connecting the generator to two-half size main transformers. Each normal station service transformer (NSST) is connected to one of the bus duct runs. The NSST are rated 100/50/50 MVA, 22-13.8 kV.

The tap bus duct to the NSST joins the generator leads between the main transformers and the two generator load break switches; the latter being installed in line with the generator leads. The isolated phase bus duct is rated at 18,000 amps. The NSST tap buses have a symmetrical fault current rating of 345 KA. The generator load break switches have an interrupting capability of 180 KA. The laser driver power is also taken from the generator output. The top busses (SF6) join the isolated phase bus duct between the generator terminals and the generator load break switch.

Generator output voltage regulation will be maintained by integrating generator field forcing with the 10 Hz voltage pulse rate of the laser driver. Generator

frequency stabilization will be maintained using a suitably custom-designed flywheel on the turbine generator.

The two half size main step up transformers are rated 22 kV-230 kV, 600 MVA. A third main transformer is also provided as a spare unit. A 230 kV switchyard is provided with three incoming lines and three outgoing lines. A breaker and a half scheme is provided. The three lines interconnecting the station and the switchyard include the two high voltage main transformer secondary lines and a third line connecting the switchyard to a three winding reserve station service transformer rated 100/50/50 MVA, 230-13.8 kV, capable of providing power to the station electrical system when the main generator output is not available and when back feed via the main trarsformer is not available.

The station electrical system configuration includes four 13.8 kV buses, four 4,160 V buses, two Class 1E, 4 kV buses, and one 13.8 kV back-up bus. Unit substations are fed from the 13.8 kV buses. Four auxiliary step drum transformers rated 10 MVA, 13.8-4.16 kV provide power to the 4 kV buses. Two 4,160 V Class 1E buses are provided with two 16 MWe dedicated standby diesel generators. In addition, a backup nonclass 1E bus is provided with two 30 MWe gas turbine generators to supply power to nonsafety but important electrical loads during loss of station power events. Part of the power furnished by the gas turbine generators is dedicated to operate the heat tracing systems and the liquid metal circulating pumps at reduced flow to ensure that the liquid metals do not solidify during an accidental outage.

The laser driver electrical load is 200 MW. The total station service load is 358 MW.

Control storage batteries and chargers are provided for control of equipment in the normal station service ac power system. Separate control storage batteries, with chargers, are provided for one redundant train of engineered safety features. A separate storage battery and charger is provided for non-safety class essential systems and for inverters to serve computers and essential 120 V ac instrument buses.

4.1.8.3 CONTAINMENT AND OTHER MAJOR BUILDINGS

The design of all equipment and the buildings in which they are housed complies with Appendix A, 10CFR50, General Design Criteria for Nuclear Power Plants, wherever applicable. Structures, systems, and components important to safety are designed to withstand the effects of natural phenomena such as earthquakes, tornadoes, hurricanes, floods, tsunami and seiches without loss of capability to perform their safety functions. Figure 4.1.8-15 is a plot plan showing all of the buildings and facilities comprising the plant and their locations and orientation relative to each other. The containment and other major buildings are discribed in the following paragraphs.

4.1.8.3.1 REACTOR BUILDING

FUNCTION

The Reactor Building houses the Reaction Chamber, the Lithium Circulating Pumps, the Intermediate Heat Exchangers, the Lithium Drain and Storage Tank, the lithium circulating piping and valves, a portion of the sodium circulating piping and valves, and provides "hot" storage for the upper half of the Reaction Chamber and the First Wall. Mirrors for the Laser Driver beams are also housed in this building.

DESIGN REQUIREMENTS

The Reactor Building is designed to support all of the housed equipment under seismic, tornado and other severe environmental loads. The building is also missile protected and provides radiation shielding from the Reaction Chamber. All areas subject to potential liquid metal spills or escaping tritium are lined with steel and are maintained at a pressure slightly below atmospheric to assure that any building leakage is inward. A 1,000 ton bridge crane is provided for handling the upper half of the Reaction Chamber, the Reactor First Wall, the circulating pumps, and other major items of equipment.

DESIGN DESCRIPTION

The Reactor Building is illustrated on the following Figures, previously shown in Section 4.1.8.1.

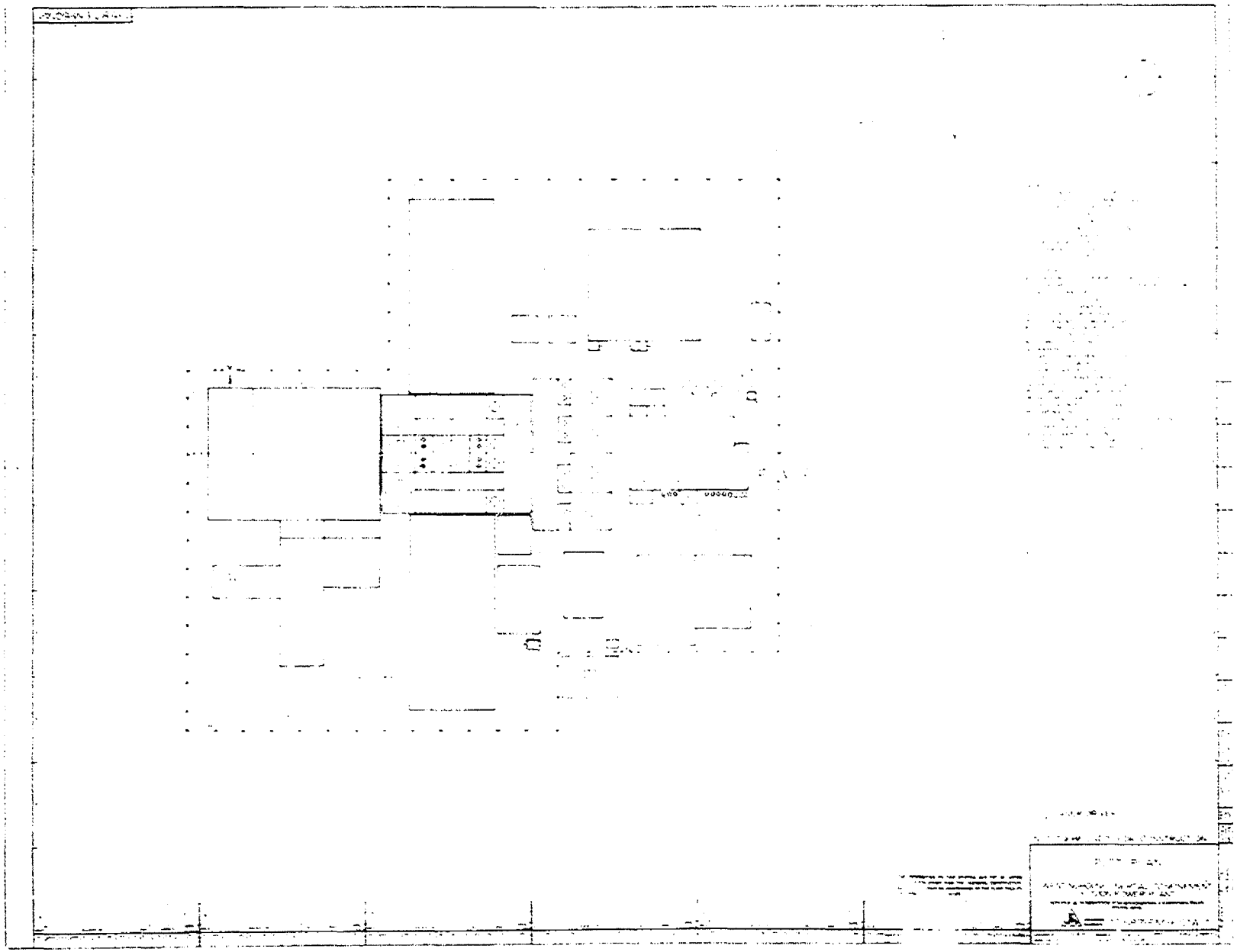

Figure 4.1.8-15. CO_2 Laser Driver Plant Arrangement, Plot Plan

Figure Title	Figure Number
Containment Structure - Plan El. 0.15 m	4.1.8-2
Containment Structure - Plan El. 42.75 m	4.1.8-3
Containment Structure - Section 1-1	4.1.8-4
Containment Structure - Section 2-2	4.1.8-5

The building is a reinforced concrete structure 125 m long by 105 m wide. The high bay area over the Reactor Chamber and Storage Area is 82.5 m high. The roof over the Intermediate Heat Exchangers and the Lithium Drain and Storage Tank is 52 m high. The Reactor Chamber, each Lithium Circulating Pump, the Lithium Drain and Storage Tank, the Storage Area, the lithium circulating piping, the sodium circulaitng piping and each Intermediate Heat Exchanger are in separate compartments. Sliding shielded doors are provided over the Reaction Chamber and at the entrance to each compartment within the Storage Area. All shielded doors slide on hydrostatic bearings and are sealed, where required, with inflatable gaskets, using argon as the inflating medium. This detail is not shown on the drawings.

The building is founded on a mat at grade. Walls are provided to support the Bridge Crane and shear walls are provided to carry lateral loads. The thickness of all walls and slabs are governed by both shielding and structural requirements. The floor and walls of each compartment are protected with an insulated steel liner to a height exceeding the depth of liquid metal that would result from a maximum possible spill. Channels, through which cooled argon is circulated continuously, are embedded in the concrete to insure against its overheating in the event of a spill. The remaining surfaces of each compartment are clad with a steel liner to insure containment of the argon that constitutes the inert atmosphere within each compartment. This detail is not shown on the drawings.

The uppermost portion of the Reaction Chamber support is subject to neutron heating, and is cooled by Freon-11 continuously circulating through tubing embedded in the concrete wall. This detail is not shown on the drawings.

4.1.8.3.2 HOT CELL FACILITY BUILDING

FUNCTION

The Hot Cell Facility Building (Figure 4.1.8-16) consists of a Hot Cell for remote work on the Reactor First Wall and other radioactive components, three separate storage sections for radioactive Reactor First Walls and/or ducts and other radioactive components, a storage compartment for a new reactor First Wall, an open storage compartment for non radioactive equipment, a receiving/assembly/dismantling area and an area with chemical cleaning cells for decontamination of equipment.

DESIGN REQUIREMENTS

The building is designed to withstand seismic, tornado and other severe environmental loads and is missile protected. All compartments in which radioactive components are stored or serviced are a minimum of one meter thick, and are furnished with shielded doors that slide on hydrostatic bearings. The Hot Cell is completely furnished with remote handling and servicing equipment and the receiving/assembly/dismantling area is equipped with a 150 tonne bridge crane. These details are not shown on the drawings.

DESIGN DESCRIPTION

The building is a reinforced concrete structure 160 m by 111 m. It is 50 m high over the receiving/assembling/dismantling area and 30 m high over the remainder of the building. It is founded at grade and is divided into separate compartments with a central transport aisle for servicing all compartments. Air float pallets are provided to furnish omni-directional/low moving force transportation for the equipment within the building. This detail is not shown on drawings.

4.1.8.3.3 STEAM GENERATOR BUILDING

FUNCTION

The Steam Generator Building houses the Steam Generators, the Sodium Drain and Storage Tank, the Sodium Circulating Pumps, and the sodium circulating piping and valves.

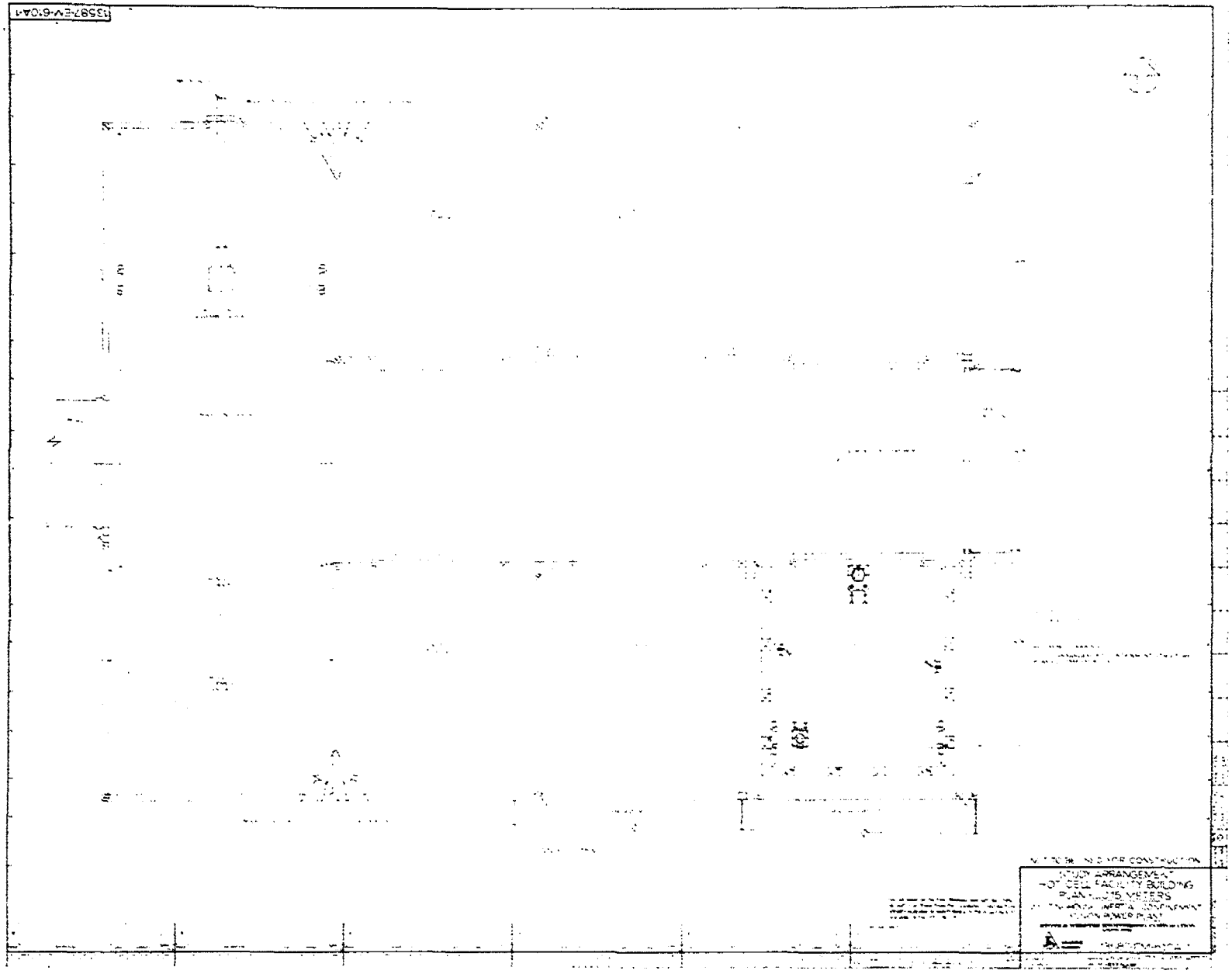

Figure 4.1.8-16. Hot Cell Facility Building, Plan El. 0.15 Meters

DESIGN REQUIREMENTS

The building is designed to support all of the housed equipment under seismic, tornado and other severe environmental loads. The building is also missile protected. All areas subject to liquid metal spills or escaping tritium are lined with steel and are maintained at a pressure slightly below atmospheric to insure that any building leakage is inward.

DESIGN DESCRIPTION

The Steam Generator Building is illustrated on the following Figures:

Figure Title	Figure Number
Steam Generator Building - Plan View	4.1.8-17
Steam Generator Building - Sections View	4.1.8-18

The building is a reinforced concrete structure 72 m by 135 m by 52 m high, and is founded on a concrete mat at grade. Each Steam Generator, each Sodium Circulating Pump, the Sodium Drain and Storage Tank and the sodium circulating piping are in separate compartments. Removable concrete slabs are provided in the roof area over each Steam Generator and each Sodium Circulating Pump in order to provide for removal and replacement of the components.

The floor and walls of each compartment are protected with an insulated steel liner to a height exceeding the depth of liquid metal that would result from a maximum possible spill. Channels, through which cooled argon is circulated continuously, are embedded in the concrete to ensure against its overheating in the event of a spill. The remaining surfaces of each compartment are clad with a steel liner to ensure containment of the argon that constitutes the inert atmosphere within each compartment. This detail is not shown on the drawings.

4.1.8.3.4 LASER DRIVER BUILDINGS

FUNCTION

The Laser Driver Buildings house the lasers, Marx generators, capacitors, mirrors, amplifiers and their coolers. There are two driver buildings, located on diametrically opposite sides of the Reactor Building.

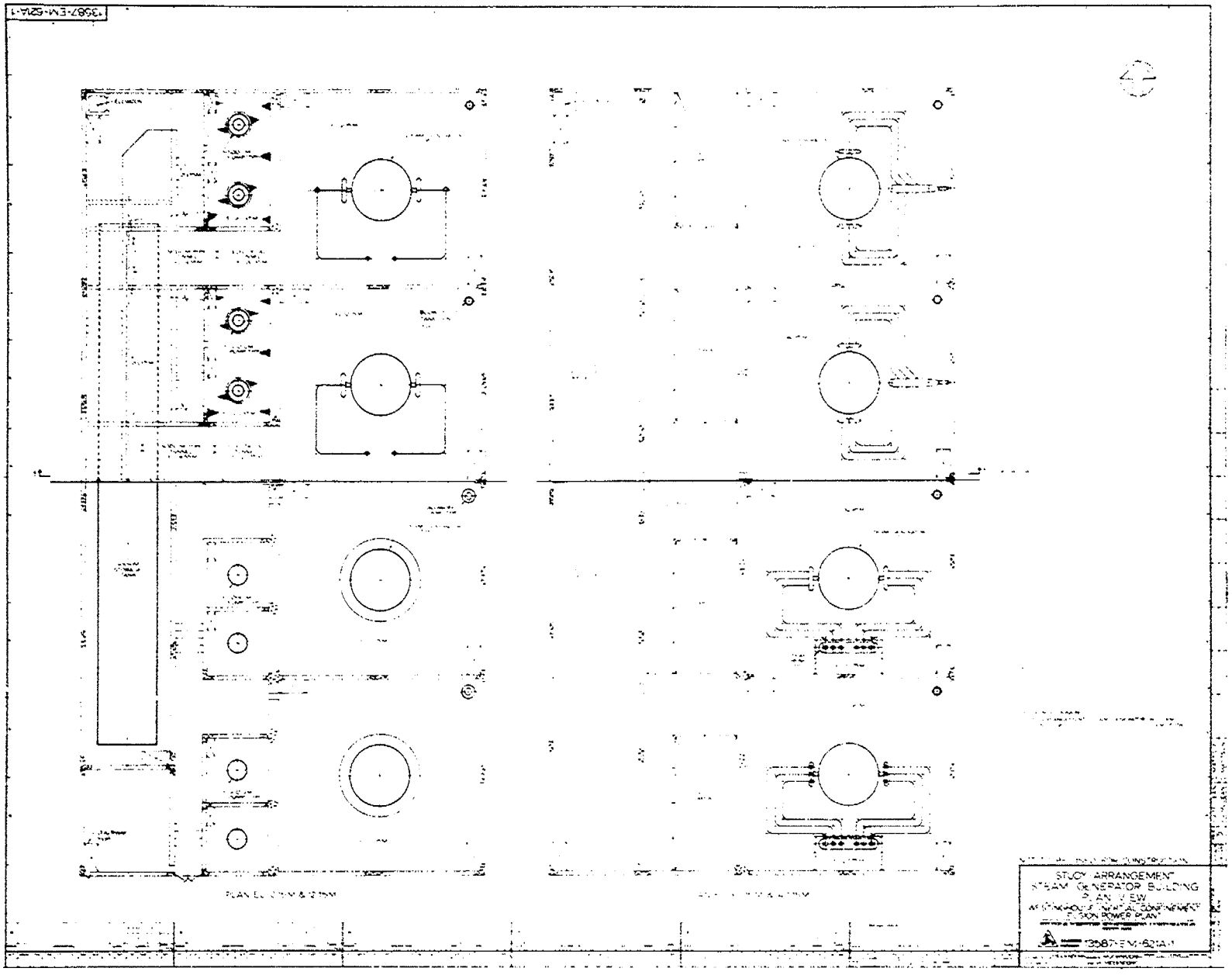

Figure 4.1.8-17. Steam Generator Building Plan View

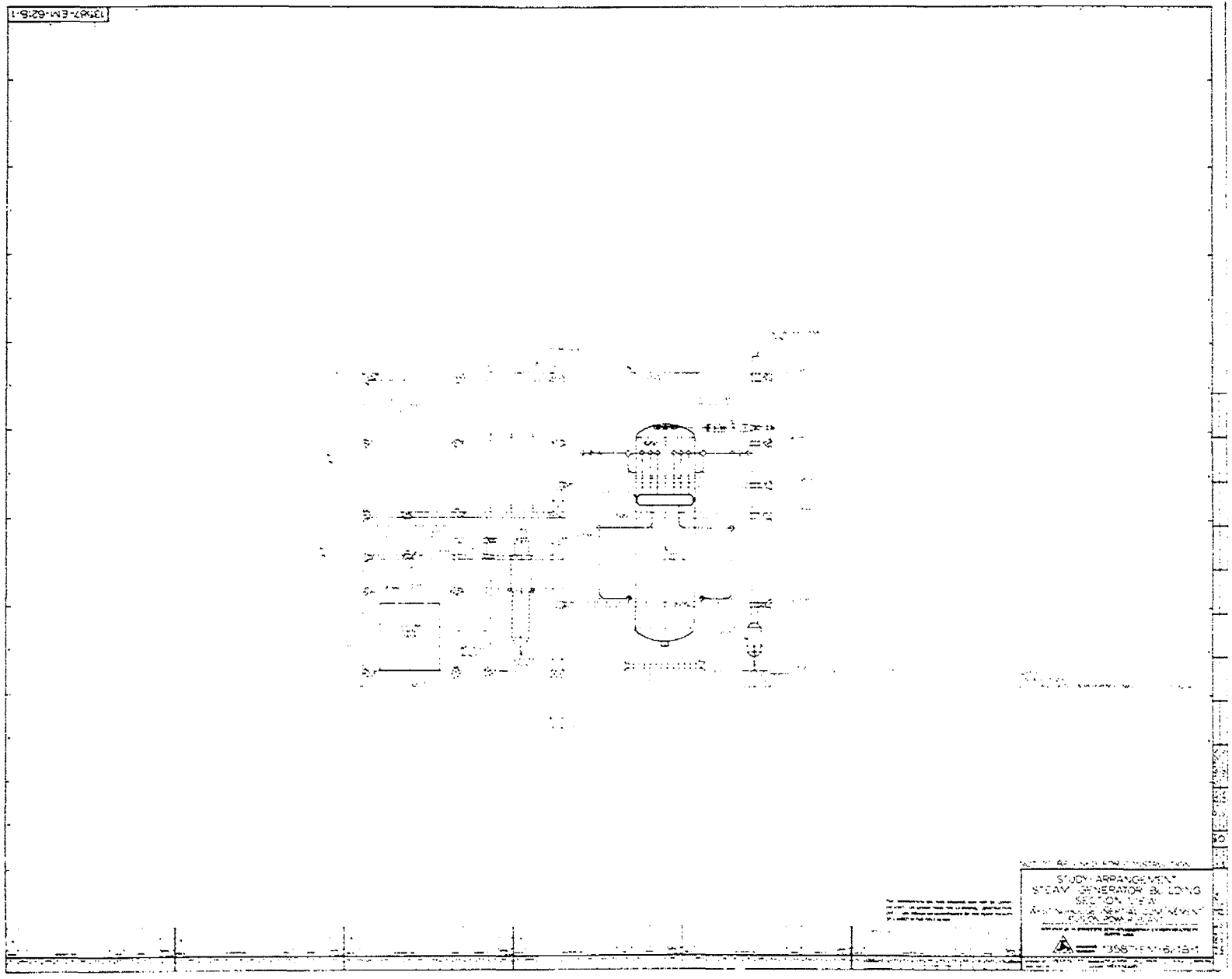

Figure 4.1.8-18. Steam Generator Building Section View

DESIGN REQUIREMENTS

The buildings are humidity controlled to maintain a dew point of -10° C (Relative humidity of 3% at 22° C) and are designed so as not to inflict any damage to the Reactor Building under seismic or tornado conditions. The mirrors are each isolated from the building slab in order to be free from all vibration.

DESIGN DESCRIPTION

Schematic drawings for these buildings are found in Section 4.1.1.

The buildings are founded at grade with reinforced concrete footings and a reinforced concrete slab. The buildings are each 175 m long by 75 m wide by 42.75 m high. The superstructure consists of a structural steel frame with insulated metal siding and roof deck and is sealed to maintain a vapor barrier to maintain the low dew point within the building. The roof deck is furnished with asphalt and gravel built-up roofing.

One wall of each building is common with a Reactor Building wall. The lower section of each of these common walls is provided with 54 salt windows for the transmission of the laser beams into the Reactor Building.

4.1.8.3.5 TURBINE BUILDING

FUNCTION

The Turbine Building houses the turbine generator, main condenser, feedwater heaters and other pertinent equipment of the power conversion system.

DESIGN REQUIREMENTS

The building is designed in compliance with the Uniform Building Code.

DESIGN DESCRIPTION

The Turbine Building is illustrated on the following figures shown in Section 4.1.8.2.

Figure Title	Figure No.
General Arrangement Turbine Building - Ground Floor	4.1.8-11
General Arrangement Turbine Building - Operating Floor	4.1.8-12
General Arrangement Turbine Building - Section 1-1	4.1.8-13

The building is a multi-story steel framed structure with insulated metal siding and and roof deck. The three general areas of the building are the turbine bay, the heater bay and the condensate polishing area. The turbine bay is 107 m long by 40 m wide by 41 m high. The heater bay is 95 m long by 24.4 m wide by 26.5 m high. The condensate polishing area is 95 m long by 13.7 m wide by 9.2 m high.

The turbine generator is set on a reinforced concrete pedestal.

Laydown space for maintenance is provided on the operating floor and is serviced by a bridge crane.

4.1.8.3.6 PELLET FACTORY BUILDING

FUNCTION

The Pellet Factory Building houses equipment for the recycling of tritium and the manufacture of the pellets.

DESIGN REQUIREMENTS

The building is designed in compliance with the Uniform Building Code and is maintained at a pressure slightly below atmospheric to insure that any building leakage is inward.

DESIGN DESCRIPTION

Schematic drawings for this building are found in Section 4.1.4.

The Pellet Factory is a rectangular building 37 m long by 25 m wide by 9 m high. At one end of the building, provision is made for two pellet towers. In this area, the building is 16 m high.

The building is steel framed with insulated metal siding and roof deck.

It is founded at grade on a reinforced concrete foundation.

4.1.8.3.7 WASTE DISPOSAL BUILDING

FUNCTION

The Waste Disposal Building houses equipment for collecting, separating, treating and packaging gaseous, liquid and solid waste products from the Pellet Factory, the Reactor Building and the Steam Generator Building.

DESIGN REQUIREMENTS

The portion of the building that houses the waste processing equipment is designed to withstand seismic, tornado and other severe environmental loads, and is missile protected. The remainder of the building is designed in compliance with the Uniform Building Code.

DESIGN DESCRIPTION

Drawings for this building have not been prepared.

The Waste Disposal Building is 121 m long by 38 m wide by 9 m high.

The portion of the building that houses the waste processing equipment is constructed of reinforced concrete and is 40 m long by 38 m wide by 9 m high. The walks and slabs are 0.6 m thick for radioactive shielding.

The remainder of the building is for drum storage and is 8.4 m long by 38 m wide by 9 m high. This portion of the building is structural steel framed with insulated metal siding and roof deck. A 15 tonne bridge crane is provided in this area.

4.1.8.3.8 CONTROL BUILDING

FUNCTION

The Control Building houses the power, control and instrumentation equipment necessary for station personnel to operate the plant and, in the event of an accident, to effect a safe shutdown of the plant. The building includes the

control room, switchgear rooms, cable spreading area, computer rooms, and environmental control equipment. The electric cables are carried to the Reactor Building in concrete tunnels on grade.

In the event that the outside atmosphere becomes contaminated with airborne radioactive contaminants, the building provides complete protection for the operating personnel within.

DESIGN REQUIREMENTS

The building is designed to withstand seismic, tornado and other severe environmental loads, and is missile protected.

DESIGN DESCRIPTION

Drawings for this building have not been prepared.

The Control Building is a reinforced concrete structure, 32 m by 35 m by 23 m high and is founded at grade. It has three floor levels, with the control room isolation area on the top floor, the cable spreading room on the second floor, and the switchgear room on the ground floor.

4.1.8.3.9 EMERGENCY GENERATOR AND STANDBY GENERATOR BUILDING

FUNCTION

The building houses two 16 MWe emergency diesel generators and two 30 MWe gas turbine generators and the equipment necessary to provide electric power to operate both the safety-related systems and nonsafety-generating equipment and off-site power.

DESIGN REQUIREMENTS

The building is designed to withstand seismic, tornado and other severe environmental loads, and is missile protected. Provisions are made for removal and replacement of all equipment housed within.

DESIGN DESCRIPTION

Drawings for this building have not been prepared.

The building is a reinforced concrete structure 30 m long by 50 m wide by 18 m high. The air intake and exhaust hoods rise above the main roof and are located at opposite ends of the building. An electrical tunnel connects this building to the control building. The generators are separated from each other by concrete divider walls.

4.1.8.3.10 EMERGENCY GENERATOR AND STANDBY GENERATOR FUEL OIL STORAGE TANKS AND PUMP HOUSE

FUNCTION

Two fuel oil storage tanks and a pump house provide fuel for the emergency and standby generators.

DESIGN REQUIREMENTS

The fuel oil tanks and pump house are designed to withstand seismic tornado and other severe environmental loads and are missile protected.

DESIGN DESCRIPTION

Drawings have not been prepared.

The fuel oil tanks are underground in a reinforced concrete vault. The pump house is located on grade on top of the vault.

4.1.8.3.11 ARGON STORAGE BUILDING

FUNCTION

The Argon Storage Building houses the argon storage tanks and the argon purification system and serves to shelter them from the elements.

DESIGN REQUIREMENTS

The building is designed in compliance with the Uniform Building Code.

DESIGN DESCRIPTION

Drawings for this building have not been prepared.

The building is a steel framed structure with metal siding and roof deck, and is 86 m wide by 92 m long by 7.6 m high. The argon tanks are supported on concrete saddles.

Louvers, ventilators, windows and doors are provided to allow cross ventilation in the building.

4.1.8.4 SAFETY AND CONTROL

SODIUM WATER REACTION WITHIN STEAM GENERATOR

In the event of a sodium tube perforation allowing contact between steam and sodium, both the escaping steam and the hydrogen produced by the resulting sodium-water reaction, are conducted to a separating drum where the steam is condensed and discharged to the cooling tower. The hydrogen, along with the argon carryover, is discharged to atmosphere.

If tritium should be detected in the discharge, the Steam Generator will be removed from service by isolating it from the sodium loops and the boiler feed and steam loops, the hydrogen will be sent to Waste Handling, the sodium contained within the tubes and chambers of the Steam Generator will be returned to the Sodium Drain and Storage Tank and the steam discharged to the condenser.

After the perforated tube has been plugged, the Steam Generator will be returned to service. This system does not appear on the drawings.

LIQUID METAL LEAKS

Both lithium and sodium, in the range of operating temperatures encountered in the plant, ignite spontaneously on coming into contact with air. The only positive means of preventing either lithium or sodium fires in the event of a leak ranging from small to catastrophic, is to inert all of the compartments in which a leak can occur, with either argon, helium or neon gas.

From the standpoint of ease of containment and cost, argon has been selected as the inerting gas for this plant. To inert, each compartment is first evacuated to 2.5 Torr, followed by filling with argon to a pressure slightly below atmospheric pressure.

Argon gas can be contaminated by contact with air; therefore, in order to be assured that no traces of oxygen or nitrogen are introduced into the Argon Storage Tanks, an argon purification system is provided. In this system, the argon is heated to a temperature range of 425 to 480° C and is passed to a Deoxidizer Unit where the oxygen contaminate is removed by a copper catalyst. The remaining argon and nitrogen gas mixture is then air-cooled, water-cooled and liquefied at approximately -196° C and essentially atmospheric pressure. Final liquefaction of the mixture is obtained by cooling with purchased liquid nitrogen. The resulting argon and nitrogen liquid mixture becomes the feed stream to the Argon Recovery Distribution Column. In the Argon Recovery Column, the nitrogen contaminate and some argon pass overhead from the column. Subsequently, the column overhead is vaporized and discarded to the atmosphere. Pure liquid argon is recovered from the bottom of the Recovery Column. The argon product is then vaporized, cooled and sent to the Argon Tanks. This system does not appear on the drawings.

TRITIUM LEAKAGE INTO REACTOR BUILDING OR STEAM GENERATOR BUILDING

Because of the necessity of inerting the Reactor Building and the Steam Generator Building with argon, it was decided to cope with escaping tritium in the following manner rather than resort to the double pipe helium purge system that is generally used for the purpose.

Each compartment within the Reactor Building and the Steam Generator Building is provided with an atmospheric clean-up system, consisting of a fan, a detritiating adsorber and a HEPA filter. Any tritium entering a compartment, either through leakage of the liquid metal or by permeation, is removed by circulating the contaminated argon atmosphere through the detritiating adsorber and HEPA filter. The removed tritium is returned to the Waste Handling Building. This system is illustrated on the Heating, Ventilating and Air Conditioning (HVAC) Diagram, Figure 4.1.8-19.

SALT WINDOWS

To prevent breach of containment and loss of vacuum within the Reactor Chamber in the event of a leak or breakage of any of the salt windows, each beam duct

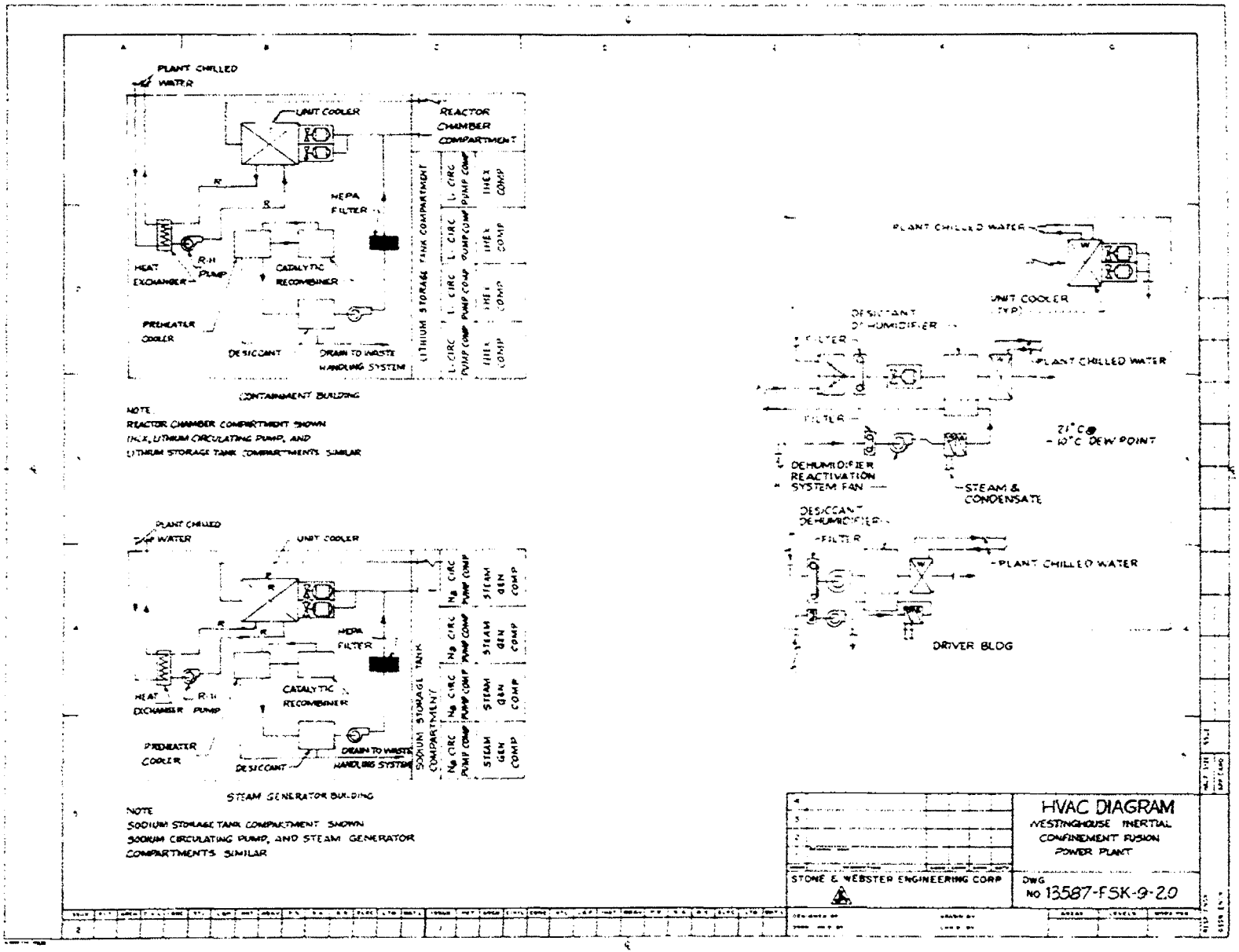

Figure 4.1.8-19. Heating, Ventilating and Air Conditioning Diagram

through which a laser beam is passed, is provided with a motor operated ball valve.

An ultrasonic detection unit is positioned within a salient chamber, made a part of each beam duct and located 0.5 m from the salt window within the Reactor Building. The rapid inrush of air flowing from the Driver Building into the beam duct through a leaking or broken salt window, will be detected by the ultrasonic detection unit and the resulting signal will sound an audible alarm in the Control Room, simultaneously identifying the broken window. The same signal will also trigger the motor operated ball valve to close, and terminate the laser beam within the duct. This system does not appear on the drawings.

LASER COOLING

Because the Main Ducts and the final laser beams turning and focusing mirrors are subject to intensive radiation from the Reactor Chamber, a cooling system is provided to maintain the surface temperatures of these items at acceptable levels.

The gas flowing through the laser amplifiers is heated by the electrical discharge and must be continuously cooled in order to maintain the gas at an acceptable temperature level (60.5° C average).

Each amplifier is furnished with a cooler and a centrifugal compressor to circulate the gas through the amplifier and the cooler.

The gas passes through the cooler tubes where it is cooled by water taken from the cooling tower. As the water leaves the cooler, it is returned to the cooling tower. The total heat removed from each amplifier amounts to 14.5 MWt. This system does not appear on the drawings.

4.1.9 ELECTRICAL SYSTEM

FUNCTION

The principal function of the electrical system will be to take power from the main generator and supply each reactor load at its required utilization voltage. In addition, the electrical system will provide adequate levels of equipment and personnel safety, during both normal facility operation and abnormal occurrences. Also, the electrical system will receive power from an emergency generator system and deliver it to the emergency reactor loads.

DESIGN REQUIREMENTS

- Distribute power to each reactor load.
- Provide the power at the appropriate voltage of each reactor load.
- Provide switching capabilities for both energizing and disconnecting loads.
- Distribute emergency power to loads designated as requiring power for safe operation after any loss of the main generator power. At the same time power will be removed from unnecessary loads.

SUMMARY DESCRIPTION

The electrical system will include primary distribution switchgear, secondary load centers, and primary and secondary distribution circuits as shown in Figure 4.1.9-1.

The primary distribution switchgear will receive power from the main generator for distribution to appropriate areas of the ICF reactor. The primary distribution points will either be facility loads or be secondary load centers if further voltage transformation is required. The switchgear will provide overcurrent protection and a means for isolating loads from the power supply. It may also provide special control functions such as motor starting. The driver power supplies are the largest reactor load and will be operated directly off the main generator terminals.

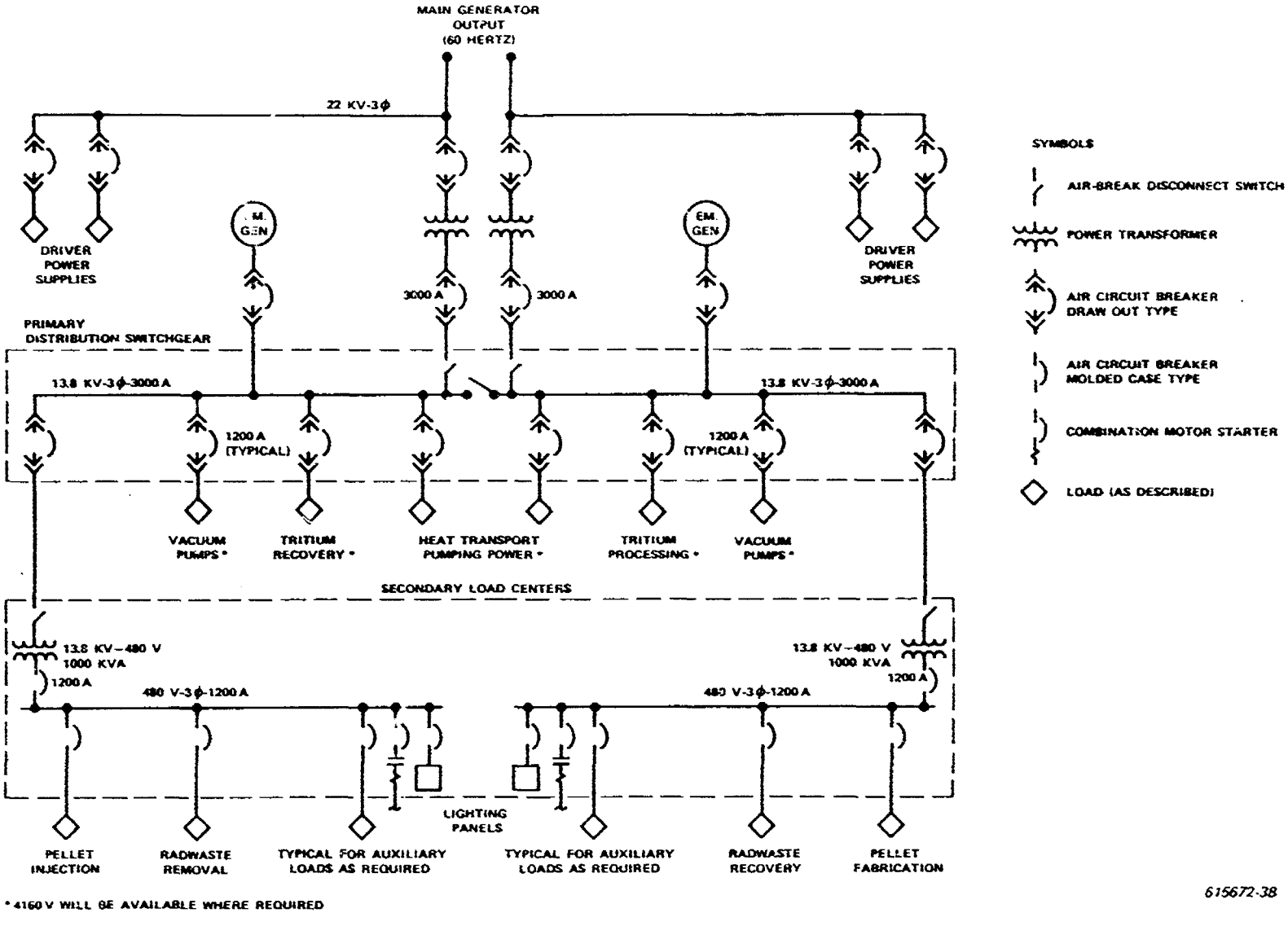

Figure 4.1.9-1. ICF Reactor Electrical Single-Line Diagram

The secondary load centers will be provided when additional voltage transformation is necessary to supply appropriate voltage levels for smaller loads. The load centers will also provide overcurrent protection, as well as motor starting and other equipment control functions. The secondary load centers will consist of transformers, main fuses, circuit breakers, motor starters, and other power conditioning equipment as required.

The primary and secondary distribution circiuts will transmit power between the various components of the electrical system. The distribution circiuts will consist of insulated power cables. The sizes and insulation type will be selected to be compatible with the voltage and current levels of the circuit, as well as the environmental conditions to which the cable will be subject.

The configuration of the reactor electrical system is dependent on the characteristics of the reactor loads. The estimated parameters of the reactor electrical system are summarized in Table 4.1.9-1 for both the laser and heavy ion driven systems. As shown, the total plant electrical load is 358 MW for the laser system and 219 MW for the heavy ion system. The driver power supply of the laser system required 133 MW of power more than did that of the heavy ion system. Table 4.1.9-1 also indicates the several voltage levels required to deliver the power, including 13,800 volts, 4,160 volts, 480 volts, and 120 volts. The laser driver power supply will be operated at 22 kV in order to operate directly off the main generator.

TABLE 4.1.9-1

ELECTRICAL DISTRIBUTION PARAMETERS

REACTOR LOAD	POWER FOR LASER SYSTEM	POWER FOR HEAVY ION SYSTEM
Driver Power Supply	200 MW	67 MW
Lithium Circulating Pumps	24	24
Sodium Circulating Pumps	48	48
Vacuum Pumps	4	4
Tritium Recovery System	2.5	2.5
Tritium Processing System	1.5	1.5
Pellet Fabrication	0.5	0.5
Pellet Injector System	0.3	0.3
Radwaste Removal System	0.7	0.7
Total Reactor Load	282 MW	149 MW
Plant Auxiliaries (Balance of Plant)	76 MW	70 MW
Total Plant Load	358 MW	219 MW

Electrical Inputs for Reactor Loads

Three-Phase, 60 Hz

13.8 kV, 4160V, 460V, and 120V

22 kV for the Laser and Heavy Ion Driver Power Supplies

Emergency Load Requirements for the Reactor System Not Including Plant Auxiliaries (Balance of Plant)

Tritium Processing Recovery	1.2 MW
Lithium Circulating Pumps	3.4
Sodium Circulating Pumps	2.4
Pellet Fabrication	0.05
Heat Tracing Loads	10.6
Total	17.65 MW

4.2 HEAVY ION BEAM DRIVEN DESIGN

4.2.1 DRIVER

FUNCTION

The function of the driver is to deliver a properly shaped pulse of energetic heavy ions to the pellet. For a heavy ion driver this implies ions of atomic mass from Xe 131 to U 238 at kinetic energies from 5 GeV to 20 GeV.

DESIGN REQUIREMENTS

These ions are to be focused on a target spot ranging from 1 mm to 5 mm in radius. The pulses are to be 6 to 20 n sec long containing 1 MJ to 10 MJ of energy per pulse.

Table 4.2.1-1 summarizes the requirements on the heavy ion driver to be used in this reference design.

TABLE 4.2.1-1

PARAMETERS REQUIRED FOR HEAVY ION DRIVER

Ion:	Xe^{+} or Xe^{++}
Ion Energy:	10 GeV
Target:	2.5 mm Radius
Beam Energy:	2 MJ
Beam Power:	150 TW
Pulse Length:	13 nsec

SYSTEM DESCRIPTION

The heavy ion driver system is divided into 7 blocks, as listed below.

1) Ion source and pre-accelerator
2) Low β accelerator $\beta < 0.1$

3) High β accelerator $\beta > 0.1$

4) Debuncher, multiplier rings, compressor

5) Storage rings

6) Beam transport lines

7) Final bending and focusing elements and reactor.

The first six of these blocks comprise the driver.

Because the charge state has an extreme influence on system size and cost, two almost identical systems meeting the design requirements are described in Tables 4.2.1-2 through 4.2.1-7. The systems are based on either Xe^{+} or Xe^{++} (single and doubly ionized xenon). When only one value of a parameter is listed it is the same for both systems. Figures 4.2.1-1 and 4.2.1-2 are schematic representations of heavy ion drivers based on a Xe^{+} or on a Xe^{++} ion. In general, all parts of the Xe^{++} system are half the size of the corresponding part of the Xe^{+} system. However, the number of storage rings required by the Xe^{++} system is four times greater than that required by the Xe^{+} system. The low β, Wideroe, accelerator ends at "a" on these figures; the high β, Alvarez, accelerator starts at "a" and continues to "b" on the figures.

The following tables will describe the seven blocks comprising the driver and reactor interface by listing important parameters and their values.

TABLE 4.2.1-2

PARAMETERS DESCRIBING THE ION SOURCE AND PREACCELERATOR

Ion	Xenon
Normalized Emittance	$\varepsilon_s = 3.2 \times 10^{-7}$ m-rad
Current per source	$i_s = 25$ mA
Charge state of ion	$Z = 1$
Atomic mass of ion	$A = 131$
Kinetic Energy of Preaccelerator	$T_0 = 2 \times 10^{-3}$ GeV
Number of Sources	$Xe^{++}, n_s = 4$ $\quad Xe^{+}, n_s = 8$

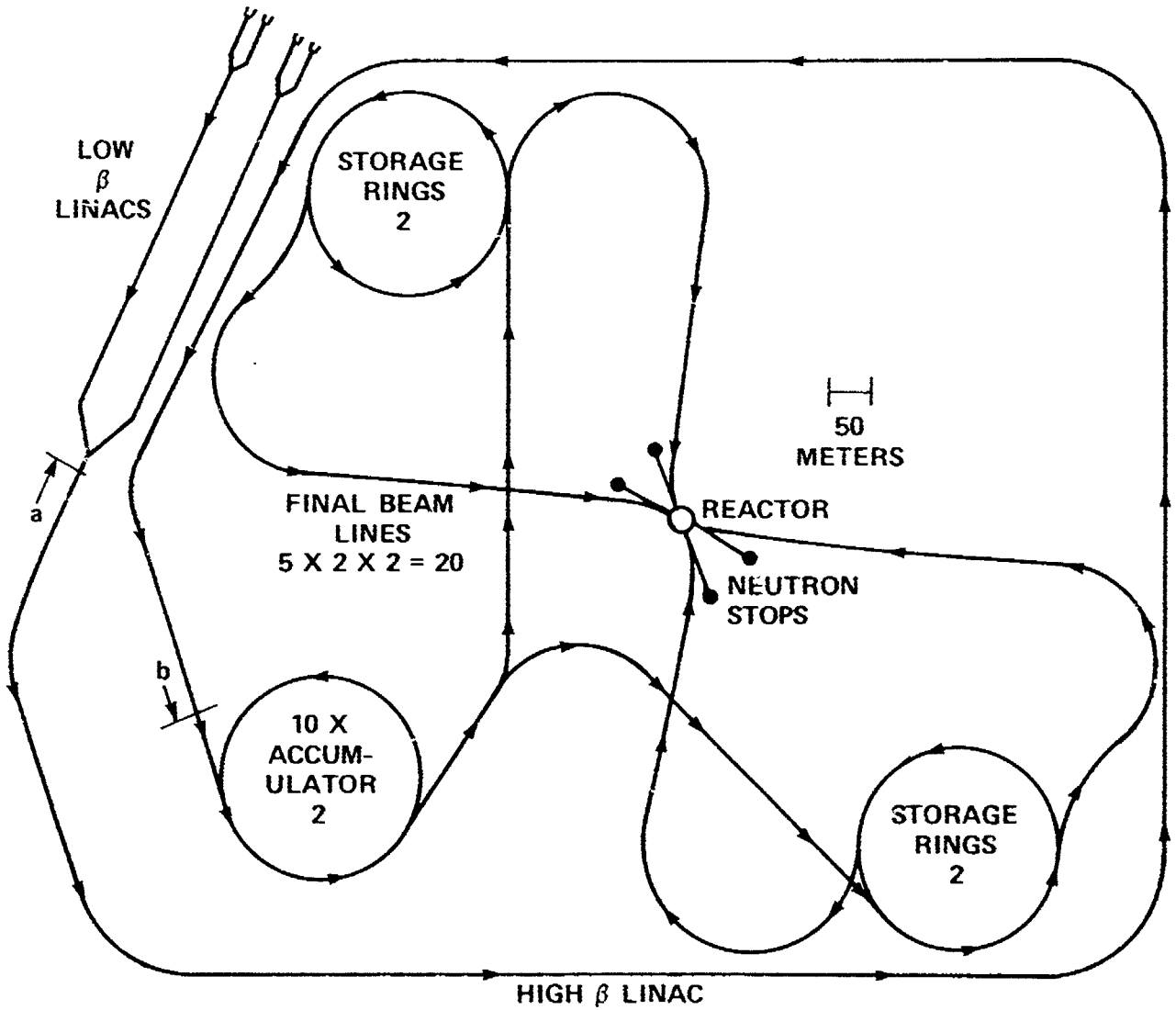

Figure 4.2.1-1. Schematic Representation of 10 GeV Xe^{+} Heavy Ion RF Linac Driver

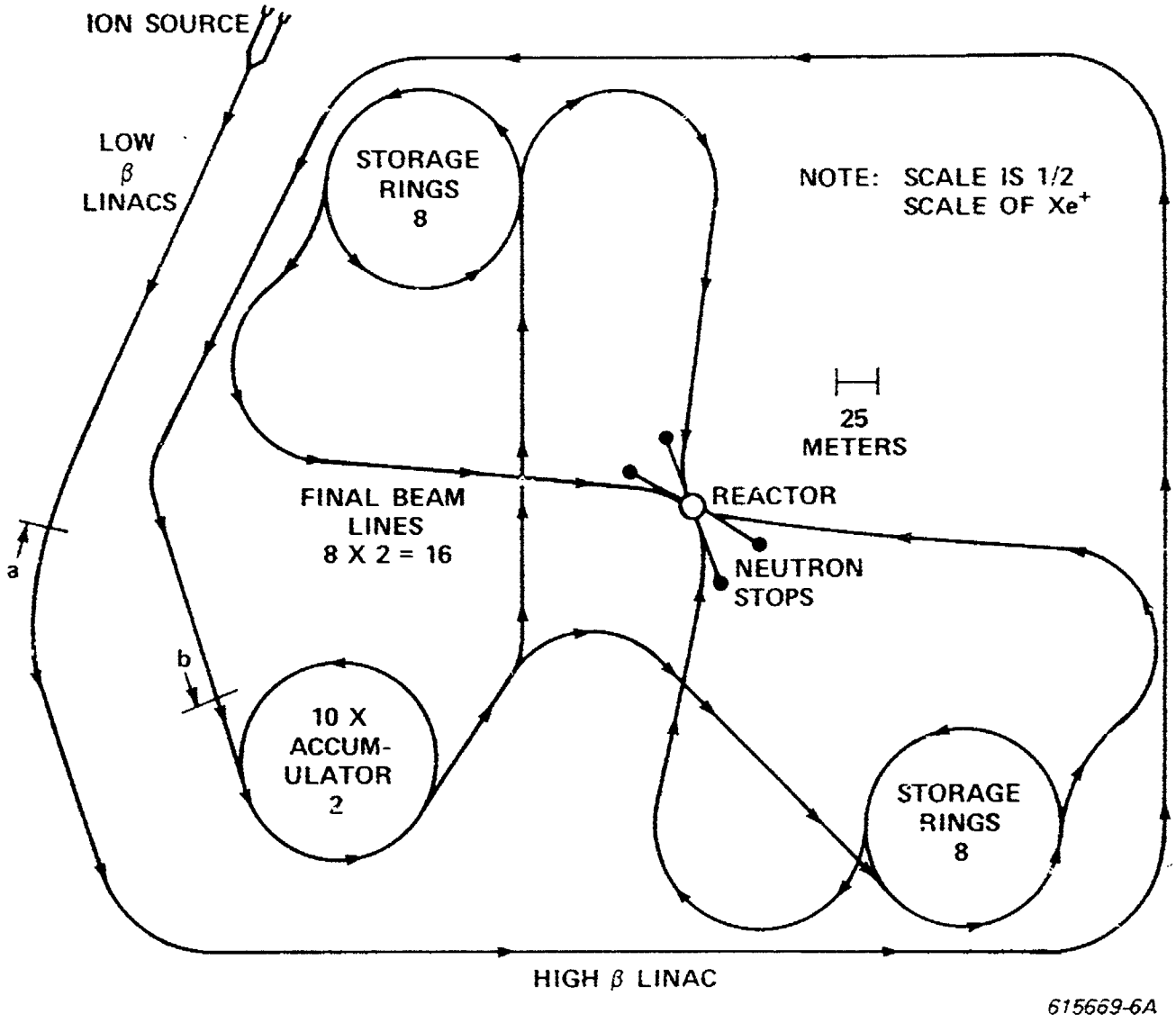

Figure 4.2.1-2. Schematic Representation of 10 GeV Xe^{++} Heavy Ion RF Linac Driver

TABLE 4.2.1-3

PARAMETERS DESCRIBING THE LOW β ACCELERATOR WIDEROE CAVITIES

Total energy 0.16 MJ

	Xe^{++}	Xe^{+}
Total power to beam	37.9 MW	75.8 MW
to cavities	58.3 MW	116.6 MW
First Section		
Operating Frequency	12.5 MHz	
2 MeV in/20 MeV out; 1:1 Beam Loading		
Magnetic Field, B	> 1 Tesla	
Number of Sections	4	8
Length of each Section	18 m	
Second Section		
Operating Frequency	50 MHz	
20 MeV in/100 MeV out; 1:1 Beam Loading		
Magnetic Field, B	~ 0.65 Tesla	
Number of Sections	2	4
Length of each Section	80 m	
Third Section		
Operating Frequency	100 MHz	
100 MeV in/800 MeV out; 2:1 Beam Loading		
Magnetic Field, B	1.67T	0.056T
Number of Sections	1	2
Length of each Section	350 m	700 m

TABLE 4.2.1-4

PARAMETERS DESCRIBING THE HIGH β LINAC ALVAREZ CAVITIES

Total energy 1.84 MJ

	Xe^{++}	Xe^{+}
Total power to beam	460 MW	920 MW
to cavities	614 MW	1227 MW
Operating Frequency	200 MHz	
0.8 GeV in/10 GeV out; 3:1 Beam Loading		
Magnetic Field, B	∿ 0.002 Tesla	
Length of Linac	2760 m	5520 m

TABLE 4.2.1-5

PARAMETERS DESCRIBING THE DEBUNCHER, MULTIPLIER RINGS AND COMPRESSOR

	Xe^{++}	Xe^{+}
Debuncher		
Operating Frequency	200 MHz	
Power	2 MW	4 MW
Length of debuncher	50 m	100 m
Multiplier Rings		
2 Rings		
10 revolutions to fill		
Average dipole field	1.8 Tesla	
Radius of Ring	45 m	90 m
Compressor		
ΔT introduced to produce compression	2% T = 0.2 GeV	
Length of compressor	55 m	110 m

TABLE 4.2.1-6

PARAMETERS DESCRIBING THE STORAGE RINGS

	Xe^{++}	Xe+
Storage time	4 msec	2 msec
Number of rings	16	4
Radius of rings	45 m	90 m
Average dipole field	1.8 Tesla	
Vacuum in Ring	1.3×10^{-9} Torr	2.7×10^{-9} Torr
Fill factor	50%	
Stacking in ring	(10 x 10)	
ε_{SR} Normalized Emittance	2.6×10^{-5} m-rad	
Number of bunches per ring	1	5
Compression in ring	7X	
Revolutions to compress	8	4
Time per revolution	2.94 μsec	5.89 μsec
Current at extraction	70 A	70 A

TABLE 4.2.1-7

PARAMETERS DESCRIBING THE FINAL TRANSPORT SYSTEM

	Xe^{++}	Xe^{+}
Number of lines	16	20
Compression from storage ring to target	26.8	10.7
Paraxial distance from storage ring to pellet	1334 m	500 m
Initial current per line	70 A	70 A
Final Current at pellet	1875 A	750 A
Current at end of transport	752 A	306 A
First quad pole tip field	0.026 Tesla	0.018 Tesla
Last quad pole tip field	0.92 Tesla	0.17 Tesla
Geometric mean B	0.025 Tesla	0.016 Tesla

Bending and Final Focusing Elements

The heavy ion driver is defined as ending with the beam transport line; the final bending and focusing elements are considered part of the reactor block because of the strong influence of the neutron flux on their design. The essential elements of the interface are: bending magnet (to bend the ion beam away from the neutron path), neutron dump (to capture the back-streaming neutrons) and final focusing triplet. These are shown in Figure 4.2.1-3. A greatly expanded vertical view of the action of the final focusing triplet is shown in Figure 4.2.1-4. The final focusing triplet causes the ion beam which is expanding after leaving the first focusing magnet to converge towards the focal spot some 15 meters away from the edge of the magnet.

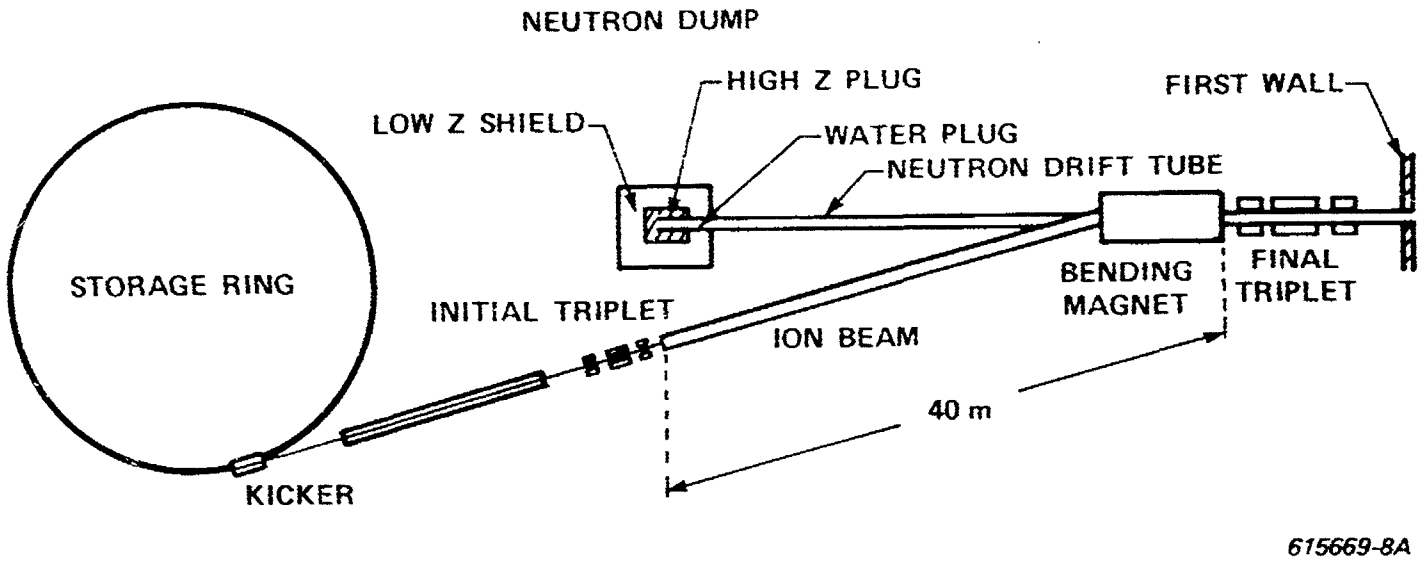

Figure 4.2.1-3. Schematic Illustration of the Interfaces Between tne Storage Ring, Focusing Triplet, Bending Magnet and Reactor Chamber in a Heavy Ion Driven ICF Power Plant

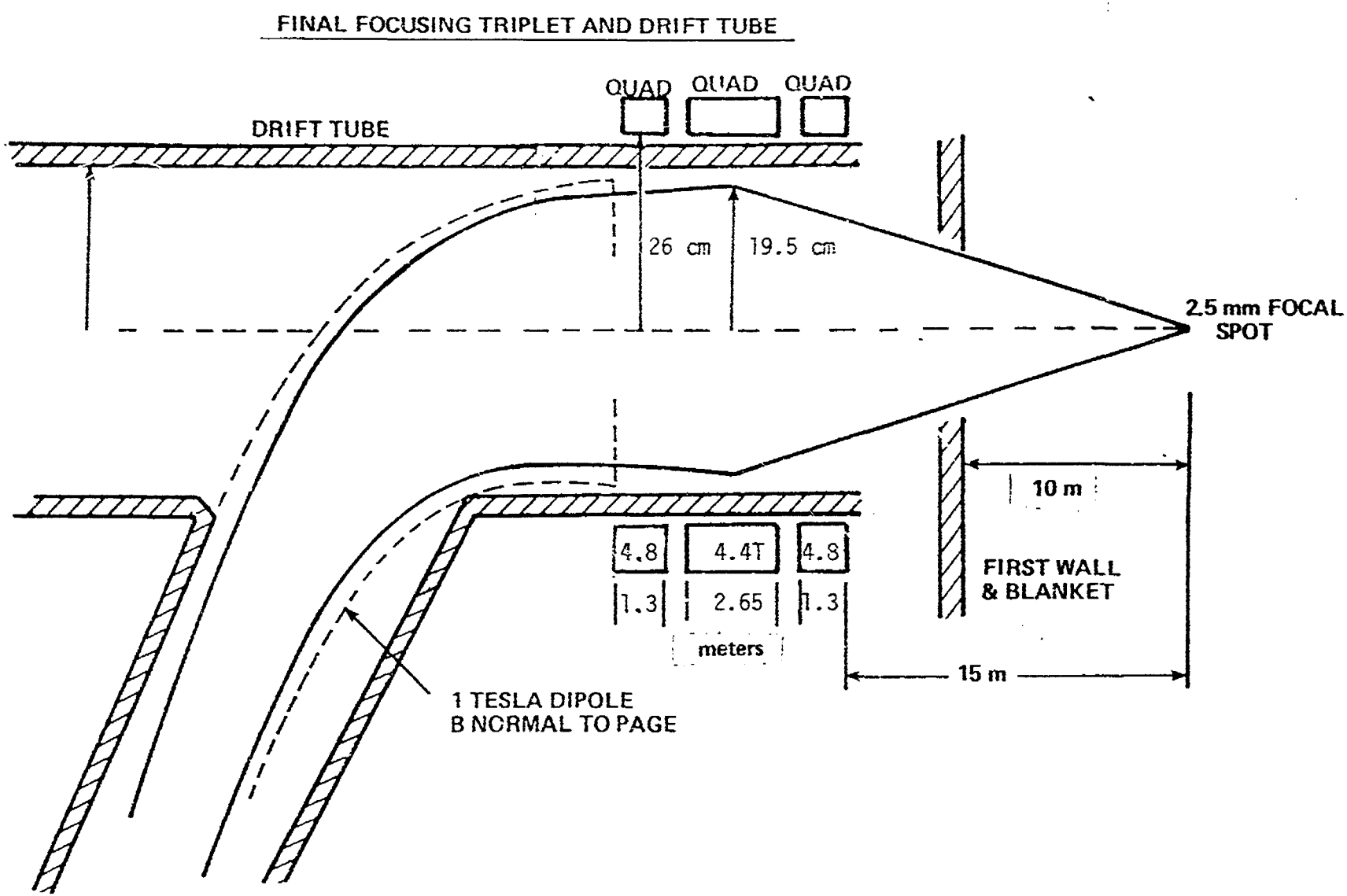

Figure 4.2.1-4. Detail of the Heavy Ion Beam Focusing Concept

TABLE 4.2.1-8

PARAMETERS DESCRIBING THE FINAL FOCUS AND REACTOR

Reactor inner radius	10 m	
	Xe^{++}	Xe^{+}
Distance from pellet to front of final focusing magnet	13.9 m	15 m
B_{max} of final element	4.1 T	4.8 T
Total length of focusing triplet	6 m	8 m
Distance from pellet to first focusing magnet	48 m	78 m

Bending Magnet for Heavy Ion Beam

FUNCTION

A bending magnet for the heavy ion beam line is needed to prevent backstreaming neutrons from drifting back into the beam line and destroying sensitive components along the way. The magnet bends the ion beam line away from the straight line path of the neutrons, allowing the neutrons to be captured in a neutron dump.

REQUIREMENTS

The magnet must bend 1 kA of 10 GeV singly charged Xe 131 ions through a small arc ($\sim 5°$). Its bore must be large enough to accommodate both the curved path of the ions and the backstreaming neutrons; to minimize the bore diameter its length should be as small as possible consistent with minimal magnetic field and cost. There will be one magnet for each of the 20 ion beams.

DESCRIPTION

The location of the bending magnet with respect to the focusing magnets, reaction chamber and beam dump is shown in Figure 4.2.1-3. Table 4.2.1-9 summarizes some of the significant features of the system.

TABLE 4.2.1-9

BENDING MAGNET INTERFACE WITH REACTION CHAMBER

Distance of Neutron Dump from Reaction Chamber	40 m
Length of Bending Magnet	9 m
Bending Angle	5.6°
Deviation of Ion Beam from Straight Line Path at Exit of 9 m long Magnet	0.44 m
Displacement of Ion Beam from Straight Line Path at Neutron Dump	3.5 m

Figure 4.2.1-5 shows the dimensional details of the bending magnet.

Focusing Magnet for the Heavy Ion Beam

FUNCTION

The focusing magnet is a quadrupole triplet which is intended to accept an expanding cloud of ions from a source located 40 to 50 meters from the focusing magnet. The ion beam will occupy a region up to 0.387 meters in radius as it passes through the focusing magnets. Beyond the focusing magnet the ion beam will converge to a 5 mm diameter at the pellet located at the center of the fusion reaction chamber and situated some 15 meters away.

REQUIREMENTS

The magnetic fields must focus a 1 kA beam consisting of singly charged 10 GeV Xenon ions. The overall design of the magnets is greatly influenced by the constraint that no stray field from any of the companion focusing magnets can distort the field produced by the magnet that is active in focusing a particular beam.

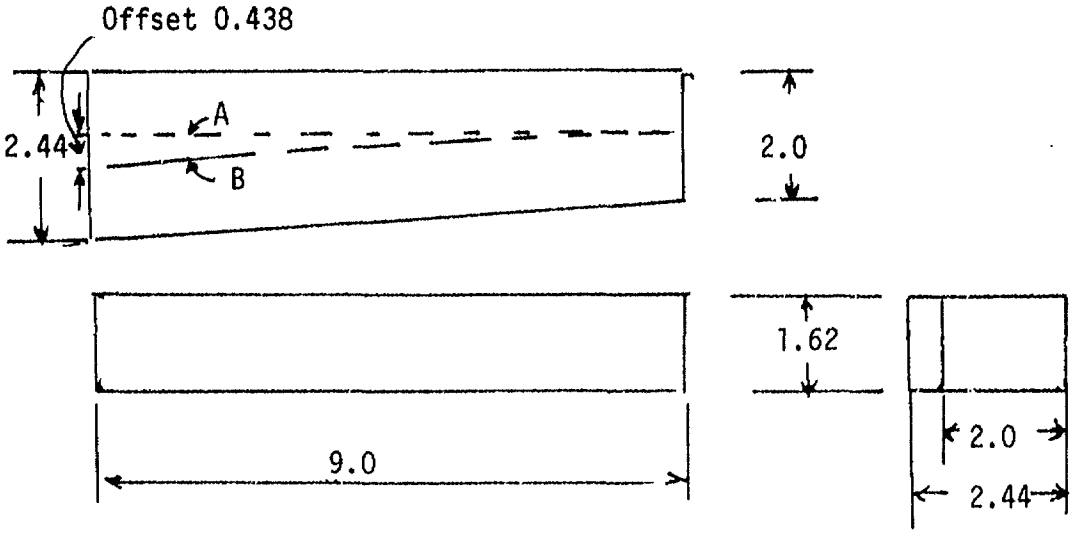

(All distances above in meters.)

Bending Magnet

A is path of neutrons
B is path of ions

Overall height	1.62 meters
Overall length	9.00 meters
Wide width	2.44 meters
Narrow width	2.00 meters
Iron weight	195 Tonnes
Copper weight	23 Tonnes
Overall weight	218 Tonnes
Excitation requirement	2.57 megawatts

Figure 4.2.1 -5. Dimensions of Bending Magnet for Heavy Ion System

DESCRIPTION

A superconducting magnet without iron in the neighborhood would, in the absence of other magnets, be a light weight effective quadrupole magnet. Without iron to collect the useful flux, the flux leakage is considerable and a shield is required. In the current application the shield is a thick cylinder of iron placed around each quadrupole winding to accept and to carry the external flux from pole to pole without giving rise to any leakage field beyond the iron cylinder. The required winding, when a shield is used, is almost identical to an air core magnet winding without a shield except that the required excitation and winding thickness would be nearly halved.

When an iron shield is used, the iron takes very little excitation if the iron section is large enough to allow the flux to flow within the iron at a density equal to or less than the saturating level for iron. The flux leakage control is ideal when appropriate shielding (enough thickness is provided) is used and the amount of superconductor needed is held to a minimum. The only drawback introduced by the iron is a slight field distortion produced if the local flux density in the iron is above the saturation level, a possibility in an area near the pole center where the useful flux entering the iron has a local flux density that is higher than the saturation level for iron.

Generally the quadrupole flux density gradient, the individual quadrupole length, the radius of the clearance bore, and the dewar insulation space requirements are known. These items are conveniently listed in Table 4.2.1-10 and described in Figure 4.2.1-6.

TABLE 4.2.1-10

PARAMETERS DESCRIBING THE THREE MAGNETS COMPRISING THE FOCUSING TRIPLET

	Magnet #1	Magnet #2	Magnet #3
Field gradient, Tesla/meter	6.0	5.25	6.0
Length, meters	2.0	4.1	2.0
Radius of clearance bore, meters	0.288	0.358	0.387
Dewar plus insulation, meters	0.100	0.100	0.100
Inner radius of S.C. winding,meters	0.388	0.458	0.487
S.C. winding thickness, meters	0.0365	0.0376	0.0503
Outer radius of S.C. winding,meters	0.4245	0.4956	0.5373
Iron thickness	0.2666	0.3181	0.4199
Outer radius, iron shield, meters	0.6911	0.8137	0.9573
Dewar plus insulation, meters	0.100	0.102	0.100
Overall radius, meters	0.7911	0.9137	1.053
Principal Iron, Tonnes	14.48	41.57	30.56
End Shield, Tonnes	2.41	3.38	5.09
Total, Tonnes	16.89	44.95	35.65
Bore diameter, meters	0.576	0.716	0.774
Length (Principal + ends),meters	2 + 1 = 3	4.1 + 1 = 5.1	2 + 1 = 3
Maximum diameter, meters	1.582	1.827	2.106
Weight, Tonnes	16.89	44.95	35.65

Overall Triplet dimensions

Gross length	11.1 meters
Maximum diameter	2.016 meters
Minimum bore	0.576 meters
Gross Tonnes	97.49 Tonnes

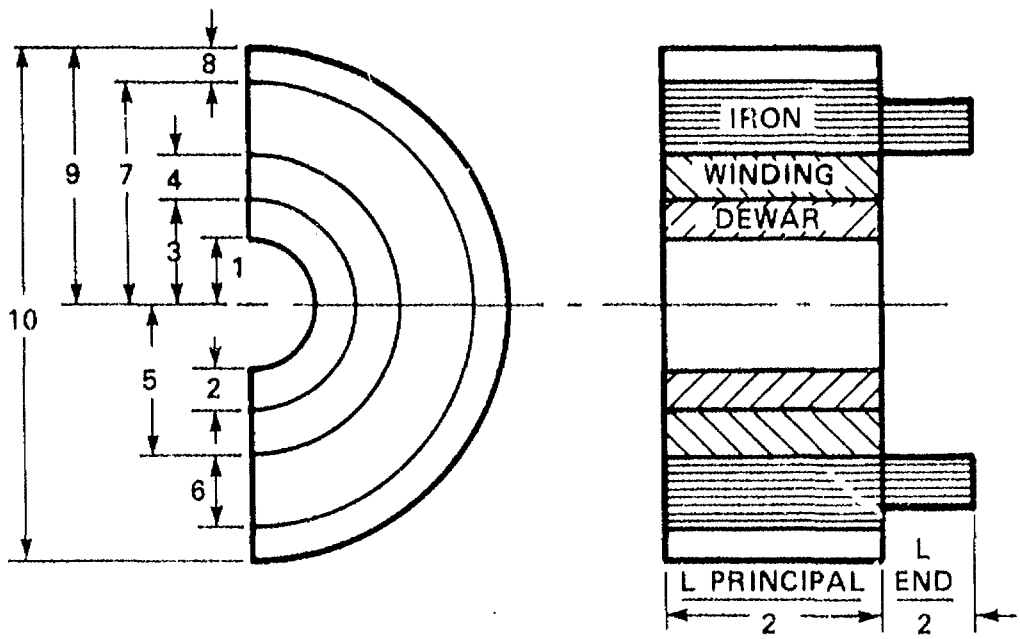

L PRINCIPAL IS THE LENGTH OF THE MAIN POLE (AXIALLY)
L END IS THE LENGTH OF END WINDING SHIELD

1. BORE RADIUS
2. DEWAR SPACE
3. INNER WINDING RADIUS
4. WINDING THICKNESS RADIALLY
5. OUTER RADIUS OF WINDING
6. IRON THICKNESS RADIALLY
7. IRON OUTER RADIUS
8. DEWAR SPACE
9. OVERALL RADIUS
10. OVERALL DIAMETER

615670-2A

Figure 4.2.1-6. Dimensions for One of the Shielded Triplet Quadrupoles

A 1 meter long iron cylinder between individual magnets of the triplet is assumed. Subsequent entries in Table 4.2.1-10 reflect calculations and serve to specify the overall geometry of the focusing magnet. The tabulation also provides tonnages for the magnet iron shield. By referring to Figure 4.2.1-7 the dimensions of each magnet may be visualized.

For scoping purposes, no account is taken of the superconductor weight as it will not appreciably increase the overall weight. The structural support size will be based on the "shield" weight and enough margin is presumed to accommodate the winding and any cryogenic supporting services.

SYSTEM OPERATIONS

The accelerator portion of the driver stores 2 MJ of energy in the storage rings in the form of energetic ions 10 times per second. Each storage ring has one kicker magnet to extract each bunch from the ring. The total time for the beam to compress is 28 μsec for Xe^{+} and 35 μsec for Xe^{++}. The beams must be in phase with each other to less than 1 nsec, but the absolute timing is not critical since the pellet travels a negligible distance in one cycle period of a storage ring. The synchronization of the beams requires a phase accuracy within the ring of $1:10^{4}$ which is well within the state of the art. The final magnet systems focus the ions onto the pellet and bend the beam into the line of sight of the pellet allowing the neutrons to stream into the neutron dumps.

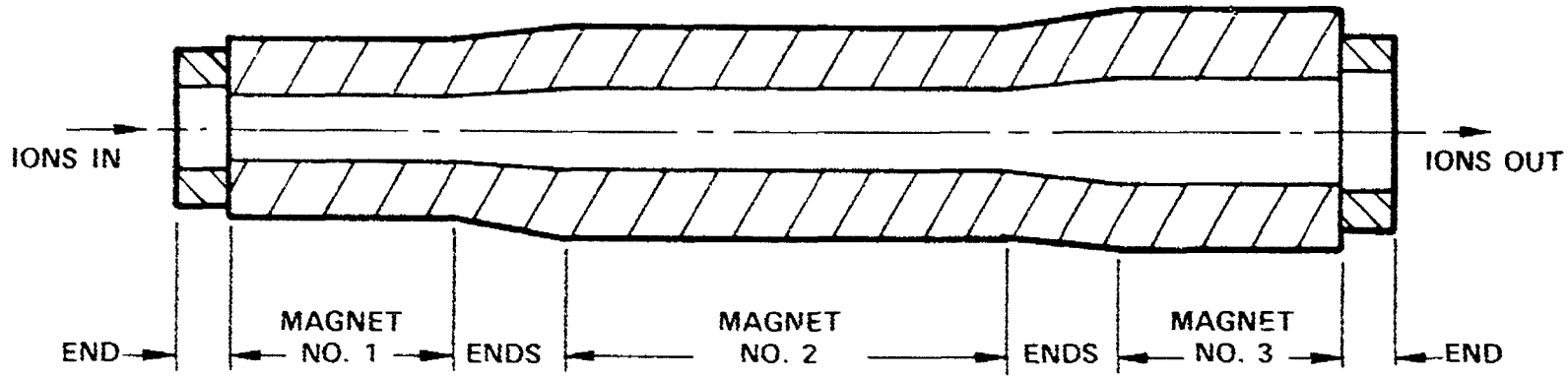

GROSS LENGTH	11.1 METERS
MAXIMUM DIAMETER	2.016 METERS
MINIMUM BORE	0.576 METERS
GROSS TONNES	97.5

615670-1A

Figure 4.2.1-7. Overall Arrangement of Focusing Magnet Triplet

4.2.2 POWER SUPPLY

FUNCTION

The power supply must convert 60 Hz line voltage into RF output power which is then delivered to individual segments of the linear accelerator.

DESIGN REQUIREMENTS

The RF power must be between 100 kW and 1 MW at frequencies between 25 MHz and 200 MHz as specified by the driver designer and delivered in pulses 2 or 4 ms long with a 10 Hz rep rate. The design should be directed toward achieving maximum reliability and availability.

DESIGN DESCRIPTION

Acceleration of the heavy ions from source to target is accomplished in several stages of the linear accelerator. Each stage requires RF power of different frequency and magnitude in order to produce its limited amount of particle acceleration.

RF energy for the linac is supplied from multiple RF power sources. Each source consists of a final power amplifier tube and associated equipment to provide RF power equal to either 500 kW or 125 kW.

Each stage consists of several RF cavities which couple RF energy to the particle beam. All cavities of a given stage operate at a single phase locked frequency as shown in Figure 4.2.2-1. As the particles accelerate to a succeeding stage, a different set of RF parameters are required. The output of an immediately preceding stage is the input to the succeeding stage so all RF systems are specified by sequentially defining output to input demands. The following tables describe the parameters of the last two stages in the linear accelerator.

The final accelerator stage contributes 92% of the total output beam energy. Efficiency of RF power input to beam acceleration is estimated to be 90% and overall beam transport efficiency is estimated to be 78%.

TABLE 4.2.2-1

RF POWER SUPPLY FOR FINAL STAGE OF LINAC

RF Output Frequency	120 MHz
Output Power	30 MW
Duty Cycle	1.0
Number of RF Cavities	2000
Number of Cavity Groups	20
Number of RF Cavities per Group	100
Number of RF Power Sources	60
RF Output Power per Source	500 KW
Input Power per Source	789 KW
Beam Particle Transport Efficiency per Cavity	0.9998

TABLE 4.2.2-2

RF POWER SUPPLY FOR PENULTIMATE STAGE OF LINAC

RF Output Frequency	60 MHz
Output Power	8.95 MW
Duty Cycle	1
Number of RF Cavities	1000
Number of Cavity Groups	20
Number of Cavities per Group	50
Number of RF Power Sources	72
RF Output Power per Source	125 KW
Input Power per Source	202 KW
Beam Particle Transport Efficiency per Cavity	0.9998

A significant difference in RF peak power requirements exists when the linac operates at a duty cycle of 0.02 or 0.04. At 0.02 duty cycle, the peak output beam power is 10^9 watts; at 0.04 duty cycle, this is reduced by a factor of 2 for the same pulse energy which would allow a corresponding reduction in the total number of RF sources.

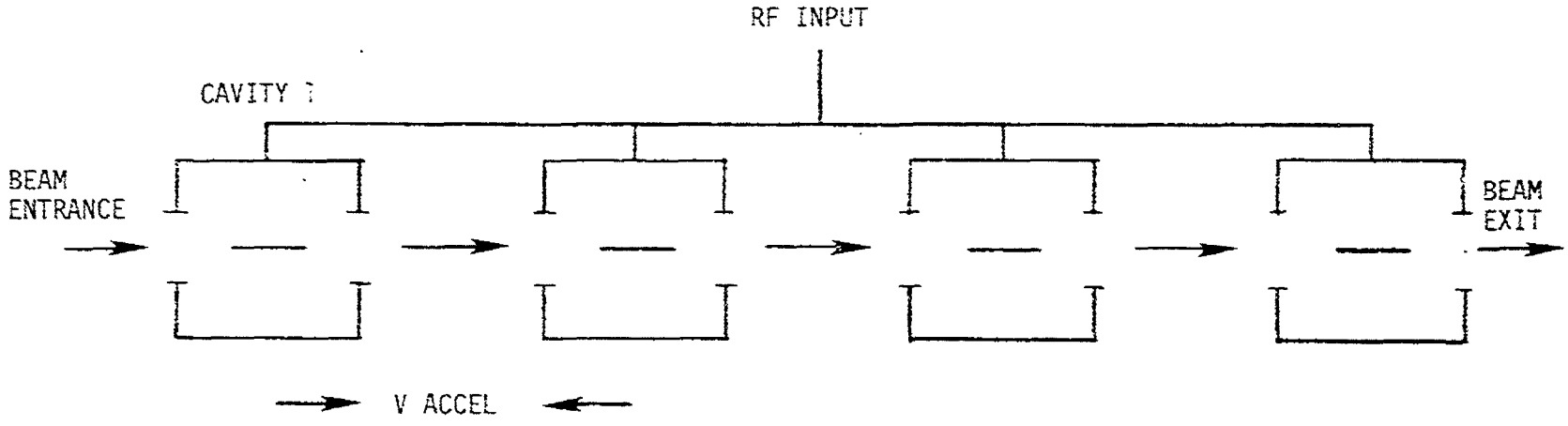

Figure 4.2.2-1. Schematic of a Single Stage Containing Several Cavities in a Linear Accelerator

4.2.3 PELLET DESIGN AND FIRST WALL PROTECTION

FUNCTIONS

The functions of the pellet design and first wall protection for the heavy ion beam driver are exactly the same as those described in Section 4.1.3 for the laser driver.

DESIGN REQUIREMENTS

The design requirements of the pellet design and first wall protection for the heavy ion beam driver are exactly the same as those described in Section 4.1.3 for the laser driver.

SYSTEM DESCRIPTION

Pellet

The heavy ion pellet selected for this study is the tamped pusher design of Bangerter and Meeker[1]. This pellet, shown in Figure 4.2.3-1, features a low Z pusher material, TaCOH, positioned between a high Z tamper, Ta, and the cryogenic fuel of DT in a 1:1 mixture. The TaCOH material is a plastic, polymerized CH_2, that has been seeded with tantalum oxide, Ta_2O_5, until the tantalum constitutes about 1 atomic percent of the pusher. R. Bangerter originally used Pb for the high Z tamper but since the choice of this material is not critical, Ta is used in this design because it eliminates the need to process an additional material, and because the major component of the pellet is then completely compatible with the first wall coating of tantalum.

This pellet has a gain of 88 for an incident energy of 1.28 MJ and can be crudely scaled to a gain of 175 for an incident energy of 2 MJ. The scaled pellet is assumed to give a ρR of 6 g/cm^2 for the compressed fuel which means that 55% of the yield will be in the kinetic-energy of thermonuclear neutrons and 45% will be in x-rays and ions[2]. This pellet has a total mass of 214.6 mg divided into 160.0 mg of tantalum, 20.0 mg of carbon, 18.6 mg of oxygen, 10.5 mg of silicon, and 5.5 mg of hydrogen and its isotopes. These masses include a nominal amount of SiO_2 from the glass shells which separate the different materials during pellet fabrication.

Although this pellet design is unclassified, it is useful in elucidating many of the functional and design requirements of heavy ion pellets and their effects on other systems of the reactor. However, the target design group at the Lawrence Livermore Laboratory has furnished a classified design which has been used for many of the classified studies which are contained in the accompanying classified report, DOE/DP/40086-2.

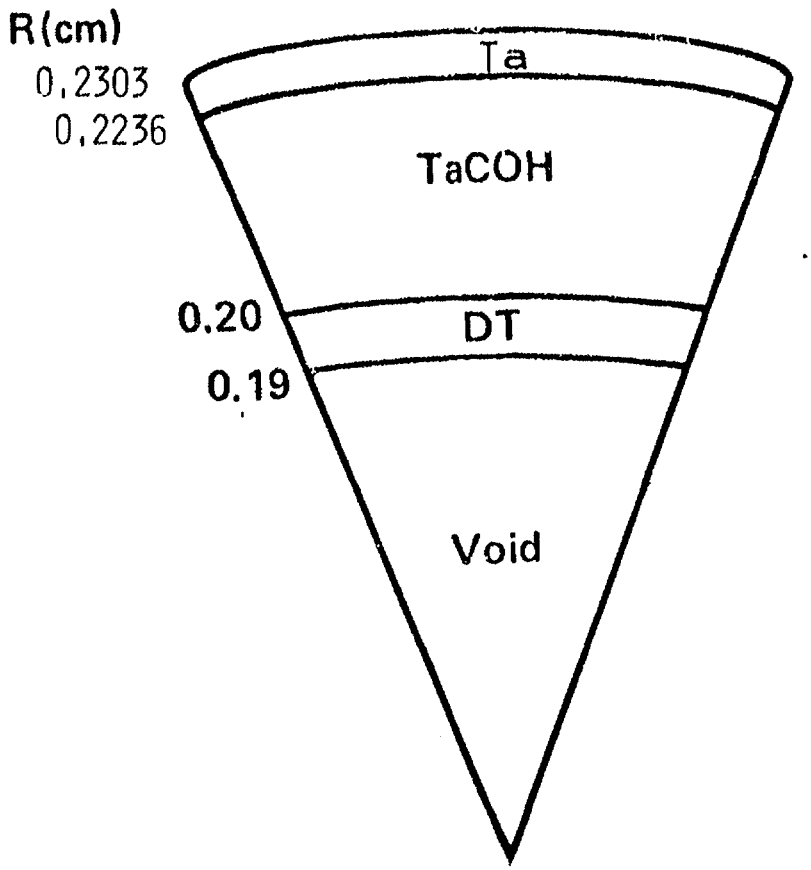

Figure 4.2.3-1. Heavy Ion Pellet Design

First Wall Protection

The concept for protecting the first wall described in Section 4.1.3 for the laser driver is also applicable to the heavy ion driver except that the gas pressure of 5×10^{-4} Torr allowed within the reactor chamber for the heavy ion beams is too low for the gas to play any role in the protection concept.

The pellet is illuminated by 20 heavy ion beams oriented within two opposing cones which have a 23° half angle. Each beam is focused to a 5 mm diameter spot size. The total energy incident on the pellet is 2 MJ and is delivered in 13 nanoseconds. This irradiation produces a pellet yield of 350 MJ. Insomuch as it is possible, the classified pellets are designed to not only have a gain of 175, but also to give x-ray and ion spectra under which the first wall and its coating can best survive (see the accompanying classified volume). In particular, the selection of tantalum for the coating, and of a properly designed pellet are all based on the premise that, in order to survive, the maximum temperature anywhere within the coating must be less than the melting temperature of the coating material.

SYSTEM OPERATION

The basic system operation as described in Section 4.1.3 is essentially the same for the heavy ion driver and the laser driver. The only differences are in the implosion process of the pellet, in the material composition of the pellet, and in the gas pressure allowed within the reactor chamber. Consequently, those aspects of system operation which are different are examined in this section, and repetition is avoided whenever it is not useful for clarification.

The heavy ions incident on the pellet penetrate the Ta tamper shell and are stopped 2/3 of the way into the TaCOH pusher. The inner third of the pusher then implodes, compressing and heating the cryogenic DT fuel to a ρR value of 6 g/cm^2, and heats the fuel to a temperature near 20 keV. The implosion and thermonuclear burn then proceed as described for the laser-driven pellet. The final result is again a total energy yield of 350 MJ, 55% of which is in the kinetic energy of the escaping neutrons, and 45% is in the form of x-rays and the kinetic energy of charged particles formed from the pellet debris.

Since the gas pressure is too low to significantly absorb any of the pellet yield, the x-rays and ions are absorbed in the Ta coating by a thin surface layer a few μm thick. If the temperature of this thin layer exceeds the melting temperature, 3269°K, of Ta, the layer will likely spall and the entire

Ta coating would be gone in a few hundred shots. In the present design with the classified pellets, the maximum temperature reached in the Ta coating is about 2960°K, compared to 2870°K for the laser driver, but still 300°K below the melting temperature and too low to initiate spallation, or to produce significant evaporation.

Since the heavy ion pellet is much more massive and contains a much higher proportion of Ta than the laser pellet, the deposition rate on the coating of the Ta will be significantly higher. In fact, the deposition rate from the heavy ion pellets is 199 μm/month or 2420 μm/year compared to 11 μm/month or 136 μm/year from the laser pellets. This higher deposition rate should be more effective in filling the surface cracks and in thickening those portions of the coating which are abnormally thin. It would also require more frequent usage of the higher yield pellets to evaporate the excess Ta from the coating. This will lead to more frequent replacement of the vacuum ducts which capture the evaporated Ta.

4.2.3 REFERENCES

1. R. Bangerter and D. Meeker, "Ion Beam Fusion Target Designs," Paper Preprint UCRL-78474 (1976).

2. J. A. Blink, P. E. Walker, and H. W. Meldner, "Target-Dependent Effects," p. 8-25, Laser Program Annual Report UCRL-50021-77 (1977).

4.2.4 PELLET FABRICATION

An unclassified heavy ion fusion pellet is shown schematically in Figure 4.2.4-1. This is taken from Reference (1) except that tantalum has been substituted for the lead outer shell. This pellet is simpler than the laser fusion pellet described in Section 4.1.4. Its fabrication would be similar to that of the inner shell of the laser fusion pellet. That is, an inner glass shell would first be manufactured by the drop tower technique. This would then be filled by gaseous DT diffusion at high temperature and pressure. The DT filled glass shell will then be coated with a TaCHO layer by vapor deposition. The tantalum outer shell could be similarly deposited by vapor deposition.

A factory to manufacture the heavy ion pellet would be similar to that for the laser pellet except that a facility for depositing the tantalum shell would be necessary while the equipment for fabricating the MODOX outer shell and suspension system would be absent.

4.2.4 REFERENCES

1. R. Bargerter and D. Meeker, "Ion Beam Inertial Fusion Target Designs," Lawrence Livermore Laboratory, Preprint UCRL-78474, October 20, 1976.

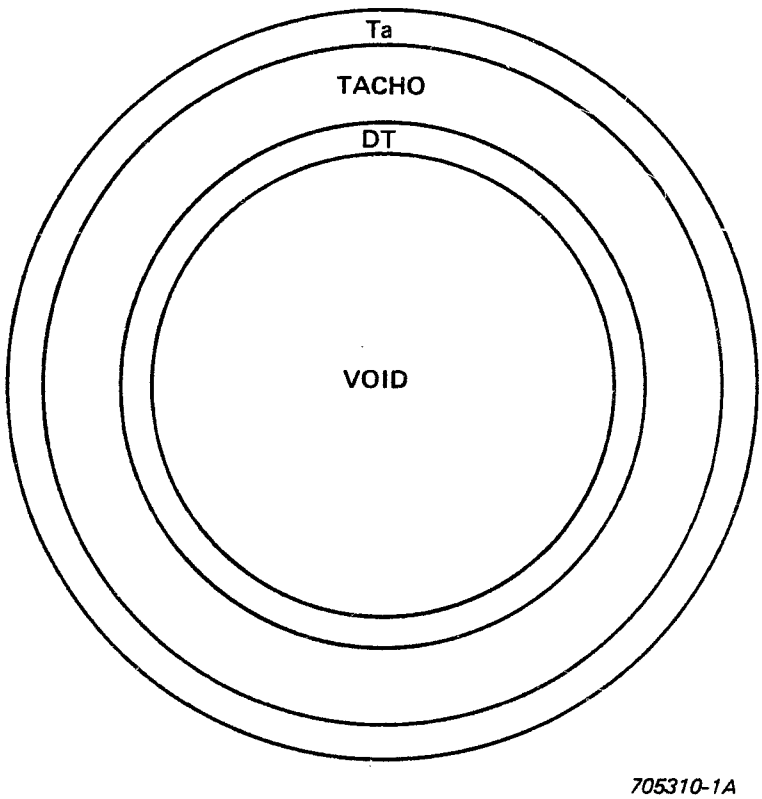

Figure 4.2.4-1. Schematic Drawing of Heavy Ion Pellet Concept

4.2.5. PELLET INJECTION AND TRACKING

Pellet injection and tracking for the Heavy Ion Driver involves a pellet of the same dimension as for the CO_2 Laser Driver and the performance specifications of this system are nearly equal. Although the mass of the pellets in the two systems is considerably different, in both cases, the pellet mass is negligibly small relative to the sabot mass. The pellet injection and tracking system is thus identical to that described in section 4.1.5.

4.2.6 REACTION CHAMBER AND SUPPORTING SYSTEMS

4.2.6.1 MECHANICAL AND STRUCTURAL CONSIDERATIONS

FUNCTION

The functions of the reaction chamber for the Heavy Ion Beam Driver are essentially the same as those described in Section 4.1.6.1-1 for the Laser Driver, except that penetrations must be supplied for the ion beams instead of lasers.

DESIGN REQUIREMENTS

The reaction chamber shall be designed with the requirements and parameters as specified in Table 4.1.6.1-1 for the HIB driver which is repeated here for convenience as Table 4.2.6.1-1.

SUMMARY DESCRIPTION

Except for the penetrations for the ion beams, the reaction chamber design concept is the same. Since operating temperatures and thermal load into the blanket and first wall are identical, the same materials, temperature limits apply for the chamber and the same design is employed. Table 4.1.6.1-2, repeated here as Table 4.2.6.1-2 shows that practically all of the parameters are identical. Exceptions occur only in the area of the chamber beam penetrations required for the ion beams and chamber pressure which will impact the vacuum pumping requirements. The reactor system is affected in the first wall,

TABLE 4.2.6.1-1. REACTOR CHAMBER REQUIREMENTS AND PARAMETERS

	LASER	HIB
PELLET THERMAL OUTPUT	3500 MWt	3500 MWt
ENERGY DISTRIBUTION		
X-RAYS AND IONS	45%	45%
NEUTRON	55%	55%
CHAMBER PRESSURE	$< 10^{-1}$ Torr	$\sim 5 \times 10^{-4}$ Torr
REACTION CHAMBER		
SHAPE	Sphere	Sphere
RADIUS TO FIRST WALL	10 m	10 m
FIRST WALL AND STRUCTURE		
MATERIAL	Steel	Steel
TEMPERATURE	500° C Max	500° C Max
PENETRATIONS/WALL COVERAGE	Consistent with achieving Tritium Breeding Ratio of $\geq$ 1.1	Consistent with achieving Tritium Breeding Ratio of $\geq$ 1.1
COOLANT	Liquid Lithium	Liquid Lithium
LIFETIME		
CHAMBER	30 Years	30 Years
FIRST WALL	5 Years	5 Years
BLANKET		
BREEDING MATERIAL	Liquid Lithium	Liquid Lithium
REFLECTOR	Graphite	Graphite
INTERFACING COMPONENTS	Laser Beams, Vacuum Pumps, Pellet Injector, Pellet Tracking Systems	Ion Beams, Vacuum Pumps, Pellet Injector, Pellet Tracking Systems
TOTAL NUMBER OF DRIVER BEAMS (2-SIDE ILLUMINATION)	108	20

TABLE 4.2.6.1-2. REACTOR SYSTEM PERFORMANCE AND DESIGN PARAMETERS

Driver	CO_2 Laser	Heavy Ion Beam
Thermal Output	3500 MWt	3500 MWt
Chamber Pressure	$\sim 10^{-1}$ Torr	$\sim 5 \times 10^{-4}$ Torr
Protective Atmosphere	Xenon	---
Reaction Chamber		
Shape	Sphere	Sphere
Radius to First Wall	10 m	10 m
First Wall Configuration	Tubular	Tubular
Material/Coating	HT-9/Ta	HT-9/Ta
Tube Diameter - Variable, OD	19.4-6.23 cm	19.4-6.23 cm
Tube Wall Thickness	0.18 cm	0.18 cm
Ta Coating Thickness	0.1 cm	0.1 cm
Tube Temperature, Max	500° C	500° C
Structural Support Sphere		
Material	HT-9	HT-9
Thickness	2.0 cm	2.0 cm
Blanket Annulus Thickness	80 cm	80 cm
Lithium Thickness	60 cm	60 cm
Graphite Reflector	19.8 cm	19.8 cm
Graphite Clad Thickness	0.1 cm	0.1 cm
Outer Sphere		
Material	HT-9	HT-9
Outer Radius	$\sim$ 11 m	$\sim$ 11 m
Thickness (Exclusive of Flanges, Fittings, etc.)	2.5 cm	2.5 cm

TABLE 4.2.6.1-2. (Cont.)

Driver	CO_2 Laser	Heavy Ion Beam
Outer Sphere Insulation		
Material	Alumina Silica	Alumina Silica
Thickness	30.5 cm	30.5 cm
Lithium Flow Requirement		
First Wall, gallons per minute (m^3/s)	261,400 (16.5)	261,400 (16.5)
Outer Blanket, gallons per minute (m^3/s)	213,900 (13.5)	213,900 (13.5)
Total Lithium Flow, gallons per minute, (m^3/s)	475,300 (30)	475,300 (30)
Maximum Velocity (m/s)		
First Wall	17.8	17.8
Blanket	1.2	1.2
Piping	9.1	9.1
Lithium Pump Requirement, gallons per minute (m^3/s)		
First Wall + Outer Blanket, 8 required	$\sim$ 60,000 (3.8)	$\sim$ 60,000 (3.8)
Lithium Inlet Pipe Size (Equiv. Dia.)		
First Wall	$\sim$ 1.5 m	$\sim$ 1.5 m
Blanket	$\sim$ 1.4 m	$\sim$ 1.4 m
Lithium Coolant Temp., (T_{in}, T_{out})	300, 369° C	300,369° C
Total No. of Beams (2-Sided Penetrations)	108	20
Chamber Beam Penetrations		
Beam Opening Requirements @ First Wall (each side)	$\sim$ 2.3 x 3.0 m	10 Openings, $\sim$ 0.3 m Dia. on $\sim$ 7.3 m Pitch Circle
Available Opening	$\sim$ 6.5 m Dia.	$\sim$ 6.5 m Dia.(1)
Beam Half- Angle	$<$ 10°	23° (Cone)

(1) Min of 4 m diameter required for vacuum pumping

TABLE 4.2.6.1-2 (Cont'd.)

Driver	CO_2 Laser	Heavy Ion Beam
Vacuum Pumps		
Type	Roots Blower	Hg Diffusion
Quantity	24	16
Pumping Speed (each)	10,000 l/sec per pump	100,000 l/sec per pump
Wt. (each)	~ 10,200 kg	~ 1600 kg
Effective Blanket Coverage, %	94.5	94.3
Electrical Power Requirements, MW		
Driver	200	67
Li Pumps (3.0 MW each)	24	24
Na Intermediate Loop (6.0 MW each)	48	48
Vacuum Pumps	4	4
Auxiliaries (steam system, HVAC, etc.)	82(2)	76(2)
Net Electric Power Output	1207 MW	1346 MW
Li Wt (Reactor Chamber Only)		
First Wall	63 Tonnes	63 Tonnes
Blanket	415 Tonnes	415 Tonnes
Toroidal Manifolds	32 Tonnes	32 Tonnes
Chamber Wt		
Tubular Wall and Ta Coating	384 Tonnes	384 Tonnes
Toroidal Manifold Assembly (2 required 31 Tonnes each)	62 Tonnes Total	62 Tonnes Total
Support Sphere	324 Tonnes	324 Tonnes
Graphite Reflector (Upper & Lower)	427 Tonnes	427 Tonnes
Outer Sphere (Upper) w/o Reflector	183 Tonnes	183 Tonnes
Outer Sphere (Lower) w/o Reflector	218 Tonnes	218 Tonnes

(2) Final Focus Magnet Not Included

the duct configuration, and to some extent in the area of maintenance. The extent to which the reactor system varies from that required for the laser driver will be discussed and clarified in the following paragraphs.

INTERFACING SYSTEMS

The reaction chamber, except as discussed below, is that described previously and is depicted in Figures 4.1.6.1-1 and 4.1.6.1-2.

HEAVY ION BEAM INTERFACES

The ion beams penetrate the reaction chamber in a conical pattern from both sides of the chamber at the horizontal centerline. The penetrations consist of 10 openings in the first wall. The penetrations are about 0.3 m in diameter and uniformly spaced on a pitch circle of 7.8 m diameter which corresponds to a beam entry cone half angle of 23°. The pitch circle for beam entry is located between the coolant inlet and outlet tori. Total penetration openings at least 4 m diameter on each side are required for vacuum pumping, therefore more than adequate area is available through the two main $\sim$ 6.5 m penetrations. Figure 4.2.6.1-1 shows the reaction chamber interface area and the beam ducts, focusing magnet duct, and vacuum pump arrangement to achieve proper interfacing.

The magnets are placed at a pitch diameter which permits installation of vacuum pumps and their ducts between magnets to minimize the length and the number of pump ducts. In addition, adequate space is available between the main ducts and magnets to shield the superconducting magnets from cavity radiation. The focusing magnets which are approximately 2 m diameter, 10 meters in length and weigh about 100 tonnes each, occupy a significant portion of the containment building.

Each of the beams enters the chamber through a small duct which penetrates chamber and first wall as shown on Figure 4.2.6.1-2. The penetration is achieved by inserting a small donut shaped manifold in a hole in the first wall tube array and welding it into position. Coolant flow enters the donut and

continues around to feed the tubes at the other side so that first wall cooling can still be accomplished around the penetration. A duct is welded to the donut and extends into the blanket. A larger mating duct can then be connected by inserting it through the chamber outer sphere and making a connecting weld from outside the chamber. A bellows is provided between this larger duct and the outer sphere to allow for any misalignment or relative motion. The ducts continue out from the chamber and magnets can then be installed.

VACUUM PUMP/MAIN DUCT INTERFACE

As in the case of the laser driver, the two main ducts which connect to the two 6.5 m openings in the reaction chamber provide the interface between the chamber and ducts to the vacuum pumps. The pumps (Figure 4.2.6.1-1) are connected in pairs to "Y" - shaped ducts each of which converges to a single penetration in the main duct. Therefore four openings in each of the two main ducts are required to accommodate the total of 16 vacuum pumps. There is a significant difference between the laser driver system main vacuum duct and this configuration. Whereas the former duct is open at the end to accommodate the laser beams, the end of this duct is closed off with a domed end which absorbs the major portion of the heat energy which escapes through the large penetration. About 45 MW of heat flux (X-rays and ions) emanates from the opening. Of this amount, approximately 15 MW are absorbed in the domed end. The remaining 30 MW heat flux is absorbed in the cooled convergent portion of the duct.

The duct cooling system was not designed or analyzed in detail since the heat flux in the front of the duct is approximately one half of that to the first wall, which is the critical point of the design. The heat flux at the domed end of the duct is approximately 22% of first wall surface heat flux. The bulk of the neutron energy will continue on through the duct and be absorbed by shielding around and behind the duct.

Removal of a main duct for maintenance requires a different procedure from that for removing the duct for the laser system, because of the proximity of the surrounding focusing magnets. This will be discussed in Section 4.2.6.8, Maintenance and Servicing.

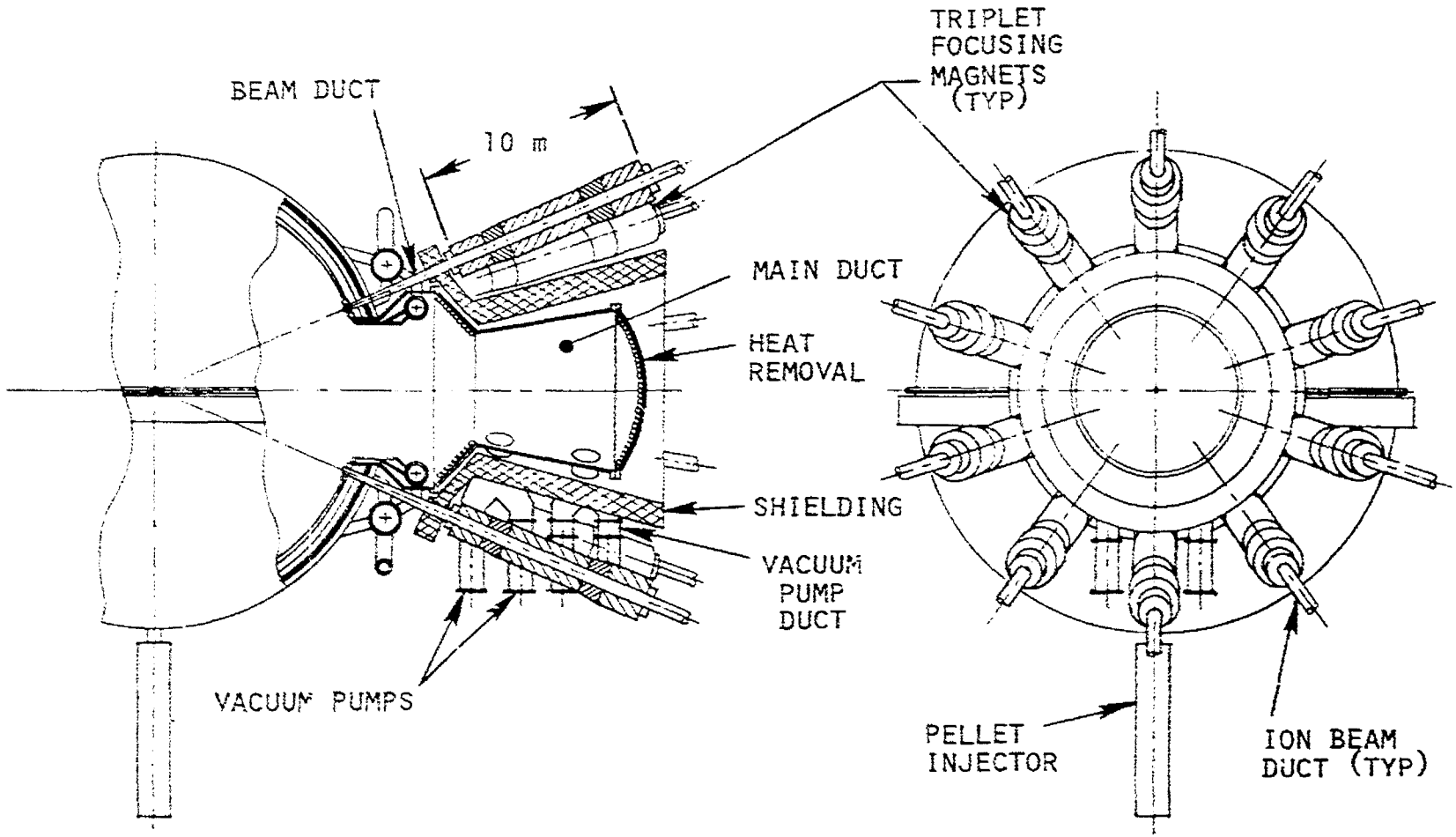

Figure 4.2.6.1-1. Reaction Chamber Interfaces Showing Relationship Between Focusing Magnets, Ion Beam Ducts and Vacuum Pumps

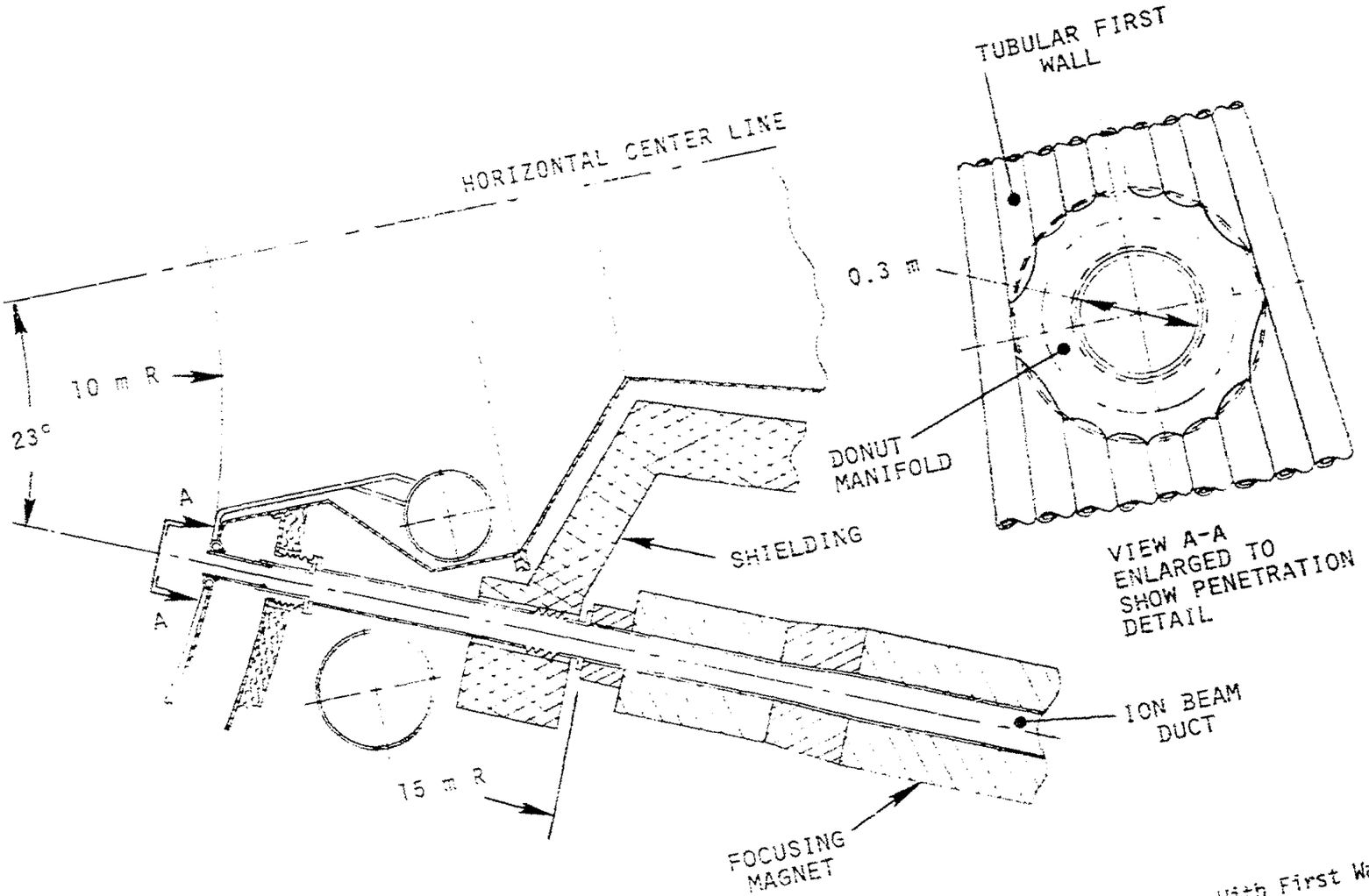

Figure 4.2.6.1-2. Focusing Magnet and Beam Duct Arrangement Showing Interface With First Wall

BEAM DUCTS, NEUTRON BEAM DUMP, AND BENDING MAGNETS

Each ion beam duct emerges from the chamber through the focusing magnet and through the containment wall; beyond which, it is bent away from the neutron dump, as shown in Figures 4.2.6.1-3 and 4.2.6.1-4, to prevent neutron streaming down the ion beam ducts toward the HIB storage system. At the point of merging, the ducts are about 60 cm in diameter and remain that size until the beam is converged in the triplet focusing magnet near the chamber. Between the focusing magnet and the reaction chamber, a smaller duct is used to minimize the chamber penetration size and collimate the particles which are emitted from the chamber as a result of the pellet microexplosion. This collimation minimizes heating of the inner bore of the superconducting focusing magnets.

The bending magnets are approximately 9 meters in length. They are rectangular in cross section and taper along the length from $\sim$ 1.6 x 2 m to 2.4 x 1.6 m at the end where the neutron drift tube and ion beam duct separate. Each magnet weighs approximately 200 tonnes.

The neutron dumps are located approximately 40 meters from the containment building outer wall. This distance is necessary to provide clearance between the ion beam duct and neutron dump without having excessively large bending magnets which would be necessary to bend the beam. The lengths of the drift tube or bending magnet have not been optimized and some tradeoffs are possible to shorten the drift tubes and permit using a smaller building (Section 4.2.8.3) to house the magnets and neutron dumps. The dump walls are approximately 2 m thick to provide adequate external shielding and are actively cooled to dissipate the energy deposited from neutron, X-ray and ion energy coming from the chamber duct penetrations. Additional shielding (not shown) is provided around the drift tubes.

A valve is incorporated in each duct near the containment building to isolate this building from the containment building. This isolation simplifies the design of the heavy ion beam driver building, since it need not be an extension of the containment building. The magnet and neutron dump structural support and valving considerations are addressed in Section 4.2.8.

4.2.6.1-3. Elevation View of Reactor Containment Building and Reaction Chamber Interfaces for Heavy Ion Driven Reactor Concept

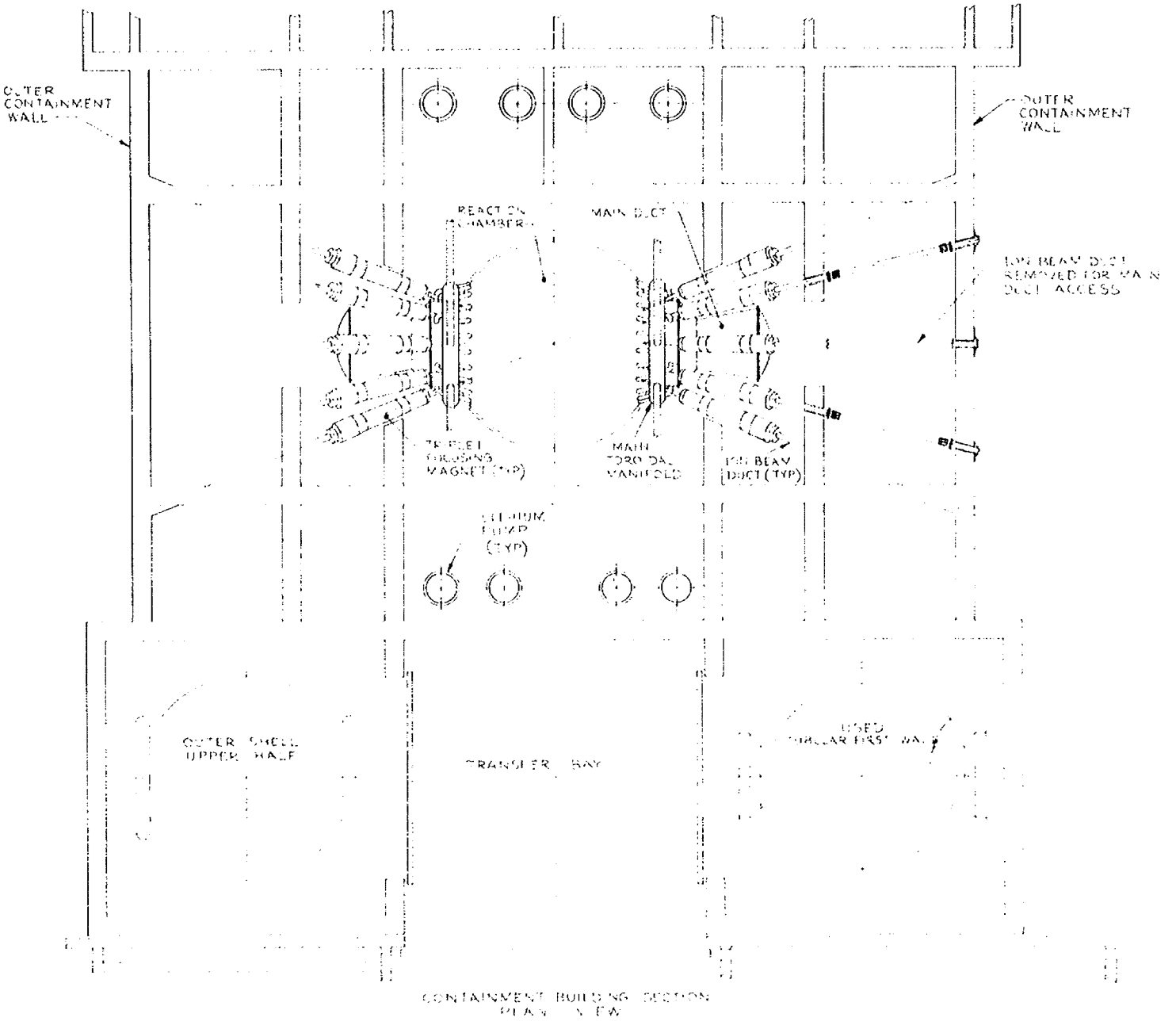

CONTAINMENT BUILDING SECTION PLAN VIEW

4.2.6.1-4. Plan View of Reactor Containment Building and Reaction Chamber Interfaces for Heavy Ion Driven Reactor Concept

4.2.6.2 MATERIALS SELECTION AND DESIGN CONSIDERATIONS

The only conditions which are different for the heavy ion beam (HIB) driven design from those of the CO_2 laser driven design which affect materials performance are the lower allowable chamber pressure and greater pellet mass for the HIB design. Both of these imply greater potential for materials-related phenomena in the HIB design case. However, the pellet composition is unchanged and there are no reasons to alter materials selections. The reader is thus referred to Section 4.1.6.2.

4.2.6.3 BLANKET AND SHIELD DESIGN

The design of this system for the heavy ion case is the same as for the laser case. The discussion in Section 4.1.6.3 applies here.

4.2.6.4 HEAT REMOVAL SYSTEM

The heat removal system for the reactor with the heavy ion driver is identical to that for the reactor with the laser driver. The thermal and hydraulic parameters of the system are therefore the same as those shown in Table 4.1.6.4-2 except that the power requirement for the heavy ion driver is 67 MWe instead of the 200 MWe required by the laser driver. For completeness the parameters table which includes the change mentioned above is reproduced here in Table 4.2.6.4-1. The total power consumption with the heavy ion driver is 219 MWe and the net electric power output is 1346 MWe. The overall plant conversion efficiency is 31.3% and the recirculation fraction is 14.0%.

TABLE 4.2.6.4-1

THERMAL AND HYDRAULIC PARAMETERS OF FIRST WALL

AND BLANKET HEAT REMOVAL SYSTEM FOR REACTOR WITH HEAVY ION DRIVER

Chamber radius, m	10
Pellet Fusion Power, MWt	3500
Percent X-Ray and Ions/Neutron, %/%	45/55
First Wall Surface Power, MWt	1489
Neutron Thermal Power, MWt (blanket multiplication = 1.54)	2811
Total Thermal Power, MWt	4300
Structural Material	HT-9 Steel
Maximum Structural Design Temperature, °C	500
Lithium Coolant Inlet Temperature, °C	300
Lithium Flow Rates:	
First Wall Tubes, m^3/sec. (gpm)	16.50 (261,000)
Blanket, m^3/sec. (gpm)	13.5 (214,000)
Total Lithium Flow Rate, m^3/sec. (gpm)	30.0 (475,000)
Lithium Temperature Rise:	
First Wall Tubes, °C	72.5
Blanket, °C	64.5
Lithium Mixed Mean Outlet Temperature, °C	369
Maximum Lithium Flow Velocity, @ First Wall Tube Ends, m/sec.	17.8
Temperature Drop Across Tube Wall, °C	87
Temperature Difference Across Tube Diameter, °C	129

TABLE 4.2.6.4-1 (Cont.)

Lithium Coolant Inlet Pressure MPa, abs. (psia)	0.41 (59)
Lithium Coolant Pressure Loss Across First Wall/ Blanket Channels, MPa (psi)	0.27 (39)
Lithium Primary Loop Hot Leg Temperature, °C	369
Lithium Primary Loop Cold Leg Temperature, °C	300
Sodium Secondary Loop Hot Leg Temperature, °C	363
Sodium Secondary Loop Cold Leg Temperature, °C	272
Total Sodium Flow Rate, m^3/sec. (gpm)	41.40 (656,000)
Steam Power Conversion System	
Steam Pressure, MPa abs. (psia)	7.24 (1,050)
Steam Temperature, °C	357
Estimated Gross Cycle Thermal Eff., %	36.4
Gross Electric Power Output, MWe	1565
Power Consumptions:	
Heavy Ion Driver, MWe	67.0
Lithium Loop, MWe	24
Sodium Loop, MWe	48
Vacuum Pumps, MWe	4.0
Tritium, Pellets & Radwaste Systems	6.0
Plant Auxiliary Power MWe	70
Total Power Consumption, MWe	219
Net Electric Power Output, MWe	1346
Overall Plant Conversion Efficiency, %	31.3
Recirculation Power Fraction, %	14.0

4.2.6.5 VACUUM SYSTEM

FUNCTION

The function of the vacuum system in the heavy ion beam case is identical to the laser driver case with one exception. Rather than finding a laser mirror protection scheme compatible with the vacuum system, an appropriate interface must be made between the driver vacuum system which is at 10^{-9} Torr and the reaction chamber vacuum system which is at 5×10^{-4} Torr.

DESIGN REQUIREMENTS

The vacuum system must maintain a chamber pressure of 5×10^{-4} Torr (evaluated at 300K) for ion beam propagation a minimum of once every 100ms. Again, the gas removal system must be closed, terminating at the beginning of a waste processing system. Interfacing with the heavy ion beam system requires that the pressure be reduced to 10^{-9} Torr at a point about 75 meters up the beamline from the first wall. The pressure should be reduced to about 5×10^{-6} Torr in the region of the final bending magnet which is about 35 meters from the first wall.

DESIGN DESCRIPTION

Table 4.2.6.5-1 describes the parameters of the vacuum system and Figure 4.2.6.5-1 is a schematic of the same. The system pumps out the gas introduced during operation via mercury diffusion pumps backed by the appropriate mechanical pumps which exhaust the noncondensible gases to a surge tank at a atmospheric pressure. The recovery and disposal system then removes the waste gas from this tank. The chamber gases are exhausted through two large (5m diameter) vacuum ducts provided specifically for this purpose. The diffusion pumps are connected to these main ducts via short secondary ducts (1.5m diameter). As in the laser driven case, the first wall is used as a condensation pump for Ta. Each of the 20 beam ducts are pumped by smaller Hg diffusion pumps in the first 35 meters and turbomolecular pumps reduce the pressure to 10^{-9} Torr along the final 40 meters to the driver interface.

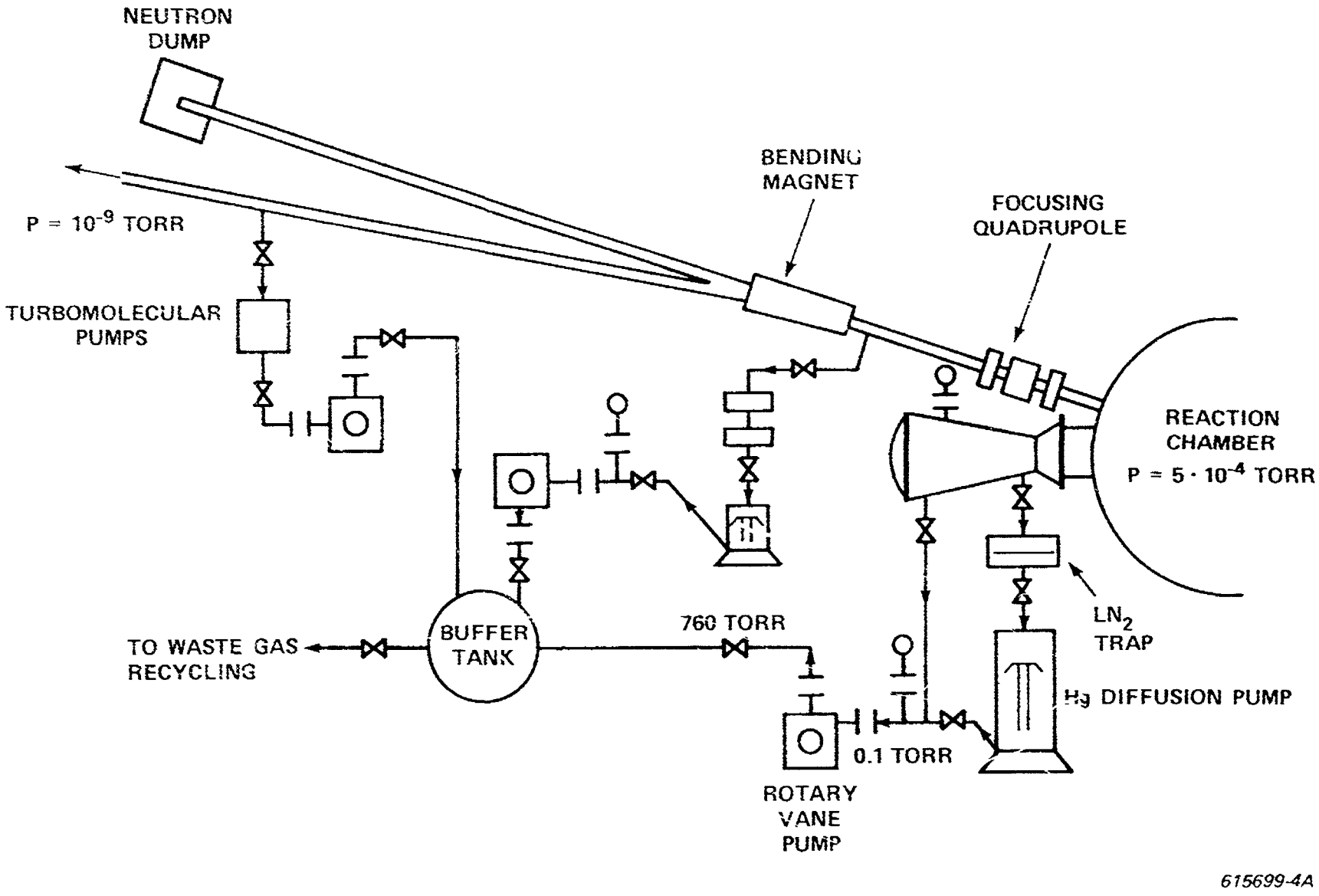

Figure 4.2.6.5-1. Vacuum System Schematic for the Heavy Ion Beam Driver Reactor

SYSTEM OPERATION

Operation is similar to the laser driven system.

TABLE 4.2.6.5-1

VACUUM SYSTEM PARAMETERS

Rep Rate	10 Hz
Chamber Pressure	5×10^{-4} Torr
Chamber Radius	1000 cm.
Chamber Volume	4.2×10^{9} cm^3
Wall Surface Temperature	800°K
Time Average Gas Temperature	800°K
Operating Debris Density	1.6×10^{13} cm^{-3}
Buffer Gas/Density	None
Per Shot Particle Load	2.4×10^{21} particles
Effective Particle Mass	13.6 amu
Single Shot Debris Density Rise	3.6%
Pump Speed at Chamber	1.5×10^{6} $\frac{\ell}{sec}$
Effective First Wall Pumping Speed for Ta	5.6×10^{7} $\frac{\ell}{sec}$
Primary Vacuum Pump	10^{5} $\frac{\ell}{sec}$ - Hg Diffusion Pumps
Number of Primary Pumps	<50
Primary Pump Size	1.2 m diam. x 2 m high
Pumping Power, Chamber Evacuation	<5.5 MW
Backing System	200 $\frac{\ell}{s}$ mechanical pumps for each diffusion pump
HIB Interface Vacuum System (one beamline)	16 - 10^{4} $\frac{\ell}{sec}$ Hg Diffusion Pumps 16 - 10^{3} $\frac{\ell}{sec}$ Turbomolecular Pumps
HIB Interface Power (one beamline)	180 KW

4.2.6.6 TRITIUM HANDLING SYSTEM

The processing requirements and the design concept for handling tritium from the Heavy Ion driver option have already been described in Section 4.1.6.6 in Tables 4.1.6.6-1 and 4.1.6.6-5 so they need not be repeated here. The reader is referred to Section 4.1.6.6 for details.

4.2.6.7 RADWASTE HANDLING SYSTEM

While the Ta content of the pellet designed for a heavy ion driver is much greater than that designed for a laser driver. The essential processes for extraction, storage and purification are the same. The schematic diagram shown in Figure 4.1.6.7-1 therefore applies to the heavy ion case. The different quantities involved are specified in Table 4.1.6.7-1 and in the text of Section 4.1.6.7. The reader is referred to that section for details.

4.2.6.8 MAINTENANCE AND SERVICING SYSTEM

The maintenance and servicing requirements for the CO_2 laser driver and the heavy ion driver are basically the same for the portions of the operation which involve the first wall assembly and removal. However, the heavy ion driver requires that the vacuum ducts be removed and replaced on a yearly basis rather than once every five years. This is due to the fact that the heavy ion pellet contains much more Ta than does the laser pellet. In addition, the design does not have protective gas flow which directs the tantalum debris from the reactor chamber to filters. The tantalum therefore deposits directly on the vacuum duct walls. This will result in a tantalum build-up on the ducts of approximately 0.6 cm (0.24 inch) thickness per year which is so heavy that it must be removed on a yearly basis.

Because the focusing and bending magnets for each of the ten beams completely surround the vacuum ducts, it is necessary to first remove the magnets that are above the duct in order to provide sufficient clearance to move the duct away from the reactor chamber. It will be feasible to remove and replace the ducts during the time of the first wall assembly replacement; the complete operation can be accomplished within the normal 30 day shutdown. Tables II and III of the Appendix list the steps required to perform this operation.

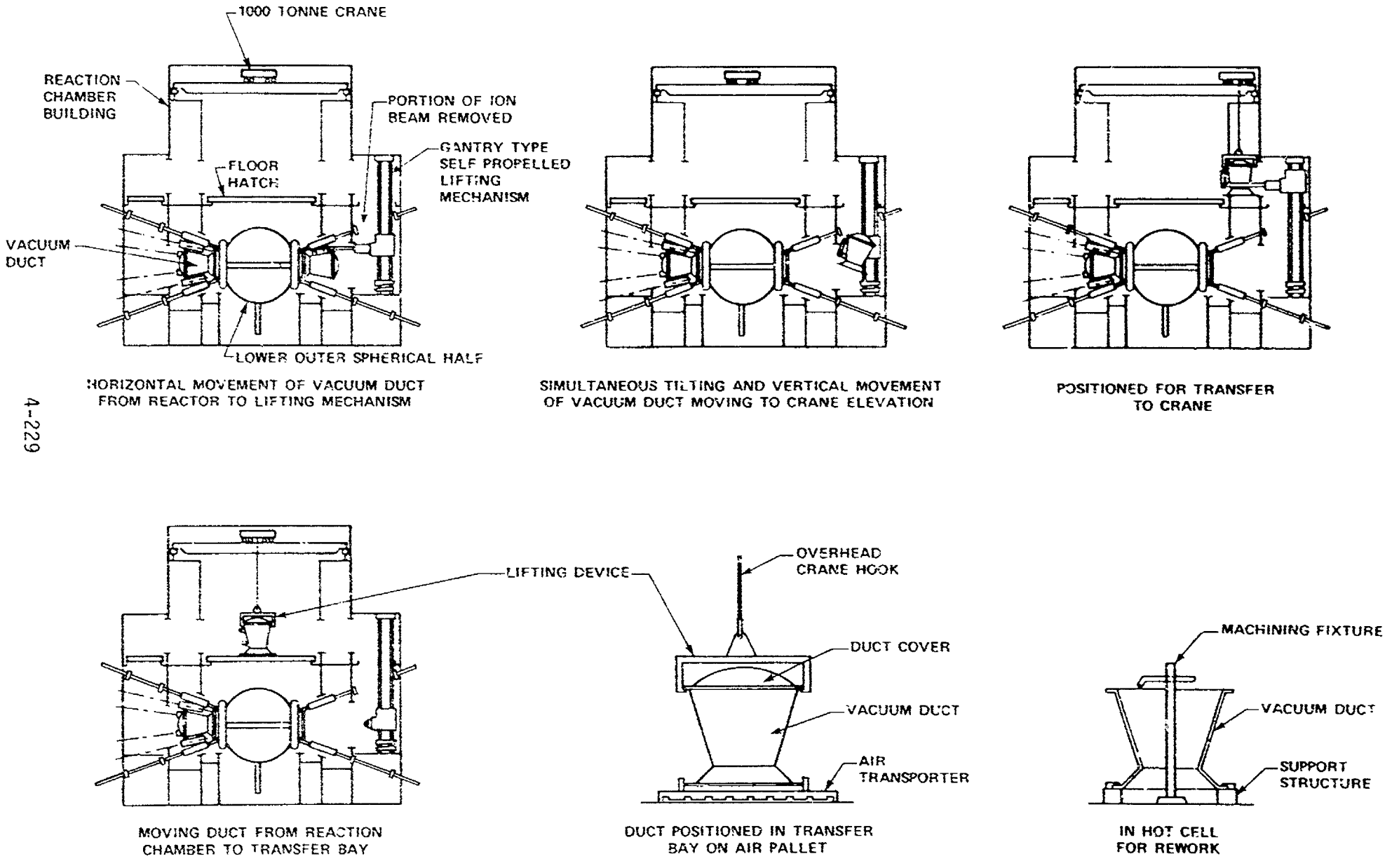

705317-38

Figure 4.2.6.8-1. Schematic Showing the Disassembly Operations for the Vacuum Duct for the Ion Driver

4 OF 4

DOE/DP

40086-1

(VOL I)

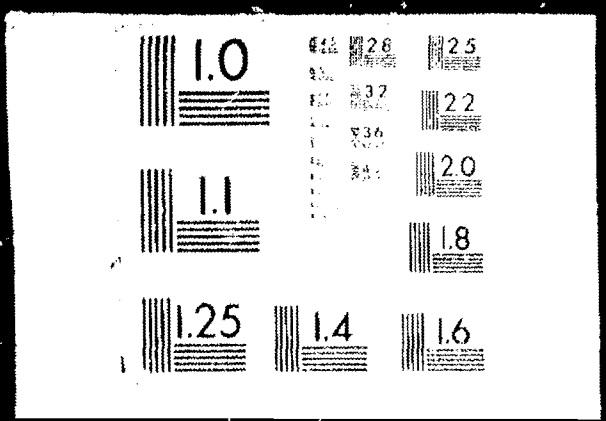

4.2.7 DATA HANDLING AND CONTROL

The system for the heavy ion driver is essentially the same as for the laser driver described in Section 4.1.7. Because of the longer time of flight of the ion beam, it is necessary to place the tracking beams earlier in the flight path in order to provide a timely abort signal. Different parameters must be measured for the two drivers, but it does not alter the basic system.

4.2.8 BALANCE OF PLANT

4.2.8.1 INTERFACE WITH REACTOR

The discussion is the same as in 4.1.8.1 except Figures 4.2.8-1 and 4.2.8-2 should be viewed in place of Figures 4.1.8-1 and 4.1.8-4.

4.2.8.2 INTERFACE WITH GRID

The discussion is the same as 4.1.8.2 except for the station electrical system which is essentially the same as for the Laser Power Concept except for the following:

The heavy ion beam driver power is also taken from the generator output. The tap buses (SF6) join isolated phase bus duct between the generator terminals and the generator load break switch.

Generator output voltage regulation will be maintained by integrating generator field forcing. Generator frequency stabilization will be maintained using a suitably custom-designed flywheel on the turbine generator.

The heavy ion beam driver electrical load is 67 MW. The total station service load is 219 MW.

4.2.8.3 CONTAINMENT AND OTHER BUILDINGS

The discussion is the same as 4.1.8.3 except that "Laser Driver Building" is replaced with the following:

HEAVY ION BEAM DRIVER BUILDING

FUNCTION

The Heavy Ion Beam Driver Building supports the ion beam ducts, bending magnets, neutron beam ducts, and the neutron dumps. There are two driver buildings, located on diametrically opposite sides of the Reactor Building.

DESIGN REQUIREMENTS

The buildings support the ion beam ducts, bending magnets, neutron dump, all other equipment and duct shielding, and are designed so as not to inflict any damage to the Reactor Building under seismic or tornado conditions.

DESIGN DESCRIPTION

Figures 4.2.8-1 and 4.2.8-2 include a conceptual rendering of the structural support for the above items. The Heavy Ion Beam Driver Buildings are each 82 m wide by 50 m long by 60 m high above grade. The superstructure consists of a structural steel frame, an internal structural system consisting of 70 steel columns, seismically braced and located to suit the beam duct arrangement and supporting horizontal steel beams on which the housed equipment are mounted.

The buildings have metal siding and roof deck. Louvers, ventilators, windows and doors are provided to allow cross ventilation in the buildings.

4.2.8.4 SAFETY AND CONTROL

The discussion is the same as 4.1.8.4 except that paragraphs titled "SALT WINDOWS" and "LASER COOLING" are replaced with the following:

BEAM DUCTS

To prevent breach of containment in the event of a leak in any of the beam ducts external to the Reactor Building, each beam duct is provided with a motor operated ball valve, located at its penetration through the Reactor Building wall.

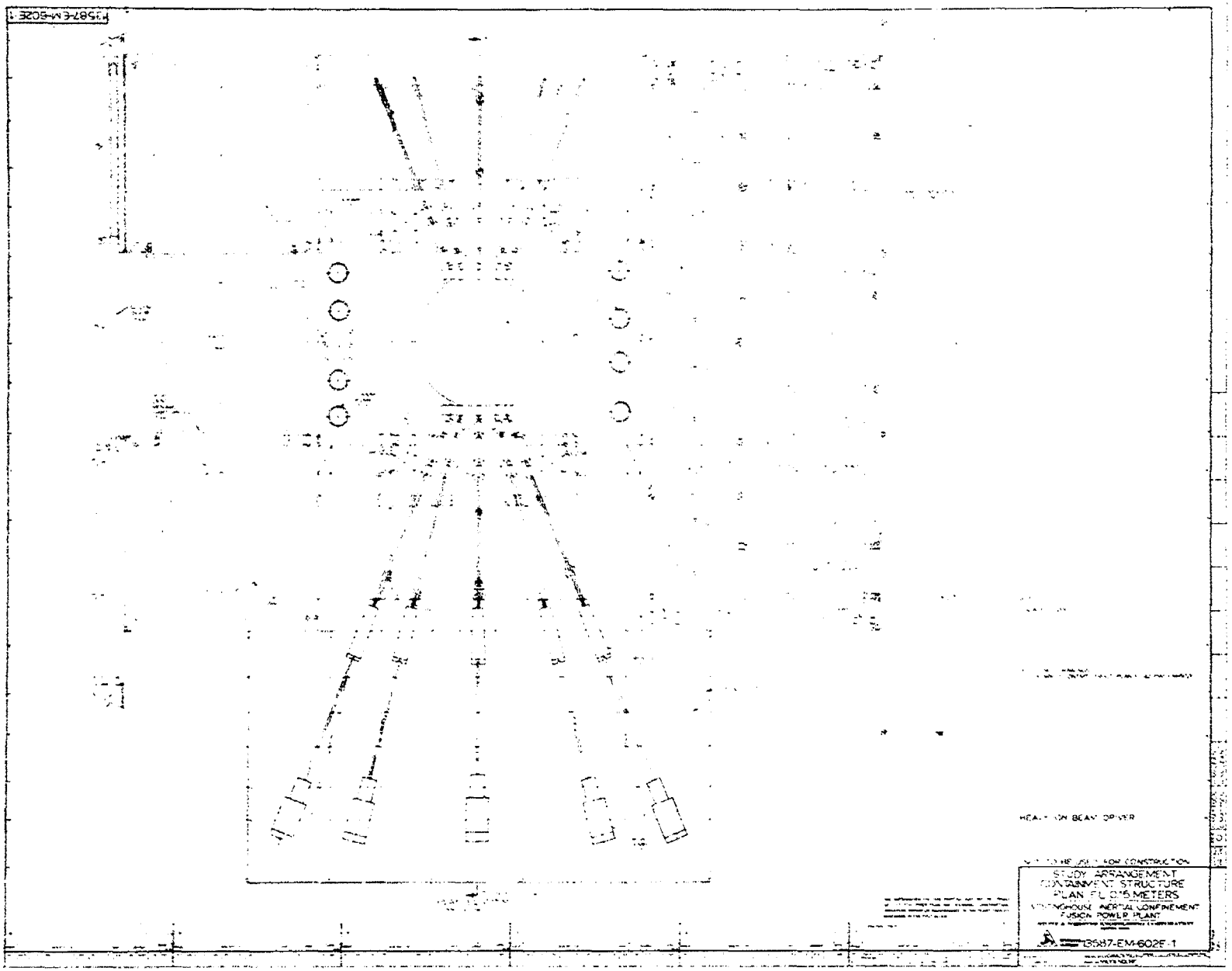

Figure 4.2.8-1. Heavy Ion Beam Driver Containment Structure, Plan El. 0.15 Meters

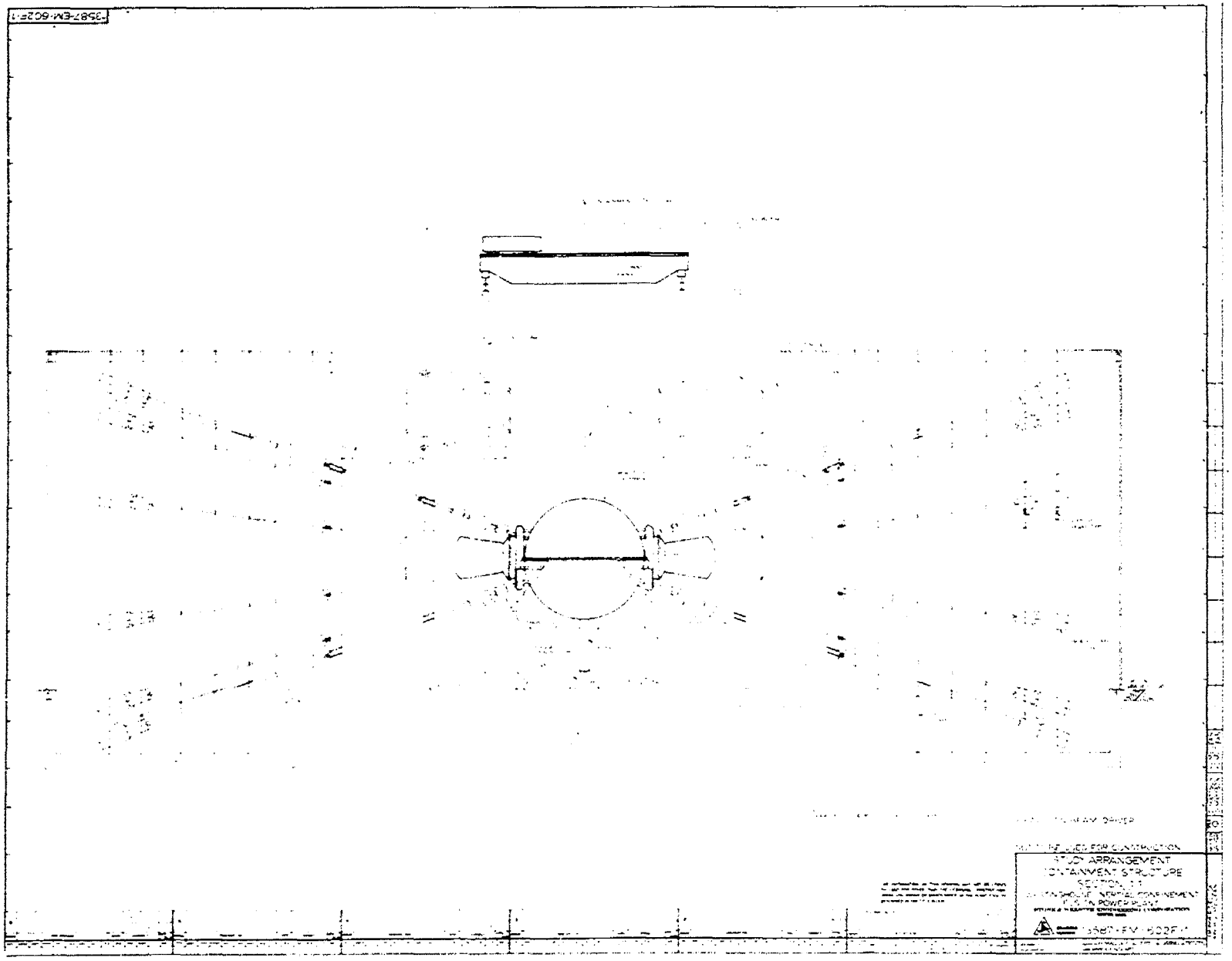

Figure 4.2.8-2. Heavy Ion Beam Driver Containment Structure, Section 1-1

An ultrasonic detection unit is positioned within a salient chamber, made a part of each beam duct and located 1 m from the ball valve, exterior to the Reactor Building. The ultrasonic emission within the beam duct resulting from the flow of air through a perforation will be detected by the ultrasonic detection unit and the resulting signal will sound an audible alarm in the Control Room, simultaneously identifying the leaking beam duct. The same signal will also trigger the motor operated ball valve to close and terminate the heavy ion beam within the duct.

This system does not appear on the drawings.

COOLING

Because the Main Ducts are subject to intensive radiation from the Reactor Chamber, a cooling system is provided to maintain the surface temperatures at acceptable levels.

The neutron dumps are also provided with a cooling system to limit the concrete temperature resulting from neutron heating.

The beam ducts are provided with a cooling system in the area of the Focusing Magnets in order to limit the load on their cryogenic system.

These systems do not appear on the drawings.

SUPPORT OF SUPERCONDUCTING FOCUSING MAGNETS

In order to minimize the transfer of heat through the supporting structure, each superconducting magnet support is furnished with a thermal barrier at each of the members at their point of attachment with the magnet cryostat.

The construction of the thermal barrier allows axial compression loads only. Because of the seismic requirement imposed on these supports, a total of six thermal barriers are required for each support point. Each magnet is furnished with two supports requiring a total of twelve thermal barriers.

The estimated thermal in-leakage per support point amounts to 90 watts for a total of 180 watts for each magnet, based on an ambient temperature of 32°C with a magnet internal support structure at -269°C. Each thermal barrier consists of a stack of 38,000 stainless steel discs, each 0.21 m in diameter by 0.02 m thick encased in an axially flexible housing in which a vacuum of 10^{-4} Torr is maintained. This system does not appear on the drawings.

END

DATE FILMED

08/13/81